A candidate gene based investigation of aberrant DNA methylation in the pathogenesis of primary cutaneous T-cell lymphoma

Jones, Christine Lisa

Awarding institution:
King's College London

Title: A candidate gene based investigation of aberrant DNA methylation in the pathogenesis of primary cutaneous T-cell lymphoma

Author: Christine Jones

A candidate gene based investigation of aberrant DNA methylation in the pathogenesis of primary cutaneous T-cell lymphoma

Christine Lisa Jones

Thesis submitted to Kings College London

for the degree of Doctor of Philosophy

Abstract

Primary cutaneous T-cell lymphoma (CTCL) is a clinically heterogeneous malignancy of mature skin-homing T-cells. Mycosis fungoides (MF) is an indolent subtype of CTCL whilst Sézary syndrome (SS) is an aggressive leukaemic variant characterised by the presence of malignant Sézary cells in the peripheral blood. A role for epigenetic mechanisms in the pathogenesis of CTCL has been proposed but not extensively investigated. In this thesis, the contribution of DNA methylation to the regulation of SHP-1, Fas and PLS3, which have been implicated in the pathogenesis of CTCL, was examined. Gene expression was assessed on the mRNA and protein levels using qPCR and flow cytometry respectively whilst DNA methylation was evaluated using bisulphite conversion and Pyrosequencing. Contrary to results in CTCL cell lines, primary malignant cells from CTCL patients did not display aberrant DNA methylation or dysregulated expression of SHP-1, a negative regulator of STAT3 signalling. Dysregulation of Fas, a key regulator of apoptosis, was observed in 34/47 SS patients with 13/47 showing over-expression compared to healthy controls and 21/47 showing under-expression, attributed to the positional hypermethylation of five CpG dinucleotides in the Fas CpG island. PLS3, an actin-binding protein not normally expressed in any haematopoietic cell, was aberrantly expressed in malignant cells from 21/35 SS patients and 3/8 MF patients with demonstrated clonal blood involvement. CpG dinucleotides 95-99 in the PLS3 CpG island were differentially methylated between healthy lymphocytes and keratinocytes, and hypomethylation of these CpG dinucleotides was observed in SS patients expressing PLS3. To investigate expression of PLS3 on the protein level a novel anti-PLS3 antibody was raised and optimised for use in Western blotting, flow cytometry and immunofluorescence. In conclusion, these data demonstrate that SHP-1 is not regulated by methylation in primary CTCL cells whilst Fas is dysregulated by hypermethylation of five key CpG dinucleotides and PLS3 is dysregulated by hypomethylation of CpG dinucleotides 95-99.

Acknowledgements

I would like to express my deep gratitude to my supervisors Tracey and Sean who have provided support and encouragement, not just towards the completion of this thesis but also towards my professional development as a scientist. It has been a joy to work with the Skin Tumour Unit team: Silvia, Rob, Jac and Isabella made every minute spent in the lab a pleasure. The ninth floor gang, particularly John, JB, Kazouyo, Grace, Joey, Guy, Olivier and Cheri provided many enjoyable discussions, both on science and more lighthearted matters. I am indebted to Mike and Felicia for their hard work maintaining the communal facilities and supplies, undoubtably making my life a lot easier. Outside of the department, I am grateful to Susan for teaching me Western blotting and providing extensive advice on my attempts to optimise uncooperative antibodies, and to Matt and Esti at the genomics centre, who provided invaluable assistance with Pyrosequencing.

I particularly appreciate my wonderful friends Kim, Hannah and Laura, who were always happy to listen, even if they had no idea what I was actually talking about. My sanity was saved on more than one occasion by Becky, who having been through the process herself always knew just what to say to keep me going. I am lucky to know the many wonderful members of JOK, SLOW and SuperChick, whose company encouraged me to venture out into the daylight occasionally and get some exercise. This thesis would not have been possible without the support of my family, which has been unwavering from the point when I declared aged 8 that I was going to do a PhD. I greatly appreciate the effort my parents put into encouraging my siblings and I to be inquisitive and excited by the world around us and can only hope to provide the same for my child. Finally, I wish to extend my heartfelt thanks to my husband for never once complaining and for providing an ever present reminder that to enjoy what one does is to be truly fulfilled.

This thesis represents my own original research work with the exception of contributions from others which are clearly noted in the text and figure legends. The data presented within each results chapter has been accepted for peer-reviewed publication in collaboration with other authors Jones *et al.* (2010), McKenzie *et al.* (2011) and Jones *et al.* (2012): copies of these articles are provided in Appendices A, B and C. Some elements of these articles appear within this thesis in line with Nature Publishing Group's terms of re-use for authors which states 'Since 2003, ownership of copyright in in original research articles remains with the Authors, and provided that, when reproducing the Contribution or extracts from it, the Authors acknowledge first and reference publication in the Journal, the Authors retain the following non-exclusive rights: To reproduce the Contribution in whole or in part in any printed volume (book or thesis) of which they are the author(s)'.

Contents

List of Figures

List of Tables

Abbreviations

5aza	5-aza-2'-deoxycytidine
5mC	5-methylcytosine
5'-UTR	5'-untranslated region
AICD	activation induced cell death
ALCL	anaplastic large cell lymphoma
ALPS	autoimmune lymphoproliferative syndrome
ATLL	adult T-cell lymphoma/leukaemia
CGH	comparative genomic hybridisation
CGI	CpG island
ChIP	chromatin immunoprecipitation
CLA	cutaneous lymphocyte antigen
CTCL	cutaneous T-cell lymphoma
DISC	death inducing signalling complex
DNMT	DNA methyltransferase
FADD	Fas-associated protein with death domain
FFPE	formalin fixed and paraffin embedded
FISH	fluorescence *in situ* hybridisation
HDAC	histone deacetylase
HDI	histone deacetylase inhibitor
MF	Mycosis fungoides
MSP	methylation specific PCR
PBMC	peripheral blood mononuclear cell
PRMT	protein arginine methyltransferase
qPCR	quantitative PCR
RT-PCR	reverse transcription PCR
SS	Sézary syndrome
SSCP	single strand conformational polymorphism
STAT	signal transducer and activator of transcription
T_a	annealing temperature
T_m	melting temperature
TCR	T-cell receptor
USP	unmethylation specific PCR

Introduction

1.1 Primary cutaneous T-cell lymphoma

Mycosis fungoides (MF), named by Alibert after the characteristic skin lesions which 'perfectly resembled morel mushrooms' was the first recognised lymphoid neoplasm presenting in the skin (Alibert, 1832). Subsequently Sézary syndrome (SS), distinguished by generalised erythroderma, lymphadenopathy and 'monstrous histiomonocytes' in the circulating blood was described by Sézary & Bouvrain (1938) as a separate disease. However, electron microscopy of the abnormal cells in both conditions revealed striking ultrastructural similarities suggesting that the two conditions may be related (Brownlee & Murad, 1970, Lutzner *et al.*, 1971). Currently, SS and MF are recognised as subtypes of primary cutaneous lymphoma, a diverse group of lymphoid neoplasms with an incidence rate of 10.7 per 1,000,000 person-years with SS and MF accounting for approximately 40% of cases. A series of consensus meetings led to the 2005 publication of the WHO-EORTC classification for cutaneous lymphomas (Willemze *et al.*, 2005) defining subtypes by the originating lineage, the most common being cutaneous T-cell lymphoma (CTCL) followed by cutaneous B-cell lymphoma and precursor haematological neoplasm. Within each lineage, subtypes are further defined based upon their clinical, histological and molecular features. The degree of relatedness between MF and SS remains a subject of frequent debate, particularly with respect to the possibility of 'disease progression' from MF to SS. The recognised subtypes of CTCL are listed in Table 1.1 along with incidence and survival data from a Dutch and Austrian cohort of 1905 cutaneous lymphoma patients (Willemze *et al.*, 2005) and a US cohort of 3885 cutaneous lymphoma patients (Bradford *et al.*, 2009).

This thesis will focus on SS and MF, both of which usually involve malignant

WHO-EORTC classification	Dutch/Austrian cohort		US cohort	
	Frequency (%)	5 year survival (%)	Frequency (%)	5 year survival (%)
Mycosis fungoides and subtypes			38	91
Mycosis fungoides	44	88		
Folliculotropic MF	4	80		
Pagetoid retuculosis	<1	100		
Granulomatous slack skin	<1	100		
Sézary syndrome	3	24	0.8	40
Adult T-cell leukaemia/lymphoma	0	NR	0.1	NR
Primary cutaneous CD30+ lymphoproliferative disorders			10.2	73
Primary cutaneous anapaestic large cell lymphoma	8	95		
Lymphomatoid papulosis	12	100		
Subcutaneous panniculitis-like T-cell lymphoma	1	82	0.6	NR
Extranodal NK/T-cell lymphoma, nasal-type	<1	NR	0.3	NR
Primary cutaneous peripheral T-cell lymphoma			20	79
Primary cutaneous peripheral T-cell lymphoma, unspecified	2	16		
Primary cutaneous aggressive epidermotropic CD8+ T-cell lymphoma	<1	18		
Primary cutaneous γ/δ T-cell lymphoma	<1	NR		
Primary cutaneous CD4+ small/medium pleomorphic T-cell lymphoma	2	75		

Table 1.1: Subtypes of CTCL

Subtypes of CTCL as defined by the WHO-EORTC and frequency and survival determined within a cohort of 1905 Dutch and Austrian cutaneous lymphoma patients (Willemze *et al.*, 2005) and a cohort of 3885 US cutaneous lymphoma patients (Bradford *et al.*, 2009). NR = not reported.

transformation of CD3+CD4+ T-lymphocytes. MF presentation is typically restricted to the skin and is characterised by lesions which begin as flat patches and then progress to raised infiltrated plaques and further to tumours (Figure 1.1a). MF is generally considered an indolent disease with progression taking place over years or even decades, however, in a small proportion of MF patients the malignancy disseminates to the peripheral blood. By contrast SS is clinically more aggressive, presenting with malignant involvement in the peripheral blood alongside widespread erythroderma demonstrating total skin involvement (Figure 1.1b). Diagnostic parameters include the presence of Pautrier's microabcesses, clusters of atypical lymphocytes within the epidermis (Schmidt-Skrabs, 2000) and presence of Sézary cells with distinct cerebriform nuclei in the blood (Taswell & Winkelmann, 1961) (Figure 1.1c). Molecular genetic analysis can be used to detect the presence of a clonal expansion of T-cells, strongly supporting diagnosis, particularly in SS where an identical clone can often be observed in skin and blood (Bench *et al.*, 2007, Ralfkiaer *et al.*, 1987, Weiss *et al.*, 1985). An estimate of tumour burden in SS can be obtained through visual inspection of a blood smear to enumerate the Sézary cells whilst disease severity in both SS and MF is staged according to an international standardised scoring system assessing the extent of disease presence within skin, lymph nodes, blood, and visceral organs (Olsen *et al.*, 2011). Prognostic factors in SS and MF include clinical entity and stage, age, sex, serum lactate dehydrogenase concentration and the presence of a clonal T-cell receptor (TCR) gene rearrangement in the peripheral blood (Agar *et al.*, 2010). No initiating molecular defect has been identified as the cause of malignant transformation in CTCL however, as discussed in detail below, a wide range of phenotypic changes have been identified along with a multitude of genetic alterations and an increasing number of epigenetic alterations that may lead to the observed phenotypic changes.

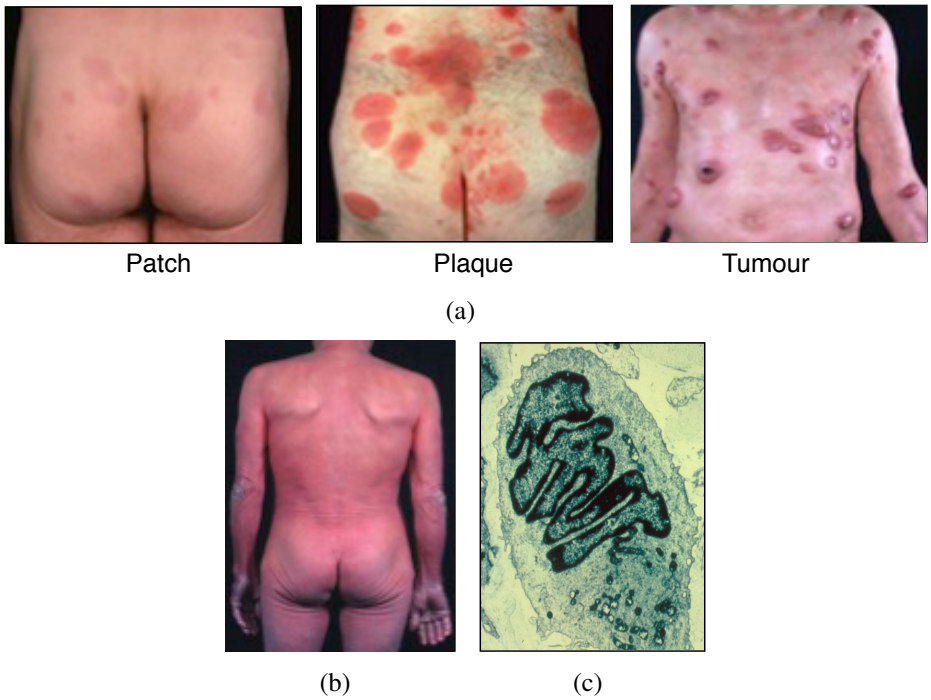

Figure 1.1: Clinical features of SS and MF

(a) Patch, plaque and tumour stage lesions of MF (b) Erythroderma in SS (c) A Sézary cell by electron micrography.

1.1.1 Phenotypic features

Extensive studies have been made to define the phenotypic features of malignant cells in CTCL. Ideally a unique and consistent marker would be identified with potential for use in diagnosis, enumeration of the malignant cells and isolation of the malignant cells. However, thus far no marker has been identified that is consistently expressed in all patients and on the entire malignant subset of each patient. CTCL is clinically heterogeneous and this is reflected in the molecular characteristics of malignant cells from CTCL patients. The origin of the malignant cells is widely agreed to be CD3+CD4+CD45RO+ mature skin-homing T-lymphocytes in typical cases, and expansion of the CD4+ subset is used as an indicator of SS (Vonderheid *et al.*, 2002). There are reports however of diminished CD3 expression ($CD3_{dim}$) in some CTCL samples (Edelman & Meyerson, 2000, Hristov *et al.*, 2011, Klemke *et al.*, 2008), which can be used to identify a subset of malignant cells. The malignant cells are a clonal expansion so molecular analysis can demonstrate clonal rearrangement of the TCRβ and TCRγ genes, which is used to support a diagnosis of CTCL (Fraser-Andrews *et al.*, 2001). Additionally, if the clonal TCRVβ gene segment has been identified for a given patient, antibodies against that TCRVβ can be used to detect the malignant cells (Gorochov *et al.*, 1995). Since this requires prior knowledge of the TCRβ gene rearrangement and a different antibody for each patient it is not of much value for diagnosis but can be used to identify the malignant cells in research studies. However, there are several limitations to this technique. Firstly, not all rearrangements are suitable for detection in this manner as the clonal rearrangement can be non-productive, leading to a TCRVβ chain that is not expressed at the cell surface. Secondly, not all Vβ segments have a corresponding antibody, limiting the repertoire that can be studied. Additionally, some of the available antibodies do not react consistently with their corresponding clone, leading to an increased false positive rate (Bigler

et al., 1996). CD158k, an immunoglobulin-like receptor found on NK cells and some subsets of T-cells has been proposed as a novel phenotypic marker, expressed on 27% of SS peripheral blood mononuclear cells (PBMCs) compared to 6% of healthy control PBMCs (Poszepczynska-Guigné *et al.*, 2004). However, 12% of patients did not show any significant over-expression of CD158k suggesting that it is not universal to all SS patients. A recent report (Clark *et al.*, 2011) suggests that a unique population of high scatter T-cells can be identified by flow cytometry of T-cells isolated from both skin lesions and peripheral blood. Co-staining with appropriate TCRVβ antibodies demonstrates that this high scatter population is restricted to the dominant clone however, in the examples shown clonal cells are also present within the 'normal' T-cell population, suggesting that high scatter is not a feature of the entire clonal population.

The skin-homing characteristics of the malignant cells have led to extensive investigation of skin-homing antigens on their cell surface, cutaneous lymphocyte antigen (CLA), which interacts with E-selectin on endothelial cells to initiate extravasation of T-cells at cutaneous sites, has been demonstrated on PBMCs from CTCL patients (Borowitz *et al.*, 1993). The proportion of PBMCs expressing CLA is greater in those with leukaemic disease than those with skin-restricted disease (Heald *et al.*, 1993). Increased expression of the skin-homing chemokine receptors CCR4 and CCR10 has also been observed on CTCL PBMCs (Capriotti *et al.*, 2007, Ferenczi *et al.*, 2002, Sokolowska-Wojdylo *et al.*, 2005a). Circulating CLA+CD4+ T-cells in SS have been found to co-express the lymph node homing receptor CCR7 whilst those from MF patients with no peripheral involvement and healthy controls did not (Sokolowska-Wojdylo *et al.*, 2005a). T-cells isolated from the skin lesions of leukaemic CTCL patients also demonstrated expression of CCR7 whilst those from MF patients with skin-restricted disease did not (Campbell *et al.*, 2010). Therefore, it appears that the malignant cells of skin-restricted CTCL express skin-homing antigens consistent with

originating from a skin resident memory T-cell subset whilst in leukaemic disease the gain of lymph node homing chemokine receptors allows the malignant cells to circulate through peripheral blood and skin compartments. Campbell *et al.* (2010) also identified co-expression of L-selectin and CD27 alongside the CCR7 expression in leukaemic CTCL, indicating that leukaemic CTCL originates from central memory T-cells whilst skin-restricted disease originates from effector memory T-cells.

Phenotypic features of healthy CD4+ T-cells that are frequently reported to be lost in malignant CTCL PBMCs include: CD7, which plays a role in T-cell interactions during lymphoid development (Stillwell & Bierer, 2001), and CD26, a peptidase that is involved in providing the co-stimulatoy signal during TCR signalling (Morimoto & Schlossman, 1998). Many groups have demonstrated an increased proportion of CD4+CD7- cells in CTCL patients when compared to healthy controls (Borowitz *et al.*, 1993, Haynes *et al.*, 1981, Washington *et al.*, 2002) and some have reported that the proportion of CD4+CD7- cells is significantly higher in advanced stage MF and SS than in early stage MF (Harmon *et al.*, 1996, Laetsch *et al.*, 2000, Scala *et al.*, 1999). However, the prognostic value of CD7 loss is unclear, with Bogen *et al.* (1996) finding a strong correlation between the percentage CD4+CD7- cells and the proportion of Sézary cells by nuclear contour analysis in those patients with a significant CD4+CD7- population, whilst Vonderheid *et al.* (2005) observed no correlation. Similarly, whilst some studies report a correlation between CD7- and appropriate Vβ+ by co-staining (Bogen *et al.*, 1996, Rappl *et al.*, 2001), another reports that this is not the case (Dummer *et al.*, 1999) and additionally that both CD4+CD7- and CD4+CD7+ populations contained clonal cells by TCRγ gene rearrangement. Interestingly, an expanded CD4+CD7- subset can be induced *in vitro* by repeated restimulation of naïve T-cells (Reinhold *et al.*, 1996) suggesting that this subset could be induced by the cellular microenvironment as an indirect consequence of the malignancy. Loss of CD26

has been similarly widely reported and is also more significant in SS than early stage MF (Scala *et al.*, 1999, Sokolowska-Wojdylo *et al.*, 2005b, Washington *et al.*, 2002). When comparing the diagnostic potential of significant CD7- or CD26- subsets, most studies have concluded that loss of CD26 is more prevalent, affecting 86%-100% of SS patients (Jones *et al.*, 2001, Sokolowska-Wojdylo *et al.*, 2005b, Washington *et al.*, 2002), however, other studies have observed a prevalence as low as 60% (Kelemen *et al.*, 2008). Since no marker is consistently observed in all patients, Klemke *et al.* (2008), who assessed the diagnostic potential of $CD3_{dim}$, CD7, CD158k+ and TCRVβ, concluded that assessment of multiple phenotypic anomalies was necessary to ensure accurate diagnosis of blood involvement in CTCL patients.

A multitude of microarray studies have been performed to delineate changes in mRNA levels associated with CTCL, some with the intention of establishing 'gene signatures' for the diagnosis of CTCL and some with the intention of highlighting potentially pathogenic gene expression changes. Key findings of these studies are summarised in Table 1.2, frequently noted changes include increases in EPHA4, PLS3, KIR3DL2, MMP9 and TRAIL and decreases in STAT4, CD26, CD40 and IL2-RB. One notable gene highlighted by these studies is PLS3 (T-plastin), initially characterised by a representational difference analysis study searching for potential biomarkers (Su *et al.*, 2003) and subsequently highlighted by several microarray studies (Booken *et al.*, 2008, Kari *et al.*, 2003, van Doorn *et al.*, 2004). PLS3 is of particular interest because it is not normally expressed in haematopoietic cells and could therefore act as a unique marker of malignant cells if its expression is consistent within and between patients. General themes emerging from gene expression studies include the down-regulation of genes involved in the polarisation towards a T_h1 effector response such as the TBX21 transcription factor and up-regulation of genes involved in the polarisation towards a T_h2 effector response such as the GATA3 transcription factor. This may

Ref	CTCL samples	Control samples	Number of differentially expressed genes	Details
1	18 SS PBMCs with high tumour burden on initial array, 27 SS PBMCs with low tumour burden for testing	9 healthy T_h2-skewed PBMCs on initial array, 1 untreated healthy PBMCs and 7 healthy T_h1-skewed PBMCs for testing	42 ↓, 93 ↑ by >2×	Identified a panel of 8 genes that could discriminate SS in patients with ≥5% tumour cells (STAT4, MGAM, IL1R2 and IL1R1 ↓: ARHB, TNFSF10, CD1D and DUSP1 ↑) and 10 genes identifying those who will survive less than 6 months from sampling, regardless of tumour burden (IL2RB, TGFBR3, BCL2, TCN1 and SFTPD ↓: P4HB, LY64, HEHU, DAD1 and BATF ↑)
2	29 MF lesions on initial array, 24 MF lesions for testing and clustering	11 assorted inflammatory dermatosis lesions	7 ↓, 20 ↑	All samples normalised against average signal from 6 healthy skin samples. Identified 6 genes (FJX1 ↓: Hs127160, STAT4, SYNE1B, TRAF1 and BIRC ↑) that can distinguish MF from ID. Unsupervised clustering of MF samples revealed 2 clusters that could be differentiated by expression of 334 genes, cluster 2 associated with more aggressive phenotypes particularly tumour stage disease and constitutive activation of nuclear STAT3. 5 genes could separate tumour stage disease from plaque stage disease (IKBKAP, FZD7, PDIR, hAC2387 and hAD7824 ↓ in tumour).
3	10 SS PBMCs with high tumour burden	CD4+ T-cells from 5 patients with assorted benign erythroderma and 3 healthy	64 ↓, 59 ↑ by >2×	Identified several genes undetected in control samples but present in SS samples EPHA4 (8/10 SS), FARSA (7/10 SS), RANKL (7/10 SS), TFAP2A (3/10 SS), and ACOX3 (3/10 SS). Consistent with reports from the literature, found JunB, versican, TRAIL, PLS3, CD158k and integrinβ1 ↑: STAT4, TGF-β receptor II, Fas and CD26 ↓. Contradictory to previous reports found TIA1 and SHP1 ↑.
4	5 SS PBMCs and 5 MF PBMCs (3 also isolated for CD4+ T-cells and 3 matched skin lesions also examined)	5 healthy PBMC and CD4+ T-cells, 4 skin biopsies from patients with non-malignant lymphoid skin infiltrates	19 ↓ 26 ↑ in SS PBMCs, 7 ↓ 47 ↑ in MF lesions, 14 ↓ 33 ↑ in MF CD4+ T-cells, 3 ↓ 5 ↑ in MF PBMCs all by >3×	Identified genes similarly regulated between MF skin and MF CD4+ (C1QBP ↓: ARPC1A ↑) and between SS PBMCs and MF PBMCs/CD4+ (ZBTB16 and CD160 ↓: HIST2H2AA, HBD, MMP-9, SNCA, YWHAE, LIR9, TOP1, S100P, STAT1, TRIB1, GLIPR1, GLUL and MS4A4A ↑). In contrast to literature CD158k ↓.
5	63 MF leisions	none	Clustering identified 3 subsets of samples showing >2×change in 593 genes	Cluster 1 enriched for stage IIB and deficient for IB, cluster 2 deficient for stage III, cluster 3 enriched for stage III and deficient for IA. ↑ of 11 genes (IL21R, MYO7A, RGS16, ANP32E, SLA, PPP1R16B, C1GALT1, IL10, TRIB2, MTHFD2 and EHD1) associated with poor response to treatment whilst ↑ of 4 genes (WIF1, KRT15, GSTA3 and PTN) associated with good response to treatment.
6	10 SS CD4+ T-cells	10 healthy CD4+ T-cells	53 ↑ by >2×	Confirmed PLS3, EPHA4, CD158k, CTLA4, SOCS3 and DUSP4 ↑ as previously identified by other studies. Confirmed ↑ five novel genes (DNM3, IGFL2, CDO1, NEDD4L, KLHDC5) by RT-PCR on 27 SS PBMCs. CDO1 and DNM3 provided best discrimination between SS patients and controls.

Table 1.2: CTCL microarray studies

Brief summary of the key findings of each of the microarray studies that has been performed on SS or MF samples. ↓ is used to indicate significant under-expression whilst ↑ is used to indicate significant over-expression. Where a minimum fold change was used this is indicated by >2× or >3×. References are as follows 1. Kari *et al.* (2003) 2. Tracey *et al.* (2003) 3. van Doorn *et al.* (2004) 4. Hahtola *et al.* (2006) 5. Shin *et al.* (2007) 6. Booken *et al.* (2008).

account for the observed development of a T_h2 cytokine profile with disease progression, which is believed to help malignant T-cells suppress the immune system response against them (Vowels *et al.*, 1992). Significant changes have also been noted in genes related to the NF-κB signalling pathway (Martínez-Delgado *et al.*, 2005) and genes of the TNF receptor superfamily (Tracey *et al.*, 2003), both of which are involved in T-cell activation.

1.1.2 Genomic abnormalities

Genomic instability is a common feature of malignancy although the molecular basis for this instability is only recently becoming understood (reviewed by Negrini *et al.* (2010)). Early attempts to examine the cytogenetics of Sézary patient PBMCs were complicated by technical difficulties, namely the inability to induce proliferation, as discussed in Section 1.1.4, which limited the generation of metaphase spreads. Those who did succeed observed highly heterogeneous karyotypes including heteroploidy, structural anomalies, ring chromosomes and minute chromosomes (Johnson *et al.*, 1985, Whang-Peng *et al.*, 1976). Improved staining methods enabled more detailed examination of the chromosome segments involved in rearrangements and a 1995 review of 56 published cases of SS concluded that the most frequently involved chromosomes were 1 and 2, affected in 43% of cases each, followed by 6, 9, 11, 13, 14 and 17 (Limon *et al.*, 1995). Unlike nodal lymphomas, where disease-specific balanced chromosomal translocations are common and can be used in diagnosis or monitoring of disease (Bench *et al.*, 2007), no unique translocation has been found to be associated with CTCL. Subsequent studies reported translocations in almost all chromosomes but consistently found around 50% of CTCL patients to be affected, with alterations of 1p, 6q, 10q, 12q, 17p and 19p occurring most frequently (Batista *et al.*, 2006, Mao *et al.*, 2002a, 2003a).

A summary of results obtained by genome-wide chromosomal rearrangement studies is presented in Table 1.3, any chromosome that was found to be altered in 2 or more studies has been included. Advances in assay resolution are apparent with more recent studies showing multiple small minimal regions of loss/gain in locations such as 10q and 17p where the older studies detected much wider regions of loss/gain. The most frequently affected chromosomes are: 1, harbouring both losses and gains, 9 which appears to be principally affected by losses, and 17 showing gains in 17q and mixed loss and gain within 17p. Whilst most studies drew their conclusions from a range of CTCL samples including both MF and SS, van Doorn *et al.* (2009) compared the two entities and concluded that the pattern of genomic alterations differed between them, suggesting potentially different molecular origins. Particularly, they found frequent gain of 7p13-7p14, 7p21-7p22, 1q31-1q32, and 1p36.2 and losses of 5q13, 9p21, and 13q14-13q31 in MF whilst SS was characterised by gain of 17q23-25 and 8q24 and loss of 17p13. Alterations in 7p21.1, 1p36 and 13q14 have also been detected in SS, suggesting that either these may not be unique to MF or the exact region and genes affected may differ between disease subtypes. Loss of 9p21 appears to be the strongest candidate for an alteration unique to MF as it is supported by another study examining only MF samples (Prochazkova *et al.*, 2007). However, loss of heterozygosity at 9p21 has been observed in SS patients in studies examining the CDKN2A-CDKN2B region (Laharanne *et al.*, 2010a, Scarisbrick *et al.*, 2002), suggesting the limited size of this deletion leads to it going undetected in genome-wide studies of SS. Of the alterations unique to SS, loss of 17p13 is supported by an independent study (Caprini *et al.*, 2009) although Prochazkova *et al.* (2007) did observe loss of the whole 17p arm in some MF patients. Notably, examination of Table 1.3 suggests losses within 10q to be unique to SS as these are not detected in either of the studies using only MF samples. However, several more detailed studies of the 10q locus using micro-satellite

markers revealed loss of heterozygosity in 12/50 MF cases (Scarisbrick *et al.*, 2001) and 15/45 MF cases (Wain *et al.*, 2005) demonstrating that this alteration does also occur in MF.

The development of array-based analysis of chromosomal rearrangement allowed integration of this data with gene expression levels, indicating those imbalances that are more likely to be responsible for disease pathogenesis. Chromosomal arms 1q, 4q and 16q contain genes that are significantly up-regulated in CTCL and this correlates with gains of these regions detected by comparative genomic hybridisation (CGH) (Hahtola *et al.*, 2006). Conversely, chromosomal arms 4q and 12q show a significant downward bias in gene expression in CTCL and losses in these regions are detected by CGH. In another study, minimal regions of loss or gain common to at least 35% of SS patients were mapped and examined for potential oncogenes or tumour suppressor genes (Vermeer *et al.*, 2008). Gain of 8q24.1-8q24.2, which harbours the MYC gene, was consistent with over-expression of MYC, whilst negative regulators of the MYC signalling pathway MXI1 and MNT were located in regions subject to frequent loss. Additional genes integrating with this pathway, including TWIST and BIM, were similarly affected at both genetic and gene expression levels suggesting that multiple genetic aberrations can lead to dysregulation of the MYC signalling pathway. A region of gain in 17q21 was narrowed down to the candidate genes STAT5A, STAT5B and STAT3, all of which are strongly dysregulated in SS (Mitchell *et al.*, 2003, Sommer *et al.*, 2004). Mao & McElwaine (2008) analysed gene expression array data in the context of previously defined regions of chromosomal loss and gain and identified 4 regions; gain of 20q11.21-13.33 (66 genes), loss of 1p36.33-22.1 (86 genes), loss of 6q24.1-24.2 (11 genes) and loss of 15q11.2 (12 genes), where the altered gene expression pattern could separate SS from healthy controls. Caprini *et al.* (2009) on the other hand, compared gene expression between samples with and without each imbalance to

SS[1]	SS[2]	SS[3]	SS[4]	MF and SS[5]	MF and SS[6]	MF and SS[7]	transformed MF and SS[8]	leukaemic CTCL[9]	transformed MF[10]	MF[11]
1p11, 1p36	↓1p26.33-22.1			↓1q	1p32-36	↑1q	↑1q25-31	↑1p36.13 ↓1q31.2	↑1p36	↑1p36.2, 1q21-22, 1q31-32
2p11-24		↓2q37 ↑2p11.2							↓2q36-qter	
		↓3q26.33			3	↑3p, 3q		↑3p11.1		
		↑4p16.1		↑4q		↓4q ↑4q				
		↓5q14.3								↓5q13
6q	↓6q24.1-24.2				6q22-25			↑6p21.1		
		↓7p14 ↑7p21.1			7		↑7p22-11.2; 7q21, 7q31	↓7q21.2	↑7	↑7p22-21; 7p15-13; 7q11.2; 7q22-23; 7q32-36
		↑8p11.2-11.1, 8q11.2-21.1, 8q22-23, 8q24.1-3	↑8p23.3-q24.3		8		↑8q23-24.3	↑8q23.3, 8p23.3 ↓8p11.21		↑8q24.2, 8q24.4
9q		↓9p13.1-12	↓9q13-21.33		9		↓9p21	↓9p21.3	↓9p21 ↑9q34	↓9p21, 9p13-11.1, 9q21, 9q22-31
		↓10p11.2, 10q22, 10q23.31, 10q23.32, 10q24-25, 10q25-26	↓10p26.3-12.1 ↑10p12.2	↓10q	10q23-26		↓10p12-11.2, 10q22-24, 10q25-26	↓10p11.22, 10p11.23, 10q23.33		
11q					11					
					12	↓12q				
						↑12q				
13q11-14		↓13q14			13					↓13q14-13q31
		↓16p11.2				↑16p, 16q		↓16p12.3		
		↓17p13.3-13.2, 17p12 ↑17p11.2, 17q21.31, 17q23, 17q24-25	↓17p11.2-13.2 ↑17p11.2-q25.3	↓17p ↑17q	17p11.2-13		↑17q12, 17q23-24 ↓17p13-q11.1	↑17q25.1 ↓17p12, 17p13.3, 17q25.3	↓17p ↑17q24-qter	↑17q21, 17q22-23, 17q25
				↓19	19p13.3				↑19	

Table 1.3: Chromosomal rearrangements frequently identified in CTCL

Summary of chromosomes found to be frequently altered in at least 2 genome-wide chromosomal rearrangement studies, for each study the minimal regions of loss/gain are given and the nature of the samples examined is provided in the column header. ↓ is used to indicate loss whilst ↑ is used to indicate gain. References 1 and 6 did not indicate the nature of the alterations. References are as follows 1. Limon *et al.* (1995) 2. Mao & McElwaine (2008) 3. Vermeer *et al.* (2008) 4. Caprini *et al.* (2009) 5. Mao *et al.* (2002b) 6. Batista *et al.* (2006) 7. Hahtola *et al.* (2006) 8. Laharanne *et al.* (2010b) 9. (Lin *et al.*, 2012) 10. Prochazkova *et al.* (2007) 11. van Doorn *et al.* (2009).

identify 113 genes whose altered expression was likely due to chromosomal rearrangement within 8p22-21, 8p12-11, 8q13, 8q21-24, 9p13, 9q13, 9q21-22, 9q21-34, 10p13, 10p15, 10q11, 10q21, 10q23, 10q24-26, 17p13-11 and 17q11-25.

In some cases the minimal region of deletion has been mapped to a much higher resolution. Locus-specific fluorescence *in situ* hybridisation (FISH) has been used to identify the gene disrupted by a translocation in 12q as NAV3, resulting in allelic loss in 50% of early MF patients and 85% of late MF and SS patients (Karenko *et al.*, 2005). This was disputed by a subsequent study (Marty *et al.*, 2008) however Vermeer *et al.* (2008) also detected a deletion affecting NAV3 in 30% of their patients suggesting methodological differences may account for the difference. The minimal region of deletion affecting chromosome 10q has been mapped using allelotyping of microsatellite markers revealing two regions of deletion, 10q23.33-24.1 and 10q24.33-25.1, and highlighting genes including Fas, PTEN, HHEX and HELLS in these loci, which could be potentially relevant to the pathogenesis of CTCL (Wain *et al.*, 2005). Other genes inactivated by allelic loss include p15 and p16, located at 9p21 (Navas *et al.*, 2000, Scarisbrick *et al.*, 2002), which are involved in cell cycle regulation. Use of genomic microarrays has identified JunB as having increased copy number that correlated with nuclear expression in 21/23 SS patients (Mao *et al.*, 2003b). Other established changes in copy number include a decrease in Bcl-2 (Mao *et al.*, 2004) and an increase in Her2/neu (Utikal *et al.*, 2006), both of which were shown to be detectable at the protein level.

Though a wide range of genes that are commonly mutated in cancer have been investigated in CTCL, very few sequence mutations have been reported. Infrequent mutations of the Fas gene have been reported in MF (Dereure *et al.*, 2002, Nagasawa *et al.*, 2004) and a novel splice variant has also been described resulting in a truncated dysfunctional protein (van Doorn *et al.*, 2002). The SS cell line HuT78 harbours a

point mutation in p53, a tumour suppressor gene implicated in many different malignancies, however results from primary malignant cells are rather more mixed. Marrogi *et al.* (1999) reported point mutations and deletions affecting the majority of their cohort of large cell transformed CTCL patients whilst a study of MF found p53 mutations in 6/17 patients with tumour stage disease but none of 12 with plaque stage disease suggesting a possible association with disease progression (McGregor *et al.*, 1999). However, Dereure *et al.* (2002) found no p53 mutations in a cohort of 44 MF patients representing all stages. Mutations of p53 also appear to be infrequent in SS patients (Brito-Babapulle *et al.*, 2000, Marks *et al.*, 1996). One study examined the nature of 14 different p53 gene mutations identified within a cohort of 55 primary cutaneous B-cell and T-cell lymphomas and found that 12 occurred at dipyrimidine sites, a feature characteristic of UVB induced DNA damage (McGregor *et al.*, 1999). NF-κB is observed to be constitutively expressed in MF skin lesions (Izban *et al.*, 2000) and a rearrangement of the NF-κB2 gene is seen in the HuT78 cell line, leading to expression of a truncated protein and constitutively activated NF-κB transcription (Zhang *et al.*, 1994) however the presence of this rearrangement in patient samples has not been investigated. Recently, Curiel-Lewandrowski *et al.* (2011) have identified mutations in the IL-16 gene in 11/11 CTCL patients, generating consistent amino acid alterations from GSA to WNG or WNS in the PDZ1 domain, required for association of pro-IL-16 with the nuclear chaperone HSC70. Since loss of nuclear pro-IL-16 has been demonstrated to induce cell cycle progression these mutations may drive proliferation in CTCL.

1.1.3 Epigenetic abnormalities

Epigenetic modifications, causing heritable changes in gene expression without altering the nucleotide sequence of DNA, have been recognised as vital to both normal

cellular function and malignant transformation. Two major categories of modifications can occur: in malignancy the more intensely characterised is DNA methylation, the addition of methyl groups to selected cytosine bases, which can lead to transcriptional silencing (Baylin & Ohm, 2006). As DNA methylation is the focus of this thesis a more thorough discussion of the discovery, mechanism and role of DNA methylation in lymphoma can be found in Section 1.2. The other class of epigenetic modification covers post-translational modifications to the histone proteins that control the packaging of DNA and hence the 'availability' of gene promoters to the transcriptional machinery. A complex code of histone modifications including mono-, di- and trimethylation, acetylation and phosphorylation has been discovered to tightly regulate the conversion between transcriptionally active euchromatin and the highly condensed, transcriptionally inactive heterochromatin (Cosgrove *et al.*, 2004).

Histone proteins were first identified as inhibitory to gene expression since nuclei depleted of histones showed enhanced levels of RNA synthesis (Allfrey *et al.*, 1963). Subsequently, acetylation of the histone proteins was observed to reverse this inhibition (Allfrey *et al.*, 1964). Since then, a multitude of histone modifications have been identified, the combinatorial role of which is to regulate the dynamics of nucleosome positioning and hence DNA accessibility (Cosgrove *et al.*, 2004). Simply establishing the baseline pattern and role of each modification presents a major challenge, the most commonly used method involves chromatin immunoprecipitation (ChIP) with antibodies specific to a particular modification followed by array profiling of the enriched DNA. However, since each nucleosome contains approximately 150bp of DNA, analysis on a mono-nucleosomal level requires an incredibly high resolution which has been overcome by the use of next-generation sequencing methods. Using this method a picture is being built of the positioning of nucleosomes in resting human CD4+ T-cells and the rearrangements that take place upon activation by TCR signalling (Schones

et al., 2008). High-resolution maps have also been generated in resting CD4+ T-cells for 19 different histone methylations and 18 histone acetylations, identifying a 'module' of 17 modifications whose presence in a gene promoter is associated with higher expression levels (Barski *et al.*, 2007, Wang *et al.*, 2008).

Such is the complexity of the histone code that identification of aberrant modifications which may play a role in malignancy has not been performed to the same extent as identification of aberrant DNA methylation. A recent review summarised those modifications that have been associated with a range of malignancies (Füllgrabe *et al.*, 2011) including loss of H4K16ac, H4K20me3, H3K4me2/me3, H4K12ac and increase of H3K56ac. Other marks, including H3K18ac and H3K27me3 show more complex results with some malignancies showing poor prognosis in correlation with increased levels and others showing the opposite. Given the cell type specificity of nucleosome positioning and modification patterns, and the coordination shown between 'modules' of modifications in CD4+ T-cells, it is perhaps unsurprising that changes in individual modifications have differing effects in malignancies of different origins. Additionally, the reviewed studies all examine histone marks on a global level, it seems likely that much remains to be elucidated through investigation of the alteration in patterns of histone modification associated with specific genes.

Although changes to the histone code have not been directly investigated in CTCL the therapeutic success of a range of compounds that act by inhibiting the histone deacetylase (HDAC) enzymes suggest that aberrant histone acetylation patterns may play a pathogenic role in CTCL. Two histone deacetylase inhibitors (HDIs), Vorinostat and Romidepsin, have demonstrated efficacy in clinical trials (Duvic *et al.*, 2007, Whittaker *et al.*, 2010) and have subsequently been approved for treatment of CTCL. In CTCL models, Romidepsin has been found to induce apoptosis of HuT78 cells (Piekarz

et al., 2004) whilst *ex vivo* incubation with Vorinostat induced a greater level of apoptosis in CTCL patient PBMCs than in healthy PBMCs (Zhang *et al.*, 2005a), suggesting that HDIs can selectively target the malignant cells. Further laboratory studies have demonstrated wide ranging changes in gene expression are induced in primary lymphocytes from CTCL and CTCL cell lines upon HDI treatment (Tiffon *et al.*, 2011). Emerging studies also suggest that the gene expression changes induced by HDI treatment may lead to modulation of the STAT3 pathway (R. McKenzie *et. al.*, manuscript submitted), which as discussed below, is constitutively activated in CTCL.

1.1.4 Dysregulation of T-cell signalling pathways

Running through the diverse array of abnormalities discussed above is a common theme of defects in genes associated with various T-cell signalling pathways. Specifically, as discussed below, PBMCs from CTCL display an absent or attenuated proliferative response to mitogen or interleukin stimulation, suggesting dysregulation of the TCR signalling pathways. Abnormal lymphocytes in CTCL have been shown to demonstrate limited *in vivo* proliferation in the peripheral blood compartment, somewhat faster proliferation in the skin and much more extensive proliferation in lymph nodes (Bunn *et al.*, 1981, Shackney & Schuette, 1983). PBMCs from SS patients are not tumourigenic when injected into nude mice through various routes, further suggesting that the peripheral malignant cells are not inclined towards spontaneous proliferation (Gazdar *et al.*, 1980). Whilst PBMCs from healthy individuals show spontaneous proliferation when placed in culture, those from CTCL patients showed no proliferation (Carney *et al.*, 1980, Gazdar *et al.*, 1980). When cultured with mitogens or interleukins the response of CTCL patient PBMCs is highly variable as summarised in Table 1.4 and despite extensive studies, no method of stimulation has been consistently demonstrated to activate the proliferative response of malignant cells in

CTCL. Some methods have shown more promise as a means of stimulating proliferation, Berger *et al.* (2002) for example, demonstrated proliferation for up to three months by stimulating with immature dendritic cells suggesting that malignant cells in SS require cellular contact to initiate proliferation. However, no follow up studies were performed to investigate the pathway leading to activation in this protocol and to the best of our knowledge no other group has successfully reproduced this method of stimulation. Although lack of proliferation may seem disadvantageous to a malignancy, T-cell signalling induced proliferation normally activates a signalling cascade that eventually leads to the elimination of the expanded cells through activation induced cell death (AICD) (reviewed by Krammer *et al.* (2007)). Thus, the lack of response to TCR and interleukin signalling could lead to resistance to apoptosis, allowing the malignant cells to persist. Evidence of the persistence of malignant cells is demonstrated by observations that they respond poorly to most chemothereapeutic agents, which are intended to trigger widespread apoptosis (Meech *et al.*, 2001). Interestingly malignant cells in CTCL often respond to phototherapy, the use of UV light to induce DNA damage, which in turn triggers the intrinsic apoptotic pathway, suggesting that resistance to apoptosis is more likely to stem from defects in the extrinsic apoptotic pathway (Meech *et al.*, 2001).

Since the lack of a proliferative response appears to be general to all mitogens and interleukins, it is unlikely to be due to deficiencies or defects in specific interleukin receptors. TCR signalling is however a dynamic process requiring rearrangement of the actin cytoskeleton to form an immunological synapse (Burkhardt *et al.*, 2008), a complex process that could be subject to dysregulation. One protein that is critical to this rearrangement is L-plastin, an actin-binding protein, which becomes phosphorylated upon co-stimulation (Wabnitz *et al.*, 2007). In the absence of L-plastin, T-cells form smaller, less stable immunological synapses (Wang *et al.*, 2010), leading to reduced

Reference	Stimulant	Result
Braylan *et al.* (1975)	PHA, ConA, PWM, ATS	3/3 MF PBMCs showed similar proliferation to healthy PMBCs but 5/5 SS PBMCs showed substantially reduced proliferation in response to all mitogens.
Carney *et al.* (1980)	PHA, ConA, PWM, SPA	Variable maximal proliferative responses in 10 SS PBMCs, 4 were nearly normal, 4 were poorly responsive, in all SS samples induction of maximal proliferation required much greater mitogen concentrations than required in healthy PBMCs.
Gazdar *et al.* (1980)	PHA, ConA, PWM, TCGF, SPA	2/5 SS PBMCs unresponsive to all mitogens, 2/5 SS PBMCs showed similar proliferation to healthy PBMCs, remaining showed some response to SPA, ConA and PHA only.
Poiesz *et al.* (1980)	TCGF	Crude TCGF ineffective however a partially purified extract enabled continuous culture of two SS PBMC samples, three MF PBMC samples and one MF bone marrow sample for at least four months.
Kaltoft *et al.* (1984), Kaltoft *et al.* (1987)	TCGF	PBMCs from 23 MF patients generated 5 EBV-transformed B-lymphoblastoid cell lines but no T-cell lines. 2 MF skin biopsies and 1 lymph node biopsy showed outgrowth of lymphocyte subsets. Elimination of CD8+ T-cells allowed CD4+ T-cells to proliferate for over three months. However, the T-cell lines generated 'have a finite lifespan and represent T-cells with normal phenotype and function'.
Bang *et al.* (2005)	IL-2 + IL-4	T-cell lines that could proliferate for up to 3 months generated from 15/19 MF skin biopsies. Cell lines generated were oligoclonal as assessed by TCRVβ gene usage and contained a mixture of CD4+ and CD8+ memory T-cells.
Dalloul *et al.* (1992)	IL-7	Proliferation observed in 12/12 SS PBMCs, 3/8 could be maintained for > 10 weeks, cultured cells retained the same TCRβ gene rearrangement as freshly isolated lymphocytes.
Foss *et al.* (1994)	IL-2 + IL-7	5/7 SS PBMCs showed synergistic effect on proliferation of both IL-2 and IL-7 as opposed to individually, 2/7 showed additive effect, only examined over 10 days.
Berger *et al.* (2002)	IL-2 + IL-7	PBMCs from 4 erythrodermic MF patients remained viable for at least a week but not longer than 10 days.
Döbbeling *et al.* (1998)	IL-7 + IL-15	2 SS PBMCs had prolonged survival but no significant proliferation.
Berger *et al.* (2002)	immature DCs	10/10 SS PBMCs proliferated for up to 3 months, cell contact required as transwell co-culture prevented proliferation.
Bensussan *et al.* (2011)	anti-CD3	Proliferation observed in 2/2 SS PBMCs but of much lower magnitude than in healthy CD4+ T-cells.
Yoon *et al.* (2008)	IL-21	No proliferation observed in 3/3 SS PBMCs.
McCusker *et al.* (1997)	PHA + anti-CD28	3/6 SS PBMCs showed proliferation that was dependent upon CD28 mediated co-stimulation.
Yagi *et al.* (1996)	SEB	Induced proliferation in lymphocytes from a patient with clonal TCRVβ17 (SEB is a superantigen for Vβ17), no proliferation observed with SEA, a Vβ3 superantigen or TSST-1, a Vβ2 superantigen.

Table 1.4: Proliferative response of CTCL cells

Summary of studies where CTCL PBMCs have been stimulated with various mitogens, interleukins and other agents and the observed proliferative response.

proliferation. Interestingly, L-plastin is closely related to PLS3, the two proteins show 80% identity and in healthy tissues there is no overlap in expression. In solid tissue malignancy, where PLS3 is normally expressed and L-plastin is aberrantly expressed (Lin *et al.*, 1993a), this dual expression leads to enhanced tumour cell invasiveness (Foran *et al.*, 2006, Klemke *et al.*, 2007) suggesting the aberrantly expressed plastin isoform can interfere with cytoskeletal dynamics. It is therefore interesting to speculate that the aberrantly expressed PLS3 in SS may influence cytoskeletal dynamics and hence impact upon TCR signalling.

Multiple signalling pathways act to integrate the myriad of signals being received by the cell at any one time and coordinate a response. The gene expression studies discussed in Section 1.1.1 highlight dysregulation of multiple genes within the NF-κB signalling pathway whilst the genomic studies identified a mutation causing constitutive activation of NF-κB in the HuT78 cell line. NF-κB is a transcription factor that has been implicated in control of the apoptotic response in malignancy (Rayet & Gélinas, 1999). Strong nuclear and cytoplasmic expression of activated p65, a subunit of the NF-κB dimer, has been identified in 21/23 MF lesions suggesting that the NF-κB pathway is aberrantly activated in MF (Izban *et al.*, 2000) and constitutive activation of NF-κB was observed in 30/30 SS patients (Sors *et al.*, 2006). Additionally, CTCL cell lines showed increased apoptosis after incubation with various inhibitors of NF-κB (Izban *et al.*, 2000), or transfection with the super-repressor IκBα (Sors *et al.*, 2006), providing evidence that inappropriate activation of NF-κB may contribute to resistance to apoptosis in CTCL.

The other central regulators of T-cell signalling that are disrupted in CTCL are the signal transducer and activator of transcription (STAT) proteins (reviewed by Mitchell

& John (2005)). Of the seven mammalian STAT family members, four show dysregulation in CTCL. Specifically, STAT4 shows significant down-regulation in gene expression studies whilst genetic studies demonstrate frequent gain of 17q21, which harbours STAT3, STAT5A and STAT5B. STAT4 is a key regulator driving T_h1 differentiation therefore the reduction in STAT4 expression is probably the underlying mechanism for the observed shift towards a T_h2 polarizing cytokine profile in CTCL (Papadavid *et al.*, 2003, Vowels *et al.*, 1992). Whilst STAT5 does not appear to be constitutively activated in SS (Zhang *et al.*, 1996), the expression of an inactive terminally truncated isoform has been observed (Mitchell *et al.*, 2003) leading to reduced STAT5 signalling. STAT3 is the most intensely investigated of the STATs in CTCL, showing constitutive activation in patient PBMCs (McKenzie *et al.*, 2011, Sommer *et al.*, 2004). Incubation of CTCL cell lines with JAK inhibitor AG490 prevents the binding of STAT3 to its consensus sequence, promoting increased expression of the pro-apoptotic Bax gene and decreased expression of the anti-apoptotic Bcl-2 gene (Nielsen *et al.*, 1999). Further to this, transfection of a dominant negative form of STAT3 into CTCL cell lines led to a significant increase in apoptosis (Sommer *et al.*, 2004), demonstrating that constitutive activation of STAT3 plays a key role in resistance to apoptosis. Recently, it has been demonstrated that one of the targets of STAT3 is miR-21 and that silencing of this microRNA leads to increased apoptosis (van der Fits *et al.*, 2011), suggesting that STAT3 mediated increased expression of miR-21 may coordinate resistance to apoptosis. Despite extensive investigation, no clear mechanism responsible for constitutive activation of STAT3 has been defined although various possibilities have been reviewed by Mitchell & John (2005). The most promising candidate is loss of SHP-1, a protein tyrosine phosphatase that has been demonstrated to be silenced by DNA methylation in some CTCL cell lines (Nakase *et al.*, 2009, Zhang *et al.*, 2000) but this has yet to be validated in primary cells from CTCL patients.

Another signalling pathway likely to be central to the observed resistance to apoptosis in CTCL PBMCs is the Fas system, which is highly regulated during the phases of a T-cell immune response. The Fas receptor, when expressed at the cell surface, interacts with its natural ligand FasL, initiating the extrinsic apoptotic pathway. Resting T-cells express marginal amounts of Fas and are resistant to apoptosis (Klas *et al.*, 1993). During the activation phase Fas is up-regulated (Ju *et al.*, 1995), although short term activated effector T-cells remain resistant to AICD (Klas *et al.*, 1993), which is thought to be due to incomplete death inducing signalling complex (DISC) formation and the presence of high levels of the apoptosis inhibitor c-FLIP (Kirchhoff *et al.*, 2000, Schmitz *et al.*, 2004). Long term activated T-cells express comparable levels of Fas to short term activated T-cells but have complete DISC formation, with concomitant down-regulation of c-FLIP expression and are therefore sensitive to Fas-mediated AICD (Dhein *et al.*, 1995). The Fas gene is located at 10q24, a region frequently found to be lost in CTCL as shown in Table 1.3, suggesting that chromosomal rearrangement could lead to the elimination of this gene. It has been demonstrated that 9/16 SS patient PBMCs are resistant to FasL induced apoptosis and that decreased Fas cell surface expression was seen in four of these cases (Contassot *et al.*, 2008). In the remaining five cases, who showed normal or enhanced Fas expression, the resistance was due to over-expression of the pathway inhibitor c-FLIP demonstrating two instances of dysregulation within the Fas signalling pathway.

1.1.5 Cell line models of CTCL

Long term cell line models are vital tools in the study of disease mechanisms and the observed absence of spontaneous or induced proliferation in CTCL PBMCs has

severely limited the range of SS/MF cell lines available for study. Of the many attempts to expand the malignant cells of CTCL *in vivo* only a few have led to the establishment of long term, stable cell lines with a validated malignant origin. Of the seven samples cultured by Gazdar *et al.* (1980) two long term cultures were established and named HuT78 and HuT102. HuT78 was derived from a patient suffering from SS and the cell surface antigens, karyotype and morphology were similar to those of the originating patient cells (Bunn & Foss, 1996) making HuT78 the first SS cell line to be successfully established. Another SS cell line, SeAx, was produced in 1987 by culturing Sézary patient lymphocytes with TCGF, producing a cell line that was dependent upon IL-2 (Kaltoft *et al.*, 1987). The SeAx phenotype is CD2+CD3+CD4-CD8-CD25+ and it has similar chromosomal abnormalities to the fresh patient peripheral clone. Sez-4, established in 1991 from a patient with stage IVa (T4 N3 B1 M0) MF/SS, was initially dependent upon IL-2 and restimulation every three months with conditioned medium from another Sézary patient's lymphocytes that had been stimulated with ConA (Abrams *et al.*, 1991). After one year the line became independent of these stimuli although IL-2 did still induce an increased rate of proliferation. This line was shown to demonstrate an identical TCR rearrangement to the predominant clone in freshly isolated patient lymphocytes. The phenotype of the cell line, CD3+CD4+CD8-CD7-CD25+, closely matched that observed on lymphocytes in the skin, blood and lymph nodes of the originating SS patient. Interestingly, in another study only one of eight patient samples proliferated upon induction with IL-2 and in this case the sample contained a high proportion of CD25+ cells (Dalloul *et al.*, 1992).

Only one MF cell line, MyLa, has ever been successfully produced, after culture of a skin biopsy from an MF patient with IL-2 and IL-4 (Kaltoft *et al.*, 1992). The MyLa cells had a CD3+CD4+CD8-CD25+ phenotype and a very complex karyotype that was genetically unstable, leading to alterations of the karyotype over multiple

passages (Kaltoft *et al.*, 1994). Some other lines that are occasionally used to model SS/MF cell lines posses features that makes them inappropriate for this use. HuT102, the other line generated by Gazdar *et al.* (1980) was produced from the lymph node tissue of a patient with multiple unusual disease characteristics who was later determined to be suffering from adult T-cell lymphoma/leukaemia (ATLL), which is associated with HTLV-1 viral infection. In fact, the HuT102 cell line proved vital to the initial characterisation of HTLV-1, the first human retrovirus to be identified (Rho *et al.*, 1981). MJ is a cell line derived from the peripheral blood of an MF patient, which also carries the HTLV-1 virus (Popovic *et al.*, 1983) whilst the IL-2 independent and CD25 negative HH cell line was also derived from a patient with ATLL (Starkebaum *et al.*, 1991). PB-1, 2A and 2B are a series of cell lines often cited as originating from a 'progressive cutaneous T-cell lymphoproliferative disorder' and occasionally used to model CTCL or anaplastic large cell lymphoma (ALCL). They reflect an incredibly complex case where the patient was originally diagnosed with MF, then additionally developed Hodgkin's disease, then lymphomatoid papulosis followed by a shift to erythroderma with circulating Sézary like cells, at which point PB-1 was established from the peripheral blood. Subsequently CD30+ ulcerating skin lesions appeared, from which PB-2A and PB-2B were established (Davis *et al.*, 1992).

1.2 DNA methylation

5-methylcytosine (5mC), the cytosine base with a methyl group added to C5 of the pyrimidine ring, was identified as a chemical constituent of the cell well before our current understanding of DNA was elucidated (Johnson & Coghill, 1925). Advances in analysis techniques enabled the proportion of 5mC to be determined in multiple sources, at which point the modification was observed to be both species- and tissue-specific (Kappler, 1971, Vanyushin *et al.*, 1973). Subsequently it was proposed that the

methylation of cytosine bases in the CpG context could contribute to X-chromosome inactivation (Riggs, 1975), stable gene regulation during differentiation (Holliday & Pugh, 1975) and imprinting (Erickson, 1985) however, experimental evidence to support these theories was limited. The key to dissecting the role of DNA methylation in vertebrates came in 1986 with the identification of 'islands' containing a high frequency of unmethylated CpG dinucleotides that tended to be located near transcriptional start sites (Bird, 1986).

It had already been recognised that the frequency with which the CpG dinucleotide appears in vertebrate DNA was much lower than might be expected given random incorporation of nucleotides (Josse *et al.*, 1961, Russell *et al.*, 1976, Swartz *et al.*, 1962). This was proposed to be due to the propensity of 5mC to spontaneously deaminate, becoming tyrosine (Coulondre *et al.*, 1978) (Figure 1.2a). Since tyrosine is a standard nucleotide base this change is less to be detected by DNA repair mechanisms, leading to the propagation of a C→T mutation in subsequent generations and a gradual decrease in the proportion of CpG dinucleotides. By contrast, if unmethylated cytosine deaminates, it becomes uracil (Figure 1.2b), which is recognised by the DNA-uracil glycosylase enzyme and replaced. Consequently vertebrate genomic DNA is found to exhibit an increased frequency of TpG, which is proportional to the deficiency in CpG and the extent of DNA methylation (Bird, 1980).

Upon digestion of vertebrate DNA with the methylation sensitive restriction enzyme *Hpa*II, which cleaves within the sequence CCGG, the majority of fragments are large (Cooper *et al.*, 1983, Gautier *et al.*, 1977, Singer *et al.*, 1979) whereas digestion with the non-methylation sensitive isoschizomer *Msp*I leads to extensive cleavage, suggesting that the majority of vertebrate CpG dinucleotides are methylated. A small proportion, comprising 0.5-2% of the *Hpa*II digest is observed to be unmethylated, generating a low molecular weight fraction with fragments averaging 120bp (Cooper *et al.*,

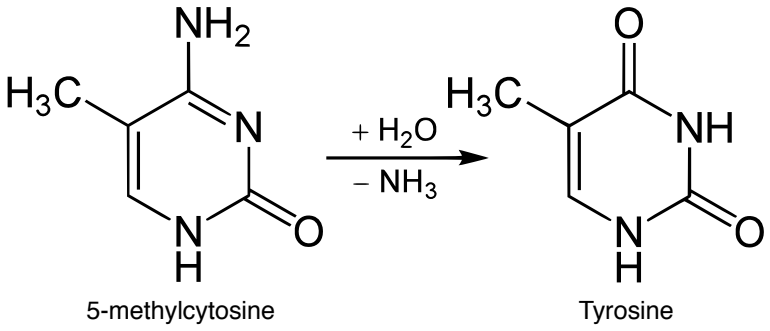

(a)

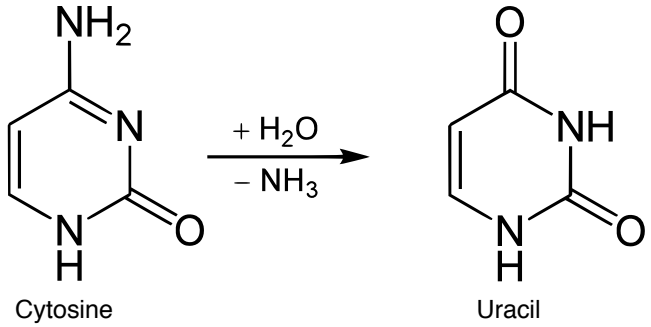

(b)

Figure 1.2: Spontaneous deamination of 5-methylcytosine and cytosine

Chemical structures showing the consequences of spontaneous deamination of: (a) 5-methylcytosine (b) cytosine.

1983) . Remarkably, this fragment length is inconsistent with the predicted frequency of CCGG sites within the genome given the reduced frequency of CpG dinucleotides discussed above. In fact, within the low molecular weight fraction it was calculated that the *Hpa*II recognition site is present at a frequency 13 times greater than expected, suggesting that unmethylated *Hpa*II sites are clustered within the genome (Cooper *et al.*, 1983). These clusters of unmethylated *Hpa*II sites, now known as CpG islands (CGIs) were described by Bird (1986) as '*Hpa*II tiny fragment islands' and were principally defined by a G+C content greater than 50% and CpG count roughly equal to GpC count at the expected frequency given the base composition of the sequence. Bird observed that most of the genes with identified CGIs were housekeeping genes and predicted that a high proportion of all islands would be gene-associated. Controversially, Bird also argued that CGIs were not involved in tissue-specific gene regulation despite evidence showing an inverse correlation between tissue-specific DNA methylation level and gene expression in globin genes (Shen & Maniatis, 1980, van der Ploeg & Flavell, 1980). He further proposed that in these cases methylation may be a secondary event following some other means of inactivation and may act to imprint the silencing.

The definition of a CGI was greatly refined by Gardiner-Garden & Frommer (1987) following an in-depth analysis of all the vertebrate genomic sequences from GenBank. The expected frequency of CpG dinucleotides within a given region was calculated by multiplying the number of Cs by the number of Gs, giving the number of CpGs that would be present if nucleotides were incorporated at random. The observed number of CpGs was then divided by the expected number of CpGs and multiplied by the total number of nucleotides in the region to give an observed/expected CpG frequency. Gardiner-Garden & Frommer (1987) calculated this observed/expected CpG frequency for a 100bp window around each nucleotide and also calculated the percentage G+C

for each window. A CGI was defined as any stretch of 200bp or more where observed/expected CpG frequency was greater than 0.6 and G+C was greater than 50%. Of the sequences examined, 68 did not contain a CGI whilst 51 contained a 5'-CGI, starting upstream of the transcriptional start site, and 11 contained a 3'-CGI, starting downstream of the translational start site. In addition, five sequences contained both 5'- and 3'-CGIs whilst two sequences contained a CGI starting between transcriptional and translational start sites. Interestingly, they found that the 5'-CGIs extended much further into the gene than was expected, in most cases covering part of the coding sequence.

All manner of interesting avenues for bioinformatic analysis became possible with the completion of the draft human genome sequence, including the chance to assess the number of of CGIs present within the genome. Using the definition proposed by Gardiner-Garden and Frommer, 28,890 CGIs were found within the repeat masked sequence (Lander *et al.*, 2001). Interestingly their density per chromosome was quite variable averaging 10.5 islands per Mb but ranging between 2.9 islands per Mb on chromosome Y to 43 islands per Mb on chromosome 19. Subsequently, analysis of SAGE tags and published cDNA sequences allowed the definition of 10,255 gene promoters within the human genome, of which 79% contained a CGI (Bajic *et al.*, 2006). This was a substantially greater proportion than the previous estimates of 55-57% (Antequera & Bird, 1993, Larsen *et al.*, 1992) highlighting the pivotal role played by CGIs in gene expression, particularly for ubiquitously expressed genes. ChIP-on-chip analysis of active promoters within fibroblasts, identified using an antibody against RNA polymerase II pre-initiation complex, defined 9328 active promoters, of which 88% contained a CGI suggesting an enrichment for CGIs in those genes that are being expressed.

Bioinformatic detection of CGIs did however highlight some issues with the sequence based definition of a CGI as many of the CGIs detected were not associated with a transcriptional unit. One particular problem is the presence of extensive tracts of repetitive DNA sequences within the genome including Alu elements, some of which are notably CpG rich (Britten *et al.*, 1988, Jurka & Smith, 1988). Takai & Jones (2002) endeavoured to adapt the CGI definition in order to exclude non-gene-related elements and found that by increasing the stringency of the thresholds to greater than 500bp in length, greater than 55% G+C and observed/expected CpG frequency of greater than 0.65 they could exclude the majority of Alu repeats and unidentified sequences from detection as a CGI. However, the length distribution of 5'-CGIs was found to be biphasic with an average length of 1300bp but a small but significant proportion of 5'-CGIs falling between 200 and 400bp in length therefore their method did exclude a small proportion of known 5'-CGIs. Subsequently, a study focussing on chromosome 21q identified 149 CGIs using thresholds of minimal length 400bp, G+C greater than 50%, and observed/expected CpG frequency of greater than 0.6, on sequence masked for Alu and LINE-1 elements, thus minimising the incidence of non-gene-associated CGIs to 26 (Yamada *et al.*, 2004). Of these, 10 contained sequences identified as tandem repeats that in 8 cases were completely methylated, suggesting that they represented repeat regions that had not been detected by the sequence masking. Of the remaining non-gene-associated CGIs, 15 were found to be unmethylated and not contain tandem repeats suggesting a potential regulatory role, either of a spatially distant gene or of a currently unidentified gene.

Yamada *et al.* (2004) also identified 123 gene-associated CGIs, 94 (76%) of which covered the 5'-untranslated region (5'-UTR) and 26 (21%) of which covered the coding sequence, introns, or 3'-UTR. Of the 5'-CGIs, 84% were found to be completely

unmethylated whilst only 19% of the 3'-CGIs were unmethylated, highlighting the potential functional difference between CGIs spanning the 5' end of the gene and those within the body and 3' end of the gene. Further to this, Bock *et al.* (2007) argued that in addition to being gene-associated, 'bone fide' CGIs ought to be largely unmethylated with strong basal promoter activity in order to have the potential for regulation by methylation. To evaluate this they compared sequence characteristics of predicted CGIs with epigenomic datasets for chromosomes 21 and 22 quantifying DNA methylation, RNA polymerase II pre-initiation complex binding, *DNase*I hypersensitivity, SP1 binding and histone modification states to identify features that imply a regulatory role. The data were used to generate a combined epigenetic score between 0 and 1, reflecting the 'strength' of a CGI. Using a threshold of 0.5 they found 21,631 'bone fide' CGIs within the human genome, available as a track in the UCSC genome browser. However, even with this refinement more than 40% do not overlap with annotated transcriptional start sites suggesting either a substantial number of undiscovered transcripts, which seems unlikely given the large number of transcriptional datasets available at the time, or a functional role for CGIs that are spatially separated from transcriptional start sites.

1.2.1 Functions of DNA methylation

The central functional role of DNA methylation is to prevent expression of nearby genes. It does this through two key mechanisms: direct blocking of transcription factor binding when present in the recognition sequence (Campanero *et al.*, 2000), and recruitment of chromatin modifying enzymes via methyl-CpG binding proteins to initiate condensation of the local chromatin (reviewed by Klose & Bird (2006)). Gene

silencing by DNA methylation is essential for normal development during embryogenesis as demonstrated by the generation of mice lacking each of the enzymes responsible for DNA methylation, which are non-viable (Li *et al.*, 1992, Okano *et al.*, 1999). *De novo* DNA methylation occurs post-implantation, following a reduction in global methylation during blastocyst formation (Howlett & Reik, 1991, Monk *et al.*, 1987). DNA methylation helps to establish the gene expression patterns that characterise each tissue by silencing those genes that are not required. The pluripotency genes Oct-4 and Nanog, for example, are expressed in embryonic stem cells but silenced by methylation in trophoblast stem cells, enabling further differentiation (Hattori *et al.*, 2004, 2007). The proportion of methylated CGIs in a selection of healthy somatic tissues varies between 5.7% in brain and 8.3% in muscle with some CGIs methylated only in one tissue whilst others are methylated in all tissues (Illingworth *et al.*, 2008). Gene ontology analysis revealed that this subset of genes regulated by DNA methylation were enriched for developmental specific genes and transcription factors highlighting their role in lineage definition.

During development, DNA methylation is responsible for X-chromosome inactivation in females, where one of the X-chromosomes is completely silenced in each cell to ensure gene dosage is the same as in males who only have one X-chromosome (Lyon, 1961, Ohno *et al.*, 1959). This process is initiated by a long noncoding RNA called XIST that coats the X-chromosome to be inactivated prior to the establishment of DNA methylation and histone modifications, which condenses the chromatin into an inaccessible state (reviewed by Goto & Monk (1998)). Interestingly XIST expression is in turn regulated by DNA methylation, the XIST promoter of the inactivated X-chromosome remains unmethylated whilst the XIST promoter on the active X-chromosome is silenced by methylation (Norris *et al.*, 1994), raising the possibility that differential methylation is responsible for both triggering and maintaining the inactivation of one

X-chromosome.

A related role of DNA methylation is genomic imprinting, whereby particular genes are expressed only from the maternal or paternal allele because the alternate allele is 'imprinted' by extensive DNA methylation. Imprinting is particularly critical in mammals, where embryos containing two sets of maternal or paternal chromosomes are non-viable (McGrath & Solter, 1984). The first characterised example of an imprinted gene was IGF-II, mutations of which were shown to be propagated only through the paternal germ-line in mice because the maternal allele is silenced (DeChiara *et al.*, 1991). IGF-II was later demonstrated to also be paternally imprinted in humans (Giannoukakis *et al.*, 1993) although some imprinted genes are species-specific, for example ASCL2 is imprinted in mice but not humans (Guillemot *et al.*, 1995, Miyamoto *et al.*, 2002). Several imprinted genes in humans have been identified through their involvement in human disease. Double gene dosage of paternally expressed ZAC following paternal uniparental disomy of chromosome 6 has been shown to be involved in transient neonatal diabetes mellitus (Varrault *et al.*, 2001) whilst Prader-Willi syndrome is caused by deficiencies of the paternally expressed genes SNRPN (Glenn *et al.*, 1993) and NDN (MacDonald & Wevrick, 1997) when their gene loci 15q12 is deleted in the paternal allele (Knoll *et al.*, 1989).

In addition to these regulatory roles, the bulk methylation of non-CGI DNA plays an important protective role in the genome, ensuring that pathogenic DNA elements such as Alu elements are inactivated. Since Alu elements, with the assistance of the L1 transposase enzyme can insert themselves throughout the genome by retrotransposition (Dewannieux *et al.*, 2003), they have the potential to cause widespread disruption by integrating within genes. One new insertion is estimated to occur in every 200 new births, contributing to 0.1% of human genetic disorders (Deininger & Batzer, 1999).

Alu repeats are extensively methylated within the genome (Schmid, 1991) and consequently undergo a high rate of 5mC →T mutation (Britten *et al.*, 1988, Jurka & Smith, 1988). The methylation of CpG dinucleotides within Alu repeats provides an important regulatory role, recruiting methyl-CpG binding proteins that promote the formation of heterochromatin (Huang *et al.*, 2004), preventing further retrotransposition and effectively silencing the Alu elements. The importance of this protective role is highlighted by ICF syndrome, a disorder where satellite DNA that should be methylated is unmethylated due to mutations in DNA methyltransferase (DNMT) 3b (Xu *et al.*, 1999). This results in widespread genomic instability, causing a phenotype characterised by immunodeficiency and facial anomalies.

The critical role of DNA methylation in somatic tissues is the transcriptional repression of genes that are not required in a given cell type. The importance of this role is highlighted by the potential for malignancy when these methylation patterns go awry. Aberrant DNA methylation has long been recognised as a key hallmark of human cancers, often silencing tumour-suppressor genes such as MGMT, CDKN2B and RASSF1A (reviewed by Jones & Baylin (2002)). Genome-wide analysis of the DNA 'methylome' in cancer has revealed extensive hypomethylation of bulk DNA in combination with hypermethylation of promoter CGIs (Weber *et al.*, 2005). In breast cancer cell lines a clear shift in methylation pattern was observed upon epithelial-to-mesenchymal transition (Ruike *et al.*, 2010), which accompanies progression to metastatic disease, whilst another study identified 5 genes whose methylation status allowed discrimination between tumour subtypes (Bediaga *et al.*, 2010). Additionally, the extent of demethylation of the LINE-1 element in colon tissue has recently been demonstrated to be predictive of colon cancer risk (Kamiyama *et al.*, 2012) suggesting that DNA methylation patterns could provide valuable biomarkers for the early detection, diagnosis and prognosis of malignancy.

1.2.2 Mechanism of DNA methylation and demethylation

DNMT3a and DNMT3b, identified by sequence similarity search with a bacterial DNMT, are capable of methylating completely unmethylated DNA (Okano *et al.*, 1998). Both are highly expressed in embryonic stem cells but down-regulated in differentiated embryoid bodies and adult somatic tissues (Okano *et al.*, 1998). In addition, inactivation of these genes in mice blocks *de novo* methylation in embryonic stem cells (Okano *et al.*, 1999) suggesting that DNMT3a and 3b represent the *de novo* methyltransferases. Each has a different specificity, conferred by the N-terminal domain, with DNMT3a crucial to parent of origin specific gene imprinting (Kaneda *et al.*, 2004) whilst DNMT3b targets centromeric minor satellite repeat regions (Okano *et al.*, 1999). A further member of the DNMT3 family, DNMT3L has mutations within the catalytic domain that prevent it from acting as a methyltransferase (Hata *et al.*, 2002). However, it is required for correct formation of the maternal imprint (Bourc'his *et al.*, 2001), acting as a stimulating factor for DNMT3a (Chedin *et al.*, 2002). Once the methylation pattern has been established it it is stably maintained through cell replication (Stein *et al.*, 1982, Wigler *et al.*, 1981). DNMT1 has been identified as the maintenance methyltransferase (Bestor *et al.*, 1988), efficiently methylating hemimethylated CpG dinucleotides but not unmethylated DNA *in vitro* (Gruenbaum *et al.*, 1982).

Demethylation of CGIs promotes formation of an open chromatin structure thus permitting gene expression in a tissue or developmental stage-specific fashion. Demethylation could occur as an active, enzyme catalysed reaction where the methyl group is cleaved from the cytosine base. Alternatively it could be a passive process whereby exclusion of DNMT1 from the replication fork prevents the maintenance of the methylation state, leading to hemimethylated DNA that upon subsequent replication events excluding DNMT1 would become completely unmethylated. Evidence for both mechanisms has been identified during embryogenesis where the paternal

genome is demethylated within eight hours post fertilisation and prior to any cell division whilst the maternal genome becomes demethylated over several rounds of DNA replication (Mayer *et al.*, 2000). Despite compelling evidence for the existence of active demethylation, both in a global (Hajkova *et al.*, 2002) and locus-specific fashion (Lubin *et al.*, 2008), the mechanism and enzymes that lead to demethylation remain contentious.

The demethylation pathway has been characterised in plants, where a 5mC-specific glycosylase removes the entire base, leaving an abasic site into which enzymes of the base excision repair pathway ligate an unmethylated cytosine base (Zhu, 2009). However, no mammalian homologue of the plant 5mC-specific glycosylases have been identified suggesting that this pathway may not be used in mammals. Base excision repair could be used following a different modification to the 5mC base such as deamination to thymidine, which would activate a mismatch repair pathway. Recent studies have shown that activation induced cytosine deaminase (AID) is involved in active DNA demethylation during reprogramming towards pluripotency (Bhutani *et al.*, 2010, Popp *et al.*, 2010). However, AID knockout mice are viable, showing a phenotype restricted to anomalies of B-cell terminal differentiation (Muramatsu *et al.*, 2000), whilst homozygous mutations of the AID gene have been identified in patients with hyper-IgM syndrome (Revy *et al.*, 2000). This suggests that whilst AID may contribute to active demethylation, loss of AID does not lead to complete disruption of demethylation pathways, which would result in developmental defects. RNF4, an E3 ubiquitin ligase, has been demonstrated to be critical to DNA demethylation through interaction with the base excision repair proteins TDG and APE1 (Hu *et al.*, 2010). Homozygous knockout of RNF4 is embryonic lethal and causes global hypomethylation in mouse embryonic fibroblasts suggesting a potential role in developmental methylation however the exact role of RNF4 is unclear, as is the glycosylase or deaminase initiating

this pathway, though the evidence suggests it is not AID (Hu *et al.*, 2010).

Other studies have suggested that GADD45a, a DNA damage response protein, is involved in in active demethylation by recruiting components of the nucleotide excision repair pathway (Barreto *et al.*, 2007, Schmitz *et al.*, 2009). However, the results are open to debate as others have failed to replicate them (Jin *et al.*, 2008) and GADD45a knockout mice do not show global or locus-specific hypermethylation (Engel *et al.*, 2009). One group has identified a protein, MBD2, with specific cytosine demethylase activity in an *in vitro* system that can directly release the methyl group from 5mC (Bhattacharya *et al.*, 1999), an impressive catalytic achievement as it involves the breaking of a thermodynamically stable carbon-carbon bond. MBD2 is required for valproate induced demethylation of a replication deficient reporter construct in HEK293 cells (Detich *et al.*, 2003) supporting its role as an active demethylase. However, another report suggests that *in vivo* MBD2 is a component of a transcriptional repression complex that strongly binds to methylated DNA without demethylating it (Ng *et al.*, 1999). Additionally, paternal demethylation in oocytes from MBD2 knockout mice proceeded normally, suggesting that MBD2 is not involved in developmental reprogramming (Santos *et al.*, 2002). All these potential DNA demethylation mechanisms are outlined in Figure 1.3.

1.2.3 Methods for quantification of DNA methylation

There are two main approaches for detecting methylation: direct methods using enzymes that recognise or are blocked by the methyl group or indirect methods using bisulphite conversion to convert all cytosines to tyrosines leaving the 5mC unconverted. The fact that some restriction enzymes are unable to cleave DNA if their recognition site contains 5mC has been used as a tool since the very early studies

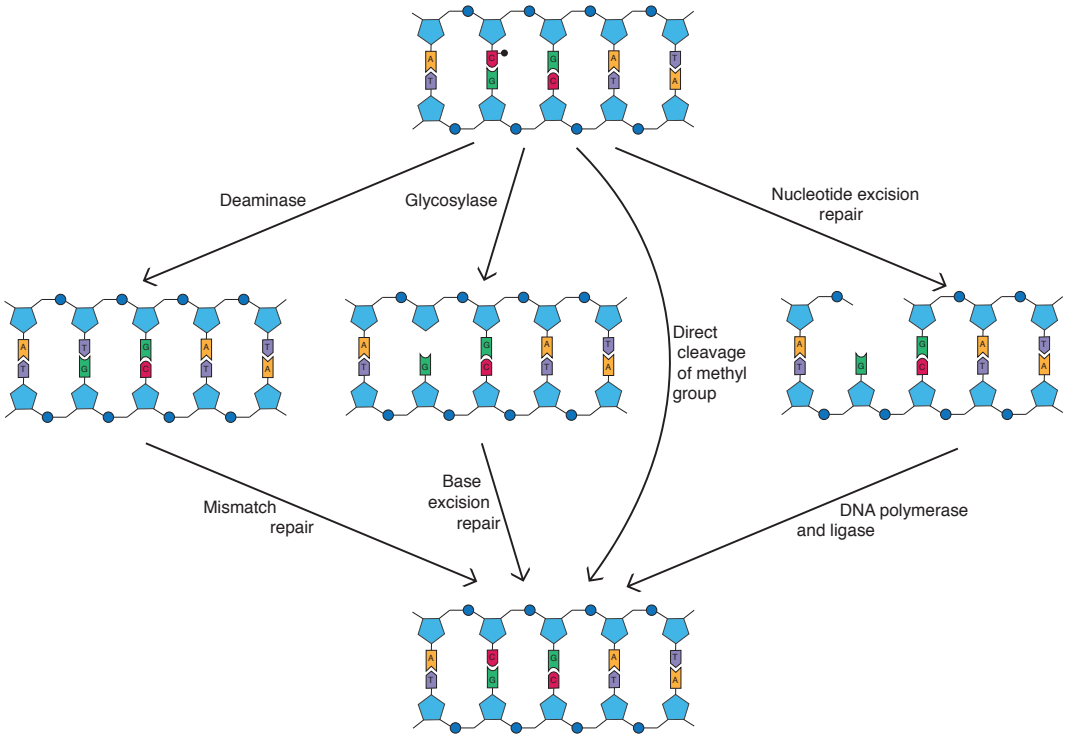

Figure 1.3: Potential DNA demethylation mechanisms

It remains unclear how DNA demethylation occurs in mammalian systems. Potential mechanisms are presented here along with a diagrammatic representation of the changes being described. Firstly methyl-cytosine could be deaminated to thymidine, which would then be detected and replaced by the mismatch repair pathway. Alternatively, the methyl-cytosine base could be excised by a glycosylase followed by replacement of cytosine by the base excision repair pathway. Another possibility, though highly chemically unlikely, is that the methyl group may be directly cleaved from the cytosine base. Finally, the entire methyl-cytosine nucleotide could be excised by the nucleotide excision repair pathway and replaced by the actions of DNA polymerase and ligase.

on DNA methylation, often in conjunction with Southern blotting to detect the methylation level in specific genes such as ApoAI (Shemer *et al.*, 1990). This is a very sensitive and accurate technique but requires large quantities of input DNA and a specific probe for the region of interest. In addition a restriction site needs to be present in the region of interest, which can limit the regions to be examined. Methyl-sensitive restriction digestion can also be used in a genome-wide manner to perform a variant of restriction landmark genomic scanning (Takamiya *et al.*, 2006) or in combination with ligation mediated PCR (Khulan *et al.*, 2006). These techniques can be used to highlight a substantial number of differentially methylated regions within the genome but are not truly 'genome-wide' as they are only interrogating methylation within the restriction sites used.

The alternative approach to direct identification of methylated DNA involves immunoprecipitation of the methylated DNA fraction using anti-5mC antibodies (Weber *et al.*, 2005) or methyl-CpG binding domain based proteins (Gebhard *et al.*, 2006). Initially the methylated and unmethylated DNA fractions were compared by hybridisation to arrays, either specifically interrogating known CGIs or on whole genome tiling arrays (Wilson *et al.*, 2006). More recently, direct sequencing of the methylated fraction has been employed (Down *et al.*, 2008) allowing a more thorough analysis. One major advantage of this method is that it can be performed in parallel with ChIP, allowing analysis of the overlap between DNA methylation and chromatin marks in identical samples. This approach has been used to determine that CGIs which are susceptible to methylation in prostate cancer cell lines are characterised by the presence of a H3K27me3 modification whilst those which are resistant to methylation are characterised by H3Ac, H3K4me3 and the presence of RNA polymerase II (Takeshima *et al.*, 2009). This pattern was maintained in breast cancer cell lines even though the subset of

methylation susceptible CGIs was substantially different between the two tissues, suggesting a possible mechanistic role in malignancy associated hypermethylation. The main limitation of these techniques is the affinity and specificity of the proteins used to isolate methyl-DNA, which can introduce a bias by isolating fractions only within a specific range of CpG densities (Robinson *et al.*, 2010).

Bisulphite conversion based techniques rely on the use of sodium bisulphite to add a sulphate group to cytosine under acidic conditions, encouraging hydrolytic deamination of the cytosine sulphonate to uracil sulphonate. However, the methyl group of 5mC protects the amino group from deamination leaving all 5mC residues unaffected (Figure 1.4). During re-purification of the DNA it is subjected to alkaline desulphonation leaving uracil residues at each position that was previously an unmethylated cytosine (Frommer *et al.*, 1992). Bisulphite conversion carries the risk of DNA degradation and incomplete conversion if not optimised and controlled properly however it does offer the opportunity to acquire extensive methylation data by detecting unmethylated C as a C→T polymorphism in downstream analysis. A popular technique for assessing methylation is methylation specific PCR (MSP), which uses primers specific to the bisulphite converted methylated sequence to detect methylated DNA and primers specific to the bisulphite converted unmethylated sequence to detect unmethylated DNA (Herman *et al.*, 1996). This is a very sensitive technique that can be used to detect a small proportion of methylated DNA within an unmethylated background but it is limited by primer design, which can cover only a few CpG dinucleotides each. One solution to this is to use bisulphite specific primers for PCR then subject the amplicon to high resolution melt analysis (Wojdacz & Dobrovic, 2007). The melting temperature will be affected by the C/T content of the amplicon and thus reflects the overall methylation of the amplicon but gives no information on the individual CpG dinucleotides.

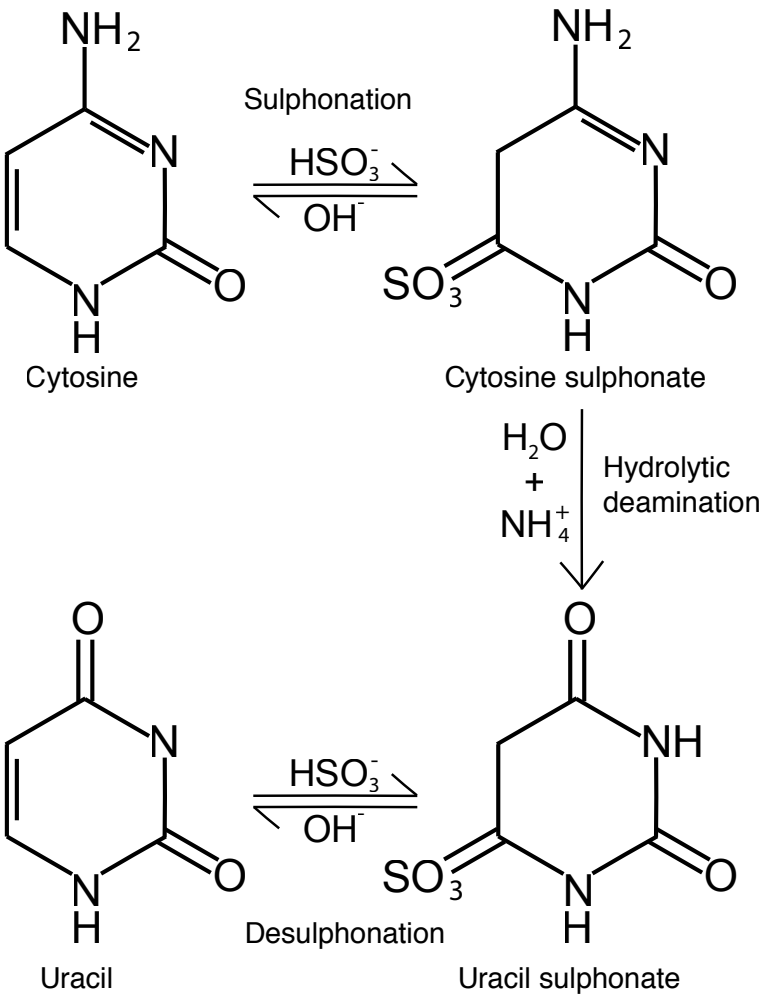

Figure 1.4: Mechanism of bisulphite conversion

Chemical structures showing the stages of bisulphite conversion. The sulphonation reaction cannot proceed in the presence of a methyl group on the cytosine base.

The most comprehensive method of downstream analysis is to sequence the bisulphite converted DNA, allowing examination of the whole CGI. Direct sequencing of bisulphite converted DNA is possible if the original sample is expected to have homogeneous levels of DNA methylation but if a mixed population of input cells has been used it is necessary to clone the bisulphite converted DNA and sequence a number of clones in order to determine the percentage of cells with 5mC at each CpG dinucleotide. Pyrosequencing, a sequencing by synthesis technique, enables quantitation of the proportions of each base present at a polymorphic site (Tost *et al.*, 2006). Pyrosequencing of bisulphite converted DNA therefore enables the proportion of DNA methylated at each CpG site within a CGI to be measured, which is useful when measuring DNA methylation in a mixed population of cells. With the reduction in cost and increase in availability of next-generation sequencing technologies, whole genome bisulphite sequencing represents an approach with the potential to generate huge volumes of DNA methylation data. However, the bisulphite conversion step reduces the complexity of the DNA sequence making the short read data generated by these technologies difficult to map to a reference genome (Xi & Li, 2009). Although still in the early stages of development, third-generation single molecule sequencing has the potential to circumvent these issues, generating read lengths in excess of 100bp and possibly much longer (Schadt *et al.*, 2010). In addition to this, nano-pore based sequencing can innately detect the difference between methylated and unmethylated cytosine (Wallace *et al.*, 2010), thus promising to remove the requirement for any manipulation of DNA prior to detection of methylation at some point in the future.

1.2.4 DNA methylation in T-cells

The importance of DNA methylation to the development of T-cell lineages was first shown in 1986 when it was observed that treatment of CD8+ T-cells with the methylation inhibitor 5-aza-2'-deoxycytidine (5aza) led to the expression of CD4 on their surface (Richardson *et al.*, 1986), suggesting that DNA methylation is responsible for silencing the CD4 antigen in CD8+ T-cells. By contrast, treatment of CD4+ T-cells with 5aza did not lead to any alteration in the cell surface marker phenotype however the previously antigen-specific cells did become self-reactive, a change that could be blocked using anti-CD3 (Richardson, 1986). Interestingly, both CD4+ and CD8+ T-cells developed thymocyte-like features upon treatment with 5aza suggesting that DNA methylation is crucial to the progression of T-cell maturation. Further supporting this theory, mature T-cells were found to contain a significantly greater proportion of 5mC than thymocytes (Golbus *et al.*, 1990). Selective inactivation of DNMT1 at different stages of thymocyte development in a transgenic mouse model led to substantial changes in their T-cell differentiation (Lee *et al.*, 2001). DNMT1 knockout in double-negative thymocytes led to a decreased proportion of TCR$\alpha\beta$ cells and an increased proportion of TCR$\gamma\delta$ cells that aberrantly expressed CD8. DNMT1 knockout in double positive thymocytes did not affect the number or proportion of CD4+TCR$\alpha\beta$, CD8+TCR$\alpha\beta$ or TCR$\gamma\delta$ cells but it did generate a reduced proportion of memory T-cells. This was due to reduced activation induced proliferation and increased cytokine mRNA expression in the naïve T-cells of these mice.

T-cells taken from patients with the autoimmune disease systemic lupus erythematosus have been found to display global hypomethylation when compared to healthy T-cells (Richardson *et al.*, 1990). In addition, the drugs hydralazine and procainamide, which have been observed to initiate a lupus-like autoimmune disease in some patients, have been shown to act by inhibition of DNA methylation (Cornacchia *et al.*, 1988) and

treatment of activated murine CD4+ T-cells with DNMT inhibitors prior to adoptive transfer into syngeneric recipients induces a lupus like disease (Quddus *et al.*, 1993). These observations suggest that hypomethylation of T-cells induces changes in gene expression that are sufficient to substantially alter the functional role of the T-cells. Fascinatingly, a more recent study (Zhao *et al.*, 2011) suggests that over-expression of miR-126 in CD4+ T-cells from lupus patients is responsible for down-regulation of DNMT1 expression, contributing to the observed hypomethylation. Thus, targeted down-regulation of miR-126 may have potential as a mechanism to reverse the hypomethylation and restore the T-cells to their original state.

Several genes critical to T-cell lineage commitment have been investigated with respect to DNA methylation and two examples have been chosen here to highlight the variety of regulatory mechanisms that DNA methylation can induce. Rapid induction of IL-2 expression is observed upon the activation of naïve T-cells: the secretion of IL-2 initiates a signalling pathway leading to rapid proliferation of the activated T-cells (Smith, 1984). Concomitant with this induction, CpG dinucleotides 2-6 in the IL-2 promoter become rapidly demethylated, an alteration which is sufficient to enhance IL-2 expression in an IL-2 promoter driven reporter construct (Bruniquel & Schwartz, 2003). Of note, demethylation was observed within seven hours of T-cell activation whilst 48 hours was required to observe any cell division. In addition, blocking of the cell cycle with rapamycin did not prevent demethylation, strongly suggesting that an active demethylation process is being observed.

T_h1 or T_h2 polarisation is induced by the cytokine milieu present during antigen presentation by dendritic cells (Kapsenberg, 2003). Polarisation induces the expression of a 'master regulator' transcription factor, T_{bet} for T_h1 (Szabo *et al.*, 2000) and GATA3 for T_h2 (Zheng & Flavell, 1997), driving expression of the relevant cytokines.

The T_h2 cytokines IL-4, IL-13 and IL-5 are coordinately regulated by the CNS-1 element (Loots *et al.*, 2000). In naïve T-cells the IL-4 promoter and intron 1 are 70% methylated whilst the CNS-1 is 90% methylated allowing only basal levels of IL-4 transcription (Makar *et al.*, 2003). Upon T_h2 polarisation the IL-4 promoter and intron 1 become hypomethylated within four days whilst the CNS-1 becomes hypomethylated over a week later (Lee *et al.*, 2002). Since IL-4 expression is induced within hours and the rate of demethylation is relatively slow, in this case passive demethylation through non-recruitment of DNMT1 to the replication fork is likely to be responsible and hypomethylation is being used to maintain rather than initiate the change in expression.

More recent studies have begun to use high throughput methods to define characteristic patterns of DNA methylation in T-cells. Examination of 27,458 CGIs revealed that only 5% were methylated in primary human CD4+ T-cells (Hughes *et al.*, 2010). In addition 388 genes were identified that had a methylation peak within -5kb and +1kb of the transcriptional start site. Of these, 72.8% were not expressed and functional network analysis revealed these genes to be involved in antigen presentation and immune response. The genes that were expressed despite the presence of a DNA methylation peak were observed to be involved in cellular signalling and proliferation. The majority of these genes were also found to have a *DNase*I hypersensitivity site spanning the transcriptional start site, suggesting that the chromatin remained accessible despite the presence of DNA methylation. Comparison of CD4+CD25^{high} T_{reg} cells to CD4+CD25- conventional T-cells using an array targeting genes that were differentially expressed between the two cell types revealed 132 regions of lineage-specific methylation associated with 53 genes (Schmidl *et al.*, 2009). Interestingly only seven of these overlapped with the transcriptional start site of a gene, including FOXP3 the major transcriptional regulator of T_{reg} cells (Fontenot *et al.*, 2003), whilst the remainder were located within gene bodies or intergenic regions. It was further determined

that a proportion of these regions showed enhancer activity that could be prevented by methylation suggesting a key functional role for gene distal methylation.

1.2.5 DNA methylation in lymphoma

DNA methylation anomalies are frequently described in malignancy and associated with all stages of tumour formation and progression (Baylin & Ohm, 2006). Aberrant DNA methylation often affects genes associated with the DNA repair and cell cycle checkpoints (Toyota *et al.*, 2009), thus releasing cells from normal growth control and increasing the rate of genetic mutations. Since correct formation and maintenance of DNA methylation is vital to the development of different T-cell lineages it is expected that disruption of DNA methylation in T-cells could lead to errors in the stability of T-cell subsets and hence the delicate balance of the immune system.

Hypermethylation of the cell cycle regulators p15 and p16 is a feature common to haematological malignancies (Herman *et al.*, 1997) and has also been repeatedly characterised in CTCL (Gallardo *et al.*, 2004, Navas *et al.*, 2000, Scarisbrick *et al.*, 2002). Other genes in which silencing by promoter methylation has been characterised in CTCL include MLH1 (Scarisbrick *et al.*, 2003) and SHP-1 (Zhang *et al.*, 2000). MLH1, a DNA mismatch repair gene, was investigated in patients showing micro-satellite instability and found to show promoter hypermethylation in 9/14 cases. In five of these, promoter hypermethylation correlated with abnormal MLH1 expression suggesting that this might contribute to micro-satellite instability. SHP-1, a tyrosine phosphatase was found to have evidence of promoter hypermethylation in the HuT78 cell line associated with a lack of mRNA or protein. Since an inhibitor of methylation restored expression, loss of SHP-1 can be attributed to promoter hypermethylation in this cell line however studies of SHP-1 methylation in primary malignant cells taken from lymphoma patients showed mixed results as discussed further in Section 3.1.

Global DNA methylation analysis of 367 haematological malignancy samples revealed that lymphoid malignancies are associated with higher levels of DNA methylation than myeloid malignancies and that DNA hypermethylation was particularly prevalent in malignancies of lymphoid precursor cells (Martin-Subero *et al.*, 2009). DNA hypomethylation was also observed with 108 genes hypermethylated and 47 genes hypomethylated across the T-cell lymphomas examined. Only one study has used an array to examine methylation of CGIs within CTCL samples. This identified 35 genes whose promoters were hypermethylated in at least 4 of 28 MF samples (van Doorn *et al.*, 2005) when compared to healthy T-cells. Bisulphite sequencing was used to confirm the presence of hypermethylation in BCL7a, TPTRG, THBS4, p15, p16, p73, MGMT, TMS1 and CHFR. Further to this, demethylation of the MyLa cell line with 5aza was demonstrated to reactivate expression of BCL7a and PTPRG. However, the array used in this study only interrogated 8640 CGIs thus missing a proportion of potentially informative CGIs and no SS samples were included.

1.3 Aims of the thesis

It is clear that a myriad of molecular defects contribute to the malignant transformation of skin-homing T-lymphocytes in SS and MF. The integration point of these defects is the T-cell signalling pathways which, through constitutive activation or signalling blockade, combine to generate a population of T-cells that proliferate only slowly but are resistant to apoptosis. Whilst extensive gene expression and genomic studies have been performed to delineate the mechanisms leading to dysregulation of T-cell signalling pathways, limited investigation of the role of DNA methylation has been performed. Therefore, the aim of this thesis was to investigate the contribution of DNA

methylation to the regulation of three genes with potentially central roles in dysregulation of T-cell signalling. A target gene approach was chosen in order to enable the investigation of CGI methylation in greater detail than is possible using high throughput methods. The genes chosen for investigation were: SHP-1, silencing of which could contribute to constitutive STAT3 activation; Fas, silencing of which could contribute to reduced AICD; and PLS3, re-expression of which could contribute to disruption of cytoskeletal rearrangements at the immunological synapse. Each gene contains a CGI upstream of or spanning the transcriptional start site and was not included in the DNA methylation arrays used by van Doorn *et al.* (2005) (Heisler *et al.*, 2005). Further background to the individual genes is provided in Sections 3.1, 4.1 and 5.1.

Materials and methods

2.1 Collection and processing of samples

All patient samples were obtained from a national approved research tissue bank (07/H10712/106) of cutaneous lymphoma samples. For all samples, informed consent was obtained in accordance with the declaration of Helsinki 1975 as revised in 2005. Blood and tissue samples were obtained from consenting patients during the course of standard clinical procedures. Healthy blood samples were obtained from volunteers with project-specific approval from the Guy's and St. Thomas' hospital research ethics committee (EC01/301) or through the national blood service.

All patients fulfilled the WHO-EORTC diagnostic criteria for CTCL (Willemze *et al.*, 2005). T-cell clonality was assessed in blood and tissue samples using TCRVβ and γ gene rearrangement studies with BIOMED-2 primer sets (van Krieken *et al.*, 2007). For each sample, total lymphocyte and lymphocyte subset counts were recorded at the time of sampling as an indicator of circulating tumour burden. For SS patients the percentage of Sézary cells in the lymphocyte population was counted in blood smears by one expert investigator at regular intervals but not alongside each sample.

Tissue samples were bisected and half was formalin fixed and paraffin embedded (FFPE) prior to immunohistochemical analysis for diagnostic purposes. FFPE blocks were then stored in the tissue bank for future research use. DNA was extracted from the remaining half of each tissue section prior to TCR gene rearrangement studies. Any remaining DNA was then deposited in the tissue bank.

Blood was collected into EDTA vacutainers prior to Lymphoprep (Axis-shield, Kimbolton, UK) gradient centrifugation to isolate PBMCs. To isolate CD4+ T-cells, blood was incubated with RosetteSep CD4+ T-cell enrichment cocktail (Stem Cell

Technologies, London, UK) prior to Lymphoprep gradient centrifugation. Negative selection was chosen as an isolation method in order to avoid activating the cells during processing, which could potentially cause changes in gene expression. Isolated PBMCs or CD4+ T-cells were suspended at 1×10^6 cells/ml in freezing medium of 90% FCS (Invitrogen Ltd., Paisley, UK) and 10% DMSO (Sigma Aldrich, Dorset, UK) then stored under liquid nitrogen until required.

2.2 Cell culture

Cell stocks were resuscitated from liquid nitrogen storage a few weeks prior to use. The SS cell lines HuT78 and SeAx, MF cell line MyLa and leukaemic cell line Jurkat were maintained in RPMI (Invitrogen) supplemented with 10% FCS (Invitrogen) and 1×penicillin/streptomycin (Invitrogen). SeAx cells were additionally supplemented with 25U/ml IL-2 (Invitrogen). HEK293 (human embryonic kidney) cells were maintained in D-MEM (Invitrogen) supplemented with 10% FCS (Invitrogen) and 1×penicillin/streptomycin (Invitrogen). Cells were passaged every 3-4 days up to a maximum of 25 passages. Kit225, HeLa and primary keratinocytes and fibroblasts were generously provided by colleagues as a cell pellet prior to lysis.

2.3 Extraction of RNA

Pelleted cells were lysed in buffer RLT from the RNeasy mini kit (Qiagen Ltd., Crawley, UK) then homogenised using a QIAshredder column (Qiagen). RNA extraction was completed using the RNeasy mini kit (Qiagen) according to the manufacturers instructions. RNA concentration was measured using the Nanodrop-1000 (Thermo Scientific, Epsom, UK). FACS sorted cells that had previously been subject to fixation were digested with proteinase K in Buffer PKD from the RNeasy FFPE kit (Qiagen)

for 15 min at 55°C followed by 15 min at 80°C in order to release the RNA from the cross linked protein matrix. RNA extraction was completed using the RNeasy FFPE kit (Qiagen).

2.4 Generation of cDNA

The high capacity cDNA archive kit (Applied Biosystems, Warrington, UK) was used to generate randomly primed cDNA from up to 1μg of RNA in a 20μl reaction according to the manufacturers instructions then reverse transcription PCR (RT-PCR) using primers against the housekeeping gene Cyclophilin was performed as described in Section 2.5 to check for successful generation of cDNA prior to further use of the cDNA.

2.5 Reverse transcription PCR

RT-PCR was performed in 25μl reactions containing GeneAmp PCR Buffer II, 0.4mM each primer, 1.5mM $MgCl_2$, 0.2mM each dNTP and 0.625U of AmpliTaq Gold DNA Polymerase (Applied Biosystems). All primers were ordered from MWG (Ebersberg, Germany) and annealing temperature (T_a) was optimised for each primer pair from a starting point of 5°C below the calculated melting temperature (T_m). PCR cycles were performed in a GeneAmp 9700 thermal cycler (Applied Biosystems) and comprised 10 min initial denaturation at 95°C followed by 25-35 cycles of 30 sec denaturation at 95°C, 30 sec annealing at the relavent T_a and 60 sec extension at 72°C, reactions were completed with a 5 min final extension at 72°C followed by holding at 4°C. Primer details and T_a for each primer set used are provided in Table 2.1. PCR products were electrophoresed through a 1.5% agarose gel and visualised using ethidium bromide. Each set of reactions included a negative control containing water instead of cDNA

Assay	Primer sequences	Size/bp	T_a/°C
SHP-1 total	GACTGTGACATTGACATCCAG	350	52
	CTTCCTCTTGAGGGAACCCTT		
SHP-1 isoform I	TGGCTTCCCCCTCCCTACAGAGA	179	60
	GTCACCTGATCCCCCACCCTGACG		
SHP-1 isoform II	CCCCCAGGATGGTGAGGTGGTT	157	60
	GTCACCTGATCCCCCACCCTGACG		
PLS3	TAAGGACAAGACGATCAGCTCC	495	55
	TATGAGCACATTTCAGGCGTGC		
Fas	ACTGCGTGCCCTGCCAAGAAG	186/295	56
	AAGACAAAGCCACCCCAAGTTAGA		
Cyclophilin	AAAGCATACGGGTCCTGGCATC	223	55
	CGAGTTGTCCACAGTCAGCAATG		

Table 2.1: RT-PCR primer details

and if available a known positive control.

2.6 Quantitative PCR

Real-time quantitative PCR (qPCR) was performed on the ABI Prism 7000 (Applied Biosystems) using the manufacturers recommended cycling profile of 10 min initial denaturation at 95°C followed by 15 cycles of 15 sec denaturation at 95°C and 60 sec annealing and extension at 60°C. The following optimised TaqMan probe/primer sets were used: Hs00192406_m1 - PLS3; Hs00236330_m1 - Fas and Hs99999904_m1 - Cyclophilin in combination with TaqMan gene expression master mix (Applied Biosystems) and cDNA generated from 50ng RNA in each 25μl reaction. Each sample was analysed in triplicate for both the target gene and an endogenous control (Cyclophilin). Target and control genes were measured on the same plate to reduce run-to-run variability and a non-template control substituting water for cDNA was included on each plate for each TaqMan probe/primer set. ΔCt calculations were used to normalise expression level in each sample relative to expression of the endogenous control whilst $\Delta\Delta$Ct calculations were used to present patient expression as a fold change relative to

the average of the healthy control group. No TaqMan probe/primer sets were available that could discriminate between the isoforms of SHP-1 so isoform-specific primer sets, listed in Table 2.1, were used at 0.3mM each primer in combination with SYBR Green PCR master mix (Applied Biosystems) to enable quantitation. PCR cycles were the same as used for TaqMan probe/primer sets with the addition of a melting curve analysis upon completion of the cycles to confirm the absence of non-specific amplification. Serial dilution of one sample was first used to ensure that the efficiency of amplification from each primer set was close to 100%.

2.7 Extraction of DNA

Pelleted cells were lysed in nuclei lysis buffer (Promega, Southampton, UK) and digested with proteinase K (Promega) for 24 hours. Proteins were removed using protein precipitation solution (Promega) prior to isopropanol precipitation of the DNA. The DNA pellet was then washed in 70% ethanol and finally resuspended in MilliQ water. DNA concentration was measured using the Nanodrop-1000 (Thermo Scientific). For extraction from FACS sorted cells where a low yield of DNA was expected, GenElute-LPA (Sigma Aldrich) was added prior to isopropanol precipitation to act as a carrier and help visualise the DNA pellet.

2.8 Generation of DNA with known methylation

For each CGI investigated, methylation level was first determined in a selection of cell lines in order to find a completely unmethylated control. An aliquot of DNA from the relevant cell line was then *in vitro* methylated in order to generate a completely methylated DNA control. 1μg DNA was incubated with 4U *M.Sss*I CpG methyltransferase enzyme (New England Biolabs, Hitchin, UK) in NEBuffer 2 (New England Biolabs)

supplemented with 160μM S-adenosylmethionine (New England Biolabs) for 4 hours at 37°C followed by heat inactivation at 65°C for 20 min. The completely methylated DNA was then isolated from the reaction mixture using a DNA clean and concentrator column (Zymo Research, Orange, CA) and mixed in varying proportions with the unmethylated DNA to create mixtures of known methylation level.

2.9 Bisulphite conversion of DNA

DNA was bisulphite treated in 10μl aliquots containing 500ng DNA using the EZ DNA methylation kit (Zymo Research) according to the manufacturers instructions. Following elution the converted DNA was made up to a total volume of 100μl in TE buffer (Sigma Aldrich).

2.10 Methylation specific PCR

Bisulphite converted DNA was amplified using the previously published (Oka *et al.*, 2002) primers. PCR was performed in 25μl reactions containing GeneAmp PCR Buffer II, 0.5mM each primer, 1.5mM $MgCl_2$, 0.25mM each dNTP, 0.625U of AmpliTaq Gold DNA Polymerase (Applied Biosystems) and 200ng bisulphite converted DNA. Cycles used were as described for RT-PCR in Section 2.5, primer details and T_a are listed in Table 2.2. Products were electrophoresed through a 2% agarose gel and visualised using ethidium bromide. Reactions with MSP and unmethylation specific PCR (USP) primers were performed concurrently for each set of samples and each PCR included completely methylated, completely unmethylated and negative controls.

Assay	Primer sequences	Size/bp	T_a/°C
SHP1MSP	GAACGTTATTATAGTATAGCGTTC	158	60
	TCACGCATACGAACCCAAACG		
SHP1USP	GTGAATGTTATTATAGTATAGTGTTTGG	161	60
	TTCACACATACAAACCCAAACAAT		

Table 2.2: Primers used for MSP

2.11 Pyrosequencing to measure DNA methylation

PCR using primers specific for the bisulphite treated DNA (Table 2.3) was performed on 50ng of the converted DNA. Reactions were performed in a total volume of 50μl containing GeneAmp PCR Buffer II, 0.2mM F and R primers, 0.2mM each dNTP, 1.5mM $MgCl_2$ and 1.25U of AmpliTaq Gold DNA Polymerase (Applied Biosystems). PCR cycles were performed in an GeneAmp 9700 thermal cycler (Applied Biosystems) and comprised 10 min initial denaturation at 95°C followed by 35 cycles of 30 sec denaturation at 95°C, 30 sec annealing at the relevant T_a and 2 min extension at 66°C, reactions were completed with a 5 min final extension at 66°C followed by holding at 4°C. Annealing temperature was optimised for each primer pair from a starting point of 5°C below the T_m. For the PLS3 primers a touchdown approach was found to be optimal therefore over 10 cycles the T_a was sequentially reducing from 62°C to 52°C followed by 25 cycles at 52°C. 10μl of each PCR product was electrophoresed through a 1.5% agarose gel and visualised using ethidium bromide to check for a good yield of product of the expected size.

In each assay either the forward or reverse PCR primer was biotinylated (denoted by bF or bR in Table 2.3) allowing the PCR product to be immobilised by incubation with 3μl streptavidin sepharose HP beads (GE Healthcare UK Ltd., Little Chalfont, UK) in binding buffer (Biotage AB, Uppsala, Sweden). A vacuum prep workstation (Biotage) was used to capture the beads with immobilised PCR product from a 96 well plate onto filter probes. After washing in 70% ethanol the complementary strand

Assay	Primer sequences	Size/bp	T_a/°C
S1-bF, S2-bR	TGTTTTATAGGGTTGTGGTGAGA	223	61
	CTCCAAACCCAAATAATACTTCA		
F5.6-bF, F7-bR	GGGATAGGAATGTTTATTTGTGTA	272	60
	CCTAAAACTCCAACCAAATCACTC		
F8-bR, F9-bF	GAGTGATTTGGTTGGAGTTTTAG	181	57
	AAATCCAAATACCCAACATAATTA		
F10.11.12.13-bR	AATTATGTTGGGTATTTGGATTTT	394	57
	ACCCTAAAACTTCCCAAACTTC		
F14-bF	TTGTTTTTTTTGGGTTTTGATG	422	62
	ACTCATTCAACCCCCATATAACT		
F15.17-bR, F16-bF	GGGGATTTTGGTTGGAGAG	263	62
	CATTCAACCCCCATATAACTTTT		
PLS39599F-bF	TGGAGTGGGGGTTAATGGTAT	205	Bisulphite
PLS39599R-bR	CCTCCCAATCCCTCTTAACAAA		touchdown

Table 2.3: Primers used for PCR prior to Pyrosequencing

was removed by denaturation in 0.2M NaOH and the resultant single stranded PCR product washed in a neutralising buffer (Biotage). Beads with bound single stranded PCR product were then deposited into a Pyrosequencing plate (Biotage) pre-filled with 3.6μmol of sequencing primer diluted in annealing buffer (Biotage). The plate was heated to 80°C and allowed to cool to room temperature in order to anneal the sequencing primer. The Pyrosequencing reaction was carried out using a PSQ HS 96 machine (Biotage) following the manufacturers instructions for methylation analysis.

2.12 Sequencing

PCR was carried out in a total volume of 50μl containing GeneAmp PCR Buffer II, 0.4mM each primer, 1.5mM $MgCl_2$, 0.2mM each dNTP and 0.625U of AmpliTaq Gold DNA Polymerase (Applied Biosystems) using the primer sets and annealing temperatures described in Table 2.5. Cycles were as described for RT-PCR in Section 2.5. Touchdown cycles were used for many of the primer sets, this comprised 10 cycles where the T_a was sequentially reducing from 62°C to 52°C followed by 25 cycles at

Assay	Primer sequence	T_m/°C
S1	CCTCCACCAACTACTTTT	51.8
S2	GGAGGAGGGAGAGATG	52.5
F5	AATTCAACAACTTAACCTAC	47.9
F6	AAACACCTATATATCACTCT	44.5
F7	TGATATATAGGTGTTTAAAG	44.0
F8	GGTTGGAGTTTTAGGGG	54.6
F9	CATAATTATTAAACAATCCT	54.8
F10	GGTATTTGGATTTTTTTATT	49.8
F11	GGGGATAGGTAAAGTG	46.9
F12	GTTGGAGATTGGTTT	44.5
F13	TTTTTTTTGGGTTTTGA	51.7
F14	CAAAACTTATCCAAAAATTC	51.1
F15	TTTGATAAGTTAAGTTAAA	42.0
F16	CCCCCATATAACTTTTTC	51.3
F17	GTAGGAAATAAGTTAGTAT	39.2
PLS39599SF	TTAAGTGGGTTGGAGAGT	51.4
PLS39599SR	AATCCCTCTTAACAAACC	49.1

Table 2.4: Sequencing primers used in Pyrosequencing

52°C. 10μl of each PCR reaction was electrophoresed through a 1-1.5% agarose gel to check for the presence of a single unique band of the expected size. The remaining 40μl of PCR product was purified through a clean and concentrator 5 column (Zymo Research) and sent for sequencing (Geneservice, London, UK) using the original PCR primers. Data were examined using Geneous (Drummond *et al.*, 2011) with a 25% peak height similarity cut off to detect potential mutations.

2.13 Single strand conformational polymorphism

PCR for single strand conformational polymorphism (SSCP) analysis was performed with primer pairs described by Beltinger *et al.* (1998) designed to amplify all nine exons and the 3' end of the promoter. PCR products were labeled by substituting α-^{33}PdCTP for a proportion of the dCTP in the dNTP mixture. PCR products were denatured for 10 min at 95°C then rapidly cooled prior to electrophoresis through non-denaturing polyacrylamide gels containing both 5% glycerol and no glycerol. Gels

Assay	Primer sequences	Size/bp	T_a/°C
PLS3mRNA2	GATTCCGAGGTGCAGAAGTT	400	Touchdown
	GAGCACAAATACCTTCTTTCCTG		
PLSmRNA5b	AAACTCATGCTGGATGGTGA	424	55
	CCAAGTTCAAGTTTTCCTGA		
PLS3mRNA7	GAAAGAGCAATCAACAAGAAGAAAC	401	Touchdown
	CCTTTTGGTGCGATTTGATT		
PLS3mRNA9	ATTTGGAAAACTCGGGCTGG	400	Touchdown
	TTGACACCAAGAGAGTTCATCC		
PLS3mRNA12	GAAACTCGTGAAGAAAGAACCTT	403	Touchdown
	TGTTCACCCAGTTCACAATGA		
PLS3mRNA15	TCAATGTCCTGGAAGATCTTGG	475	Touchdown
	AATGGCCAAGAGTTCCTTAAGC		
PLS3mRNA16	ATGATTCGCAGGTCAGCTAT	453	Touchdown
	CGGCAAATTTTCAGTACTAC		
PLS3mRNA17	ATGAGTATCCTTTGCTTATC	504	Touchdown
	CATTTCTTTGTTTCAGGTGT		
PLS3CGIT1	TTATTTTTTTTGGGTGTTTAT	263	Failed to
	CAAAATCCTAAATCTAACCC		optimize
PLS3CGIT2	AGTGGGGGTTAATGGTATTTGAT	204	Bisulphite
	TCCTCCCAATCCCTCTTAACA		touchdown
PLS3CGIT9	TGGTTTTAGAGTTATAGTTGTAAA	418	Bisulphite
	ACCCAAAACTAACAACAAATT		touchdown
PLS3CGIT12	TTAGTTTTGGGTTGGAGTTTTAGA	531	Failed to
	TTTACCTCTCTCTCTCCAAAAATC		optimize
PLS3PROPCR1	TCCCTCAAACTCTGGCTCTC	999	55
	GGCGCCTACAAAGCACTTAC		
PLS3PROPCR2	TCGGACCAATGTAAGCTTTTT	965	55
	GAGAGCCAGAGTTTGAGGGA		

Table 2.5: Primer pairs for PLS3 mRNA and promoter sequencing

were dried on to 3-mm Whatman paper and exposed to X-ray film to visualise the bands. A negative control substituting water for the DNA was performed for each primer pair. DNA from healthy individuals was used as a positive control.

2.14 Extraction of whole cell lysates

7×complete mini protease inhibitor and 10×complete mini phosphatase inhibitor cocktails (Roche) were prepared from tablets once every three months and kept at -20°C. RIPA lysis buffer (Santa Cruz Biotechnology Inc., Santa Cruz, CA) was supplemented

with protease and phosphatase inhibitors immediately prior to cell lysis using 1ml of complete RIPA buffer per 2×10^7 cells. After one hour of disruption on ice the lysate was centrifuged to remove solid debris. Protein concentration was colourimetrically assessed using the bicinchoninic acid kit (Sigma Aldrich) and measured on the Nanodrop-1000 (Thermo Scientific).

2.15 Western blotting

Whole cell lysates containing 5μg protein were denatured by boiling with Laemmli sample buffer (Bio-Rad Laboratories, Hemel Hempstead, UK) for 5 min at 95°C then loaded onto an 8% PAGE gel. After electrophoresis the proteins were transferred to PVDF membrane using the XCell II blot system (Invitrogen). Blots were blocked in 3% BSA/0.1% Tween/PBS or 1% Marvel/0.1% Tween/PBS and then sequentially incubated with optimised dilutions of primary antibody (see Table 2.6) and HRP-conjugated anti-mouse or anti-rabbit secondary antibody at 1 in 10,000 (Abcam, Cambridge, UK). Chemiluminescent visualisation was performed using the ECL plus Western blotting detection system (GE Healthcare) followed by exposure to X-ray film. Precision plus protein WesternC standards (Bio-Rad) were included on each gel to enable monitoring of the gel running and transfer. Biotin-linked HRP (Bio-Rad) was added at 1 in 10,000 to the secondary antibody dilution to enable visualisation of the molecular weight marker via the integrated Strep-tag.

2.16 Anti-PLS3 antibody generation

All stages of antibody production were completed by Cambridge Research Biochemicals (Billingham, UK). An antigenic peptide unique to PLS3 (Ac-MATTQISKDELDE-LKC-amide) was synthesised and used to immunize two rabbits six times at two-week

Target	Dye	Isotype	Manufacturer	Dilution
SHP-1	Unconjugated	Rb pIgG	Atlas Antibodies	1 in 5000
pSTAT3	Unconjugated	Mo mIgG1	NEB	1 in 1000
STAT3	Unconjugated	Mo mIgG2a	NEB	1 in 1000
CD45RO	PacificBlue	Mo mIgG2a	Biolegend	1 in 50
Fas	PE	Mo mIgG1	BD Bioscience	1 in 20
CD4	PE-TexasRed	Mo mIgG2a	Caltag	1 in 50
CD25	PE	Mo mIgG1	ebioscience	1 in 30
CD26	APC	Mo mIgG2a	Miltenyi	1 in 10
CD3	PE-Cy7	Mo mIgG1	ebioscience	1 in 50
CD7	PE-Cy5	Mo mIgG1	ebioscience	1 in 10
PLS3	DyLight488	Rb pIgG	CRB	1 in 50 for FACS 1 in 5000 for Western
CD158k	APC-Cy7	Mo mIgG2a	Dr. Bagot	1 in 100
β-actin	Unconjugated	Mo mIgG1	Abcam	1 in 5000

Table 2.6: Antibodies used for immunodetection

intervals. One week after each immunisation blood samples were taken and antibody titre was assessed by ELISA. After three months, antisera was harvested and subject to affinity purification on thiopropyl sepharose 6B derivatised with the antigen. Purified antisera was then eluted using both TEA and glycine. Serum from the final bleed was provided for testing along with the TEA and glycine purified eluates. An aliquot of the antigenic peptide was also provided and used as a blocking peptide when testing the antibody specificity.

2.17 Labelling of antibodies

The CD158k and PLS3 antibodies were fluorescently labelled prior to use in flow cytometry. Since the PLS3 antibody contained glycerol which interferes with the conjugation reaction, antibody was dialysed against PBS for 3×3 hours using a slide-a-lyzer mini dialysis device (Thermo Scientific) then returned back to its original concentration by dialysis against slide-a-lyzer concentrating solution (Thermo Scientific). The DyLight microscale antibody labelling kit (Thermo Scientific) was then used to label

100μg of antibody with DyLight 488. An isotype control was labelled alongside the specific antibody and fluorescence:protein ratio was calculated from A_{280} and A_{493} to confirm successful staining at similar molar ratios for both specific and isotype control. The quantity of CD158k antibody provided was insufficient for use in the DyLight microscale kit so the Lightning-Link APC-Cy7 kit (Innova Bioscience, Cambridge, UK) was used to conjugate APC-Cy7 to CD158k antibody and its isotype control according to the manufacturers instructions.

2.18 Staining for flow cytometry

Aliquots of frozen lymphocytes were thawed rapidly at 37°C, resuspended in pre-warmed RPMI (Invitrogen) then washed twice in PBS (Invitrogen) containing 2% FCS(Invitrogen) and 2mM EDTA (Sigma Aldrich) prior to incubation with the appropriate cocktail of antibodies from Table 2.6. SHP-1, pSTAT3 and STAT3 antibodies were visualised using Alexa Fluor 488 conjugated anti-mouse or anti-rabbit secondary antibody diluted to 1 in 1000 (Invitrogen). For intracellular staining, fixation in 1% paraformaldehyde (Sigma Aldrich) followed by permeabilisation in methanol (Sigma Aldrich) was required to allow the antibody to access its antigen. To ensure any non-viable cells were excluded from the analysis, cells were incubated with LIVE/DEAD fixable aqua dye (Invitrogen) prior to fixation. Prior to multi-parameter staining including both intracellular and cell surface antigens optimisation experiments were performed to investigate the effect of fixation on cell surface antigens. CD26 and CD158k antibodies were shown to be specific only when applied prior to fixation whilst CD3, CD4, CD45RO, CD7, and CD25 could be applied post fixation.

2.19 Flow cytometry analysis

Flow cytometry analysis was performed on a FACSAria II (BD Bioscience, Oxford, UK) and data were analysed using FlowJo software (Tree Star Inc., Ashland, OR). Each tube was first gated on the viable population of lymphocytes using either FSC/SSC, for live stained cells, or LIVE/DEAD fixable aqua dye for fixed cells. Gates were then defined using the isotype controls for each dye used then the stained tubes were gated by the population of interest to determine the percentage positive cells.

2.20 Fluorescence activated cell sorting

Cells were stained as described in Section 2.18 immediately prior to sorting and kept on ice during the procedure. Accudrop fluorescent beads (BD Bioscience) were used to set up the FACSAria II stream ready for sorting. Single stained control tubes were used to calculate the compensation matrix to account for spectral overlap between the fluorescent dyes. Data acquired from the isotype control and n-1 control tubes were used to set up sorting gates. Cells were sorted into tubes containing 1ml of PBS/2% FBS/2mM EDTA then pelleted prior to either RNA or DNA extraction as described in Sections 2.3 and 2.7.

2.21 Immunofluorescent staining

One PLS3 expressing patient and one healthy PBMC sample were used to test the use of the PLS3 antibody for immunofluorescent staining. 1×10^6 cells per well were dispensed into a 96 well plate which was then spun at 800g for 5 min to attach the cells to the bottom of the plate. Cells were then fixed and permeabilised using a range of

reagents prior to blocking and staining with anti-PLS3 or rabbit polyclonal isotype control. A DAPI counterstain was used to visualise the nuclei then the fluorescent staining was examined using a Zeiss Axio Observer Z1 inverted microscope. The final protocol, found to yield strong specific staining was fixation with 1% paraformaldehyde for 15 min followed by permeabilisation in ice cold methanol for 30 min. Following a brief wash in PBS/0.1% Tween, blocking was performed using 5% Marvel in PBS/0.1% Tween followed by primary antibody at 5μg/ml and secondary antibody at 2μg/ml.

2.22 Patient-specific qPCR assay

The diagnostic DNA sample from the patient who provided sample R164 was retrieved from the tissue bank and subject to PCR using the BIOMED-2 primer set incorporating α-^{33}PdCTP. PCR products were subject to SSCP gel electrophoresis as described in Section 2.13. All clonal bands were excised from the gel and submerged in 60μl water, the PCR product was allowed to elute for 24 hours at 4°C then 5μl was used for a second round of PCR with the BIOMED-2 primer set. PCR products were recovered using the clean and concentrator 5 kit (Zymo Research) and sent for sequencing (Geneservice) using multiplexed forward or reverse primers from the BIOMED-2 primer set. Once the rearranged TCRβ gene sequence had been determined, a rearrangement specific forward primer was designed to cover the end of the V region, part of the D region and the N region. J region specific reverse primers and probes were ordered according to published sequences (Brüggemann *et al.*, 2004). Patient-specific assays were validated using the diagnostic sample as a positive control and pooled healthy lymphocyte DNA as a negative control. Sensitivity was tested and a standard curve generated by spiking a synthetic positive control into pooled healthy lymphocyte DNA. qPCR was performed on an ABI 7000 using 150ng DNA, 300nM each primer and 250nM

Assay	Primer and probe sequences	Size/bp	T_a/°C
R164_VB4-2_JB2-2	CCAGCAGCCAAGATCCCA CAACCGCCTCCTTACCCA FAM-CGGGCACCAG- GCTCACGGTC-BHQ1	90	60
BCMA_CN	CGACTCTGACCATTGCTTTCC AAGCAGCTGGCAGGCTCTT FAM-CAACCATTCTTGTC- ACCACGAAAACGAA-BHQ1	101	60
SDC4_CN	CAGGGTCTGGGAGCCAAGT GCACAGTGCTGGACATTGACA FAM-CCCACCGAACCCAAG- AAACTAGAGGAGAAT-BHQ1	129	60

Table 2.7: Primer and probe sets used for patient-specific qPCR assay

each probe in TaqMan universal master mix II (Applied Biosystems). In order to determine the proportion of tumour cells present in each cell subset, patient-specific Ct values were normalised against Ct values from previously validated assays detecting the diploid genomic control regions SDC4 and BCMA (Preter *et al.*, 2002). Primer sequences and annealing temperatures for all assays are provided in Table 2.7.

2.23 Cloning by overlap extension PCR

This protocol was based on the method of Bryksin & Matsumura (2010), a schematic of the cloning procedure is shown in Figure 5.13. The PCR amplification primers shown in Table 2.7 were ordered with the sequence CTTACGCGTGCTAGCCCGGG added to the 5' end of each forward primer and ACCAACAGTACCGGAATGCCAAGC added to the 5' end of each reverse primer. These tails were designed to be complementary to the pGL3 plasmid (Promega). PCR was carried out in a total volume of 25μl using Phusion HF buffer, 0.6mM each tailed primer, 0.2mM each dNTP, 0.5U Phusion hot start II DNA polymerase (New England Biolabs) and 50ng template DNA (R164 diagnostic sample for R164 specific rearrangement and healthy PBMCs for BCMA and SDC4). 30 cycles of PCR were performed with an annealing temperature of 65°C. 5μl

of each PCR reaction was electrophoresed through a 2% agarose gel to check for the presence of a single unique band of the expected size. The remaining PCR was purified through a clean and concentrator 5 column (Zymo Research) and the concentration was determined using a Nanodrop-1000 (Thermo Scientific). The insertion PCR was then performed in a total volume of 25μl using Phusion HF buffer, 0.2mM each dNTP, 20ng pGL3 plasmid, 150ng tailed insert and 0.5U Phusion hot start II DNA polymerase (New England Biolabs). 20 PCR cycles were performed with an annealing temperature of 60°C and an extended extension step of 2 min to allow for copying of the whole plasmid. To check for incorporation of the insert, 5μl of the completed insertion reaction was digested with 10U *Xba*I and 10U *Xho*I in NEB buffer 4 whilst 5μl was mock digested. The sizes of the fragments generated was assessed by electrophoresis through a 0.8% agarose gel. The remaining insertion reaction was digested with 10U *Xho*I to linearise any remaining empty vector followed by digestion with 10U exonuclease I and 2.5U λ exonuclease to remove the linearised empty vector. Insert containing vector was purified through a clean and concentrator 5 column (Zymo Research) and then transformed into competent E.coli, plated onto ampicillin LB agar and incubated at 37°C overnight. Colony PCR was then performed to identify those colonies that contained vector with insert. For each transformation, 10 colonies were streaked onto fresh ampicillin LB agar plates then the pick was agitated in 20μl PCR mix containing 2% Tween-20 and the following pGL3 specific primers which should amplify across the insert, F-TGTCCCCAGTGCAAGTGCAGG R-GCGGATAGAATGGCGCCGGG. Amplicon size was assessed by electrophoresing an aliquot of PCR product through a 1.5% agarose gel then the remainder was sent for sequencing to confirm the correct insert sequence was present.

2.24 Statistical analysis

Data summarisation was performed using pivot tables in Microsoft Excel then imported into R (http://www.r-project.org/) for statistical calculations and graphing. A p value of less than 0.05 was considered significant in all cases. All comparisons between healthy and patient groups were made using Student's t-test. Comparisons between three or more groups were made using ANOVA. In some cases a non-parametric test was considered more appropriate for multiple group comparisons in which case Wilcoxon unpaired U-test was used. Comparisons between subsets of cells or multiple samples from the same patients were made using paired Student's t-test. Correlation was assessed using Pearson's product moment correlation coefficient. Confidence intervals for healthy population limits were calculated using 2 standard deviations (95%) or 3 standard deviations (99%) either side of the mean.

SHP-1

3.1 Introduction

SHP-1 is a non-receptor type protein tyrosine phosphatase that has a key role controlling the intracellular phosphotyrosine level in lymphocytes thus providing a threshold for activation or initiating an activation terminating signal (Wu *et al.*, 2003). SHP-1 has been shown to act through dephosphorylation of JAKs (Jiao *et al.*, 1996, Pandey *et al.*, 2009) to regulate STAT3 signalling. Lack of SHP-1, as observed in the 'moth-eaten' mouse model that contains a splice site mutation in the mouse homologue of SHP-1, results in unregulated TCR signalling and consequent hyper-proliferation of T-cells (Lorenz *et al.*, 1996).

The structure of the SHP-1 gene was first characterised by Banville *et al.* (1995) who found that two alternate promoters regulate the expression of SHP-1, promoter I located upstream of exon 1 and promoter II located between exon 1 and exon 2 (Figure 3.1). Exons 1 and 2 are mutually exclusive and each contains a translational initiation codon therefore expression from promoter I generates transcript I including exon 1 but not exon 2 whilst expression from promoter II generating transcript II containing exon 2 but not exon 1. Banville *et al.* (1995) found that expression of the two isoforms of SHP-1 is tissue-specific with transcript I expressed only in non-haematopoietic tissue and transcript II expressed only in haematopoietic cells. However, it was subsequently shown that activation of haematopoietic cells with PHA can lead to an up-regulation of SHP-1 transcript I although transcript II remains the predominant form (Tsui *et al.*, 2002).

The two mRNA transcripts differ in their 5'-UTR and in the first few coding nucleotides, SHP-1 isoform I begins MLSRG whilst SHP-1 isoform II begins MVR (Tsui

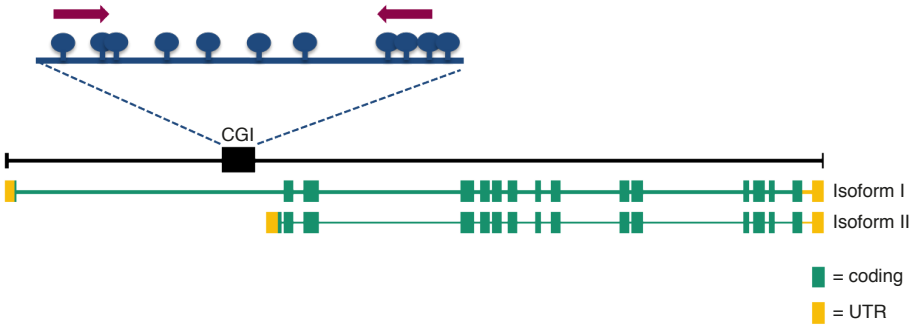

Figure 3.1: Diagram of SHP-1 CpG island

Diagram showing the exon structure of the SHP-1 gene. The black box represents the CGI, in the amplified section above each CpG dinucleotide is represented by a circle. The binding sites of the MSP primers is represented by the red arrows.

et al., 2006), the remainder of the coding sequence is identical. Since the difference in protein sequence does not affect the catalytic domains of SHP-1 (Walton & Dixon, 1993), these differences are not expected to have any impact on the catalytic activity of SHP-1 however this has not been biochemically assessed. The minimal differences in protein coding sequence led Tsui *et al.* (2002) to conclude that the two different isoforms existed principally to enable differential regulation from the different promoters rather than to generate functionally different protein isoforms.

Located upstream of SHP-1 promoter II is a short CGI that has been shown to contribute to the tissue-specific expression of SHP-1 isoform II mRNA whilst promoter 1 does not have an associated CGI. The promoter II CGI is methylated in epithelial tissue, which does not express isoform II and unmethylated in haematopoietic cells, which do express isoform II (Ruchusatsawat *et al.*, 2006). Aberrant SHP-1 CGI methylation has been identified in many haematological malignancies using the MSP primers described in Oka *et al.* (2001) however the frequency of methylation observed in different studies of the same malignancy can be quite varied as highlighted in Table 3.1. CGI methylation is also observed in HTLV-1 transformed cell lines and has been shown to correlate with loss of SHP-1 mRNA expression in these lines (Cheng *et al.*, 2004).

Treatment with the demethylating agent 5aza has been used to restore SHP-1 expression in cell line models of chronic myeloid leukaemia (K-562), B-cell lymphoma (BC-3), SS (HuT78), Adult T-cell leukaemia (EDS and MT1), B-cell acute lymphoblastic leukaemia (KW) and Hodgkins disease (HDLM2 and L428) (Koyama *et al.*, 2003, Oka *et al.*, 2002, Reddy *et al.*, 2005). SHP-1 expression could also be recovered by 5aza treatment of an NK cell (NK-TY2) and a T-cell (IWA3) line immortalised with HTLV-I (Oka *et al.*, 2002).

Disease	Frequency of methylation (n)			
BCR/ABL-negative meloproliferative disorder	7% (112)[1]	0% (28)[2]		
Myelodysplastic syndrome	0% (70)[3]			
Monoclonal gammopathy of undetermined significance	32% (19)[4]	20% (20)[5]		
Multiple myeloma	84% (32)[4]	15% (40)[5]	79% (34)[6]	
Chronic myeloid leukaemia	30% (23)[7]	100% (11)[8]		
Adult T-cell leukaemia	90% (20)[8]			
NK/T-cell lymphoma	91% (11)[8]			
Acute myeloid leukaemia	5% (20)[1]	11% (121)[3]	52% (50)[9]	90% (10)[8]
Diffuse large B-cell lymphoma	78% (46)[10]	70% (108)[11]	94% (45)[12]	
MALT lymphoma	82% (17)[12]			
Mantle cell lymphoma	75% (4)[12]			
Follicular lymphoma	96% (24)[12]			
Plasmacytoma	100% (5)[12]			
Acute lymphoblastic leukaemia	12% (336)[13]	24% (25)[9]	63% (8)[8]	
Anaplastic large cell lymphoma	64% (14)[14]			
Non-Hodgkins lymphoma/leukaemia	97% (90)[15]			

Table 3.1: SHP-1 methylation in haematological malignancies

Summary of the frequency of methylation observed in all studies of haematological malignancies using the MSP primers described in Oka *et al.* (2001). The number of patients examined (n) is included in brackets. References are as follows 1. Capello *et al.* (2008) 2. Jost *et al.* (2007) 3. Johan *et al.* (2005) 4. Chim *et al.* (2007) 5. Reddy *et al.* (2005) 6. Chim *et al.* (2004a) 7. Amin *et al.* (2007) 8. Oka *et al.* (2002) 9. Chim *et al.* (2004b) 10. Amara *et al.* (2008) 11. Amara *et al.* (2007) 12. Koyama *et al.* (2003) 13. Roman-Gomez *et al.* (2005) 14. Khoury *et al.* (2004) 15. Shivapurkar *et al.* (2004).

Some controversy exists over the demethylation of U266, a multiple myeloma cell line. Koyama *et al.* (2003) could not induce SHP-1 expression upon treatment with 5aza however Reddy *et al.* (2005) and Chim *et al.* (2004a) succesfully demethylated the SHP-1 CGI, inducing expression of SHP-1. Chim *et al.* (2004a) found dephosphorylation of STAT3 upon demethylation of the SHP-1 CGI whilst Reddy *et al.* (2005) did not observe any phosphorylation of STAT3 in U266 cells. Han *et al.* (2006) observed SHP-1 expression alongside STAT3 phosphorylation in U266 cells and did not identify any changes in SHP-1 expression or STAT3 phosphorylation after 5aza treatment. In ALK+ ALCL cell lines (Karpas 299 and SUDHL-1) SHP-1 methylation has been successfully reversed using 5aza and shown to correlate with restoration of

SHP-1 expression and concurrent decreases in JAK3 and STAT3 phosphorylation (Han *et al.*, 2006), A complex containing DNMT, pSTAT3 and HDAC has been identified to be responsible for methylation of the SHP-1 promoter in SUDHL-1 (Zhang *et al.*, 2005b).

Lymphocytes from SS patients display constitutive activation of STAT3 (McKenzie *et al.*, 2011, van Kester *et al.*, 2008) suggesting an impairment somewhere upstream in the signalling pathway. Loss of SHP-1 gene expression through CGI methylation is a potential candidate mechanism that could lead to the constitutive activation of STAT3. Reduced SHP-1 mRNA expression has been observed in the SS cell line HuT78 and found to be associated with CGI methylation (Nakase *et al.*, 2009) however the role of SHP-1 has not yet been investigated in primary Sézary cells.

3.2 Aim

The aim of this study was to establish whether SHP-1 silencing through promoter methylation contributes to aberrant STAT3 activation in SS. This was approached by assessing the expression of SHP-1 at the mRNA and protein level in SS patient PBMCs as compared to healthy control PBMCs to determine if any loss of SHP-1 was detectable. The methylation level of the SHP-1 CGI was also assessed in SS patient PBMCs as compared to healthy control PBMCs. Finally SHP-1 expression and methylation were compared to determine whether there is any correlation and both measures were also compared with patient tumour burden.

3.3 Results

3.3.1 Quantification of SHP-1 mRNA expression

Expression of SHP-1 mRNA in cell lines, healthy control and patient PBMCs was determined by RT-PCR. The primer sequences, reaction conditions and expected product size are listed in Table 2.1. RNA and cDNA were prepared as described in Section 2.3 and Section 2.4 and RT-PCR was performed as described in Section 2.5. A previously published primer pair binding in exons 14 and 16 (León *et al.*, 2002) was used to detect total SHP-1 mRNA. In order to detect the specific isoforms, primer pairs were designed to anneal to exons 1 and 3 (isoform I) or in exons 2 and 3 (isoform II).

Primers were first tested on cell line cDNA using 30 PCR cycles to verify the specificity. Each primer set gave a band of the expected size in at least one sample and no additional bands were observed. Figure 3.2 shows expression of SHP-1 mRNA by the MF cell line MyLa, the leukaemic cell line Jurkat and healthy CD4+ T-cells, which can be mainly attributed to isoform II expression although Jurkat and healthy CD4+ cells do show some isoform I expression. Primary keratinocytes show weaker expression of SHP-1, which can be attributed to isoform I expression whilst HEK293 and Kit225 cells show no expression of SHP-1. SeAx, HuT78 and HeLa cells show very weak expression of SHP-1 total mRNA but no bands are visible for the individual isoforms suggesting that the total expression is only just strong enough to be detectable on a gel.

Once the primers had been validated, they were used to examine total SHP-1 mRNA expression in 11 SS patient PBMC samples and 11 healthy control PBMC samples. The Jurkat cell line was used as a positive control and the cell line Kit225 as a negative control (Figure 3.3). Reactions were performed using a sub-threshold number

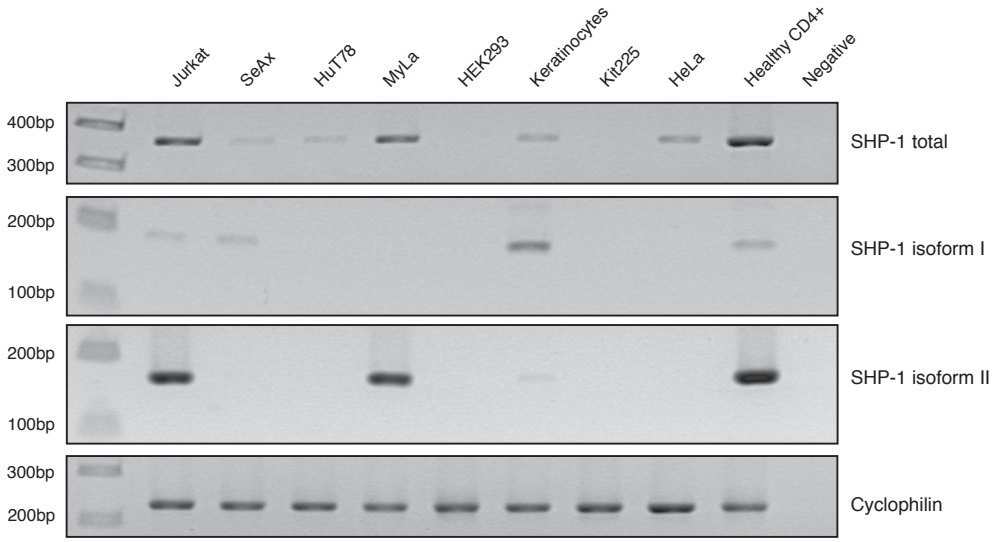

Figure 3.2: SHP-1 isoform expression in cell lines

RT-PCR was performed on 7 cell lines and 2 primary cell populations to assess total and isoform specific SHP-1 expression. cDNAs were also amplified with primers specific to the housekeeping gene Cyclophilin to ensure sample integrity. A negative control using water as a template for the RT-PCR reaction was included in each experiment.

of 25 cycles to generate semi-quantitative data. No clear difference in the band intensities of the SHP-1 amplicon was discernible between SS and healthy samples. Patient samples were derived from PBMCs rather than a purified population of malignant cells since, as discussed in Section 1.1.1 there is currently no suitable immunophenotypic marker for the isolation of Sézary cells. SHP-1 mRNA is clearly expressed by non-malignant cells of the peripheral blood, as demonstrated by the healthy control PBMC samples in Figure 3.3. It is therefore possible that SHP-1 mRNA from non-malignant cells is masking any loss of SHP-1 mRNA in malignant T-cells. Also, since RT-PCR examines the end stage of the PCR reaction, it is not accurately quantitative, although this experiment was performed using a sub-threshold number of PCR cycles in order to enhance the sensitivity of quantification.

Since some expression of both isoforms was observed in the healthy CD4+ sample by RT-PCR, expression of both isoforms was further quantified using qPCR. SYBR green was used to detect amplification using SHP-1 isoform I, SHP-1 isoform II or Cyclophilin primers as described in Section 2.6, then the expression of each isoform was normalised against Cyclophilin. Cyclophilin was chosen as a reference gene as previous studies in our lab have shown that it is the most stable housekeeping gene in lymphocytes with no change in expression upon lymphocyte stimulation. qPCR was performed on CD4+ lymphocyte cDNA samples from 11 healthy controls and 18 SS patients. Student's t-test was performed as described in Section 2.24 to compare expression between SS patient and healthy samples and revealed no difference in expression of total SHP-1 mRNA (Figure 3.4c) or of SHP-1 isoform I (Figure 3.4a) or SHP-1 isoform II (Figure 3.4b). Since the distribution of expression in SS patients was wider than that in healthy controls, a 99% confidence interval was generated as described in Section 2.24 to define the limits of the healthy population and SS patient values were compared to this limit. Using this method five of the 18 patient samples were observed

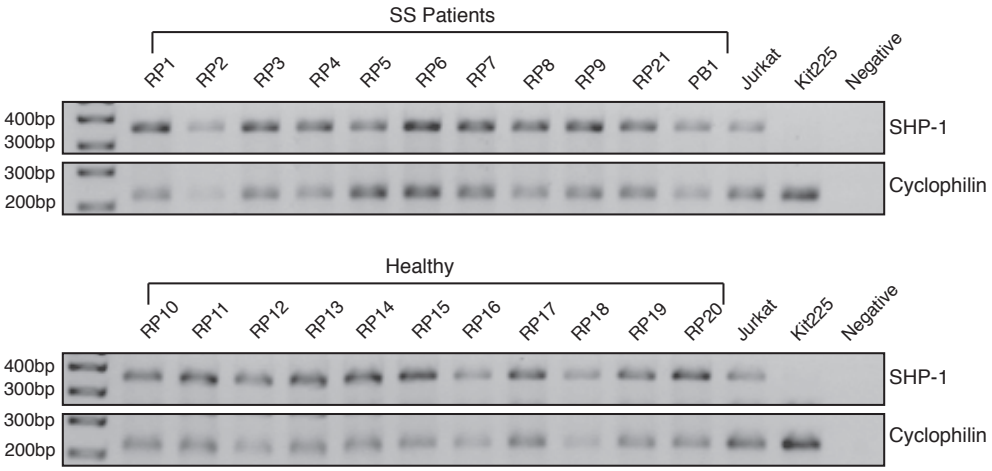

Figure 3.3: SHP-1 expression in SS patient and healthy control PBMCs

RT-PCR was performed on 11 SS patient cDNA samples and 11 healthy control cDNA samples using primers specific to all isoforms of SHP-1, which should generate a band of 350bp. cDNAs were also amplified with primers specific to the housekeeping gene Cyclophilin (223bp) to ensure sample integrity. The cell line Jurkat was included as a positive control for SHP-1 expression and Kit225 as a negative control for SHP-1 expression. A negative control using water as a template for the RT-PCR reaction was included in each experiment.

to have a significant reduction in SHP-1 total mRNA and SHP-1 isoform II suggesting that only isoform II is down-regulated in those patients with decreased SHP-1 total mRNA.

The correlation between isoform I and isoform II expression was also examined as described in Section 2.24 (Figure 3.4d) and found to be strongly positive with a correlation coefficient of 0.866 ($p<0.001$) for the healthy samples suggesting that the two isoforms are produced in a similar ratio in healthy lymphocytes. Some of the patient samples clustered with the healthy samples whilst the others clustered along a line of slightly shallower gradient suggesting a slight increase in the isoform I:isoform II ratio. Overall the patient samples maintained a weak positive correlation however this did not achieve significance.

The level of expression of SHP-1 mRNA was compared with total lymphocyte count, CD4+ count, percentage CD4+, CD4:CD8 ratio and percentage Sézary cells across the patient cohort using Pearson's product-moment correlation as described in Section 2.24. It was observed that total lymphocyte count correlated very strongly with CD4+ count (correlation co-efficient=0.998 $p<0.05$) therefore only total lymphocyte count is shown in the plots in Figure 3.5. A weak negative correlation (correlation coefficients between -0.5 and -0.54 $p<0.05$) was observed between SHP-1 mRNA quantity and each of the measures of tumour burden, with the exception of Sézary cell percentage. The patient samples that clustered with the healthy controls in terms of isoform I:isoform II ratio were also compared to those that didn't to see if there was any difference in tumour burden between the two groups however no notable differences were observed.

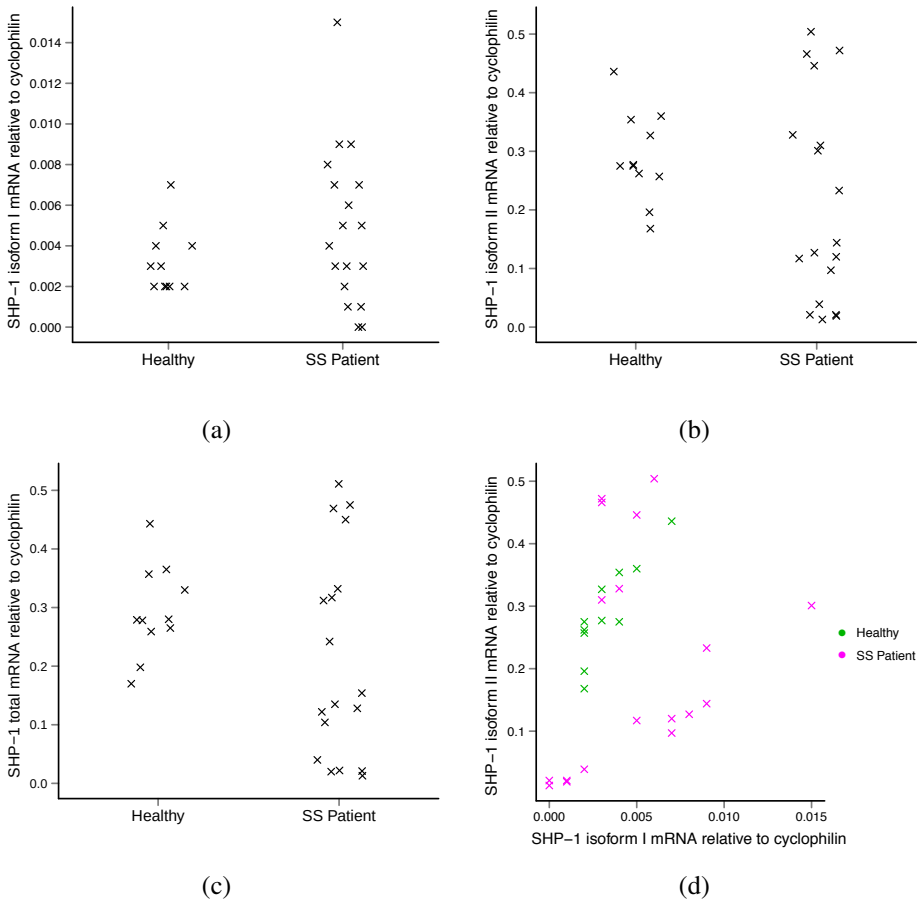

Figure 3.4: qPCR quantification of SHP-1 mRNA

Quantitative PCR analysis of SHP-1 mRNA expression in cDNA samples from 18 SS patients and 11 healthy controls. Measurements were performed in triplicate and expressed relative to the expression of Cyclophilin.(a) Comparison of SHP-1 isoform I mRNA expression (b) Comparison of SHP-1 isoform II mRNA expression (c) Comparison of total SHP-1 mRNA expression (d) Scatter plot showing the correlation between isoform I and isoform II expression.

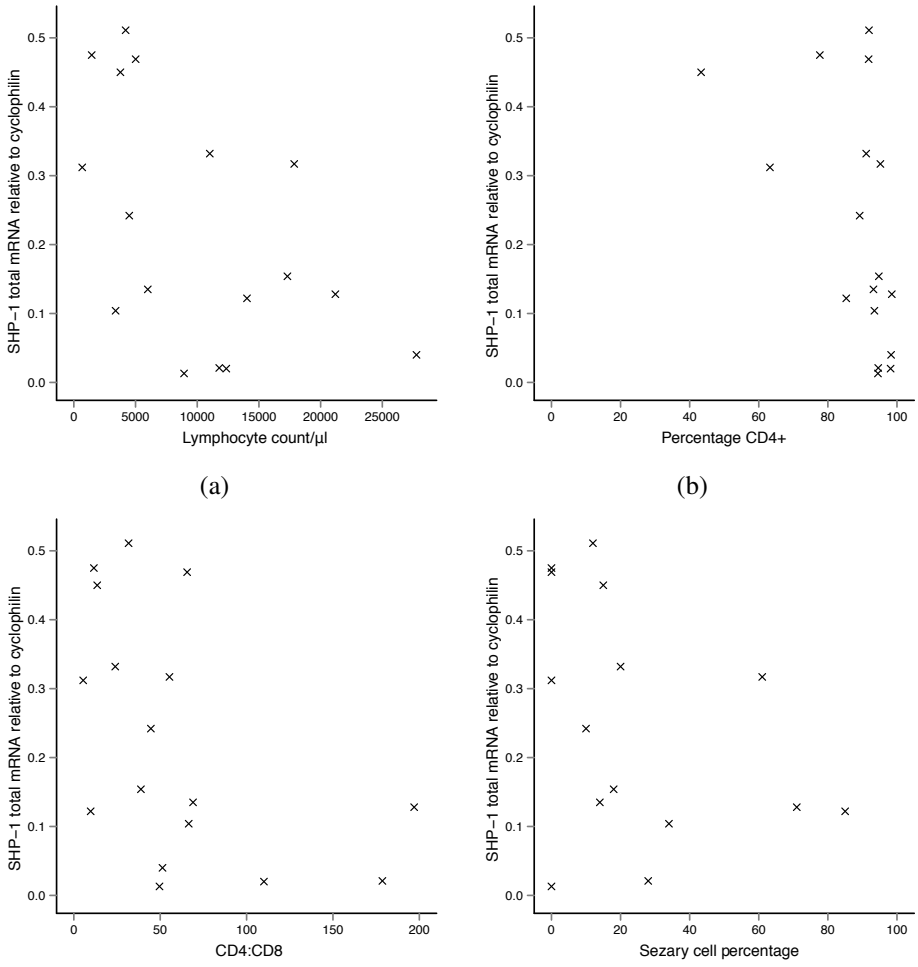

Figure 3.5: Relationship between SHP-1 mRNA quantity and measures of tumour burden

Plots to show the relationship between SHP-1 mRNA quantity, expressed relative to Cyclophilin, and measures of tumour burden: (a) Total lymphocyte count (b) Percentage CD4+ cells (c) CD4:CD8 ratio (d) Sézary cell percentage.

3.3.2 Quantification of SHP-1 protein expression

Western blotting was performed as described in Section 2.15 to investigate whether loss or decrease of SHP-1 was evident on the protein level (Figure 3.6). Whole cell lysates from six SS patient PBMC samples, two healthy control samples and the MyLa cell line were examined. In addition to the SHP-1 antibody, blots were probed using antibodies against pSTAT3, to confirm STAT3 activation status, STAT3 to confirm the presence of STAT3 and β-actin, as a loading control. Details of all antibodies and dilutions used are summarised in Table 2.6 and the Western blotting was kindly performed by Robert McKenzie. High levels of pSTAT3 were observed in all the SS patient samples and in the MyLa cell line whereas no pSTAT3 was observed in the healthy control samples. Similar amounts of total STAT3 were observed in all samples suggesting that the lack of pSTAT3 in healthy control samples is not due to a lack of STAT3. No difference in SHP-1 protein level were observed between SS patient and healthy control samples.

Since the SHP-1 antibody had proved highly specific it was further optimised for use in flow cytometry of fixed and permeabilised cells in order to accurately quantitate the level of SHP-1 protein present. Fixation, permeabilisation and intracellular staining was performed as described in Section 2.18. Data acquisition was performed on a BD FACS Aria II and analysed using FlowJo software as described in Section 2.19. Staining was performed on four healthy control CD4+ T-cell samples and nine SS patient CD4+ T-cell samples, including those five patients that showed a significant reduction in SHP-1 mRNA. A much wider distribution of SHP-1 expression was observed in SS patient than in healthy controls but no significant difference was observed between the two groups (Figure 3.7) using Student's t-test as described in Section 2.24. No significant correlation was observed between SHP-1 mRNA and protein expression in the patient cohort and the patients with reduced SHP-1 mRNA expression do not appear

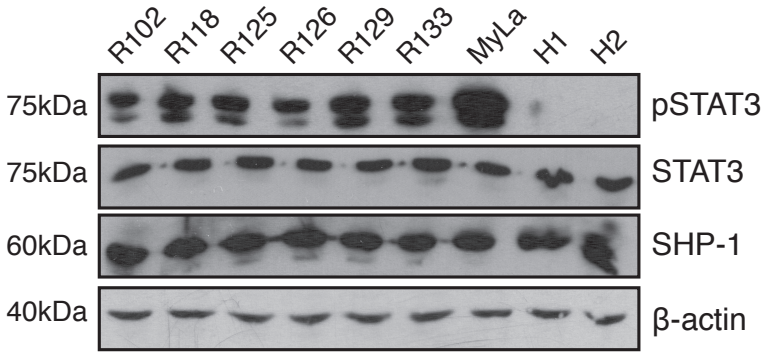

Figure 3.6: pSTAT3 and SHP-1 Western blot

Western blot analysis of pSTAT3, STAT3 and SHP-1 expression in 6 SS patients (R102-R133), the MF cell line MyLa and 2 healthy control samples (H1 and H2). β-actin was used as a loading control. Data kindly provided by Robert McKenzie.

to have any coincident reduction in SHP-1 protein expression.

Intracellular staining and flow cytometry was also used to examine the expression of SHP-1 in the SS cell lines HuT78 and SeAx, the MF cell line MyLa and the leukaemic cell line Jurkat (Figure 3.7). Expression of SHP-1 was much lower in all the cell lines than in healthy and SS patient samples. This corresponds with the RT-PCR results shown in Figure 3.2 where the healthy CD4+ sample showed a much stronger band than any cell line and expression was lower in HuT78 and SeAx than in MyLa and Jurkat.

3.3.3 Methylation specific PCR of the SHP-1 CGI

As mentioned previously, methylation of the SHP-1 CGI has been widely studied in other haematopoietic malignancies using MSP. In MSP DNA is first bisulphite converted, transforming all unmethylated cytosine residues to uracil but not affecting those cytosine residues that are methylated. Primers are then designed to be complementary to either the methylated sequence (MSP primers) or the unmethylated sequence (USP primers) and used to amplify the bisulphite converted DNA. After separation on an agarose gel the intensity of MSP and USP bands are compared to determine whether the samples are methylated, unmethylated or partially methylated. The primers are generally designed to cover several CpG dinucleotides in order to provide maximum discrimination. In this study the primers used in the majority of published MSP studies of SHP-1 CGI methylation were used, encompassing two CpG dinucleotides in the forward primer and three CpG dinucleotides in the reverse primer as shown in Figure 3.1.

Bisulphite conversion of DNA was performed as described in Section 2.9. MSP and USP was performed on bisulphite converted DNA from 47 SS PBMC samples and 11 healthy PBMC samples as described in Section 2.10 using the primers and reaction

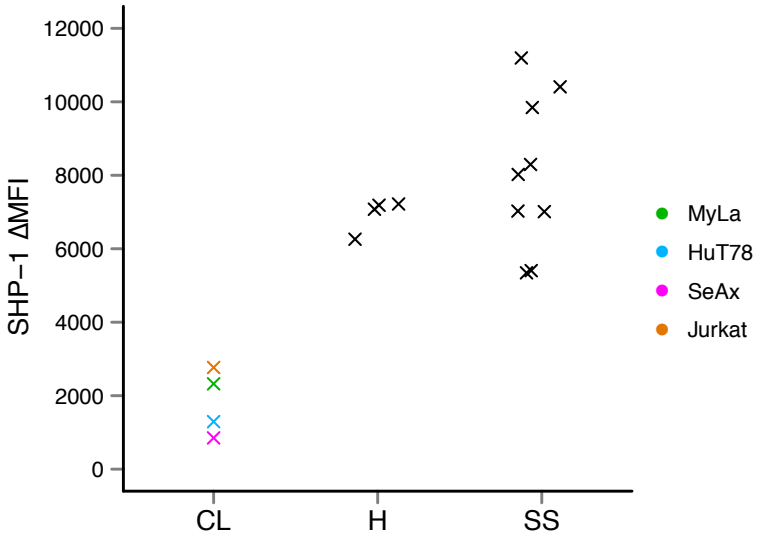

Figure 3.7: SHP-1 protein quantified by intracellular staining and flow cytometry

The cell lines (CL) MyLa, Jurkat, HuT78 and SeAx and CD4+ T-cells isolated from 9 SS patients (SS) and 4 healthy controls (H) were fixed in 1% PFA, permeabilised in methanol then fluorescently stained using a SHP-1 antibody. ΔMFI was calculated by subtracting the mean fluorescent intensity obtained using an isotype control antibody from the mean fluorescent intensity obtained using the SHP-1 specific antibody.

conditions detailed in Table 2.2. A methylation specific band was observed in only one of 47 SS samples and one of 11 healthy samples. An example gel image of MSP and USP amplicons is shown in Figure 3.8. MSP and USP were also performed on cell line DNA, detecting methylation in HuT78 and SeAx, partial methylation in MyLa and no methylation in Jurkat. Each set of PCR reactions included an artificially methylated positive control for the MSP reaction, a completely unmethylated positive control for the USP reaction and a negative control using water as the template.

3.3.4 Pyrosequencing analysis of the SHP-1 CGI

Since the MSP/USP assays do not cover all CpG dinucleotides in the SHP-1 CGI it is possible that some changes in methylation were missed by these assays therefore Pyrosequencing assays S1 and S2 (Tables 2.3 and 2.4) were developed to cover the 232bp CGI to give a more detailed and quantitative view of the methylation at each CpG dinucleotide as discussed in Section 1.2.3. The PSQ assay design program was used to design primers against the bisulphite converted sequence of the SHP-1 CGI with all potentially methylated cytosines, those occurring in the context of a CG dinucleotide, highlighted as potential C/T polymorphisms. Assays were designed such that the PCR and sequencing primers did not cover any CpG dinucleotides in order to avoid biasing the PCR reaction towards selective amplification of only the unmethylated template and therefore to allow the Pyrosequencing to be quantitative.

The PCR primers were first optimised without including the biotin tag to ensure they produced only one discrete band as any misprimed or truncated amplicons have the potential to interfere with accurate quantitation. It was observed that the yield of fully optimised PCR reactions using bisulphite converted DNA was noticeably lower than what would be expected from a standard PCR using DNA as a template. Initially this was attributed to the increase in fragmentation produced by the bisulphite reaction,

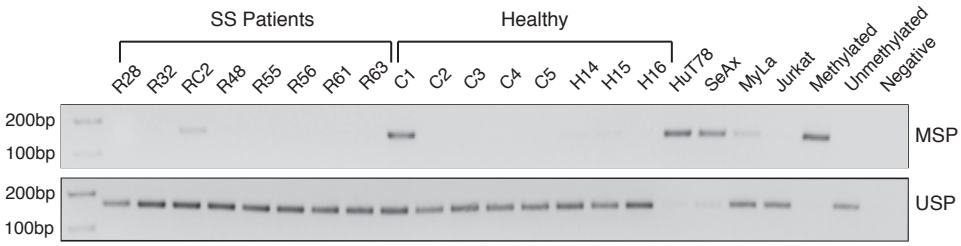

Figure 3.8: SHP-1 methylation specific PCR

Representative gel images showing the results of PCR amplification of bisulphite converted DNA using MSP and USP primers specific to the SHP-1 CGI.

which is known to have a degrading effect on DNA (Warnecke *et al.*, 2002). However, tests with increased input DNA concentration did not yield any noticeable improvement suggesting that fragmentation was not the main factor affecting the efficiency of the PCR. Several methods are available for improving PCR amplification of CG rich sequence, which can be particularly hard to amplify due to the increased stability of secondary structure within the amplicon. However, bisulphite conversion, by converting cytosine to tyrosine, creates AT rich sequence that should therefore have less secondary structure. Discussions on the Protocol Online Bioforum (http://www.protocol-online.org/forums/index.php) proposed that in particularly AT rich sequence the polymerase becomes displaced from template more easily, leading to decreased amplification efficiency and Nakase *et al.* (2009) confirmed that decreasing the extension temperature could counteract this effect. Therefore the extension temperature of bisulphite PCR reactions was decreased to 66°C, resulting in a substantial increase in PCR product yield.

Once the PCR reaction was optimised to generate a strong, specific product, one primer was exchanged for a biotin tagged version to allow capture in the next stage of the process. The Pyrosequencing reaction was then performed as described in Section 2.11, firstly testing 100% methylated and 0% methylated control DNA samples generated as described in Section 2.8. Each plate included a series of controls to ensure accuracy of the results: biotinylated PCR template with no sequencing primer was included to ensure that secondary structure within the amplicon could not prime the Pyrosequencing reaction; water was used as a template for the biotinylated PCR and then taken on into the Pyrosequencing reaction to identify any contamination; sequencing primer only and biotinylated PCR primer only were included to check for mis-priming caused by homo-dimerisation of these primers; finally one well contained annealing buffer only to identify contamination during the Pyrosequencing reaction.

The highly quantitative nature of the assays was then assessed by mixing 100% methylated DNA with 0% methylated DNA in varying proportions and plotting the measured degree of methylation (Figure 3.9). The relationship between proportion of methylated DNA added and proportion of methylated DNA measured is not linear as might be expected. This is due to the fact that bisulphite conversion leads to the presence of two slightly different templates for PCR with unmethylated template DNA containing a greater proportion of Ts than methylated template DNA. Whilst the primers are designed to avoid variable positions, subtle differences in the structure of the template is likely to lead to a difference in the kinetics of primer binding. This contributes to a 'PCR bias' whereby either the methylated or unmethylated template is amplified slightly more efficiently than the other. Despite the small departure from linearity, Figure 3.9 shows clear differentiation between samples with a 10% difference in methylation, confirming the choice of Pyrosequencing as appropriate for the measurement of DNA methylation in samples that may contain a mixed population of malignant and reactive T-cells and therefore show only a small change in methylation.

Controls were also incorporated to check the detection limit of the Pyrosequencer and the completion of the bisulphite conversion. This was done by altering the known sequence to be incorporated such that the proportion of C to T was measured at a known T and a C not in the CpG context. The T should be measured as 0% methylated, confirming the detection limit on the Pyrosequencer whilst the C not in a CpG context should also be measured as 0% methylated if the bisulphite conversion reaction has occurred to completion. These internal controls have been included in all the assays and have consistently returned values of 0-5%. Where a sample measured greater than 5% in either of these controls a fresh bisulphite conversion reaction was performed prior to repeating the Pyrosequencing.

The optimised and calibrated SHP-1 Pyrosequencing assays were then performed

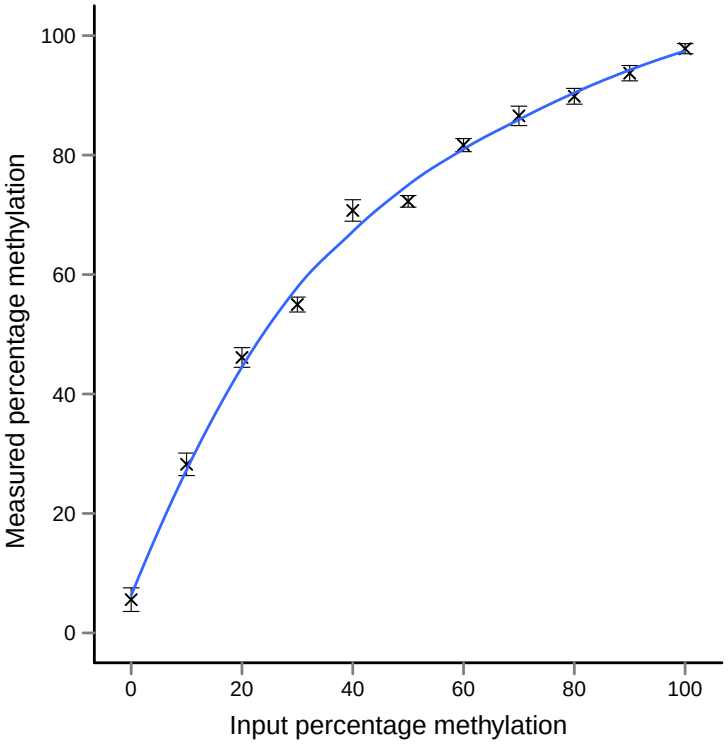

Figure 3.9: Assessment of SHP-1 Pyrosequencing sensitivity

Known input methylation samples were created by mixing 100% methylated DNA with 0% methylated DNA in various proportions prior to bisulphite conversion. Measured percentage methylation is plotted as an average across the 11 CpG dinucleotides of the CGI with error bars representing the SEM. The line of best fit has been added in blue.

on seven healthy PBMC samples and nine SS patient PBMC samples, including the five patients shown to have reduced SHP-1 mRNA and the patient shown to have methylation by MSP. None of the 11 potential CpG sites showed any increase in methylation level between patient and healthy samples (Figure 3.10). The level of SHP-1 methylation was averaged across the 11 CpG dinucleotides of the CGI for each patient and compared with total lymphocyte count, percentage CD4+, CD4:CD8 ratio and percentage Sézary cells using Pearson's product-moment correlation as described in Section 2.24. No correlation was observed between SHP-1 CGI methylation and total lymphocyte count, percentage CD4+ or percentage Sézary cells (Figure 3.11). A negative correlation was observed between SHP-1 CGI methylation and CD4:CD8 ratio (correlation co-efficient=-0.72 $p<0.05$). This is the reverse of what would be expected if tumour burden was affecting SHP-1 methylation since those patients with a higher CD4:CD8 ratio actually appear to have less SHP-1 methylation.

Assays performed on the cell line DNA confirmed the results of the MSP in that HuT78 and SeAx were found to be fully methylated (Figure 3.10) whilst Jurkat was found to have a minimal level of methylation, similar to that observed in healthy PBMCs. MyLa was determined to have a similar level of methylation to Jurkat in contrast to the MSP/USP assays which suggested that MyLa was partially methylated. The SHP-1 CGI methylation of primary keratinocytes was also assessed, confirming the presence of tissue-specific methylation of the SHP-1 CGI in healthy tissue.

Finally, the relationship between SHP-1 expression and CGI methylation was assessed in the patient samples (Figure 3.12). No correlation was observed between SHP-1 mRNA expression and SHP-1 CGI methylation however, these data were biased by the selection of those samples with low SHP-1 mRNA quantities as input for the methylation assays. A negative correlation did appear between SHP-1 protein expression and SHP-1 CGI methylation upon examination of Figure 3.12b. This correlation

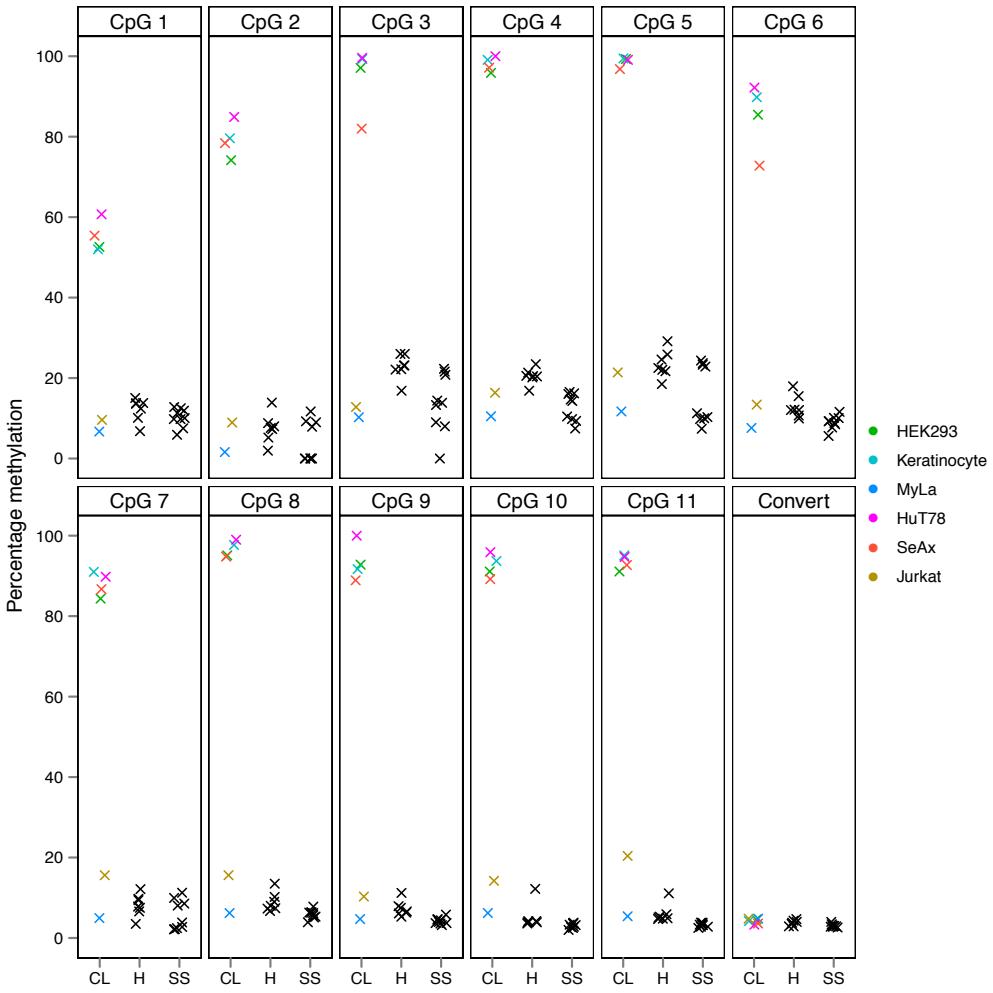

Figure 3.10: SHP-1 Pyrosequencing of cell lines, healthy and SS samples

Summary of data obtained by Pyrosequencing of bisulphite converted DNA from 6 cell lines (CL), 7 healthy controls (H) and 9 SS patients (SS). Percentage methylation in each of the 11 CpG dinucleotides is plotted for each sample, which are grouped by type. The cell lines have been identified by use of coloured points. Convert is the conversion control, performed by measuring 'methylation' at a cytosine that cannot be methylated, if the bisulphite conversion reaction has worked to completion this should measure 0.

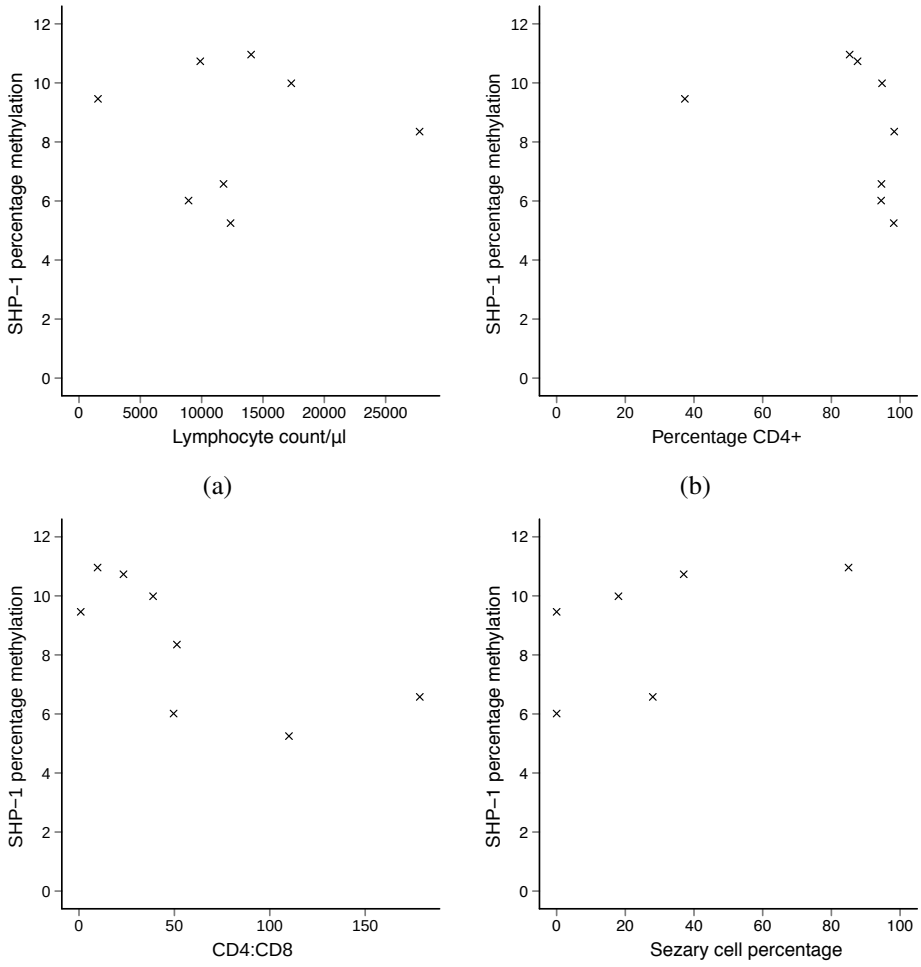

Figure 3.11: Relationship between SHP-1 CGI methylation and measures of tumour burden

Plots to show the relationship between SHP-1 CGI methylation, averaged across the 11 CpG dinucleotides, and measures of tumour burden: (a) Total lymphocyte count (b) Percentage CD4+ cells (c) CD4:CD8 ratio (d) Sézary cell percentage.

had a coefficient of -0.85 but did not reach significance (p=0.06) reflecting the limited number of data points available. The correlation could have occurred by random chance and a much larger cohort would need to be assessed to determine its relevance. In the absence of significant methylation in any sample, this was felt unnecessary.

3.4 Discussion

SHP-1 plays a complex role in the immune system, the motheaten mouse model has myriad defects in haematopoeisis leading to widespread inflammation and autoimmunity (mouse genome informatics database MGI:1856073 Blake *et al.* (2011)) Mice with homozygous conditional knockout of SHP-1 in their single positive T-cells have naïve CD8+ T-cells with a lower threshold for peptide activation and greater expansion upon antigen stimulation than those from control mice (Fowler *et al.*, 2010). However, heterozygous conditional knockout mice have a similar threshold for peptide activation and capacity for expansion upon antigen stimulation to that found in control mice, suggesting that a complete absence of SHP-1 is necessary to cause dysregulation of the activation and expansion of naïve T-cells. The same study also examined central memory CD8+ T-cells lacking SHP-1 and found that expansion upon antigen challenge was negatively proportional to SHP-1 quantity, suggesting a more sensitive mode of regulation in mature T-cells.

In addition to its role in determining the threshold for TCR signalling, SHP-1 plays a more active role in the inhibition of T-cell responses. Antagonistic peptides have been described that can prevent the proliferation induced by agonistic peptides (Evavold *et al.*, 1993). Increased SHP-1 activity is observed following treatment of pre-stimulated T-cells with antagonistic peptides and the presence of a dominant negative version of SHP-1 completely abrogates the inhibitory effect of the antagonistic peptides (Kilgore

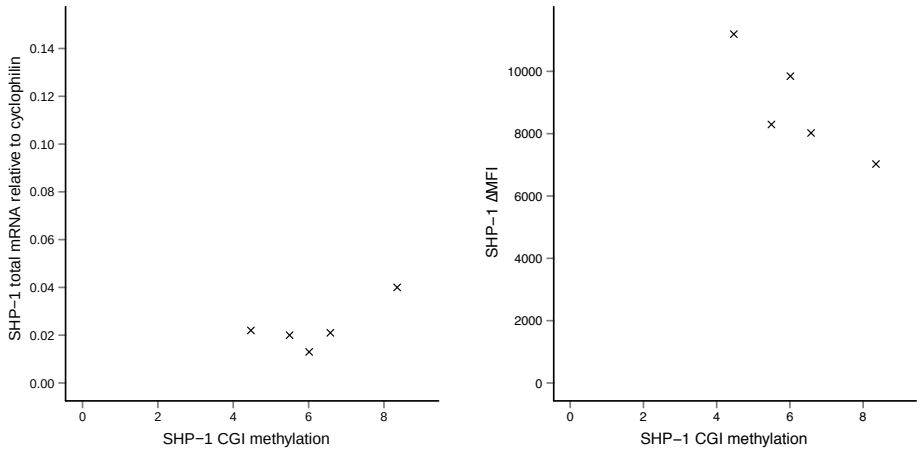

(a) (b)

Figure 3.12: Relationship between SHP-1 CGI methylation and SHP-1 expression

Plots to show the relationship between SHP-1 CGI methylation, averaged across the 11 CpG dinucleotides, and: (a) SHP-1 total mRNA expression (b) SHP-1 protein expression.

et al., 2003). Similarly, IL-10 can prevent CD2 induced proliferation through direct recruitment of SHP-1 to the CD2 signalling complex. Expression of dominant negative SHP-1 or silencing of SHP-1 expression with siRNA removes the inhibitory effect of IL-10 on CD2 induced proliferation (Taylor *et al.*, 2009).

Given the potential for uncontrolled expansion in the absence of SHP-1 it is no surprise that SHP-1 deficiencies have been widely observed in haematological malignancies, as discussed Section 3.1. In the majority of cases, the mechanism leading to decreased expression of SHP-1 has been identified as DNA methylation of the promoter II CGI, as summarised in Table 3.1. A few reports have identified aberrant SHP-1 mRNA splicing (Jin *et al.*, 1999, Ma *et al.*, 2003) in cell lines and RNA hyper-editing has been observed in AML (Beghini *et al.*, 2000) whilst there are no published reports of SHP-1 loss through gene deletion.

SHP-1 is known to be directly involved in the regulation of STAT3, the drugs 5-hydroxy-2-methyl-1,4-naphthoquinone and acetyl-11-keto-β-boswellic acid have been found to inhibit both constitutive and IL-6 induced activation of JAK2 and STAT3 in multiple myeloma cell lines via the induction of SHP-1 expression (Kunnumakkara *et al.*, 2009, Sandur *et al.*, 2010). Constitutive STAT3 activation is recognised as a key pathogenetic mechanism in CTCL with pSTAT3 positive malignant cells observed in MF tumours (Sommer *et al.*, 2004) and SS lymphocytes (Eriksen *et al.*, 2001, McKenzie *et al.*, 2011, van Kester *et al.*, 2008, Zhang *et al.*, 2010) however, upstream events leading to this constitutive activation are currently unclear. Therefore, loss of SHP-1, if present, represented a pathogenetic mechanism that could be targeted by agents inducing SHP-1 transcription or demethylation of the SHP-1 CGI, in order to down-regulate constitutive STAT3 activation.

The results of this study however suggest that loss of SHP-1 does not occur in SS

patient tumour cells. Interestingly, although loss was observed at the mRNA level in five SS patients, this did not correspond to loss on the protein level. A weak negative correlation was observed between various measures of tumour burden and SHP-1 total mRNA quantity (Figure 3.5), indicating that there may be some down-regulation of SHP-1 expression in patients with a higher tumour burden. However, no down-regulation of SHP-1 was observed at the protein level and there was no correlation between SHP-1 mRNA and SHP-1 protein levels. This suggests that SHP-1 expression is regulated at the translational level in addition to the transcriptional level. Since down-regulation of SHP-1 mRNA level is not reflected in down-regulation at the protein level it is unlikely to play a functional role. Another study performed in our lab found no correlation between SHP-1 protein and pSTAT3 in a cohort of 18 SS patients assessed by intracellular staining and flow cytometry (McKenzie *et al.*, 2011), providing further evidence that SHP-1 is not involved in the aberrant activation of STAT3 in SS.

Previous investigation of SHP-1 in CTCL had been performed on immortalised cell lines rather than primary tissue and suggested that SHP-1 methylation may play a role in contributing to aberrant STAT3 activation (Nakase *et al.*, 2009, Zhang *et al.*, 2000). In this study, whilst SHP-1 silencing through promoter methylation was not observed in the SS patient lymphocyte samples it was observed in two SS cell lines, SeAx and HuT78. It appears therefore that where methylation is observed in SS cell lines this is a feature of the cell lines rather than their originating primary tissue and may have been a contributing factor to their transformation. Methylation as a consequence of immortalisation has been previously recognised (Jones *et al.*, 1990). A survey of multiple CGIs revealed that in the majority of loci methylation status in cell lines reflected that in the original primary tissue however there are infrequent instances of methylation arising as a consequence of the escape from senescence (Ueki *et al.*, 2002), as has happened

in the case of SHP-1 methylation in CTCL cell lines.

The detection of SHP-1 methylation in primary epithelial cells however does confirm that methylation of this CGI plays a role in healthy tissues, contributing to the tissue-specific expression of particular isoforms of the protein. It is unclear what role these tissue-specific isoforms play since there is only a two amino acid difference between the two, which is not predicted to have any impact on the catalytic activity. One possibility is that the use of different promoters in different tissues allows the gene to be regulated by different signalling pathways and transcription factors in different tissues. Promoter I for example has been shown to have binding sites for NF-Y and USF1/USF2 (Tsui *et al.*, 2002, Xu *et al.*, 2001) whilst promoter II has binding sites for PU.1 Sp1 and Oct1, which mediate recruitment of NF-κB (Cheng *et al.*, 2007, Nakase *et al.*, 2009, Wlodarski *et al.*, 2007). In a murine CNS glial culture system promoter I transcription can be induced by IFN-β and IFN-γ acting through STAT-1 and IRF-1 whilst promoter II transcription can be induced by IFN-β and IL-6 acting through STAT3 (Christophi *et al.*, 2008). Use of different activating pathways may be necessary to allow SHP-1 to function in alternative roles in different tissues whilst the presence of the CGI in promoter II permits an additional level of control whereby one isoform can be completely silenced.

The literature on SHP-1 methylation in various haematological malignancies, as summarised in Table 3.1 displayed a surprising range of methylation frequencies for the same conditions despite using the same experimental technique, MSP. This was particularly notable for AML where the frequencies observed across four studies varied between 5% and 90%. This is probably influenced in part by the exact factors used to define patient inclusion in individual studies, however, when working with this technique it became clear that a reasonable proportion of this variation may be due to technical differences. Although all studies utilised the same primer sequences, very

few state the PCR reaction conditions used and, during the optimisation of the MSP reactions shown in Section 3.3.3 it was observed that annealing temperature, $MgCl_2$ concentration and cycle number could all dramatically affect the results therefore a comprehensive range of controls was necessary to ensure the validity of any conclusion drawn. This is a consequence of the fact that rather than directly measuring the methylation in a CpG dinucleotide, MSP represents the kinetics of a PCR reaction where two or three CpG dinucleotides may contribute unequally to the primer binding and that the efficiency of the MSP and USP reactions are unlikely to be equal. The technique of MSP also relies on the assumption that all CpG dinucleotides in a CGI are either 100% methylated or 0% methylated, which is rarely likely to be the case, particularly when the sample is made up of a mixed population of cells.

Pyrosequencing of bisulphite converted DNA enables the proportion of DNA methylated at each CpG site within the SHP-1 CGI to be measured. This allows identification of DNA methylation even if present in only a small proportion of cells and will also establish whether different regions of the island are subjected to differential methylation. Hence, Pyrosequencing of bisulphite converted DNA was used as a sensitive and comprehensive method for the analysis of DNA methylation in the SHP-1 CGI. Since Pyrosequencing is a much more labour intensive technique than MSP a small selection of samples were chosen for Pyrosequencing analysis, including those that had shown methylation by MSP. Even with careful controlling of the MSP reactions some differences were observed between the MSP and Pyrosequencing results. In particular, MyLa was observed to be partially methylated by MSP whilst Jurkat was completely unmethylated however, by Pyrosequencing they had very similar levels of methylation. One possible explanation for this is that the quantity of template was slightly greater in the MyLa sample than Jurkat so the very low level of methylation present was amplified sufficiently to produce a band only in the MyLa sample. Using

Pyrosequencing the proportion methylation is calculated from the relative difference in height between C and T peaks at a particular CpG dinucleotide thus rendering this method independent of template quantity.

A further observation was that of the two samples, one SS, one healthy that showed methylation by MSP, the SS patient sample failed Pyrosequencing quality control with signals too low for accurate quantification, suggesting a restricted template quality may have led to the presence of a band in the MSP. The healthy sample that showed methylation by MSP had similar methylation to the other healthy samples over CpG dinucleotides 1-5 but noticeably higher methylation over CpG dinucleotides 6-11. The reverse primer was sited over CpG dinucleotides 8-10, which had a methylation level of around 12% suggesting that this level of methylation was sufficient to generate an MSP amplicon. Given that all samples showed higher methylation in the first half of the island it is possible that the MSP reaction was becoming primed and extended in the forward direction in all samples but the reverse primer could only bind in a few samples to generate exponential amplification. Through the use of MSP screening of a large cohort and Pyrosequencing to examine a small subset of patients at much higher level of detail, it has been comprehensively demonstrated that there is an absence of SHP-1 methylation in SS patient lymphocytes.

Having excluded loss of SHP-1 as a mechanism for constitutive STAT3 activation in SS, further work in this area will remain focussed on determining what mechanism is responsible. Other known regulators of the STAT3 activation pathway include SOCS proteins, which bind to activated JAKs to prevent their kinase activity (Endo *et al.*, 1997, Naka *et al.*, 1997, Starr *et al.*, 1997), and PIAS3, which binds to activated STAT3 blocking its DNA binding activity (Chung *et al.*, 1997). SOCS3 has been found to be constitutively expressed in MF and SS cell lines however, this constitutive expression appears to be being driven by the constitutive activation of STAT3 rather than driving

the constitutive activation of STAT3 since transfection of dominant negative STAT3 into these cell lines leads to down-regulation of STAT3 (Brender *et al.*, 2001). PIAS3 is normally constitutively expressed and located in the nucleus in complex with another protein MITF, preventing it from binding to activated STAT3. Under certain cytokine signalling conditions MITF becomes phosphorylated and releases PIAS3, allowing it to sequester STAT3 thus preventing STAT3 target gene expression (Yagil *et al.*, 2010). Since this mechanism of action occurs downstream of STAT3 phosphorylation its dysregulation is unlikely to be able to induce the constitutive phosphorylation of STAT3 observed in SS.

Studies in our lab (McKenzie *et al.*, 2011) have examined JAK activation in SS patient samples and found that JAK1 and JAK2 are also constitutively activated in SS. Inhibition of JAK activation using the pan-JAK inhibitor P6 leads to a decrease in JAK activation and concurrent decrease in STAT3 activation in *ex vivo* SS patient CD4+ T-cells. Furthermore, this inhibition leads to widespread changes in STAT3 driven gene expression and ultimately to an increased level of apoptosis in primary SS tumour cells that, without P6 treatment, are known to be resistant to apoptosis. These data strongly implicate JAK1 and JAK2 activation in the constitutive activation of STAT3 in SS. Ongoing work has ruled out the most common activating mutations, JAK1V658F and JAK2V617F as the mechanism for persistent activation of JAK1 and JAK2 in SS however a complete mutational screen remains to be completed. Investigations will also be extended to receptors upstream of JAK activation, however a complex and incompletely delineated network of signalling occurs between over 40 receptors, 4 JAKs and 7 STATs (Murray, 2007) so pinpointing the original defect will become increasingly challenging as the search is extended to include receptors.

Another mechanism that could potentially be involved in the regulation of STAT3 is methylation of a conserved arginine residue by protein arginine methyltransferase

(PRMT), which is suggested to be essential for prompt dephosphorylation of STATs (Zhu *et al.*, 2002). Arginine methylation of STAT1 (Mowen *et al.*, 2001) and STAT6 (Chen *et al.*, 2004) has been demonstrated to have have a regulatory effect on their ability to activate transcription and STAT3 has been identified amongst the proteins immunoprecipitated by an anti-methyl-arginine antibody (Rho *et al.*, 2001) suggesting that STAT methylation is a frequently used regulatory mechanism. In contrast to these results, (Komyod *et al.*, 2005) did not observe arginine methylation of STAT1 and STAT3 in melanoma cell lines. Recently, STAT3 methylation mediated by PRMT2 has been characterised in mouse hypothalamus and shown to lead to prolonged STAT3 phosphorylation and altered transcriptional activity (Iwasaki *et al.*, 2010). This suggest that STAT3 methylation is a critical regulatory mechanism in some tissues and investigation of STAT3 methylation may be of particular interest in SS lymphocytes, where the timescale of dephosphorylation has been substantially altered.

In summary, no significant difference in expression of SHP-1 was observed in SS patients at the mRNA level (Section 3.3.1) or at the protein level (Section 3.3.2) compared to healthy controls. In addition no difference was observed in the methylation status of the SHP-1 CGI between SS patient PBMCs and healthy controls (Section 3.3.4). These results indicate that SHP-1 silencing through promoter methylation in not a contributory factor to aberrant STAT3 activation in SS cells *in vivo*. Silencing of SHP-1 expression through methylation of the SHP-1 promoter II CGI was however observed in the cell lines SeAx and HuT78 indicating that this feature is an artefact of the immortalisation process. Further work is ongoing to determine the mechanism that leads to aberrant STAT3 activation in SS.

Fas

4.1 Introduction

The death receptor Fas (CD95/APO-1) plays a crucial role in regulating T-cell homeostasis, contributing to negative selection of immature T-cells (Dautigny *et al.*, 1999) and regulating the induction of apoptosis via AICD in mature T-cells (Alderson *et al.*, 1995). Fas has also been implicated in non-specific and antigen-specific Ca^{2+}- independent T-cell mediated cytotoxicity (Rouvier *et al.*, 1993).

As discussed in Section 1.1.4, malignant cells in CTCL display substantial defects of the normal T-cell signalling and homeostasis mechanisms resulting in their persistence. A report in 2008 demonstrated frequent resistance (9/16 cases) to FasL induced apoptosis in freshly isolated primary Sézary cells (Contassot *et al.*, 2008) suggesting that dysregulation of the Fas signalling pathway may contribute to the persistence of malignant cells in SS. Heterogeneity of Fas expression levels was observed, with five cases showing normal or increased Fas expression and four cases showing reduced Fas expression. In those cases with normal or enhanced Fas expression, resistance to apoptosis was attributed to increased expression of the apoptosis inhibitor c-FLIP. However, the mechanism mediating reduced Fas expression was not addressed.

The Fas gene is located on chromosome 10q, a region of frequent genomic loss in many malignancies (Cappellen *et al.*, 1997, Komiya *et al.*, 1996) including CTCL (Vermeer *et al.*, 2008, Wain *et al.*, 2005). The gene is made up of nine exons separated by eight introns and generates a 48kDa protein consisting of three cysteine-rich extracellular subdomains, a transmembrane helix and an intracellular portion that includes the death domain (Behrmann *et al.*, 1994, Cheng *et al.*, 1995). Fas is activated by its natural ligand (FasL/CD95L) enabling the formation of a multi-molecular complex

called the DISC at the cell surface. The DISC comprises a tetrameric arrangement of Fas receptors and Fas-associated protein with death domain (FADD) proteins (Scott *et al.*, 2009) and this aggregation of death domains exposes binding sites for caspase 8, which self-activates through auto-proteolysis. This in turn triggers a cascade of caspase activation that constitutes the activation phase of apoptosis.

Seven alternatively spliced transcript variants are listed in the NCBI genome annotation (Figure 4.1) however, only three have associated protein coding sequence. Bioinformatic analysis suggests that transcripts 4-7 are candidates for nonsense-mediated decay (Hillman *et al.*, 2004), explaining why no protein isoforms corresponding to these mRNA isoforms have been observed. Isoform 2 lacks exon 6 which encodes the transmembrane domain, leading to the expression of a soluble protein that may negatively regulate apoptosis (Cascino *et al.*, 1995, Papoff *et al.*, 1996). Soluble Fas expression is found to be increased in patients with systemic lupus erythematosus where it may contribute to the development of autoimmunity (Cheng *et al.*, 1994). In resting PBMCs only isoforms 1 and 6 are expressed in appreciable quantities (Liu *et al.*, 1995). Activation of PBMCs leads to increased isoform 1 expression and decreased isoform 6 expression generating an increase in cell surface Fas receptor (Liu *et al.*, 1995). This suggests that the expression of alternative transcripts represents a regulatory mechanism for Fas gene expression.

Heterozygous germ line mutations of the Fas gene have been identified in patients with autoimmune lymphoproliferative syndrome (ALPS), a condition characterised by accumulation of double negative T-cells and autoimmune responses (Drappa *et al.*, 1996). Studies of T-cells from ALPS patients have confirmed that Fas-mediated apoptosis is defective as a result of the identified mutations (Fisher *et al.*, 1995). In severe cases where immunosuppression is insufficient to relieve the symptoms of ALPS, bone

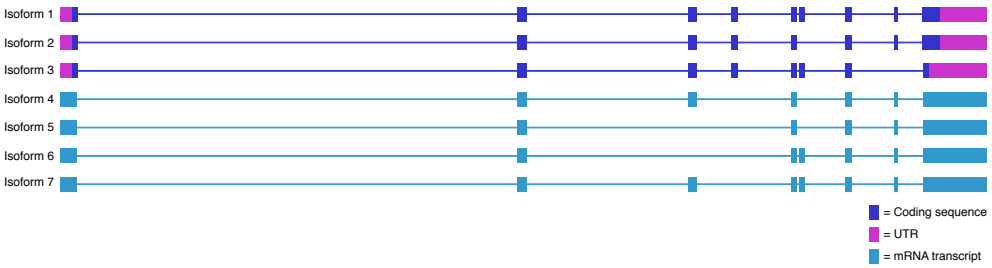

Figure 4.1: Diagram showing the exon structure of the Fas gene

marrow transplantation has been used to reconstitute the immune system with lymphocytes carrying a functional Fas receptor (Benkerrou *et al.*, 1997, Kahwash *et al.*, 2007, Sleight *et al.*, 1998). In the lpr mouse, which harbours a germ line spontaneous mutation of the Fas gene, lentiviral gene transfer has been used to introduce normal Fas cDNA into haematopoietic stem cells, leading to expression of functional Fas receptors on the surface of lymphocytes. Interestingly, ALPS patients have been found to have a significantly higher risk of both Hodgkin and non-Hodgkin lymphomas, suggesting that loss of functional Fas receptor can contribute to the development of lymphoma (Straus *et al.*, 2001).

Substantial rearrangement, allelic loss or amplification of the Fas gene has been detected at a low frequency (6/70) in non-Hodgkin lymphoma but not in 31 Hodgkin lymphoma samples (Xerri *et al.*, 1995). Somatic loss of function Fas mutations have been described in both lymphoid (Takakuwa *et al.*, 2002, Wohlfart *et al.*, 2004) and non-lymphoid (Lee *et al.*, 1999, Park *et al.*, 2001, Takayama *et al.*, 2002) malignancies and in some cases have been found to inhibit FasL induced apoptosis in a dominant negative mode (Wohlfart *et al.*, 2004). Somatic Fas gene mutations have been described rarely in tumour cells isolated from skin lesions of MF (Dereure *et al.*, 2002, Nagasawa *et al.*, 2004) whilst SSCP analysis performed in our lab by Dr. Mary Wain covering all 9 exons and the promoter region of Fas identified band shifts in 4/20 SS samples (Jones *et al.*, 2010). Sequencing of these bands revealed that one corresponded to a previously reported silent polymorphism of exon 3 (250A→G) whilst the other three anomalies were found to be single base substitutions within the promoter region (one -274C→A and two -34A→G). It remains to be determined if these mutations contribute to Fas dysregulation however, a similar frequency of promoter and exon 3 polymorphisms was observed in 20 healthy controls suggesting they play a minimal role.

The Fas gene contains a 1072bp CGI that spans the transcriptional start site and exon 1. Murine CD8+ cells have been shown to down-regulate Fas in response to *in vitro* antigen-specific restimulation, rendering the clones resistant to FasL induced apoptosis. This down-regulation of Fas could be reversed by treatment of the clones with 5aza suggesting that DNA methylation was responsible for the silencing of Fas expression. Interestingly, the same phenomenon was not observed after *in vivo* antigen-specific restimulation, indicating that whilst DNA methylation can lead to silencing of Fas expression, it may not be doing so under normal physiological conditions. There are no reports of tissue- or development-specific Fas methylation events in humans however, hypermethylation of the Fas gene promoter has been described in colon, prostatic and small cell lung carcinoma (Hopkins-Donaldson *et al.*, 2003, Petak *et al.*, 2003, Santourlidis *et al.*, 2001) and associated with decreased Fas gene expression in these malignancies. Petak *et. al.* also used 5aza to demethylate the Fas promoter in a colon carcinoma cell line, leading to induction of Fas expression and increased sensitivity to FasL induced apoptosis.

4.2 Aim

The aim of this study was to examine Fas promoter hypermethylation as a potential contributor to the dysregulation of Fas expression in tumour cell populations from patients with SS. The expression of Fas at the mRNA and cell surface protein level was first determined a cohort of SS patient PBMC samples with expression status determined by comparison with PBMCs derived from healthy controls. The methylation level across the Fas CGI was then measured in patient and healthy PBMCs to identify any hypermethylated CpG dinucleotides and these were compared with Fas mRNA expression.

4.3 Results

4.3.1 Quantification of Fas mRNA expression

qPCR was used to determine Fas mRNA expression levels in CD4+ T-cells isolated from the peripheral blood of SS patients and healthy controls. qPCR was performed using TaqMan primer/probe sets as described in Section 2.6. The TaqMan assay chosen spans intron 2 and thus should quantify expression of isoform 1 but not isoform 6 and should therefore reflect the expression of functional cell surface Fas receptor. The expression of Fas mRNA was measured in 47 SS patients and compared to average expression levels from 24 healthy controls (Figure 4.2a). Student's t-test was performed as described in Section 2.24 to compare expression between SS patient and healthy samples and revealed no difference in average expression between the two groups. It is however evident from Figure 4.2a that whilst Fas mRNA expression in the healthy control samples showed little variation, expression in SS patients was highly heterogeneous, ranging from a three fold increase to a thirty fold reduction as compared to healthy controls. A 99% confidence interval was generated to define the limits of Fas mRNA expression from the healthy control samples as described in Section 2.24. Expression from a patient sample was considered significantly different to healthy if it lay outside of this interval. Overall, 21 patients showed significant under-expression and 13 showed significant over-expression of Fas mRNA. The obtained Fas mRNA expression data represent a fold change in expression that, if displayed on a linear scale would give a two fold increase much greater prominence than a two fold decrease. For this reason, data are plotted on a logarithmic scale to allow equivalence between over- and under-expression in terms of visual deviation from the healthy average of 1.

Two samples were available from 12 patients of the original cohort, allowing investigation of changes in Fas mRNA expression over time. Figure 4.2b shows the change

in expression for each patient between their first and second samples. The general trend is towards a decrease in Fas expression over time which was shown to be significant using a pair-wise t-test ($p=0.021$) as described in Section 2.24 however, a notable subset of patients maintained a consistent level of Fas expression. Each sample was classified as either over-expressing, under-expressing or normal relative to the healthy control samples. Overall four patients remained within normal expression over time, one had consistent over-expression and two had consistent under-expression. Five patients showed a change in expression category with one decreasing from over-expression to normal expression, two decreasing from over-expression to under-expression and two decreasing from normal expression to under-expression.

To determine whether Fas expression status correlated with any of the features of blood tumour burden, Fas mRNA expression was compared to total lymphocyte count, CD4+ count, percentage CD4+, CD4:CD8 ratio and percentage Sézary cells across the patient cohort using Pearson's product-moment correlation as described in Section 2.24. It was observed that total lymphocyte count correlated very strongly with CD4+ count (correlation co-efficient=0.979 $p<0.05$) therefore only total lymphocyte count is shown in the plots in Figure 4.3. No correlation was observed between log transformed Fas mRNA quantity data and total lymphocyte count (Figure 4.3a) or percentage Sézary cells (Figure 4.3d). A weak negative correlation was observed between Fas mRNA quantity and percentage CD4+ (correlation co-efficient=-0.28 $p<0.05$)(Figure 4.3b) and between Fas mRNA quantity and CD4:CD8 ratio (correlation co-efficient=-0.30 $p<0.05$)(Figure 4.3c).

Figure 4.3 demonstrates no clear association between the observed decrease in Fas expression and changes in tumour burden suggesting this decrease is not simply due to an increase in tumour burden. Looking at the paired data samples in Figure 4.3, most

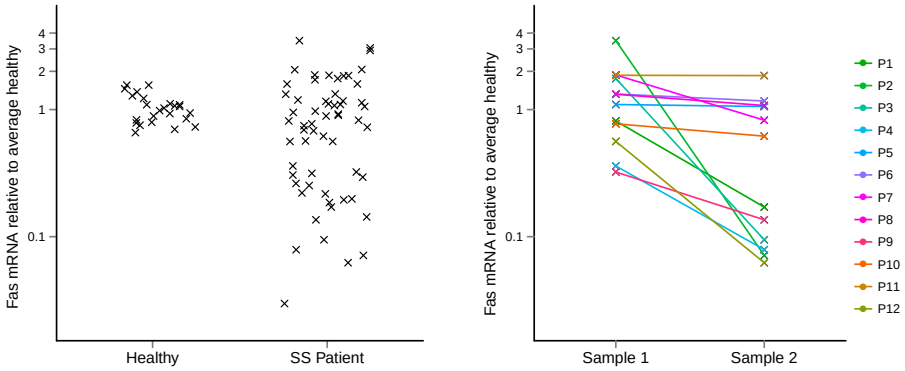

(a) (b)

Figure 4.2: Expression of Fas mRNA in SS patient samples

qPCR analysis of Fas mRNA expression in 47 SS samples expressed as a fold change in amount of mRNA relative to the average healthy control value. Measurements were performed in triplicate and normalised against Cyclophilin. (a) Comparison of the SS patient samples to the healthy controls (b) Change in Fas mRNA expression over time in 12 SS patients where a second sample was available.

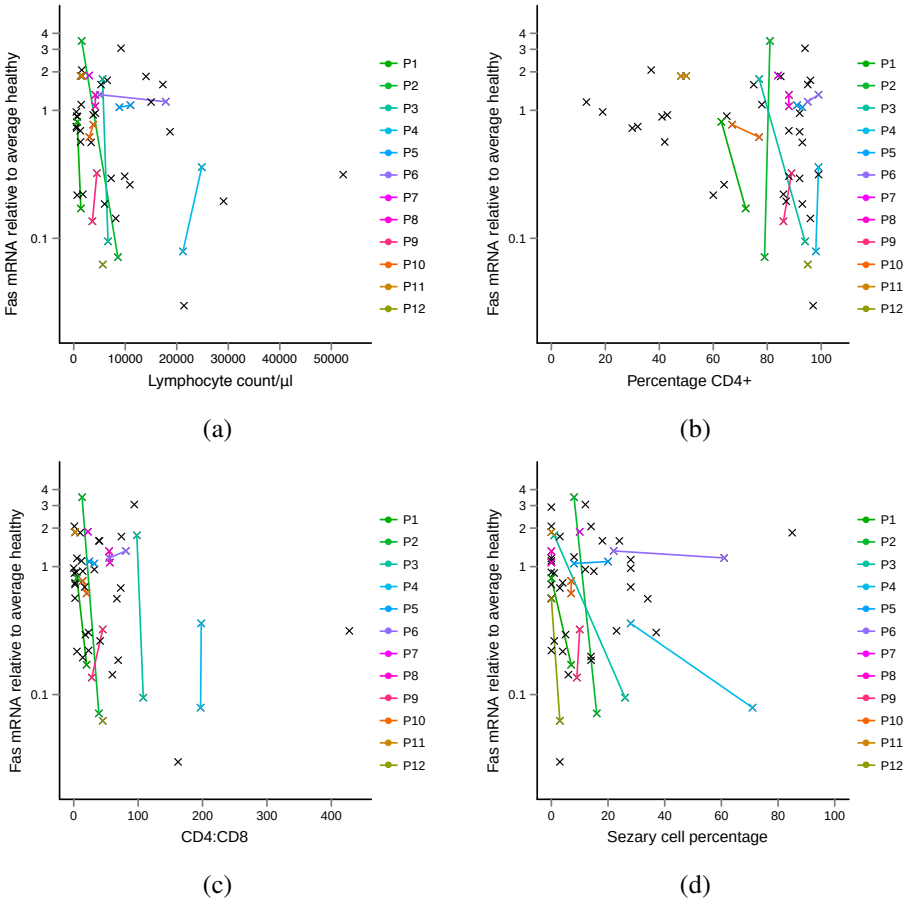

Figure 4.3: Relationship between Fas mRNA quantity and measures of tumour burden

Plots showing the relationship between quantity of Fas mRNA and: (a) Total lymphocyte count (b) Percentage CD4+ cells (c) CD4:CD8 ratio (d) Percentage Sézary cells in 59 samples taken from 47 SS patients. In the 12 cases where two samples from the same patient were measured they are connected by a line.

patients maintained fairly consistent tumour burden counts despite significant reductions in Fas expression as identified by the vertical connections. Exceptions include patient 6 (P6), where the increase in lymphocyte count and Sézary cell percentage corresponded to only a small reduction in Fas mRNA and patient 5 (P5), where the increase in Sézary cell percentage is coincident with the reduction in Fas expression however, this is not mirrored by changes in lymphocyte count, percentage CD4+ or CD4:CD8 ratio.

4.3.2 Quantification of Fas cell surface protein expression

To validate the Fas mRNA expression data the level of cell surface protein expression of Fas on the CD3+CD4+CD45RO+ T-cell population was determined by flow cytometry using PBMCs from 10 SS patients and 6 healthy controls as described in Sections 2.18 and 2.19. Cell surface Fas expression was also examined on the Sézary cell lines SeAx and HuT78 and the MF cell line MyLa. Figure 4.4 shows representative Fas histogram plots for one healthy individual (H6), two SS patients (P3, P17) and the cell lines. Whilst HuT78 and MyLa expressed Fas, SeAx displayed a complete absence of cell surface Fas protein.

The proportion of Fas positive cells within the CD3+CD4+CD45RO+ population was calculated for each sample (Figure 4.5a). Consistent with previously published work (Miyawaki *et al.*, 1992), nearly all of the memory T-cells in healthy control samples expressed Fas protein on their cell surface (range: 95.2-99.4% Fas +ve). Patient samples however showed loss of cell surface Fas expression in a proportion of their memory T-cells (range: 1.5-96% Fas +ve). Patient samples were considered significantly different to healthy if the proportion of Fas positive cells within the CD3+CD4+CD45RO+ cell population was less than 80.7% (mean healthy proportion - 10 standard deviations). The threshold was defined more stringently than the usual 99%

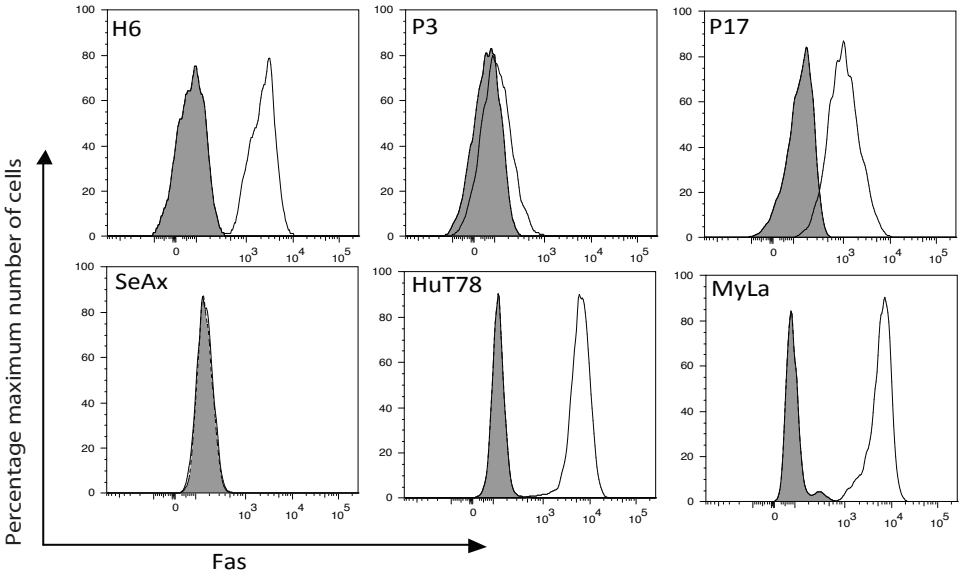

Figure 4.4: Fas cell surface protein expression by flow cytometry

Histogram plots showing the expression of Fas in one healthy control (H6), two SS patients (P3 and P17) and the SeAx, HuT78 and MyLa cell lines. The isotype control is shown with the curve filled in grey.

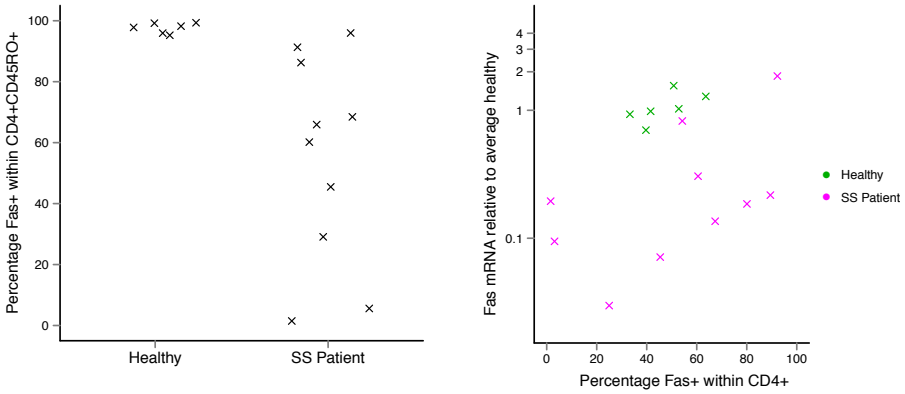

(a) (b)

Figure 4.5: Fas cell surface protein expression in SS patient samples

PBMCs from 6 healthy controls and 10 SS patients were stained with antibodies against CD3, CD4, CD45RO and Fas and 10,000 events per sample were acquired on a FACSAriaII. (a) Percentage Fas+ cells were assessed in the CD3+CD4+CD45RO+ populations and compared between SS patient samples and healthy controls (b) Correlation of Fas mRNA quantity with percentage Fas+ in the CD3+CD4+ subset.

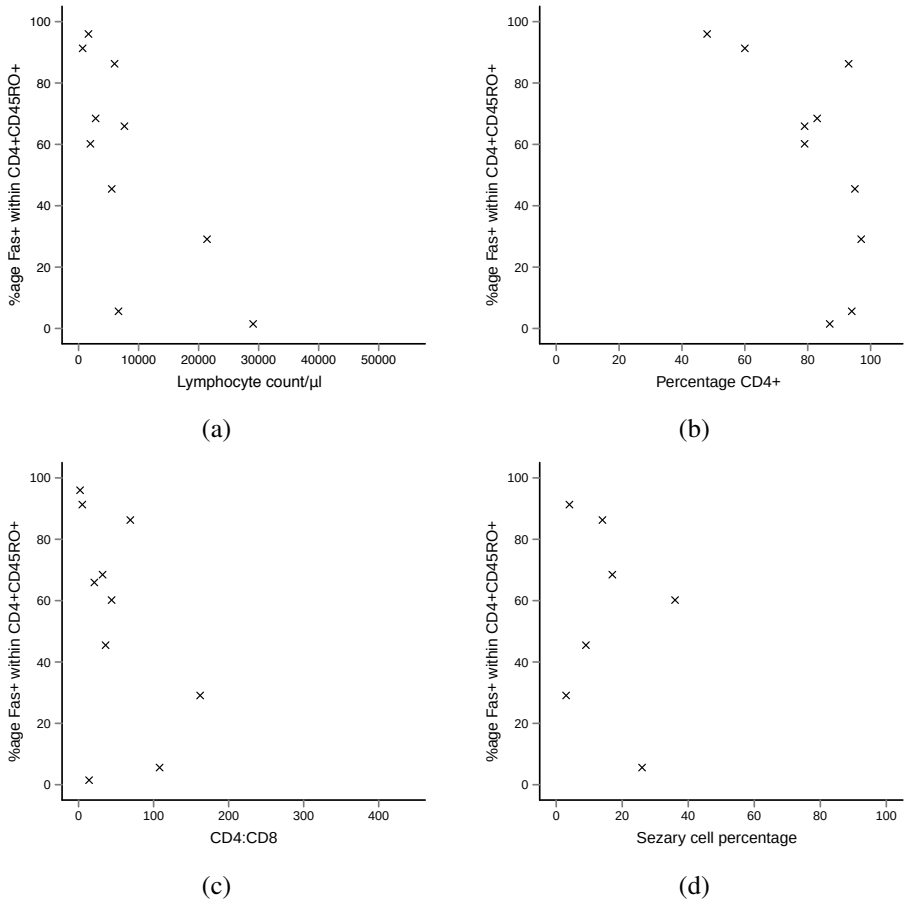

Figure 4.6: Relationship between Fas cell surface protein expression and measures of tumour burden

Plots showing the relationship between percentage Fas+ cells within the CD4+CD45RO+ subset and: (a) Total lymphocyte count (b) Percentage CD4+ cells (c) CD4:CD8 ratio (d) Percentage Sézary cells in 10 SS patient samples. Three patients did not have a Sézary cell count associated with the sample used for flow cytometry so only 7 SS patients are included in part (d).

interval using three standard deviations because of the small number of healthy samples measured and the lack of deviation between them. Whilst this may be indicative of the population wide results, without further measurements it is difficult to extrapolate and use of 10 standard deviations was considered necessary to ensure only those samples with very definite loss of Fas cell surface protein expression were classified as having loss. Overall 7/10 SS patients showed a significant loss of Fas cell surface protein expression on their memory T-cell population.

Since Fas functions at the cell surface it was of interest to establish whether Fas mRNA quantity accurately reflected the quantity of Fas protein at the cell surface. SS patient samples show a positive correlation between relative quantification of Fas mRNA in the CD4+ population and the percentage Fas+ cells within the CD4+ population (correlation co-efficient=0.53) (Figure 4.5b) however the correlation does not reach significance ($p=0.11$). This may be due to the use of a proportion of positive cells as the measurement for Fas protein where each cell may have different expression levels. Absolute mean fluorescent intensity values cannot however be used as these data were obtained in multiple experiments and therefore the absolute fluorescence level is not comparable between the sets of samples.

The relationship between cell surface Fas and measures of tumour burden was also assessed. No correlation was observed between percentage Fas+ cells within the CD3+CD4+CD45RO+ subset and CD4:CD8 (Figure 4.6c) or percentage Sézary cells (Figure 4.6d) however, a negative correlation was observed between percentage Fas+ cells within the CD3+CD4+CD45RO+ subset and lymphocyte count (correlation coefficient=-0.725, $p<0.05$) (Figure 4.6a) and between percentage Fas+ cells within the CD3+CD4+CD45RO+ subset and percentage CD4+ (correlation coefficient=-0.661, $p<0.05$) (Figure 4.6b).

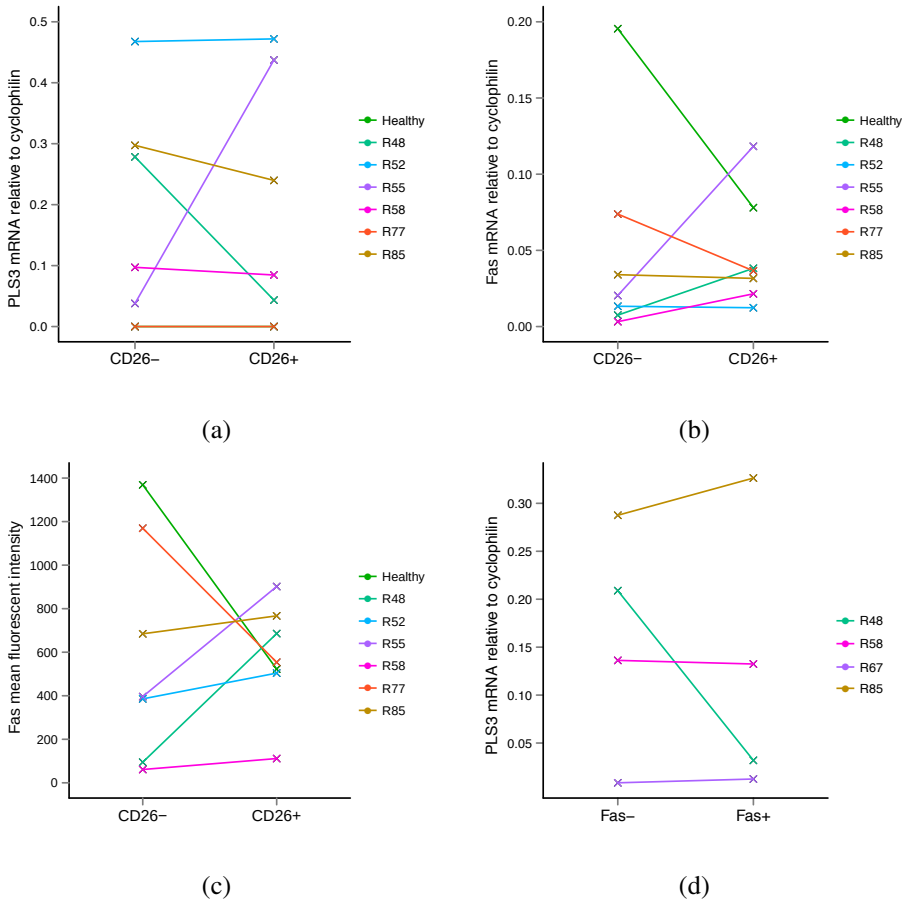

Figure 4.7: PLS3 and Fas expression within FACS sorted SS patient cells

Lymphocytes from six SS patients and one healthy control were stained and sorted into subsets prior to mRNA extraction and qPCR: (a) PLS3 mRNA distribution was compared between CD26- and CD26+ subsets. The healthy control demonstrated no PLS3 mRNA in either subset. (b) Fas mRNA distribution was compared between CD26- and CD26+ subsets (c) Fas mean fluorescent intensity distribution was compared between CD26- and CD26+ subsets (d) PLS3 mRNA distribution was compared between Fas- and Fas+ subsets. Only four samples were available for analysis in this experiment, R67 is a sample from the same patient as R55 taken one month later.

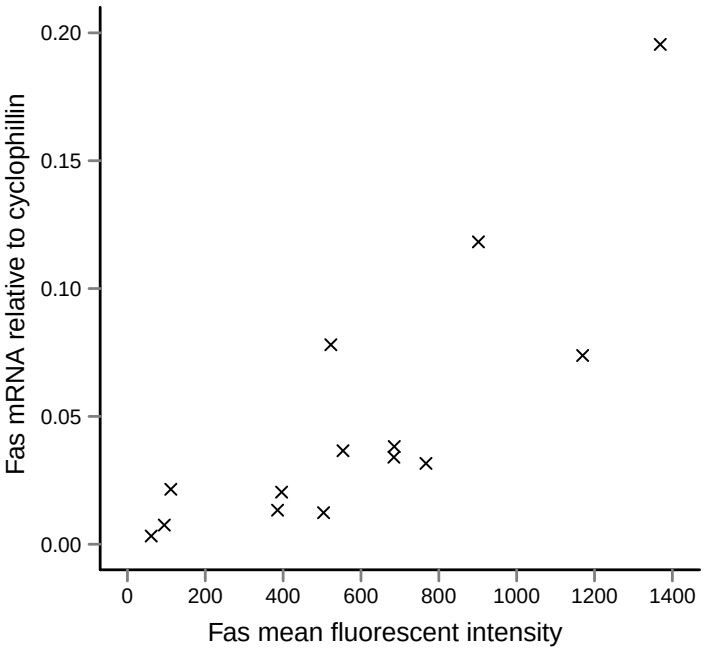

Figure 4.8: Correlation between Fas protein and mRNA

Mean fluorescent intensity of Fas cell surface protein expression was compared to Fas mRNA expression in both CD26- and CD26+ subsets from six SS patients and one healthy control.

When this work was submitted for publication it was suggested by the reviewers that loss of the cell surface marker CD26 could help further identify the tumour cell population to establish whether Fas loss was restricted to these cells. This was based upon the assumption that the frequent loss of CD26 in SS patients (Jones *et al.*, 2001) is restricted to the tumour cell population. To determine whether this was the case, anti-CD26 antibody was added to the FACS antibody staining cocktail and the CD3+CD4+CD45RO+CD26+ and CD3+CD4+CD45RO+CD26- subsets were isolated as described in Section 2.20. RNA was extracted and qPCR used to detect the expression of PLS3 in each subset as described in Sections 2.3, 2.4 and 2.6. Since PLS3 is not normally expressed in any haematopoietic cells (Lin *et al.*, 1993b) but is expressed in a proportion of SS patients the expression of PLS3 is likely to be unique to the malignant cells. An enrichment for PLS3 would therefore be expected in the CD26- subset if loss of CD26 expression is an immunophenotypic marker of the tumour cells. The approach of sorting cells and extracting mRNA for analysis was chosen because no antibody was available at the time for the detection of PLS3 through flow cytometry. In five SS patients, both CD26+ and CD26- subsets had detectable PLS3 expression and a paired t-test revealed no significant difference between the two subsets (Figure 4.7a). One healthy and one SS patient sample showed no PLS3 expression in either subset and the absence of PLS3 mRNA was further confirmed in the corresponding PBMC samples. Fas mRNA expression (Figure 4.7b) and Fas mean fluorescent intensity (Figure 4.7c) were also assessed in each subset. Results from the healthy control sample suggest that Fas is more highly expressed in the CD26- subset than the CD26+ subset however, no pattern is seen within the SS patient samples with no significant difference between CD26- and CD26+ subsets on either the mRNA or protein level using a paired t-test.

To investigate whether loss of Fas could be used as a marker to enrich for tumour

cells, stained cells were also sorted into CD3+CD4+CD45RO+Fas+ and CD3+CD4+-CD45RO+Fas- subsets and examined for PLS3 expression (Figure 4.7a). Sample R67 was taken from the same patient as R55 but one month later. R48 does show an enrichment for PLS3 expression in the Fas- subset suggesting that in this case the Fas- cells may further define the tumour cell subset however, the other three samples show roughly equivalent expression between Fas- and Fas+ subsets suggesting that Fas is not a consistent marker of the tumour cell population. Since these experiments generated absolute quantification of Fas mRNA and protein in identical populations, the two measurements were compared (Figure 4.8). This demonstrated a strong correlation between Fas mRNA expression and cell surface protein expression (correlation co-efficient=0.816 $p<0.01$) suggesting that Fas mRNA quantity accurately reflects cell surface protein expression and the failure to achieve a significant correlation between Fas mRNA and cell surface protein expression in Figure 4.5b was in fact due to the limitation of using percentage positive cells as a proxy for absolute quantity of Fas protein.

4.3.3 SSCP analysis of Fas promoter and coding sequence

As mentioned previously, SSCP analysis had already been used to establish that the frequency of Fas promoter and coding sequence polymorphisms within a cohort of 20 SS samples was similar to that observed in 20 healthy controls (Jones *et al.*, 2010). PBMC DNA samples from patient 3 (P3), patient 14 (P14) and the SeAx cell line were subject to further SSCP analysis as described in Section 2.13 to determine if promoter or coding sequence polymorphisms were contributing to the down-regulation of Fas in these samples. P3 and P14 were selected because less than 10% of their CD3+CD4+CD45RO+ population expressed cell surface Fas protein suggesting a substantial down-regulation of Fas had occurred in these samples. Similarly, Fas mutations

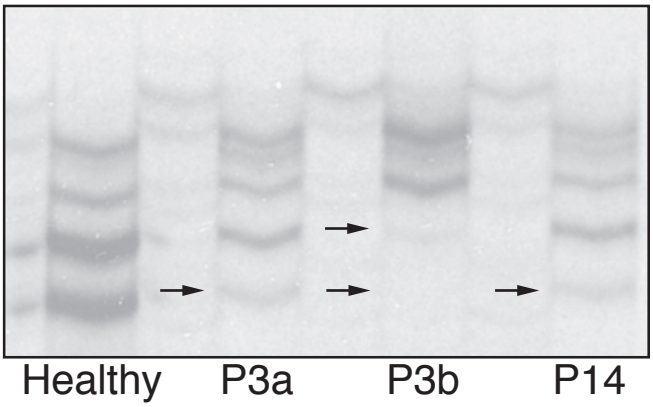

Figure 4.9: SSCP analysis of the Fas gene in SS patients

Sequential samples from Patient 3 and one sample from Patient 14 who showed minimal cell surface protein expression of Fas by flow cytometry; arrows indicate the decreased intensity of bands in exon two consistent with allelic loss.

were further investigated in the SeAx cell line because it showed a complete absence of cell surface Fas expression.

PCR amplification of SeAx DNA revealed no bands for any of the exons of the Fas gene, suggesting that the Fas gene has been deleted in this cell line. Further investigation revealed a complete absence of Fas mRNA in SeAx cells in addition to the absence of Fas protein. In the two patients who showed minimal cell surface Fas expression, SSCP analysis revealed a loss of some bands using primer pairs 1.1 (P3a, P3b and P14), 2 (P3a, P3b and P14) and 3 (P14). This suggests that allelic loss of some exons may have occurred in the malignant cells of these patients (Figure 4.9).

4.3.4 Pyrosequencing analysis of the Fas CGI

To establish if promoter methylation contributes to the down-regulation of Fas gene expression in CTCL, Pyrosequencing was used as described in Section 2.11 to elucidate the methylation status of the 74 CpG dinucleotides within the Fas CGI in healthy and CTCL patient PBMC samples. Assays F5-F18 (Tables 2.3 and 2.4) were designed to cover the whole CGI and optimised as described in Section 3.3.4. The sensitivity of the assays was tested using DNA that had been artificially methylated using the *M.Sss*I CpG methyltransferase enzyme as described in Section 2.8 and then mixed in varying proportions with unmethylated DNA prior to bisulphite conversion. Average methylation across the CGI was plotted for each of these mixtures (Figure 4.10), this shows a linear relationship across the entire range of measurements suggesting no PCR bias. However, the graph only achieved a maximum methylation measurement of 80%. This is likely to be due to the CpG methyltransferase reaction not proceeding to completion rather than any deficiency in the actual measurement. Controls were also incorporated to check the detection limit of the Pyrosequencer and the completion of the bisulphite conversion as described in Section 3.3.4.

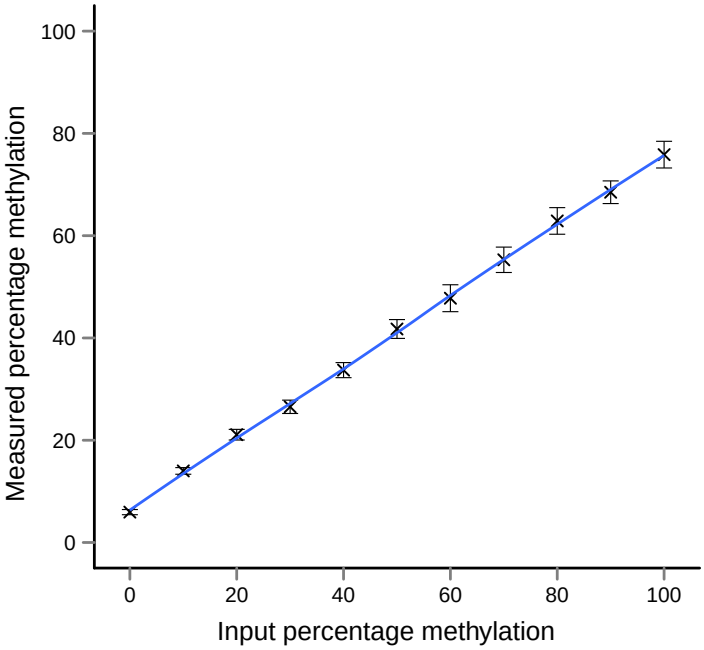

Figure 4.10: Assessment of Fas Pyrosequencing assay sensitivity

Mixtures of artificially methylated and unmethylated DNA were quantified at each CpG dinucleotide. Data represent the mean methylation across all CpG dinucleotides ± SEM. The line of best fit has been added in blue.

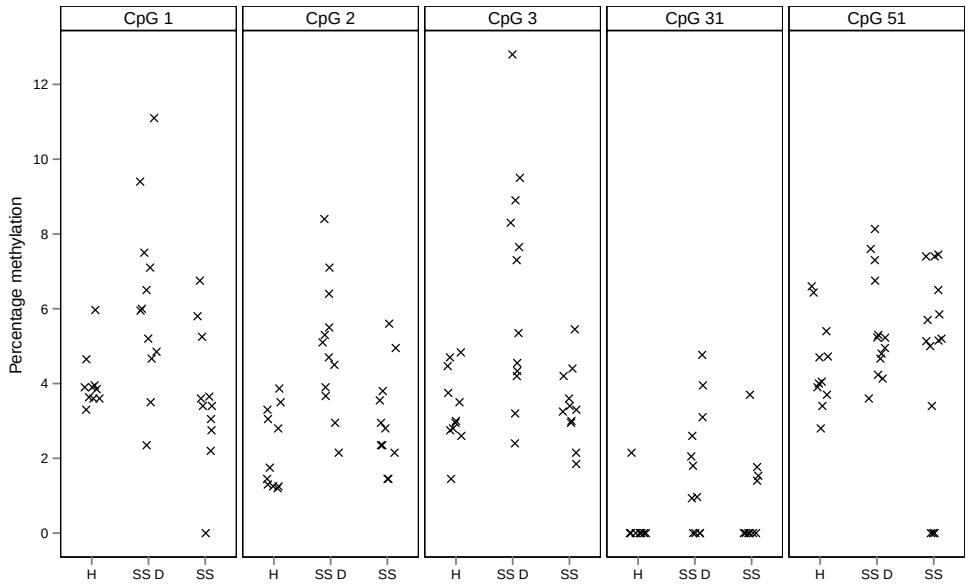

Figure 4.11: Quantification of methylation in the Fas CGI

Methylation in each sample at five CpG dinucleotides showing significantly increased methylation in SS patients with down-regulation of Fas mRNA (SS D) but not the remainder of the SS samples (SS) when compared to the 11 healthy samples (H).

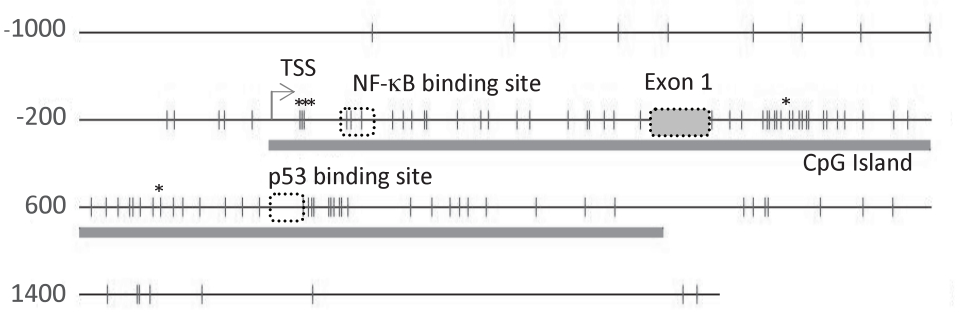

Figure 4.12: Diagram of the Fas CpG island

Diagram of the region around the Fas promoter numbered relative to the transcriptional start site (TSS). CpG dinucleotides are marked by a vertical dash, the 5 hypermethylated CpG dinucleotides are highlighted by * and important gene regulatory elements within the CGI are marked.

Methylation of each CpG dinucleotide was then measured in bisulphite converted DNA from 10 healthy control samples and 35 patient samples comprising 16 who showed down-regulation of Fas mRNA expression, 9 who showed normal Fas mRNA expression and 10 who showed up-regulation of Fas mRNA expression. The quality control procedure within the Pyrosequencer software checks for low signal, unexpected sequence and incorrect total height of C/T variable peaks and scores each well as passed, some errors or failed. All results with errors were examined by eye to determine the cause, on several occasions the nucleotide dispensing tips had become blocked during a run and this had led to no further nucleotide incorporation peaks. Where this occurred, CpG positions measured before the blockage were manually adjusted to pass as the data up until the blockage was considered valid. In addition to this any plate where the negative controls showed signal were failed in their entirety. It was observed early on that whilst most samples had run-to-run variability of <1%, a few samples had run-to-run variance of up to 10%. Further examination revealed that all samples showing this property were generating much smaller peaks during Pyrosequencing. It was determined that the first single nucleotide peak needed to measure 100U in order to generate reproducible data. A method was therefore developed for post-processing of the data in excel in order to exclude those traces where the first single nucleotide peak measured less than 100U.

All data passing the quality control procedure were summarised as described in Section 2.24 and the percentage methylation in each CpG dinucleotide was hence determined for each sample. Wilcoxon unpaired U-test was used to compare the methylation in each group of patients with that in healthy controls at each CpG dinucleotide as described in Section 2.24. Five CpG dinucleotides (1, 2, 3, 31 and 51 numbered from the start of the CGI) were found to have significantly more methylation in the

patient group showing down-regulation of Fas mRNA expression than in healthy controls (Figure 4.11). No significant excess of methylation was observed in patients with normal Fas mRNA expression or up-regulation of Fas mRNA expression compared to healthy controls in these CpG dinucleotides. The CpG dinucleotides that showed hypermethylation in patients with down-regulated Fas mRNA expression have been highlighted on the schematic diagram of the Fas CGI shown in Figure 4.12. Also highlighted are the experimentally validated NF-κB (Chan *et al.*, 1999) and p53 (Schilling *et al.*, 2009) transcription factor binding sites and the transcriptional start site and first exon of the gene.

4.4 Discussion

Induction of an immune response following antigen challenge leads to rapid clonal expansion and differentiation of naïve T-cells resulting in a large pool of effector T-cells. During the termination phase of the immune response the vast majority of effector T-cells are eliminated via AICD with only a small proportion surviving AICD and entering the memory T-cell pool (reviewed by Krammer *et al.* (2007)). Several studies have revealed that the Fas system is highly regulated during the phases of a T-cell immune response. Resting T-cells express marginal amounts of Fas and are resistant to apoptosis (Klas *et al.*, 1993). During the activation phase Fas is up-regulated (Ju *et al.*, 1995), although short term activated effector T-cells remain resistant to AICD (Klas *et al.*, 1993), which is thought to be due to incomplete DISC formation and the presence of high levels of the apoptosis inhibitor c-FLIP (Kirchhoff *et al.*, 2000, Schmitz *et al.*, 2004). Long term activated T-cells express comparable levels of Fas to short term activated T-cells but have complete DISC formation with concomitant down-regulation of c-FLIP expression and are therefore sensitive to Fas-mediated AICD (Dhein *et al.*, 1995). Given the fundamental role of the Fas system in the development of a T-cell

response and the dysregulation of T-cell signalling observed in CTCL, dysregulation of Fas represents a strong candidate pathomechanism in the development of CTCL.

This study observed a distinct heterogeneity in Fas mRNA levels, with significant under-expression in 21/47 (45%) and over-expression in 13/47 (28%) of patient-derived CD4+ T-cells compared to healthy controls (Figure 4.2a). These data are consistent with the findings of Contassot *et al.* (2008) who reported disparity in the levels of Fas expression in a cohort of 16 SS patients. Furthermore, analysis of samples taken at least 6 months apart demonstrated a trend for decreased Fas mRNA expression over time (Figure 4.2b). No clear correlation between Fas expression and tumour burden was observed (Figure 4.3) however, review of the clinical observations suggested that those patients with the most significant reduction in Fas mRNA expression had experienced an increase in disease severity over time. Because of the small numbers of patients studied these observations remain speculative and it would be of great interest to perform a longitudinal study of Fas expression to determine how closely it relates to disease progression. Immunostaining of MF lesions has been used to show that loss of Fas expression occurs in a greater proportion patients with tumour stage or CD30 negative large cell transformed disease than in plaque stage disease (Zoi-Toli *et al.*, 2000). Staining of serial samples from patients who had progressed from plaque-stage to tumour-stage MF identified a significant decrease in Fas expression associated with disease progression (Zoi-Toli *et al.*, 2000). Taken together, these results suggest that Fas expression level may be linked to disease progression across the whole spectrum of CTCL in both circulating and skin-restricted disease.

Examination of the cell surface protein expression of Fas using flow cytometry validated the observed down-regulation of Fas mRNA expression in Sézary cells (Figure 4.5). Sézary cells are generally derived from CD3+CD4+CD45RO+ memory T-cells and show variable loss of expression of CD7 and CD26 (Steinhoff *et al.*, 2009).

At present there are no tumour-specific cell surface biomarkers available to isolate Sézary cells. In this study it was demonstrated that loss of CD26 does not clearly distinguish between Sézary and reactive cell populations (Figure 4.7a). In healthy individuals a large proportion of the CD4+CD45RO+ T-cell population show cell surface Fas expression (Miyawaki *et al.*, 1992, Muench *et al.*, 2003), consistent with the findings reported here demonstrating Fas expression in at least 95% of the CD3+-CD4+CD45RO+ T-cells. In contrast, loss of Fas expression was observed in 7/10 SS patients affecting between 32% and 94% of the CD4+CD45RO+ population and was associated with down-regulation at the mRNA level. The detection of tumour cells within both the Fas- and Fas+ subsets and the CD26- and CD26+ subsets highlights the marked heterogeneity present within the tumour cell population which has previously been reported by our lab in relation to CD25 expression (Tiemessen *et al.*, 2006) and will be investigated further in Chapter 5.

Loss of cell surface Fas expression has been reported in several studies of SS lymphocytes and cell lines (Contassot *et al.*, 2008, Dereure *et al.*, 2000, Osella-Abate *et al.*, 2001, Wu *et al.*, 2009) and is associated with the failure of extracorporeal photochemotherapy to generate haematological remission (Osella-Abate *et al.*, 2001). Contassot *et al.* (2008) demonstrated that SS lymphocytes displaying both over- and under-expression of Fas show resistance to apoptosis and further established that over-expression of of the inhibitory protein c-FLIP was responsible for the observed resistance to apoptosis in the patient group showing over-expression of Fas. The mechanism mediating down-regulation of Fas has not yet been determined and down-regulation of Fas was the dominant mode of Fas dysregulation in the patient cohort investigated here. Therefore this study focussed on further investigation of the patient group exhibiting down-regulation of Fas. To address putative molecular mechanisms that may mediate the observed down-regulation of Fas in Sézary cells, a comprehensive mutational

scan of the Fas gene was performed and the CGI around the Fas promoter region was analysed for methylation events.

Two mutational studies of Fas have been performed in MF, reporting mutations in 14% and 18% of cases respectively (Dereure *et al.*, 2002, Nagasawa *et al.*, 2004). As mentioned in Section 4.1, SSCP studies by Dr. Mary Wain have identified a polymorphism of exon 3 in 1/20 SS patients and 1/20 healthy controls (Jones *et al.*, 2010). Promoter polymorphisms were also found in 3/20 SS patients and 2/20 healthy controls suggesting that, while the functional relevance of these polymorphisms are unknown, they are unlikely to contribute to the down-regulation of Fas in SS. In the current study, SSCP was used to further investigate the Sézary cell line SeAx, which has no cell surface Fas expression, and two SS patients in which less than 10% of CD3+CD4+CD45RO+ T-cells displayed cell surface Fas expression. The SeAx cell line was found to have a deletion of all exons of the Fas gene resulting in the complete absence of Fas protein and mRNA. This observation is supported by a FISH study that found the Fas gene to be completely absent in SeAx (Wu *et al.*, 2011). No disruption of the neighbouring PTEN gene was observed, suggesting that the region of deletion is relatively small . Wu *et al.* (2011) also found an increased prevalence of the germline -671 GG SNP within their CTCL cohort than was recorded in the control cohort. Functional analysis demonstrated no effect on basal Fas expression but this SNP did affect interferon induced up-regulation of Fas, suggesting that this SNP, which was not covered by the SSCP primers used for mutational screening of Fas, may contribute towards a dynamic imbalance in Fas expression during immune responses. In the two SS patient samples examined by SSCP no band shifts were observed, suggesting that no mutations were present. However, in exons 1, 2 and 3 there was a notable reduction in the band intensity of some bands suggesting that allelic loss may have occurred in

these exons (Figure 4.9). These results lead to the conclusion that specific Fas mutations are uncommon in SS however, given that loss of heterozygosity in the region of 10q23.31 spanning the Fas gene has been detected in 50% of SS patients (Vermeer *et al.*, 2008, Wain *et al.*, 2005) it is likely that chromosomal deletion/loss may also contribute to loss of Fas protein expression in SS.

Epigenetic events are known to be a critical mechanism of gene dysregulation in malignancy and aberrant Fas promoter methylation with associated loss of Fas expression has been previously described in colon, prostatic and small cell lung carcinoma (Hopkins-Donaldson *et al.*, 2003, Petak *et al.*, 2003, Santourlidis *et al.*, 2001). Recent studies of disease-specific methylation events have demonstrated that complex methylation patterns exist within CGIs (Brakensiek *et al.*, 2007). As discussed in Section 1.2.3 a wide variety of methods exist for determining the methylation status of DNA. This study required a technique that specifically examined the Fas promoter region in detail and could detect methylation in a mixed population of cells. MSP, using primers specific to the bisulphite converted sequence to detect methylated DNA, has previously been used to detect methylation of the Fas CGI (Hopkins-Donaldson *et al.*, 2003, Petak *et al.*, 2003, Santourlidis *et al.*, 2001) however it only allows examination of a limited number of CpG dinucleotides in positions suitable for primer design. Petak *et al.* (2003) and Santourlidis *et al.* (2001) investigated some samples in further detail using direct sequencing of bisulphite converted DNA however this is only useful in cell lines or pure populations of tumour cells. Pyrosequencing of bisulphite converted DNA was therefore chosen as the most suitable method as it facilitates the examination of each individual CpG dinucleotide within a CGI to allow a thorough evaluation of the methylation status across the whole island (Brakensiek *et al.*, 2007, Oprea *et al.*, 2008, Tost *et al.*, 2003). In addition, this technique allows quantitative detection of changes in methylation in a mixed cell population and

therefore is ideally applicable to the study of SS cells, overcoming the problems of analysis of a heterogeneous population of tumour cells admixed with non-malignant cells. Five hypermethylated CpG dinucleotides within the Fas CGI were found to be significantly associated with reduced Fas expression in SS patients. It is recognised that the methylation status of even a single CpG within a CGI can be responsible for the control of tissue-specific gene expression (Arányi *et al.*, 2005, Kitazawa & Kitazawa, 2007) and for aberrant gene silencing in cancer (Zou *et al.*, 2006). Three of the hypermethylated CpG dinucleotides in the Fas promoter are clustered around the transcriptional start site and therefore could be directly responsible for preventing the binding of the transcriptional machinery. Furthermore, other studies of the Fas CGI have identified hypermethylation of CpG dinucleotides located at or near transcription factor binding sites, namely the p53 binding site in colon carcinoma (Petak *et al.*, 2003) and the NF-κB binding site in prostatic carcinoma (Santourlidis *et al.*, 2001). Other mechanisms by which DNA methylation affects gene expression include recruitment of methyl-binding domain proteins that impair binding of transcriptional machinery and recruitment of histone modifying factors inducing condensation of the local chromatin structure (Newell-Price *et al.*, 2000).

At present there is no direct functional evidence to provide a link between hypermethylation, Fas expression and resistance to apoptosis in primary SS lymphocytes. Such studies are currently impossible since the demethylating effect of 5aza requires cellular proliferation in order to become incorporated into DNA and prevent maintenance of methylation. As discussed in Section 1.1.4, primary cultures of Sézary cells do not proliferate to any significant degree and therefore cannot be used for such studies. The commonest SS cell lines SeAx and HuT78 respectively exhibit homozygous deletion of the Fas gene and absence of methylation of the Fas CGI. However, studies of human colon carcinoma cell lines demonstrating hypermethylation of Fas and

reduced Fas expression, show that Fas expression and Fas-mediated apoptosis can be restored by treatment with demethylating agents (Petak *et al.*, 2003). Since this study was completed, Wu & Wood (2011) have published data investigating Fas methylation in some additional CTCL cell lines. In line with the data presented here, they found no methylation within the Fas CGI of HuT78 and also found no methylation in the MF cell line MyLa. They did however find positional methylation in the SS cell line Sez-4, which correlated with low Fas expression at both the mRNA and protein levels. They further demonstrated that the magnitude of methylation could be reduced by treatment with 5aza and that this led to increased Fas expression and corresponding increased sensitivity to FasL. Interestingly, they also showed that increased DNA methylation correlated with decreased NF-κB binding to the Fas promoter and that demethylation with 5aza led to increased NF-κB binding, supporting the proposal that hypermethylation of CpG dinucleotides is directly preventing the binding of transcription factors to the Fas promoter.

It is now apparent that in addition to loss of heterozygosity in the Fas gene locus, multiple molecular mechanisms can mediate Fas dysregulation and resistance to apoptosis in SS. A recent study (Wu *et al.*, 2009) reported similar findings to those reported here by identifying reduced Fas expression in SS and in CTCL cells from lesional skin of MF patients. Reduced Fas expression was shown to correlate with loss of sensitivity to Fas-mediated apoptosis. Contassot *et al.* (2008) have demonstrated that in SS patients with over-expression of Fas, resistance to Fas-mediated apoptosis is still observed and can be attributed to a concomitant increase in expression of the apoptosis inhibitory protein c-FLIP. Another study, Klemke *et al.* (2009), suggests that attenuated TCR signalling leading to loss of FasL up-regulation also contributes to apoptosis resistance in patients with normal expression of Fas. Fas-mediated apoptosis represents a key mechanism underlying AICD. These findings all combine to suggest that

dysregulation of Fas signalling plays a pivotal role in the pathogenesis of SS and occurs via a myriad of mechanisms.

In summary, this study of a large cohort of SS patients demonstrates that down-regulation of Fas gene expression is a common feature of Sézary cells. Mutational events were found to be uncommon and are not linked to the observed loss of Fas expression in the majority of patients. Significantly, aberrant promoter hypermethylation appears to be the most frequent mechanism that is associated with loss of Fas expression in SS.

PLS3

5.1 Introduction

T-plastin, encoded by the PLS3 gene on chromosome Xq23, is an actin bundling protein composed of four calponin homology actin-binding domains and one EF-hand motif containing two calcium binding sites. Three transcript variants are listed in the RefSeq database, each comprising 16 exons. Transcripts 1 and 2 differ only in the 5'-UTR and are predicted to generate a 630 amino acid protein whilst transcript 3 uses an alternative splice site in exon 2 to generate a 603 amino acid protein. However, transcripts 2 and 3 are based upon bioinformatic analysis of the genomic sequence and a literature search revealed no experimental evidence to support their existence whereas transcript 1 is well characterised (Lin *et al.*, 1988, 1990, 1993b). Therefore for the purposes of this study, only transcript 1 was considered.

PLS3 is one of a family of closely related plastin isoforms, displaying 80% identity with L-plastin and 75% identity with I-plastin. All three isoforms have the same domain structure (Figure 5.1), binding actin in a calcium dependent manner. The three plastin isoforms are expressed in a highly tissue-specific manner, in healthy tissue L-plastin is restricted to haematopoietic cells (Lin *et al.*, 1993b) whilst I-plastin is expressed in the small intestine, colon and kidneys (Lin *et al.*, 1994). PLS3 is more widely expressed in all cells of solid tissues with replicative potential but crucially is not expressed in any haematopoietic compartment (Lin *et al.*, 1993b). Overproduction of T- or L- plastin in epithelial cell lines leads to isoform-specific shape changes (Arpin *et al.*, 1994) suggesting that, despite their sequence similarity, the plastin isoforms

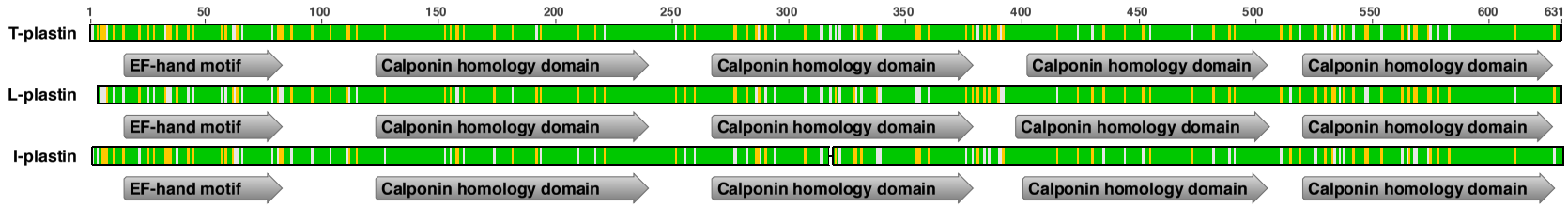

Figure 5.1: Alignment of the three plastin isoforms

The three plastin isoforms were aligned in Geneous to generate a consensus amino acid sequence. Each residue was then compared to the consensus and coloured by similarity. Green residues are 100% similar to consensus, yellow residues are 60-100% similar and white residues are <60% similar. Also highlighted are the EF-hand motif, which contains two calcium binding sites, and the calponin homology domains, which each contain an actin-binding site.

each function differently. L-plastin is the most thoroughly characterised of the plastin isoforms, becoming rapidly phosphorylated in response to IL-2 stimulation in T-cells (Zu *et al.*, 1990) and enabling T-cell signalling through the formation of the immunological synapse (Wang *et al.*, 2010). As discussed in Section 1.1.4, the aberrant expression of L-plastin in solid tissue malignancies leads to enhanced tumour invasiveness (Foran *et al.*, 2006, Klemke *et al.*, 2007), presumably through its ability to influence cytoskeletal rearrangement. PLS3 is believed to be involved in responding to DNA damage (Ikeda *et al.*, 2005, Sasaki *et al.*, 2002), a theory that is supported by its over-expression in cells resistant to agents that cause DNA damage such as cisplatin (Hisano *et al.*, 1996) or UV light (Higuchi *et al.*, 1998). PLS3 has also been suggested to play a role in regulating actin dynamics (Giganti *et al.*, 2005) and thus may be involved in cell motility. I-plastin appears to have a less dynamic function maintaining the structure of the intestinal brush border microvilli (Grimm-Günter *et al.*, 2009).

In SS, PLS3 expression has been identified at the mRNA level in peripheral blood lymphocytes by a representational difference analysis study searching for potential biomarkers (Su *et al.*, 2003). The aberrant expression of PLS3 in SS was subsequently confirmed by several microarray studies (Booken *et al.*, 2008, Kari *et al.*, 2003, van Doorn *et al.*, 2004) and proposed as part of a five gene qPCR expression signature for SS (Nebozhyn *et al.*, 2006). Interestingly, aberrant expression of L-plastin has been described as a marker for many human cancer cells of non-haematopoietic origin (Lin *et al.*, 1993b) and aberrant L-plastin expression has been shown to enhance the invasiveness of colon cancer cells (Foran *et al.*, 2006). Given the stringency of tissue restricted plastin isoform expression and its potential role in cytoskeletal rearrangements, which are vital to T-cell migration and activation, aberrant expression of PLS3 could be crucial to the development of SS however, it is unclear how widespread this alteration is within the SS patient population.

The mechanism by which aberrant expression of PLS3 occurs in SS has not yet been addressed and could provide valuable insight into the pathogenesis of the disease. One study has defined the basal promoter region of the PLS3 gene and identified a putative enhancer (Lin *et al.*, 1999) that could be affected by somatic mutations. The PLS3 gene also harbours a 1585bp CGI that has been shown to display partial or complete methylation in K562, Jurkat, CEM and Molt-4 cell lines, which do not express PLS3, and no methylation in HT-1080, HuT-12 and MCF-7 cell lines, which do express PLS3 (Lin *et al.*, 1999). However, this study also identified no methylation within the PLS3 CGI in primary lymphocytes, suggesting that the cell lines may not accurately reflect the situation in primary tissues. The choice of method, methylation sensitive restriction enzyme digest followed by Southern blotting, also restricts this study to examination of a few CpG dinucleotides rather than the whole CGI so it is possible that methylation of another region of the CGI could play a part in the regulation of PLS3 expression.

Diagnosis of SS and MF is made using a combination of clinical, histological and molecular features since there are no characterised biomarkers unique to CTCL. In SS, a measure of circulating tumour burden can be obtained by visual inspection of a blood smear to quantify those cells with abnormal cerebriform nuclei. Whilst large Sézary cells can be easily identified, the majority of patients have small Sézary cells that can be difficult to distinguish from normal activated T-cells on morphology alone (van der Loo *et al.*, 1981). Since PLS3 is not normally expressed by any cell of haematopoietic origin it has the potential to be used as a biomarker for the tumour cells if it is found to be present on the whole population of Sézary cells.

Previous studies have suggested a characteristic phenotype typical of SS including loss of CD7 (Haynes *et al.*, 1981), loss of CD26 (Jones *et al.*, 2001), and presence of CD158k (Bagot *et al.*, 2001). Increasingly, these phenotypic features are being used in

research studies to enrich for the malignant cells (Contassot *et al.*, 2008, Yoon *et al.*, 2008). However, a study comparing the utility of the different phenotypic markers as diagnostic tools concluded that no individual marker is present in all cases and a combination of markers is required for flow cytometric diagnosis (Klemke *et al.*, 2008). In addition, genetically defined tumour cells have been identified in FACS sorted CD7 and CD26 positive subsets from SS patient samples (Steinhoff *et al.*, 2009), suggesting that these markers may not be appropriate for enrichment of the malignant cell population. PLS3 expression could also be used as a tool to evaluate the utility of these proposed markers for the identification of SS tumour cells.

5.2 Aim

The aim of this study was to assess the extent of aberrant PLS3 expression in a cohort of CTCL patients and to examine PLS3 mutations and promoter hypomethylation as potential regulatory mechanisms leading to the aberrant expression of PLS3 in SS. A further goal was to test the utility of PLS3 as a marker for malignant cells and use this tool to investigate immunophenotypic heterogeneity in SS.

5.3 Results

5.3.1 Assessing aberrant expression of PLS3 mRNA

RT-PCR primers specific to PLS3 were first optimised in order to confirm the expression of PLS3 in SS patient lymphocytes but not in healthy control lymphocytes. The primer sequences, reaction conditions and expected product size are listed in Table 2.1. RNA and cDNA were prepared as described in Section 2.3 and Section 2.4 and RT-PCR was performed as described in Section 2.5. The primers were carefully designed

in order to prevent cross-reaction with either L- or I- plastin. RT-PCR primers were tested on cell line cDNA, demonstrating the presence of abundant PLS3 mRNA in HEK293 cells and primary keratinocytes, presence of PLS3 mRNA in HuT78 and SeAx cells and no expression in MyLa or Jurkat cells. Examination of a group of SS patient lymphocyte samples demonstrated PLS3 expression in approximately 70% of patients whilst no PLS3 mRNA was detected in healthy control lymphocyte samples (representative data shown in Figure 5.2).

A large variability in RT-PCR band intensity was observed, suggesting a substantial range of expression levels of PLS3 mRNA may be present within the patient cohort. To quantify the aberrant expression of PLS3 more accurately, qPCR with primers specific to PLS3 was performed and expressed relative to Cyclophilin mRNA as described in Section 2.6. qPCR was able to detect a negligible amount of PLS3 mRNA in 11 healthy controls representing only 0.001 times the amount of Cyclophilin mRNA present. A threshold for positive detection of PLS3 mRNA was set at 0.01 times the amount of Cyclophilin mRNA and using this definition 60% (21/35) of SS patients express PLS3. A group of 18 MF patients, eight of whom had advanced stage disease (Stage IV) with demonstrated clonal blood involvement (Stage B0b) and 10 of whom had skin-restricted disease (Stage IB-III B0a) were also examined. Three of eight MF patients with blood involvement expressed PLS3 (38%) whilst all those with skin-restricted disease were PLS3 negative. Comparison of average PLS3 mRNA expression between the three groups by ANOVA demonstrated a significant increase in PLS3 expression in SS patients compared to healthy controls (Figure 5.3). Comparison of the expression of PLS3 with measures of tumour burden such as CD4+ count and CD4:CD8 ratio revealed only a weak correlation (Pearson's product-moment correlation coefficient = 0.33 $p<0.05$) with percentage CD4+ cells (Figure 5.4).

In order to further assess the potential correlation between PLS3 mRNA expression

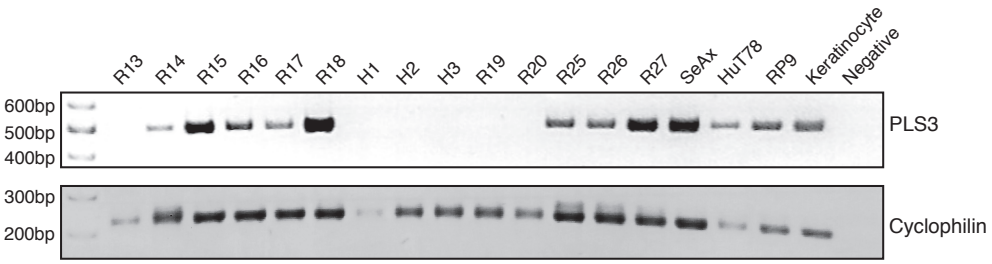

Figure 5.2: PLS3 mRNA expression in SS and healthy lymphocyte samples

RT-PCR with primers specific to PLS3 was performed on 12 SS patient lymphocyte samples (R13-27 and RP9), three healthy lymphocyte samples (H1-3), the cell lines SeAx and HuT78, and a healthy keratinocyte sample. cDNAs were also amplified with primers specific to the housekeeping gene Cyclophilin to ensure sample integrity. A negative control using water as a template for the RT-PCR reaction was included in each experiment.

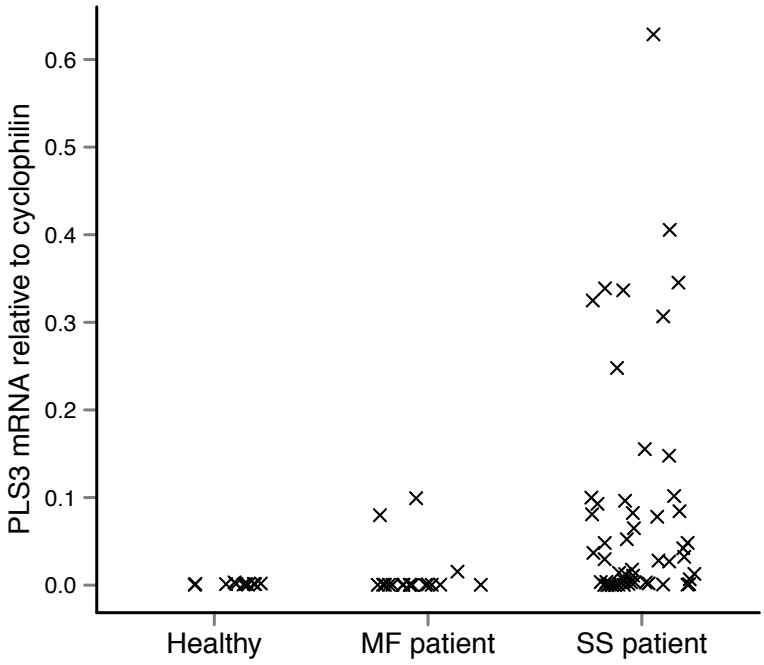

Figure 5.3: Quantification of the aberrant expression of PLS3

qPCR was used to assess the expression of PLS3 mRNA in CD4+ lymphocytes from 11 healthy controls, 18 MF patients and 35 SS patients. Measurements were performed in triplicate and expressed relative to the quantity of the housekeeping gene Cyclophilin. A significant difference between healthy and SS expression was demonstrated by one way ANOVA.

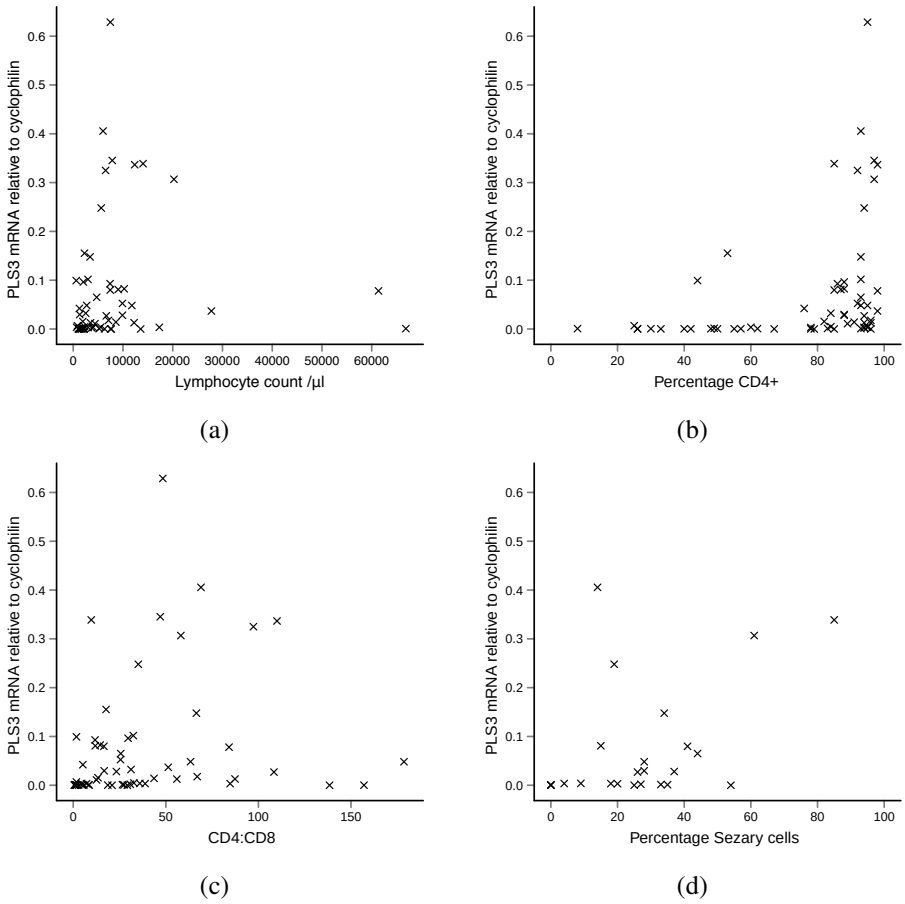

Figure 5.4: Relationship between PLS3 mRNA quantity and measures of tumour burden

Plots showing the relationship between quantity of PLS3 mRNA, expressed relative to Cyclophilin, and measures of tumour burden: (a) Total lymphocyte count (b) Percentage CD4+ cells (c) CD4:CD8 ratio (d) Percentage Sézary cells.

and markers of tumour burden, PLS3 mRNA expression was plotted relative to the date of sampling in five patients from whom multiple samples were available over a 15 month period. Lymphocyte count, percentage CD4+ and CD4:CD8 were also plotted over this period. Percentage Sézary cells was not included as this is not routinely measured with each sample. There were insufficient data points to examine correlation on a per patient basis but the general trends can be seen in Figure 5.5. None of the patients showed a large change in the quantity of PLS3 mRNA over the time period examined. P7 and P9 demonstrated a small reduction over time that was mirrored by CD4:CD8 in P7 but not P9 whereas P13 showed an increase in PLS3 mRNA expression however, lymphocyte count and CD4+ count were notably reduced over the same period. Percentage CD4+, which showed a weak correlation with PLS3 RQ in the overall patient cohort, remained constant over time in all patients, despite the variation in PLS3 RQ.

5.3.2 Assessing PLS3 expression at the protein level

In order to investigate PLS3 expression at the protein level, an antibody was required that was specific to PLS3 but did not cross react with L-plastin. This is challenging since the two proteins share 80% identity. Two commercially available antibodies were first tested by Western blotting as described in Section 2.15. ab45769 (Abcam) was tested first and observed to produce very high background staining. Further optimisation of blocking and washing conditions reduced this background however, no specific bands of the expected size were apparent (Figure 5.6a). sc-16655-R (Santa Cruz) generated bands of the expected size however these were also observed in samples from healthy lymphocytes (Figure 5.6b), suggesting that this antibody is pan-plastin reactive rather than specific to the PLS3 isoform.

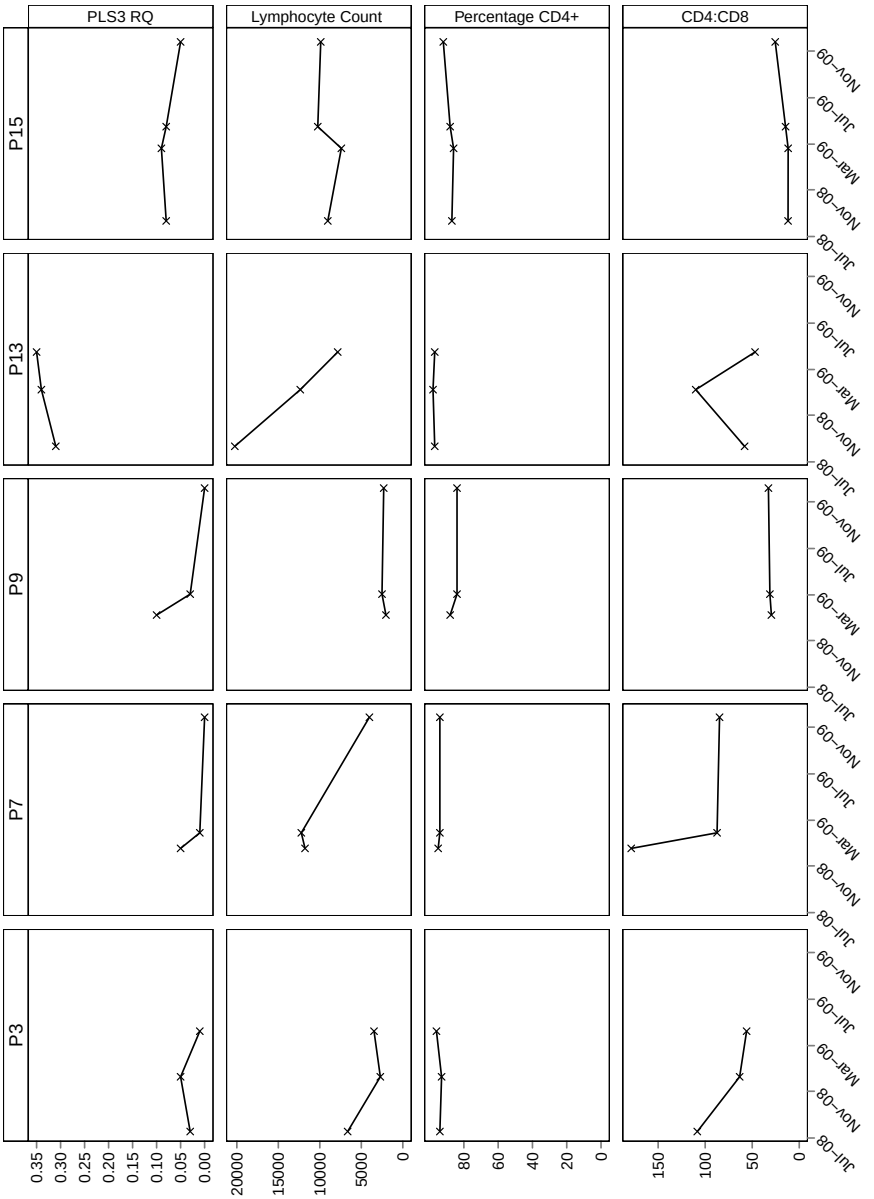

Figure 5.5: Changes in PLS3 mRNA quantity and lymphocyte subsets over time

Five SS patients (P3, P7, P9, P13 and P15) had their PLS3 mRNA expression assessed on three or more occasions. The change in expression (PLS3 RQ panel) over time is plotted above changes in lymphocyte count per μl, percentage CD4+ cells and CD4:CD8 such that corresponding changes can easily be compared.

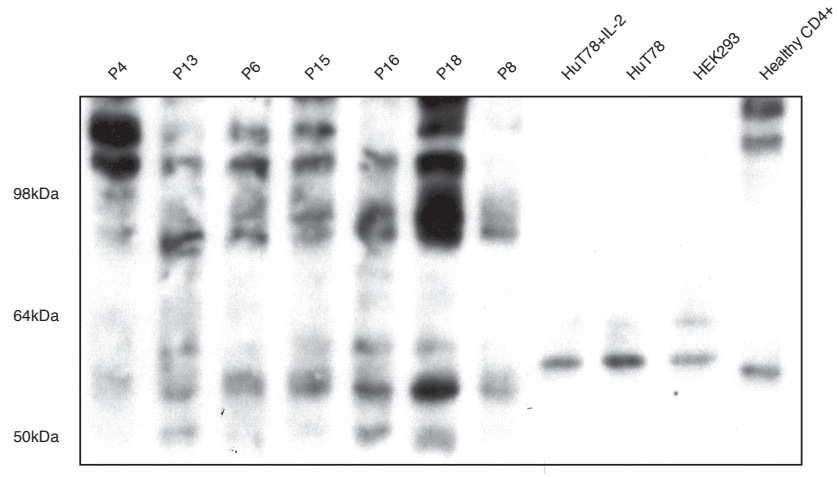

(a)

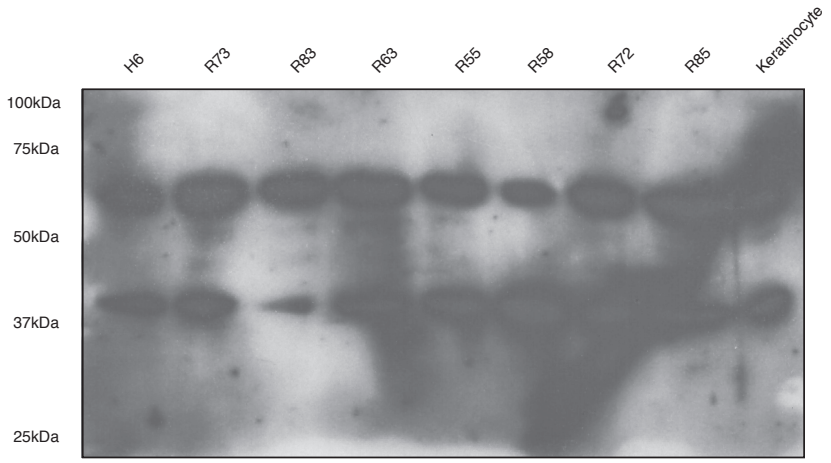

(b)

Figure 5.6: Commercially available antibodies are not specific for PLS3

Example Western blots using commercially available PLS3 antibodies (a) ab45769 demonstrates a large number of non-specific bands with none around the expected size of 70kDa (b) sc-16655-R demonstrates a band between 50kDa and 75kDa that may correspond to PLS3 however this band is present in a healthy sample (H6) in addition to the patient and keratinocyte samples, suggesting the antibody may be detecting all plastin isoforms. This blot also demonstrates a band just above 37kDa, which corresponds to re-probing with a β-actin loading control.

Therefore, a polyclonal antibody was raised against PLS3 as described in Section 2.16. Western blotting using the serum from rabbit 3852 generated a lot of background staining but serum from rabbit 3851 generated a relatively clean blot with a band just below 75kDa in a fibroblast whole cell lysate (Figure 5.7a), consistent with the detection of PLS3. Incubation of the serum with a 5 times excess of the immunogenic antigen prior to blotting leads to complete absence of this band (Figure 5.7b) confirming that this band does indeed correspond to detection of PLS3. Glycine and TEA eluates from the affinity purification of 3851 serum were then tested by Western blotting and the glycine eluate was found to generate bands in healthy keratinocytes but not in healthy lymphocytes when used at a dilution of 1 in 1000 following membrane blocking using 5% Marvel in PBS with 0.1% Tween. This antibody, termed PLS3-3851G was then used to assess the expression of PLS3 protein in SS patient samples that had already had their PLS3 mRNA status determined. Each blot, an example of which is shown in Figure 5.8, included a healthy PBMC sample and a healthy keratinocyte sample as negative and positive controls and was re-probed with β-actin following PLS3 detection to control for protein loading. Expression status of PLS3 protein in SS PBMCs was broadly consistent with the expression status of PLS3 mRNA. 8/11 SS samples previously shown to contain PLS3 by qPCR were found to demonstrate expression of PLS3 protein by Western blotting whilst 2/3 SS samples with PLS3 mRNA levels below the threshold showed no PLS3 protein expression. The one sample where PLS3 was detected on the protein but not the mRNA level was only just below the mRNA detection threshold and had a high protein loading level on the Western blot as revealed by β-actin staining, which may account for this inconsistency.

PLS3-3851G was then optimised for use in immunostaining. In order to compare multiple combinations of staining conditions, staining was performed in a 96-well flat-bottomed tissue culture plate as described in Section 2.21. For each experiment half

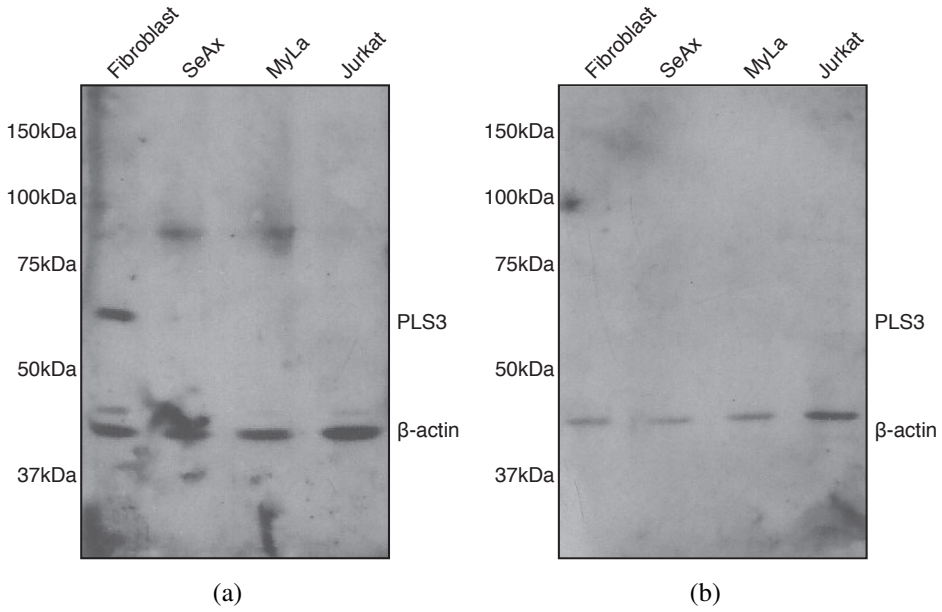

Figure 5.7: Western blot to show specificity of serum from rabbit 3851 for PLS3

Western blot analysis using (a) serum from rabbit 3851 demonstrates a band specific to fibroblasts, which do express PLS3 mRNA and that is close to the expected size of 70kDa (b) serum from rabbit 3851 pre-incubated with a 5×excess of immunogenic peptide has no band between 50 and 75kDa, suggesting that the PLS3 antigen has successfully blocked the antibody binding site. Both blots were re-probed for β-actin to demonstrate protein loading.

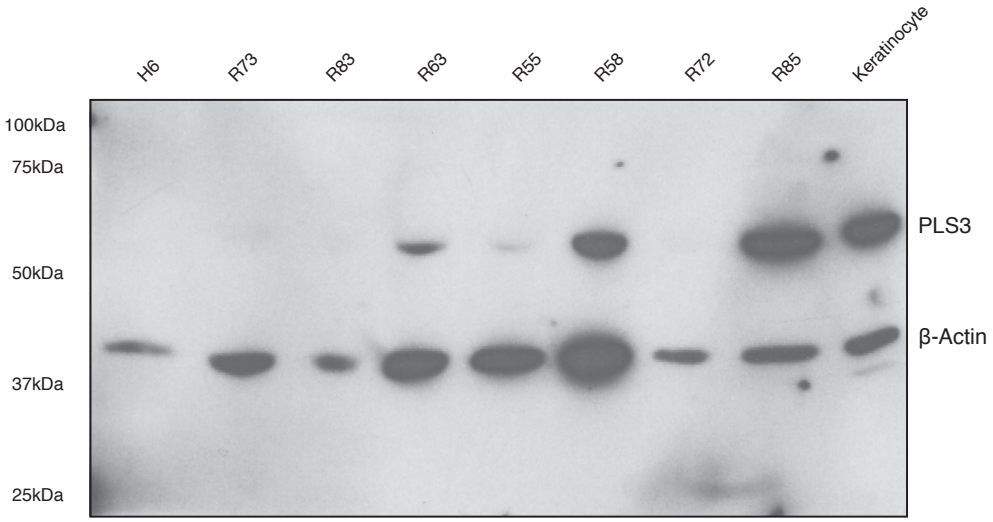

Figure 5.8: Western blot to detect PLS3 protein expression by SS patient lymphocytes

Seven SS patient lymphocyte samples (R55-85), one healthy control lymphocyte sample (H6) and a keratinocyte sample were probed using the PLS3-3851G antibody, demonstrating expression of PLS3 protein in four SS samples and the keratinocyte sample, but not in healthy lymphocytes. The blot was subsequently re-probed for β-actin, revealing rather uneven protein loading.

the wells contained healthy CD4+ lymphocytes as a negative control whilst half contained an SS patient CD4+ lymphocyte sample that had been demonstrated to contain PLS3 protein by Western blotting. Firstly a range of fixation and permeabilisation conditions were examined by bright-field imaging and compared to untreated cells in order to exclude any conditions that disrupted the morphology of the cells. The DAPI nuclear stain was also examined, leading to exclusion of some conditions where nuclear integrity had been compromised. Four conditions were then tested with a primary antibody concentration of 25μg/ml and secondary antibody concentration of 10μg/ml to determine which condition generated the clearest difference in staining intensity between isotype control and PLS3 specific antibody and between PLS3 specific staining in the positive and negative control cells. Both antibody concentrations were then titrated across a range in order to pinpoint the combination that gave minimal background staining with optimal PLS3 specific staining.

Using the optimised PLS3 immunostaining protocol as described in Section 2.21, PLS3 protein expression was observed in a proportion of the PBMCs from one PLS3 positive SS patient (Figure 5.9). The staining observed suggested that the PLS3 protein is localised in the cytoplasm. It was hoped that the relationship of PLS3 protein with the actin cytoskeleton could be determined however the only permeabilisation strategy that generated strong PLS3 staining was to use ice cold methanol, which disrupts the phalloidin binding site of actin, preventing the use of phalloidin for a dual stain.

5.3.3 PLS3 correlation with other markers

To quantify PLS3 expression on a single cell level the conditions used for immunostaining were tested and successfully applied to suspension cells, allowing their analysis by flow cytometry. In order to allow dual staining with other antibodies, PLS3-3851G was directly conjugated to DyLight 488 as described in Section 2.17. The antibody

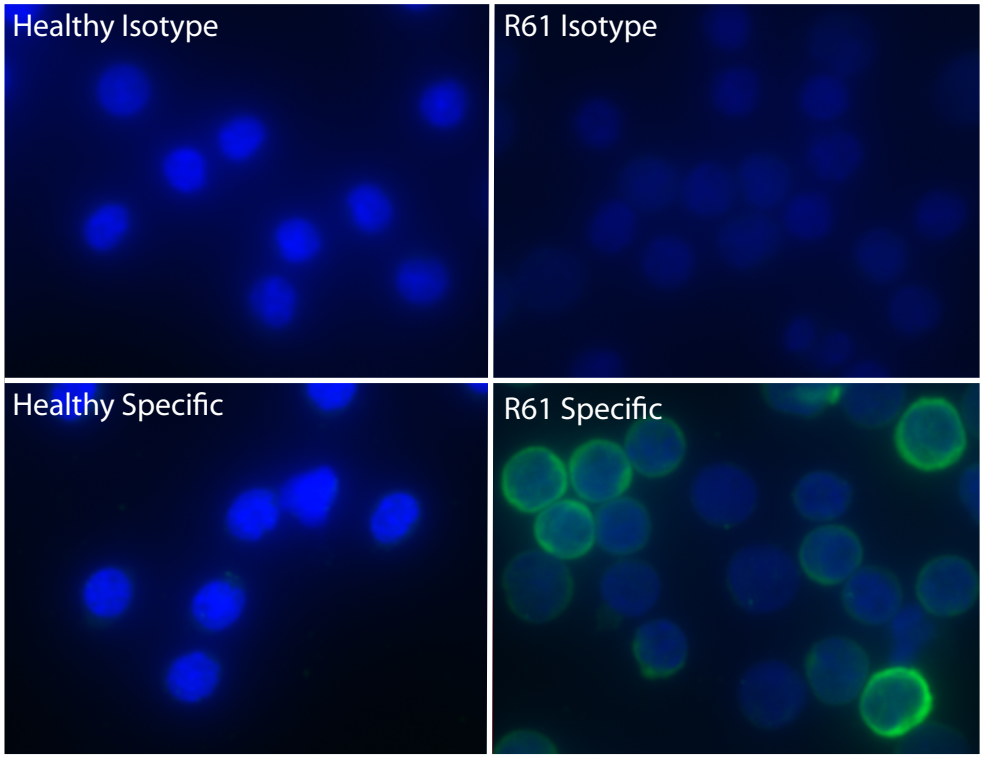

Figure 5.9: Immunostaining using PLS3 antibody

CD4+ lymphocytes from a healthy volunteer and a SS patient (R61) were spun onto slides, fixed in 1% paraformaldehyde, permeabilised with ice cold methanol and then immunostained using the PLS3 specific antibody. Goat anti-rabbit Alexa Fluor 488 (green) was used to visualise the staining and nuclei were counterstained with DAPI (blue).

dilution was then titrated to generate the optimal signal to background ratio. Multi-parameter flow cytometry was then performed as described in Section 2.18 and used to examine the correlation of PLS3 expression with other immunophenotypic markers including CD3, CD4, CD45RO, CD7, CD26, CD25 and CD158k. Individually stained controls were included in each experiment in order to check the compensation set up, which was initially performed using BD compbeads incubated with the relevant antibodies. Additionally, the distribution of each marker when individually stained was compared to the distribution in multi-parameter staining to check for any interaction between the antibodies. Five healthy control and 16 SS PBMC samples were stained over several experiments and analysed as described in Section 2.19. None of the healthy control PBMC samples contained PLS3+ cells. 11 of 16 SS samples contained PLS3+ cells and in all cases the PLS3+ population also expressed CD3 and CD4 (Figure 5.10). In those samples expressing PLS3 the PLS3+ cells comprised between 3% and 76% of the CD4+ peripheral blood lymphocytes.

Next, the distribution of various phenotypic markers within the PLS3+ and PLS3- populations of each sample was examined (Figure 5.11). Notably, in all 11 samples the CD4+PLS3+ population showed almost complete loss of CD26 whereas the corresponding CD4+PLS3- subsets expressed a significantly greater proportion of CD26 ($p=0.0006$) suggesting that loss of CD26 is associated with gain of PLS3. However, no other significant association was found between any of the other phenotypes and PLS3 expression. Notably, Figure 5.11 shows a wide range of CD45RO expression with four patients demonstrating significantly lower proportions of CD45RO+ in the CD4+ subset than the healthy average of 47% and three patients showing significantly greater ($p<0.05$). The distribution of expression between PLS3- and PLS3+ subsets was variable however, in three patients showing significant loss of CD45RO PLS3 expression was confined to the CD45RO- population.

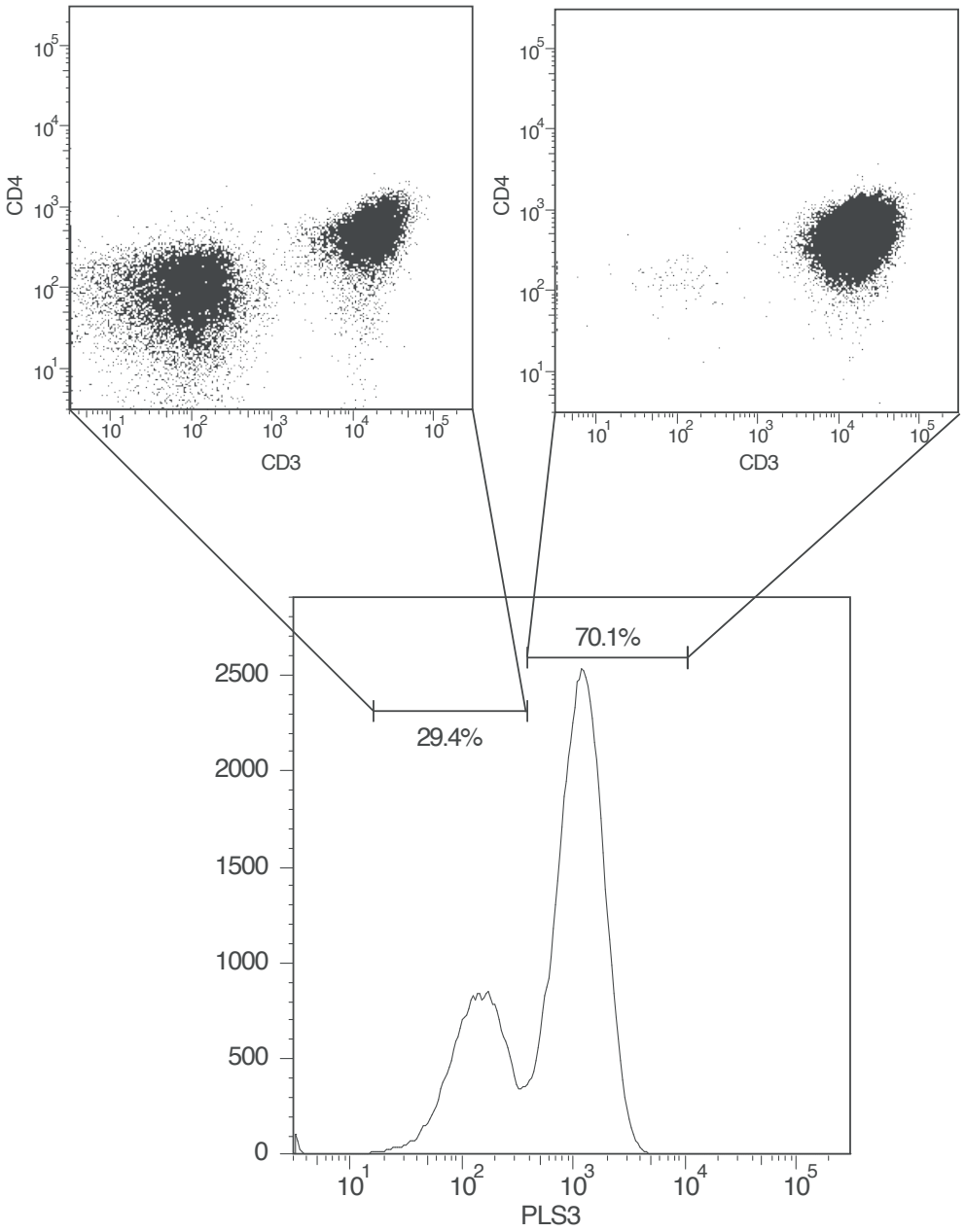

Figure 5.10: PLS3+ cells are all CD3+CD4+

Example histogram showing PLS3 expression within the R164 sample gated to show only viable cells. The dot plot inserts show the CD3/CD4 expression of PLS3- and PLS3+ subsets.

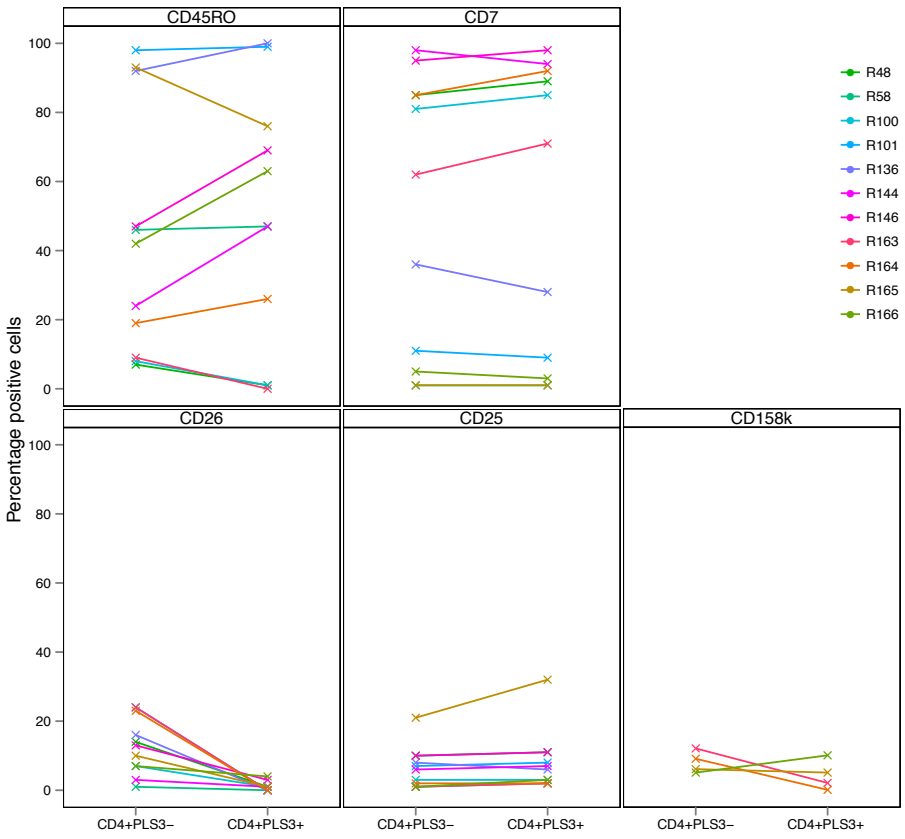

Figure 5.11: Heterogeneity in expression of T-cell differentiation markers between PLS3+ and PLS3- subsets

Viable cells were gated into CD4+PLS3- and CD4+PLS3+ populations then the percentage of positive cells was assessed for each other differentiation marker (CD45RO, CD7, CD26, CD25 and CD158k) in each subset.

5.3.4 Quantification of malignant cells in PLS3 subsets

To assess whether PLS3 expression is heterogeneous in tumour cells from an individual patient, FACS was used to isolate PLS3+ and PLS3- cell populations from one well-characterised SS sample (R164) as described in Section 2.20. A genetic assay was developed, taking advantage of the presence of a unique clonal TCRβ gene rearrangement in the malignant cells as described in Section 2.22. An overview of the assay design procedure can be found in Figure 5.12. Briefly, the sequence of this rearrangement was first determined by sequencing the clonal SSCP bands generated after amplification with the BIOMED-2 primer set. The rearrangement was found to involve Vβ4.2, Dβ1 and Jβ2.2 with the hyper-variable joining sequence shown in Figure 5.12. A TaqMan qPCR assay was then designed to specifically detect this sequence and assays for two diploid genomic regions (SDC4 and BCMA) were also obtained to normalise the input DNA quantity, primer sequences can be found in Table 2.7. The patient-specific forward and reverse primer pair were firstly analysed by standard PCR followed by agarose gel electrophoresis to ensure that a band was observed in the patient sample but not in a healthy control. BCMA and SDC4 primer pairs were similarly tested and observed to generate strong bands in a range of patient samples and healthy.

In order to test the sensitivity and specificity of the assays and generate standard curves, the rearranged TCRβ, BCMA and SDC4 sequences were cloned into the pGL3 plasmid using overlap extension PCR (Bryksin & Matsumura, 2010) as described in Section 2.23, a summary of the steps along with example agarose gel pictures for each step is provided in Figure 5.13. Given the known size of each construct (pGL3-R164 4885bp, pGL3-BCMA 4896bp and pGL3-SDC4 4924bp) the plasmids were then diluted such that 10^8 copies were present per 5μl. The qPCR assays were then performed on a dilution series of each construct covering a range from 100,000 copies per well down to 1 copy per well. The Ct values for each concentration were plotted and the

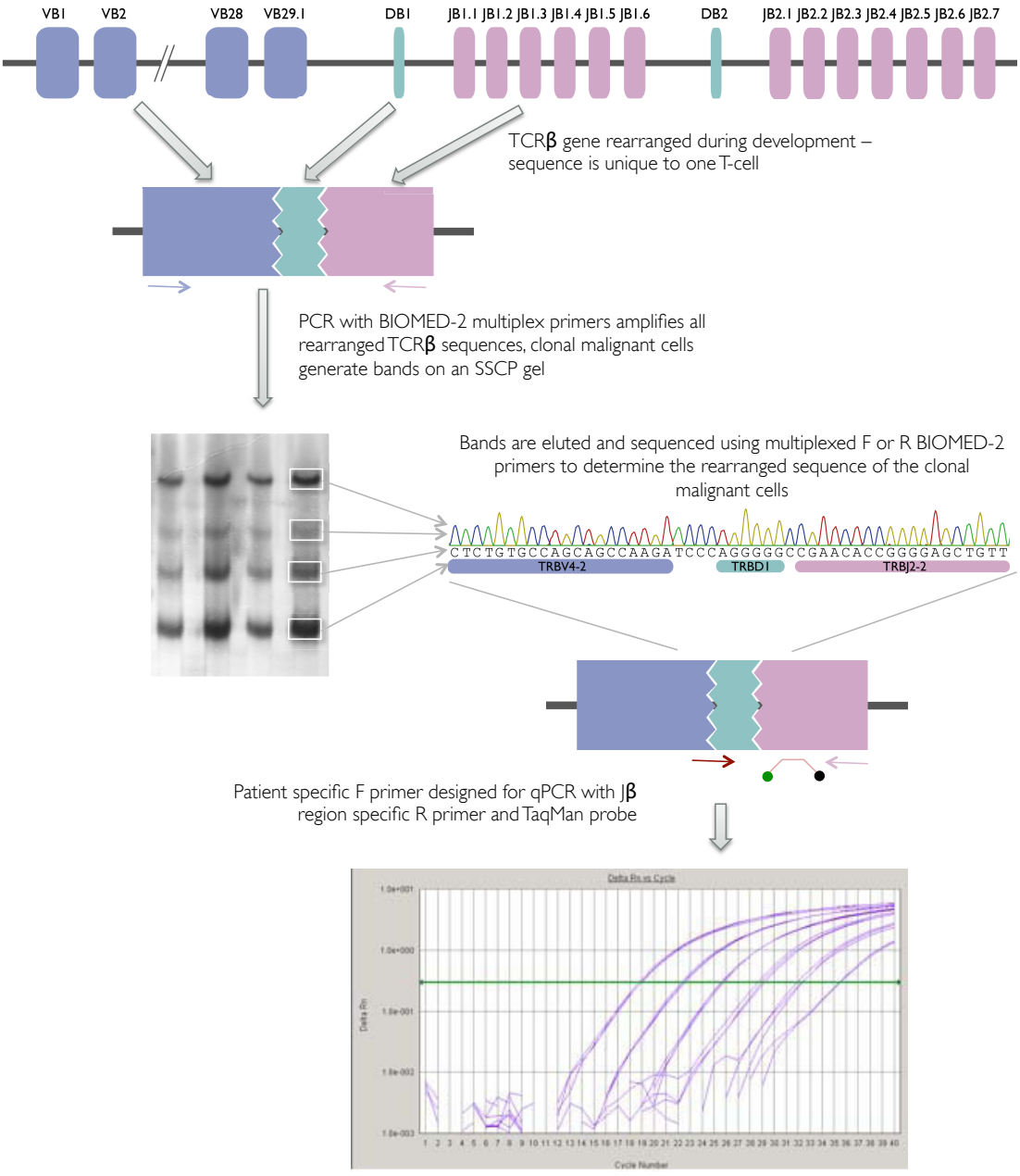

Figure 5.12: Schematic overview of the steps used to generate a qPCR assay for the quantification of malignant cells from R164

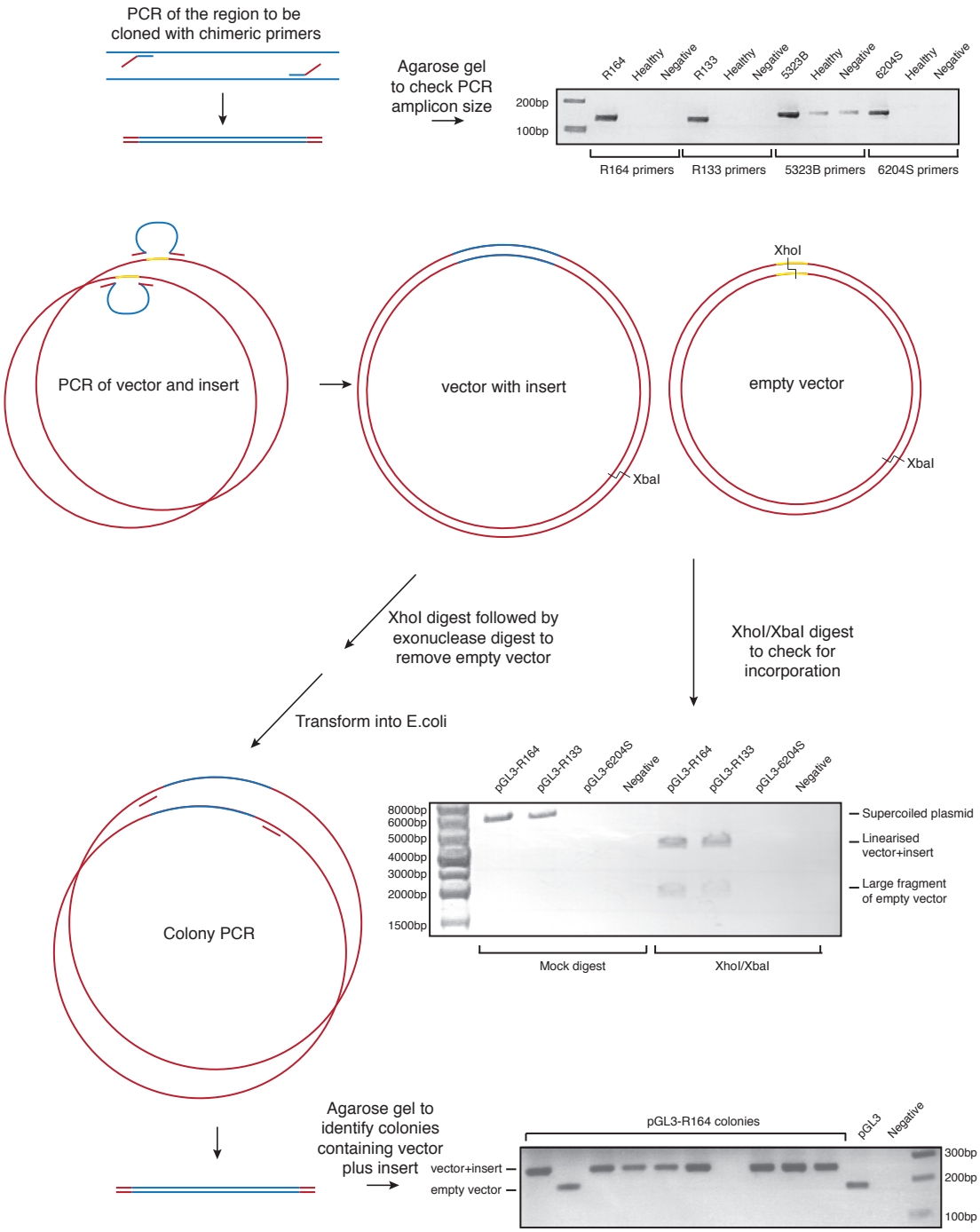

Figure 5.13: Schematic overview of overlap extension PCR

Blue lines represent genomic DNA sequence and complementary primers, red lines represent plasmid pGL3 DNA sequence and complementary primers, yellow lines represent the section of the plasmid sequence that is removed upon successful insertion of the required genomic DNA region. This region contained a unique *Xho*I site which was used to eliminate empty vector by linearisation prior to exonuclease digestion.

gradient of the resultant graphs used to calculate the PCR efficiencies, which were 98.6% for the R164 assay (Figure 5.14a), 100.4% for the BCMA assay (Figure 5.14b) and 101.4% for the SDC4 assay (Figure 5.14c). These graphs also demonstrate that 10 copies per well is the detection limit of these assays as the Ct values for 1 copy per well were inconsistent between replicates and often undetected. In order to test the specificity of the R164 assay, seven healthy controls were mixed in order to ensure a full range of TCR rearrangements was represented and diluted such that 10,000 copies could be dispensed in 5μl. qPCR was then performed on the R164 construct diluted in this healthy sample instead of water to determine the sensitivity of the R164 assay (Figure 5.14d). The efficiency of the R164 assay when conducted in the presence of other TCR rearrangements was 99.2%, very similar to the efficiency when diluted in water, suggesting that the specificity of the the assay is very good. Additionally, 10 copies per well could be accurately detected against a background of 10,000 other TCR rearrangements, giving a sensitivity of 1 in 1000 cells. The healthy control alone was also assessed (0 copies per well) and although some signal was observed in two of the three wells measured, the Ct values were inconsistent, highlighting the importance of checking replicates for generating valid data.

Once the assays were completely optimised, DNA from the PLS3+ and PLS3- populations of R164 was subject to qPCR with R164, BCMA and SDC4 assays. The previously generated standard curves (Figure 5.14) were used to convert the obtained Ct values into a copy number and the R164 copy number was normalised against the average of BCMA and SDC4 to calculate the percentage of cells within the population that contained the R164 rearrangement. Using this method the PLS3+ population was found to contain 84% (confidence interval 69%-99% $p<0.05$) cells with the patient-specific clonal TCRβ gene rearrangement, whilst the PLS3- population contained 28% (confidence interval 14%-43% $p<0.05$) cells with the patient-specific clonal TCRβ

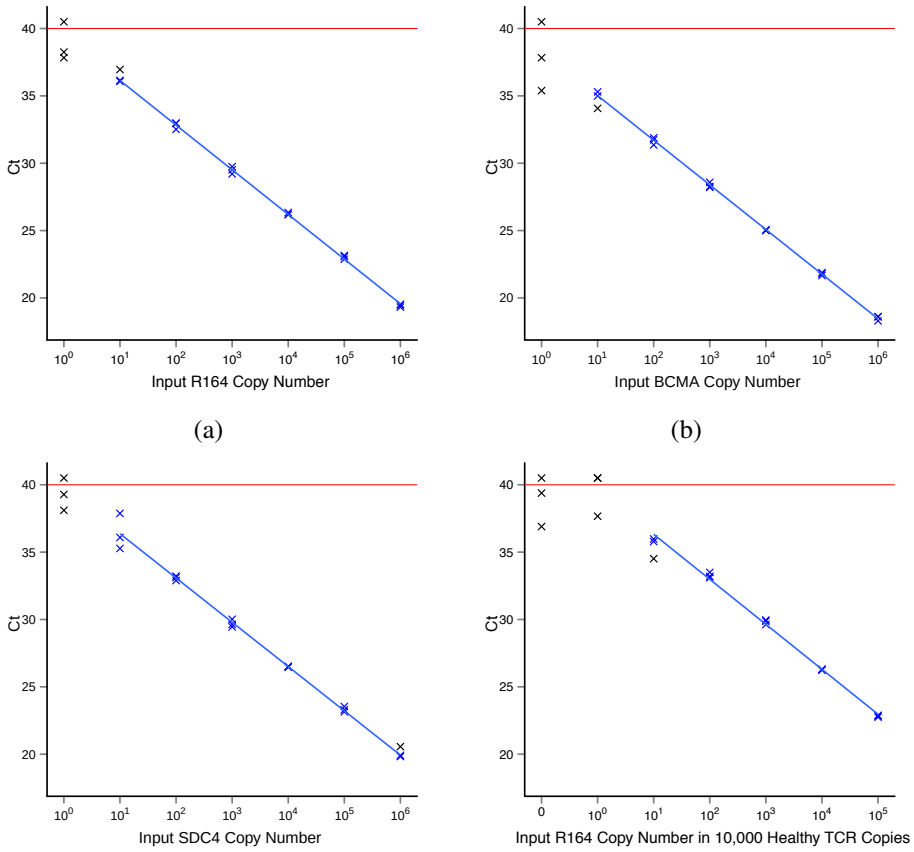

Figure 5.14: Standard curves for qPCR assays

qPCR was performed on a known input copy number of the relevant sequence for the (a) R164 assay (b) BCMA assay (c) SDC4 assay (d) R164 assay diluted in a mixed healthy control. All samples were assessed in triplicate, inconsistencies can be seen in the wells containing only 1 or 0 copies per well due to the sensitivity limit being reached. Wells where the signal did not reach the threshold fluorescence and therefore no Ct was defined are plotted just above 40, and the 40 cycle limit is shown with a red line. The linear part of each plot was used used as a standard curve and to calculate the PCR efficiency, some outliers were excluded on the basis that they were probably due to pipetting errors. The wells that were used for the generation of the standard curve are marked in blue.

gene rearrangement.

5.3.5 Mutational screen of PLS3

The aberrantly expressed PLS3 mRNA was directly sequenced in six SS patient lymphocyte samples to check whether the transcript being expressed was equivalent to that being expressed in other tissues. Eight overlapping PCR amplicons were designed to cover the entire coding sequence and 953bp of the 1111bp 3'-UTR (Figure 5.15a). Each PCR was sequenced in both the forward and reverse directions and the overlapping amplicons allowed confirmation of the sequence present at primer binding sites. Sequencing was performed as described in Section 2.12 using the primers and conditions detailed in Table 2.5. In all patients each PCR generated only one band of the expected size suggesting that no exon skipping had occurred (Figure 5.15b). All sequences were aligned to the PLS3 mRNA reference sequence NM_005032, ambiguous bases were identified and the sequences were inspected for mismatches with the reference. No mutations were detected within the coding sequence of the six patients examined however, a G/C polymorphism was observed in exon 1, 390bp up-stream of the translational start site, in two patients. Further investigation revealed this site to be a known C/G SNP, rs757124, which in the HapMap european population displays genotype frequencies of 37% C/C, 27% C/G and 37% G/G.

The promoter region of 12 patients and six healthy controls was also directly sequenced to look for polymorphisms that might be causing the aberrant expression. The patient cohort included three SS patients who had not been seen to express PLS3 mRNA, eight SS patients expressing PLS3, and one MF patient with detectable PLS3 expression. Since the CD4+ T-cell population used for sequencing would not contain a pure population of tumour cells, patients were selected on the basis of a high tumour burden, as judged by increased CD4+ count, proportion CD4+ or CD4:CD8 ratio at

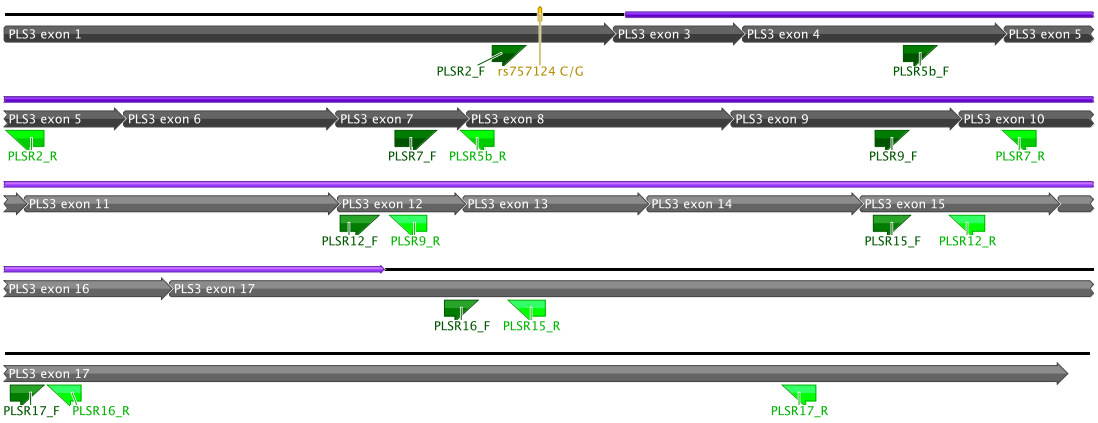

(a)

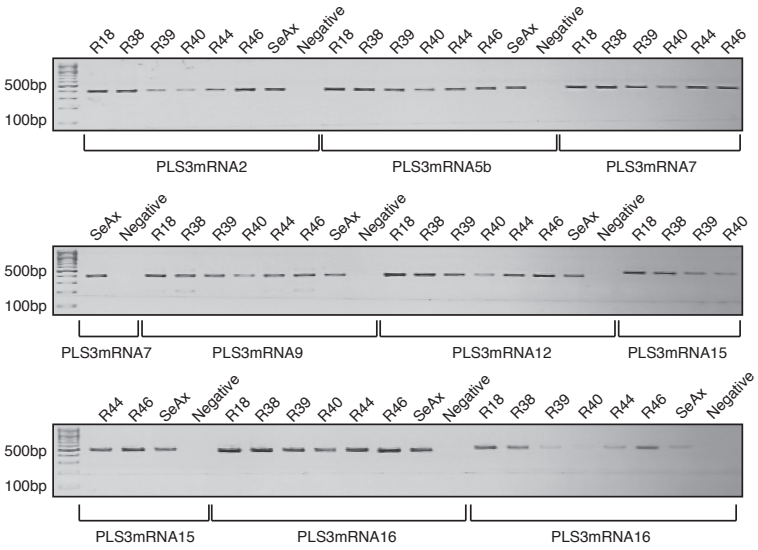

(b)

Figure 5.15: PLS3 mRNA sequencing

(a) Diagram showing the binding sites of the PLS3 mRNA sequencing primers. The purple arrow highlights the coding sequence, grey arrows represent the exons, dark green arrows the forward primers and light green arrows the reverse primers. Also marked is the C/G SNP rs757124. (b) PCR gel showing amplification of each of the PLS3 mRNA sequencing primer pairs from a selection of patient cDNA samples.

the time of sampling, in order to maximise the chance of detecting any polymorphisms. Two PCR amplicons were designed to cover from 1845bp upstream of the transcriptional start site to 99bp downstream of the transcriptional start site however, it was not possible to design amplicons with sufficient overlap to sequence over the primers leading to a gap of approximately 80bp in the sequencing coverage. Sequencing was performed as described in Section 2.12 using the primers and conditions detailed in Table 2.5

The promoter sequencing amplicons also covered the rs757124 SNP and two of the samples used for mRNA sequencing had matched DNA available, allowing comparison of results. One sample, sequenced as C in the transcript was sequenced as homozygous C at the DNA level, whilst the other sequenced as G in the transcript was sequenced as homozygous G at the DNA level. Within the healthy group, two samples were sequenced as homozygous C and three as homozygous G. Across the whole population of 12 patients, seven were homozygous for G, three were homozygous for C and two were heterozygous. The genotype at this SNP did not appear to show any association with PLS3 expression status in these patients.

Promoter sequencing reads were aligned with the reference sequence in Geneious (Drummond *et al.*, 2011) then the find heterozygotes tool was used with a peak similarity setting of 25%. This should allow the sensitive detection of polymorphisms however, it also leads to false positive detection of heterozygotes, particularly towards the ends of sequencing reads where the peaks overlap more. All annotated alignments were therefore examined by hand to exclude heterozygote calls that did not occur in both forward and reverse sequencing reads. The only polymorphisms detected within the 1845bp upstream of the transcriptional start site corresponded to known SNPs in the region (Table 5.1). Whilst a much larger cohort is required to conclusively test for an association between genotype and PLS3 expression, no clear pattern emerged from

Sample	PLS3 expression	rs3813931	rs1557770	rs757124
R67	+	C/C	T/T	G/G
R73	-	C/C	T/G	G/C
R82	+	nd	G/G	C/C
R83	+	C/C	T/T	G/G
R84	+	C/C	T/T	G/G
R85	+	C/C	T/T	G/G
R89	+	C/C	T/T	G/G
R118 (MF)	+	C/C	T/T	G/G
R122	-	T/T	T /T	C/C
R125	+	C/C	T/G	G/C
R126	-	C/C	T/T	C/C
R133	+	C/C	T/T	G/G

Table 5.1: Genotypes of the three SNPs within the PLS3 upstream region

the 12 patients studied.

The presence of SNPs proved a useful tool for assessing the sensitivity of direct sequencing for the detection of polymorphisms within a mixed population of cells. One sample homozygous for G was spiked into a sample homozygous for T at varying ratios and then sequenced. Data were analysed using Geneous as described above to detect heterozygotes with a 25% peak similarity (Figure 5.16). Interestingly, this revealed that G was detected much more sensitively than T but even T was detected when present in 50% of the cells. Given the lymphocyte subset counts, all samples examined for mutations are expected to contain >50% tumour cells and hence mutations should have been detectable if they were present.

5.3.6 Assessing DNA methylation in the PLS3 CGI

Although Lin *et al.* (1999) suggested that the PLS3 CGI was unmethylated in primary lymphocytes, their study used digestion with the methylation sensitive *Xma*I enzyme followed by Southern blotting to detect methylation. This assay quantifies only a few CpG dinucleotides within the *Xma*I restriction site and does not provide an overview of the methylation level across the whole island. Since methylation can vary across the

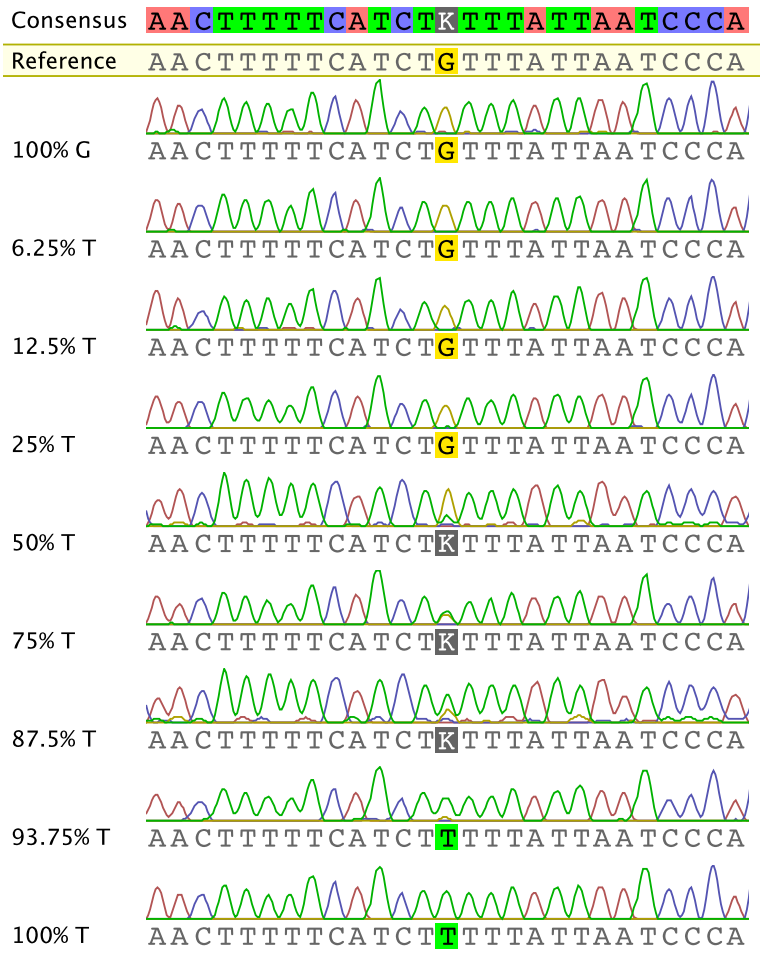

Figure 5.16: Assessing the sensitivity of direct sequencing for detection of polymorphisms

Comparison of the sequencing chromatograms from mixtures of samples containing G and T in different proportions. The potential polymorphism (K) is highlighted in grey in the consensus sequence and those mixtures where a polymorphism was detected.

CGI, and as previously demonstrated in the Fas gene, positional methylation may play a role in gene regulation, it was decided to examine the methylation of the entire PLS3 CGI.

Whilst previously, Pyrosequencing of bisulphite converted DNA had been used to examine methylation of the Fas and SHP-1 CGIs, in PLS3 the assays proved technically difficult to design. CpG dinucleotides were so densely packed within the PLS3 CGI, as shown in Figure 5.17a that there were very few spaces of sufficient length (15-20nt) to place the Pyrosequencing primers such that they did not overlap any CpG dinucleotides. Furthermore, where there was space to place them the bisulphite conversion had frequently reduced the sequence complexity such that there were homopolymeric tracts unsuitable for primer placement. In addition, Pyrosequencing amplicons have a maximum length of around 400nt so many amplicons would be required to cover the 1585bp CGI.

To circumvent this issue it was decided to use direct sequencing of bisulphite converted DNA from healthy lymphocytes to screen for any methylation of the PLS3 CGI that could be subject to dysregulation in SS patients. Although the reduced sequence complexity made primer design challenging, primers were placed as shown in Figure 5.17a and detailed in Table 2.5 covering most of the PLS3 CGI. However, upon testing these primers, only two amplicons, PLS3CGIT2 and PLS3CGIT9 could be optimised to produce the strong PCR band required for sequencing (Figure 5.17b) allowing investigation of approximately half of the PLS3 CGI. In addition to the healthy lymphocyte samples, one healthy keratinocyte sample was also sequenced as this was expected to have no methylation within the PLS3 CGI since keratinocytes strongly express PLS3. In healthy lymphocytes the majority of the region investigated was observed to be completely unmethylated, however, one small region containing CpG dinucleotides 95-99 was found to be partially methylated in four healthy lymphocyte

samples but not in the keratinocyte sample (Figure 5.18).

Several SS lymphocyte samples from patients with strong PLS3 expression were also directly sequenced however, it was difficult to quantify the proportion of C and T at the mixed base positions. Therefore, to investigate this region in further detail a Pyrosequencing assay was designed to cover CpG dinucleotides 95-99 and used to quantify methylation in four cell lines and lymphocyte samples taken from 24 healthy controls and 36 SS patients as described in Section 2.11. Healthy lymphocytes were found to contain an average of 32% methylation of CpG dinucleotides 95-99 compared to the SS patient average of 30%. Dividing the SS patients into groups based on PLS3 expression level revealed that those who expressed PLS3 had a significantly reduced methylation level of 21% ($p<0.05$) whilst those who did not express PLS3 had an average methylation level of 46%, which was not found to be different to the healthy control lymphocytes (Figure 5.19). HEK293 was unmethylated, reflecting the expression of PLS3 and lack of methylation in healthy keratinocytes, whilst 86% methylation was present in Jurkat cells that did not express PLS3. In the two SS cell lines, SeAx and HuT78 that did express PLS3, methylation levels were 39% and 49% respectively indicating a reduction in comparison with Jurkat.

DNA from the previously sorted PLS3- and PLS3+ populations from sample R164 was also analysed for methylation status of the PLS3 CGI at sites 95-99. In the pre-sort sample DNA methylation across these sites was 16% whilst after sorting the PLS3+ subset, representing 79% of the pre-sort sample, was found to be 10% methylated and the PLS3- subset 43% methylated showing that hypomethylation of CpG dinucleotides 95-99 is restricted to the PLS3+ cells.

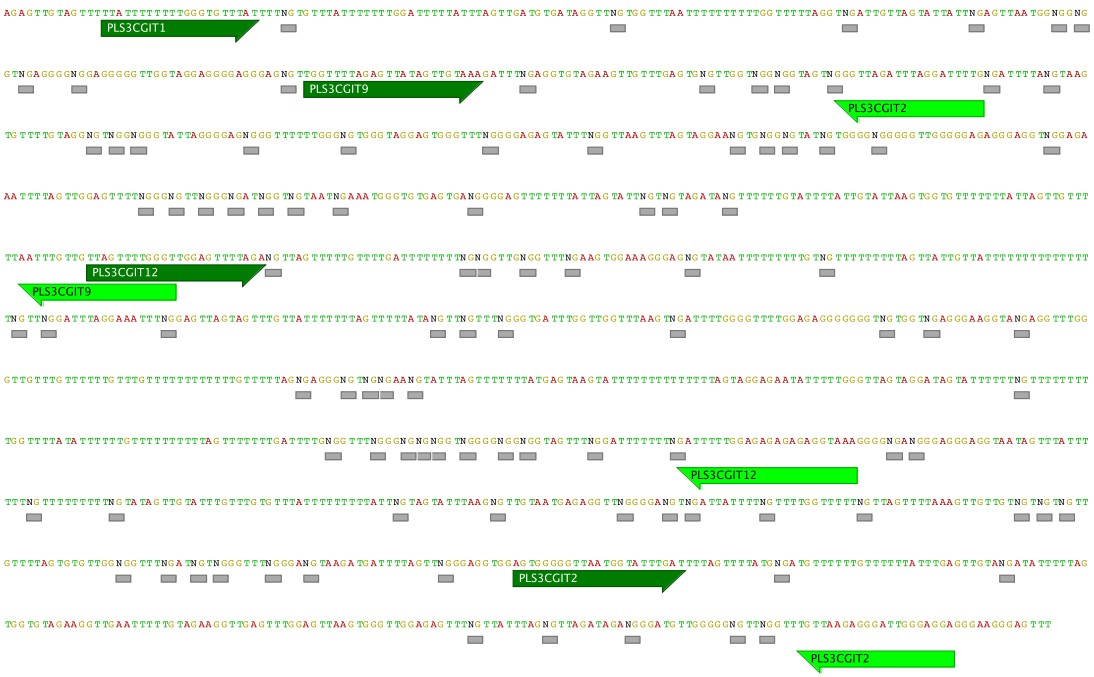

(a)

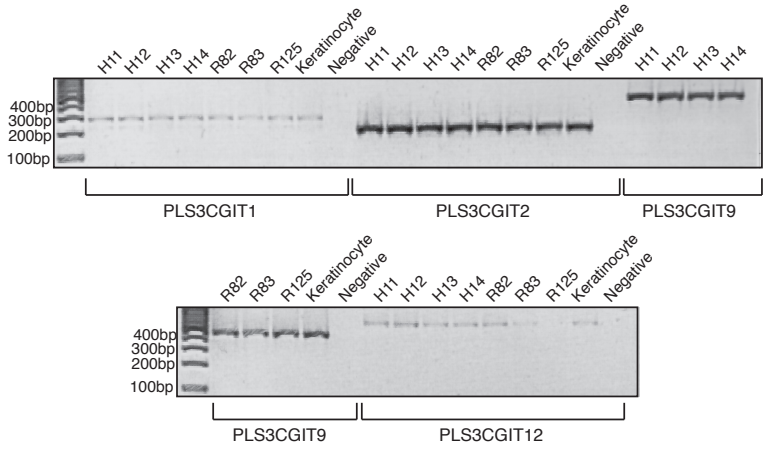

(b)

Figure 5.17: Optimisation of bisulphite sequencing primers for the PLS3 CGI

(a) Sequence of the PLS3 CGI showing the densely packed CpG dinucleotides (highlighted by grey boxes) and the frequently homopolymeric tracts in between. The designed sequencing primers pairs are highlighted with forward primers as dark green arrows and reverse primers as light green arrows. (b) PCR gel showing amplification of each of the PCR products from a selection of healthy and patient bisulphite converted DNAs. PLS3CGIT1 and PLS3CGIT12 do not generate strong enough bands for successful sequencing despite extensive optimisation of the PCR conditions.

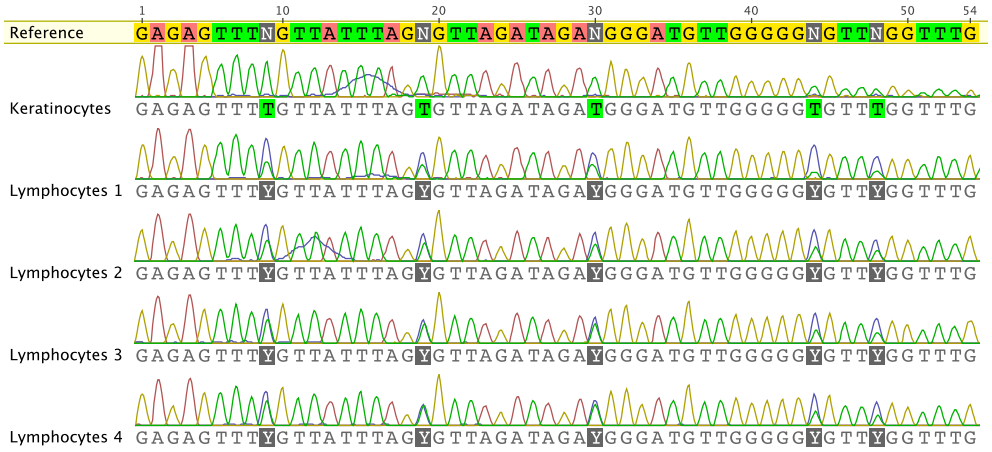

Figure 5.18: Hypomethylation of CpGs 95 - 99 in keratinocytes

Bisulphite converted DNA from four healthy lymphocyte samples and one healthy keratinocyte sample were sequenced to assess DNA methylation across the PLS3 CGI. The section shown covers CpG dinucleotides 95-99. The bisulphite converted reference sequence shows potentially methylated cytosine residues (N) and the resultant C+T mixed base (Y) highlighted in grey.

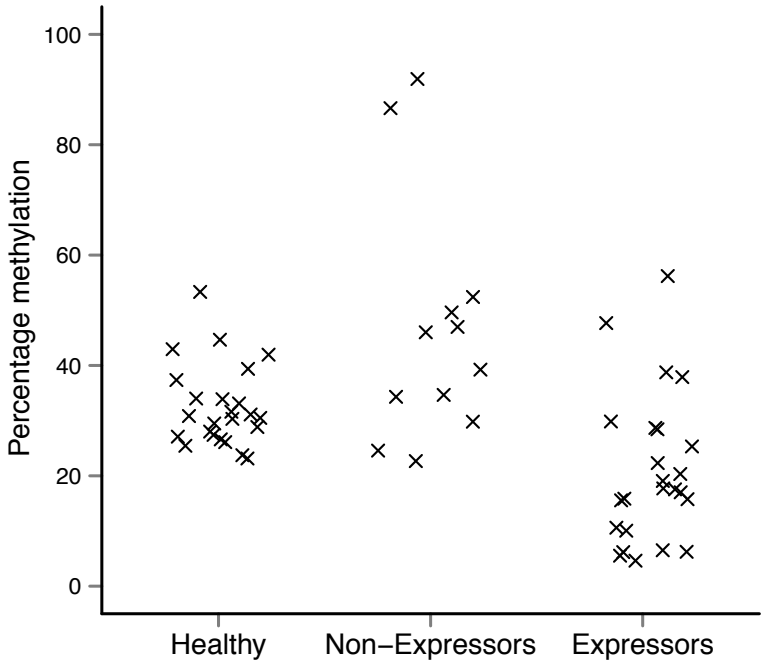

Figure 5.19: Quantification of methylation in the PLS3 CGI

Pyrosequencing was used to assess the methylation in CpG dinucleotides 95-99 of the PLS3 CGI. Average methylation across the island is plotted for 24 healthy controls, 12 SS patients who did not express PLS3 and 24 SS patients who did express PLS3.

5.4 Discussion

This study has demonstrated that aberrant expression of PLS3 in circulating lymphocytes is a feature of 60% of SS patients (Figure 5.3). In accordance with other studies (Capriotti *et al.*, 2008, Kari *et al.*, 2003, Nebozhyn *et al.*, 2006, Tang *et al.*, 2010) a negligible quantity of PLS3 mRNA was detected in healthy PBMCs using qPCR. A threshold of over ten times this amount was then used to define statistically significant PLS3 mRNA expression in patient samples. PLS3 mRNA expression status determined using this threshold was found to be consistent with PLS3 protein expression status in 10/14 patients. The inconsistency observed in 4/14 patients are likely to be due to differences in the sensitivity threshold of the detection methods and could potentially indicate regulation on the translational level.

This is the first study to quantify the proportion of patients expressing statistically significant levels of PLS3 mRNA in a large cohort. Su *et al.* (2003) demonstrated SS mRNA over-expression by RT-PCR in 8/9 patients whilst the microarray studies showed only a fold increase in the patient group compared to healthy controls. Capriotti *et al.* (2008) found expression in all 31 of their samples however their figures show that some patient samples are within the range of normal healthy samples so it is unclear how many had significant over-expression. Tang *et al.* (2010) found significant expression in a group of 8 SS patients as compared to MF patients with no blood involvement, psoriasis/PRP patients and healthy controls but their results showed only the mean and variance for each group so it is unclear what proportion of the 8 SS patients were PLS3+. Defining each sample as PLS3+ or PLS3- will be crucial to further investigation of how PLS3 status affects prognosis, a cutaneous lymphoma prognostic index has recently been validated (E. Benton *et. al.*, manuscript submitted) and it would be interesting to determine whether the addition of further molecular markers to this model could provide any further refinement.

Three MF patients demonstrating a T-cell clone in blood that was identical to the T-cell clone in their skin lesions, were also show to express significant amounts of PLS3 (Figure 5.3). Of these, one demonstrated 41% Sézary cells by morphological analysis suggesting that this patient had in fact developed SS. The presence of PLS3 in the other two raises the question of whether the expression of PLS3 is an early sign that these patients have developed SS or whether PLS3 expression is also a feature of circulating cells in MF. It has been demonstrated by Campbell *et al.* (2010) that the clonal T-cells from SS patients, as identified by expansion of one TCRVβ subfamily to greater than 50% of the total T-cell population, express CCR7/L-selectin/CD27 characteristic of central memory T-cells whilst clonal T-cells from MF express CCR4/CLA characteristic of effector memory T-cells. Skin resident T-cells in SS were shown to retain their effector memory phenotype with the additional expression of the skin-homing addresin CLA. It would be interesting to further investigate the expression of T effector memory and T central memory markers on PLS3 expressing circulating T-cells from MF patients with blood involvement and such a study may provide evidence to add to the debate over whether MF and SS are separate clinical entities or different stages of one disease.

PLS3 mRNA expression level was compared with various lymphocyte subset counts in order to determine if there was any correlation with tumour burden (Figure 5.4). A weak correlation was observed with percentage CD4+ cells however, close examination of the graph would suggest this is due to the majority of PLS3+ samples having greater than 80% CD4+ cells with a wide range of PLS3 expression levels. In contrast to Capriotti *et al.* (2008), this study found no correlation between Sézary count and PLS3 mRNA level however, Capriotti *et al.* (2008) used absolute Sézary count whereas this study used percentage Sézary cells which may account for the difference. Given that the percentage of PLS3+ cells within the CD4+ population varied between

3% and 76% it appears that PLS3+ cells comprise only a subset of the tumour cells so it is not expected that any measure of tumour burden would correlate with PLS3 mRNA level in a cohort of patients. It may however be possible to follow changes in tumour burden in individual patients by monitoring PLS3 expression. Five patients had multiple samples available over the course of 15 months and these were plotted alongside lymphocyte counts however no clear patterns emerged (Figure 5.5). Tang *et al.* (2010) followed one patient who progressed from MF to SS then received a bone marrow transplant. Large changes in PLS3 expression were observed, following the pattern of Sézary cell percentage closely, suggesting that PLS3 expression may be of use in monitoring patients but further data is necessary to confirm this.

PLS3 and L-plastin are closely related actin-bundling proteins that normally demonstrate tissue-specific expression (Lin *et al.*, 1993b). However, aberrant L-plastin expression has been demonstrated in a wide range of epithelial malignancies (Lin *et al.*, 1993b) and shown to induce proliferation and invasion in colon cancer cells (Foran *et al.*, 2006) and melanoma cells (Klemke *et al.*, 2007). Aberrant PLS3 expression has been identified in SS but the functional role it plays has yet to be identified. As discussed in Section 5.1 L-plastin plays a vital role in healthy T-cells, leukocytes deficient for L-plastin are incapable of killing pathogens despite showing normal migration, adhesion, spreading and phagocytosis (Chen *et al.*, 2003). Given the importance of actin cytoskeletal dynamics in formation of the immunological synapse (reviewed by Gomez & Billadeau (2008)) and the deficiencies in T-cell signalling observed in CTCL, aberrantly expressed PLS3 may interfere with assembly of the immunological synapse and has the potential to play a functional role in the pathogenesis of SS. Further investigation is necessary to determine the extent of any functional role and whether it represents a therapeutic target. Here, an antibody specific to PLS3 has been developed and demonstrated not to cross-react with L-plastin. The antibody has

been optimised for use in Western blotting (Figure 5.8), intracellular staining for flow cytometry (Figure 5.10) and immunofluorescent staining (Figure 5.9). It is anticipated that this antibody will enable future studies to examine the functional role of aberrantly expressed PLS3 in SS.

The mechanism leading to aberrant expression of PLS3 in CTCL has not yet been defined. No mutations were found in the coding or regulatory regions of the PLS3 gene to account for aberrant PLS3 expression in CTCL. Consistent with other studies (Lin *et al.*, 1999, Oprea *et al.*, 2008) no methylation was observed across the bulk of the CGI in healthy PBMCs, however, in a region not previously investigated, covering CpG dinucleotides 95-99, methylation was observed in healthy lymphocytes but not in keratinocytes (Figure 5.18). Further, hypomethylation of this region was found only in SS patients displaying expression of PLS3 (Figure 5.19) and upon sorting the PLS3+ and PLS3- populations from one patient, hypomethylation was found to be restricted to the PLS3+ population. These observations strongly suggest that methylation of this region may contribute to the regulation of PLS3 expression, both in terms of the healthy tissue-specific context, and in aberrant disease-specific expression. Ideally, this hypothesis would have been tested by transfecting cell lines with a reporter construct containing the PLS3 promoter and CGI with or without methylation of CpG dinucleotides 95-99 and measuring the resultant expression of the reporter gene. Unfortunately this turned out to be a particularly complex proposal as no method exists for the selective methylation of specific CpG dinucleotides, currently the only agent that can be used to methylate cytosines in the CpG context is *M.Sss*I methyltransferase, which will methylate all CpG dinucleotides present. One option would have been to isolate the DNA segment containing CpG dinucleotides 95-99 and methylate this prior to ligation back into the plasmid however, an elaborate cloning strategy was required to do this which was not possible within the time available. New methods are

emerging that endeavour to use the sequence specificity of zinc finger binding domains linked covalently to a methyltransferase domain to target methylation to a particular sequence (Meister *et al.*, 2010) however, these technologies require further development before they can be used for the application proposed above.

It has previously been demonstrated by members of our group that malignant cells in SS are present within CD4+CD26+, CD4+CD26-, CD4+CD25+ and CD4+CD25- populations by quantifying PLS3 mRNA within sorted cell subsets (Jones *et al.*, 2010, Tiemessen *et al.*, 2006). In this study the correlation between T-cell differentiation marker expression and PLS3 expression was further explored, finding loss of CD26 to be significantly associated with the PLS3+ subpopulation, whereas loss of CD7 and gain of CD158k were not (Figure 5.11). Interestingly, Capriotti *et al.* (2008) observed a weak correlation between PLS3 mRNA quantity and absolute CD26- count but not absolute CD7 count in their cohort of patients suggesting that there may be a mechanistic link between loss of CD26 expression and gain of PLS3 expression. It was also observed that malignant cells were not necessarily confined to the CD45RO+ population as widely assumed. Indeed, in three samples with significant loss of CD45RO it was confirmed that the PLS3 expression was confined to the CD45RO- population suggesting that the neoplastic cells have in these cases lost expression of CD45RO. Similar results have been reported recently by Campbell *et al.* (2010) who saw heterogeneity in both CD45RO and CD45RA expression which in some cases included co-expression, suggesting dysregulation of the mechanisms that normally lead to the switch between CD45RA and CD45RO upon development from naïve to memory T-cell (Dutton *et al.*, 1998).

In all samples examined, PLS3 expression was observed to be restricted to CD3+ CD4+ T-cells (Figure 5.10), suggesting that PLS3 expression is a feature of the malignant cells rather than being induced in other haematopoietic compartments by the

malignant microenvironment. The wide range of proportions of PLS3+ cells observed suggests that PLS3 expression is confined to a subset of malignant cells rather than the whole population. This hypothesis is further supported by the detection of genetically defined tumour cells within the PLS3 negative population in one patient. Whilst loss of CD7 and CD26 and gain of CD158k have been tested as diagnostic tools it is not established if any of these markers can be used to quantify tumour burden accurately. The current observations of phenotypic heterogeneity within the malignant cells with respect to PLS3 co-expression are supported by a previous study which determined that genetically defined tumour cells are not restricted to CD7- or CD26- subpopulations (Steinhoff *et al.*, 2009). The results presented here preclude the use of PLS3 sorting to isolate malignant cells in SS patients expressing PLS3 as doing so may lead to the exclusion of a proportion of the malignant cells. In addition, cell sorting based upon CD45RO, CD7, CD26 or CD158k is found to be likely to identify only a subset of malignant cells, whilst still potentially including reactive cells. Therefore isolation of the CD4+ subset still provides the most reliable approach for the enrichment of the malignant cell population in SS.

In order to quantify genetically defined tumour cells within sorted cell subsets a patient tumour cell-specific real-time TCR copy number assay was developed based upon those used in acute lymphoblastic leukaemia (Brüggemann *et al.*, 2004, van der Velden & van Dongen, 2009). Quantification using a genetic assay was chosen in preference to the use of TCRVβ antibodies in order to enhance the specificity of detection and to avoid excluding cells where cell surface TCRβ chain was not being produced from the rearranged TCR gene. It was demonstrated that it is possible to determine the exact sequence of the clonal TCRβ gene rearrangement by multiplex sequencing of SSCP bands and thus identify the V, D and J regions along with the hyper-variable joining segments (Figure 5.12). Identical sequences were obtained from diagnostic

skin and blood samples from the patients investigated, confirming that the clonal T-cells in the two sites are in fact identical. Assays were designed for four patients and although only one had sufficient sorted cells for use in investigating the PLS3+ and PLS3- populations, the testing process highlighted necessary steps in the development of such assays and also demonstrated a sensitivity of 1 in 1000 cells was consistently achievable. Patient tumour cell-specific real-time TCR copy number assays have potential for future use in quantifying tumour burden allowing detailed monitoring of response to therapy and with such a high sensitivity and specificity they could also be used to monitor minimal residual disease following bone marrow transplantation.

In summary, the prevalence of aberrant PLS3 expression has been determined in a large cohort of SS patients and demonstrated to be associated with hypomethylation of CpG dinucleotides 95-99 in the PLS3 CGI. The expression of both PLS3 and pan-T-cell differentiation markers in SS patient CD4+ T-cells is shown to be heterogeneous and hence unsuitable for further enrichment of the malignant cells. In the course of these investigations an antibody specific to PLS3 has been developed, which should provide a valuable tool for further studies into the functional role of PLS3. In addition a method for designing and optimising patient tumour cell-specific real-time TCR copy number assays was developed, which could be used for future monitoring of tumour burden in SS patients.

General discussion

In this thesis, three genes potentially key to the pathogenesis of SS were investigated to determine whether DNA methylation could act as a regulatory feature. In all three genes, DNA hypermethylation was observed to correlate with decreased gene expression suggesting a regulatory role. SHP-1 hypermethylation and correspondent down-regulation of isoform-specific expression was however only observed in cell lines and keratinocytes, no aberrant hypermethylation was observed in SS patient PBMCs. Hypermethylation of certain CpG dinucleotides in Fas was observed in PBMCs from SS patients showing down-regulation of gene expression. Positional hypermethylation of PLS3 was observed in healthy lymphocytes but not healthy keratinocytes, with substantial hypomethylation in PBMCs from SS patients showing aberrant gene expression. Thus, these candidate genes effectively demonstrate the role of gene silencing by positional hypermethylation in both tissue-specific gene regulation and disease-specific dysregulation of gene expression. Notably, this is the first report of gene-specific hypomethylation in CTCL. Below, several interesting features observed during this study are discussed in terms of their consequences for the study of epigenetic dysregulation in SS.

6.1 Magnitude of methylation changes

Using the bioinformatic definitions of a CGI discussed in Section 1.2, SHP-1 contains the weaker CGI of the three genes, only just covering the minimum length of 200bp defined by Gardiner-Garden & Frommer (1987) and not having sufficient 'strength' according to the functional analysis of Bock *et al.* (2007). Fas and PLS-3 by contrast, contain much longer CGIs of over 1000bp, which are predicted by Bock *et al.*

(2007) to play a strong functional role. Interestingly, the hypermethylation observed in SHP-1 tissue-specific isoform II regulation was of a much greater magnitude than that observed in Fas and PLS3, affecting all 11 CpG dinucleotides and averaging 90% methylation in healthy keratinocytes compared to 12% methylation in healthy lymphocytes. The hypomethylation of the PLS3 CGI by comparison, affected only 5 CpG dinucleotides and corresponded to an average methylation difference of only 12% between healthy control CD4+ T-cells and SS patient CD4+ T-cells with dysregulated gene expression.

One possible explanation for this difference is that only a subset of T-cells have their PLS3 gene expression silenced by CGI methylation whereas the entire population of keratinocytes have their SHP-1 isoform II expression silenced by CGI methylation. Another possibility is that 'stronger' CGIs are in a more sensitive equilibrium where methylation of a single CpG site can perturb gene expression whereas 'weaker' CGIs require more extensive methylation to bring about silencing of gene expression. Since the CGI strength algorithm proposed by Bock *et al.* (2007) was based upon histone modifications and chromatin accessibility, the 'strong' CGIs may be in a state that is poised ready for methylation induced silencing whilst 'weaker' CGIs require more modification to reach the same state. This is of particular relevance given the number of studies looking to define a DNA methylation pattern characteristic to specific healthy tissue types and disease states. Smaller changes in methylation may not be detected by the high throughput methods used in these studies although they may have strong functional relevance to the disease under study. Similarly, a more sensitive assay may be limited in terms of how many samples it is feasible to study or how many CpG dinucleotides within each CGI can be examined. Further study of these factors may enable better design of high throughput assays to enable the accurate detection of

functionally relevant changes in DNA methylation.

6.2 Methylation in cell lines

Whilst the level of methylation in the cell lines examined broadly reflected the situation in primary tissue, several notable exceptions were observed. The SHP-1 promoter II CGI was heavily methylated in the keratinocyte cell line HEK293T and unmethylated in the leukaemic cell line Jurkat, consistent with the methylation observed in primary keratinocytes but not in primary lymphocytes. However, within the CTCL cell lines methylation was observed in SeAx and HuT78, which is inconsistent with the lack of methylation observed in SS patient lymphocytes suggesting that SHP-1 promoter II methylation is a consequence of the immortalisation of these cell lines. No Fas methylation was observed in the cell lines examined as the absence of Fas expression in SeAx was attributed to gene deletion. Wu & Wood (2011) examined further cell lines and demonstrated positional methylation of the Fas CGI in the SS cell line Sez-4. The demonstration of positional Fas methylation in 1/3 SS cell lines appears consistent with the situation in primary cells where a proportion of SS patients demonstrate down-regulation of Fas gene expression and consequent positional methylation of the Fas CGI. In sites 95-99 of the PLS3 CGI, methylation in cell lines broadly reflected the situation in primary cells with no methylation in HEK293, consistent with the absence of methylation and presence of expression in primary keratinocytes whilst substantial methylation was present in Jurkat cells that did not express PLS3. SeAx and HuT78, which did express PLS3 demonstrated reduced methylation levels compared to Jurkat however, all three lymphocyte cell lines demonstrated a greater proportion of methylation than healthy CD4+ lymphocytes, which do not express PLS3. This may be due to the cell lines being a purer population of cells than CD4+ lymphocytes and may

support the suggestion that PLS3 is only silenced by methylation in a subset of CD4+ lymphocytes. Alternatively, it may suggest that methylation level alone does not determine the expression status of PLS3 and additional regulatory mechanisms are in use.

The inconsistencies observed between cell lines and primary tissue, particularly in SHP-1, highlight the issues with extrapolating from studies examining only cell lines in the case of DNA methylation. Generally it is assumed that since DNA methylation is preserved between generations, it will be preserved across multiple passages in a cell line. Several studies have been performed to assess the consistency between cell lines and the primary tissues they were derived from. Paz *et al.* (2003) compared the methylation frequency of 15 genes between cell line and primary tissues of colon, breast and lung carcinoma and leukaemia and observed significant differences in frequency of methylation in up to three genes dependent upon the tissue type. Interestingly, only one gene showed an excess of methylation in cell lines from several tissues, all the other genes identified as differentially methylated between cell line and primary tissue were unique to that tissue suggesting that the subset of genes that become differentially methylated due to immortalisation may be tissue-specific. Another investigation demonstrated that 42/50 genes that had been identified as differentially methylated in colon cancer cell lines were differentially methylated in clinical tissue samples (Ehrich *et al.*, 2008). Together these results suggest that a small but measurable proportion of differentially methylated regions are a consequence of immortalisation rather than than reflecting the situation in primary tissue. This study also identified a greater magnitude of differential methylation between normal and cancer cell lines than observed between normal and malignant clinical tissue, similar to the results observed for PLS3 methylation discussed above. Ehrich *et al.* (2008) conclude that this effect is likely to be due to

the heterogeneity of clinical samples. The relative impact of differential methylation between cell lines and primary tissue may differ dependent upon the disease model and mode of immortalisation. For example, clustering analysis of the methylation profile of lung tumour cell lines, which proliferate spontaneously in the appropriate serum-free growth factor supplemented medium (Oie *et al.*, 1996), showed grouping by disease subtype with cell lines and primary tissue clustered together suggesting these cell lines represent an accurate model (Toyooka *et al.*, 2001). In contrast, EBV-transformed lymphoblastoid cell lines cluster separately to their originating PBL samples, indicating that 'methylation differences between peripheral blood lymphocyte- and lymphoblastoid cell line-derived DNA samples from a single individual are actually greater than the methylation profile differences between individuals' (Brennan *et al.*, 2009). Given this complex picture and the inconsistencies observed, particularly in SHP-1 CGI methylation, it is concluded that assessment of the DNA methylation profile of genes in SS is best carried out on primary tissue. Cell lines remain a valuable tool for functional studies, for example assessing the effect of demethylation using 5aza, however, DNA methylation in the gene of interest should first be characterised in cohort of SS patients before determining if any of the available cell lines act as a good model for the observed pattern.

6.3 Measuring tumour burden

For each of the three genes studied, the correlation of mRNA expression level with lymphocyte count, CD4+ count, percentage CD4+ and percentage Sézary cells was examined as a proxy for tumour burden. The most useful measure was observed to be percentage CD4+ cells, which correlated negatively with SHP-1 and Fas mRNA

expression and positively with PLS3 mRNA expression. Additionally, CD4:CD8 ratio correlated negatively with SHP-1 and Fas mRNA expression and lymphocyte and CD4+ counts correlated negatively with SHP-1 mRNA expression. It is possible that the absence of strong correlations between lymphocyte or CD4+ count and gene expression is due to the skewed nature of these data in the patient data set, with some patients recording values that are orders of magnitude greater than the normal range. Pearson's product-moment correlation does not require a normal distribution in the source data (Kowalski, 1972) but it is strongly susceptible to outliers (Devlin *et al.*, 1975) hence the skewing could suggest the use of rank based measures of correlation may be more appropriate. Re-analysis of the correlation data using Spearman's rank correlation revealed no differences for Fas and SHP-1 expression but did reveal significant correlation between PLS3 mRNA expression and lymphocyte count, CD4+ count and CD4:CD8 ratio and validated the previously observed strong correlation with percentage CD4+. Since this effect was limited to one gene it is likely this is due to the skewing observed in the PLS3 mRNA expression dataset and does not suggest any benefit to using Spearman's rank when examining correlation of expression data with lymphocyte or CD4+ counts.

Interestingly, whilst percentage Sézary cells showed a weak correlation in the appropriate direction in each gene, this did not reach significance in any of the genes examined, whether by Pearson's or Spearman's tests. This may be due in part to the difficulty in accurately quantifying Sezary cells based upon morphology alone (Lutzner *et al.*, 1973). Additionally, a subset of patients display a clear TCRVβ clone in blood but have no morphologically defined Sézary cells, suggesting that morphological analysis may not identify all the malignant cells present. Ideally, a marker would be identified that clearly enumerates the population of malignant cells, however, as shown in

Section 5.3.3 and discussed in Section 5.4, none of the markers proposed to date are expressed on all malignant cells in all patients. The method described in Section 5.3.4 for determining the TCRVβ gene rearrangement in an individual patient and hence designing a qPCR assay to specifically detect the clonal malignant cells has potential for the accurate enumeration of malignant cells. Due to the patient-specific nature of this method it is probably not viable for routine analysis in all patients however, for longitudinal studies examining response to treatment in a small cohort of patients it could provide a very accurate means of monitoring tumour burden, particularly given the high sensitivity.

6.4 Heterogeneity within the tumour cell population

In Section 5.3.3 a detailed investigation of the expression of PLS3 on a single cell level and the correlation with other immunophenotypic markers demonstrated the high level of heterogeneity in marker expression both within and between patients. Heterogeneity was also observed in the Fas studies, with Fas expression both up- and down-regulated and no correlation observed between Fas, CD26 and PLS3 expression. Based upon these results it was concluded that enrichment of CD3+CD4+ T-cells remains the optimal means of isolating the entire malignant cell population. This observation of extreme heterogeneity is interesting because it suggests no individual gene or set of genes are serving as a driver for the malignancy, which would lead to much more consistent dysregulation over the tumour population. This suggestion is supported by the absence of chromosomal rearrangements unique to CTCL as discussed in Section 1.1.2. Heterogeneity is observed in many different cancers and two theories of cancer development can explain the observation of heterogeneity in cancer cells (Shackleton *et al.*,

2009). The cancer stem cell model suggests that a cancer is driven by a small subpopulation of cancer stem cells that generate progeny with the potential to differentiate, creating heterogeneity within the tumour cell population (Jordan *et al.*, 2006). Additionally these progeny will have an increased likelihood of picking up further genetic and epigenetic mutations, adding to the heterogeneity of gene expression observed. If this is the case then a subset of genetic, epigenetic and phenotypic features may be identified that define the cancer stem cells. The clonal evolution model proposes that as the malignant cell population develops further genetic and epigenetic mutations some will confer a selective advantage, allowing outgrowth of a particular clone until further mutations occur (Nowell, 1976). However, clones are not necessarily mutually exclusive and heterogeneity may arise if several sub-clones have developed which show differing phenotypic features.

6.5 Dysregulation of T-cell signalling

The pathways affected by dysregulation of the investigated genes are discussed in greater detail in the individual results chapters however, a common feature of the selected candidate genes is their potential contribution to dysregulation of the T-cell signalling pathways and hence to the persistence of the malignant cells highlighted in Section 1.1.4. Aberrant expression of PLS3 was confirmed in Chapter 5 and it is hypothesised that this aberrant expression may disrupt T-cell interactions due to the similarity between PLS3 and L-plastin, which is critical to the formation of the immunological synapse (Wang *et al.*, 2010). The signals encountered during these T-cell interactions are critical to the establishment of cell type subsets and may initiate an anergic state whereby it is difficult to promote proliferation or the subsequent apoptotic clearance of these cells. In addition to this, loss of Fas receptor as demonstrated

in Chapter 4 and gain of the downstream pathway inhibitor c-FLIP (Contassot *et al.*, 2008) combine to increase the threshold for initiation of apoptosis, allowing these cells to persist further. Although SHP-1 was not found to be dysregulated in primary SS tissues, constitutive phosphorylation of STAT3 was underlined as a common feature of SS (McKenzie *et al.*, 2011). STAT3 is a crucial integrator of cytokine signalling pathways and it's constitutive activation contributes to immune evasion by tumour cells through the promotion of T-cell tolerance (Yu *et al.*, 2007). As discussed in Section 3.4, it has recently been discovered that methylation of the STAT3 protein on an arginine residue may directly influence the phosphorylation state opening up the possibility that imbalances of methylation may impact directly upon the STAT3 pathway.

Conclusions

From the data presented in this thesis the following major conclusions are proposed:

- SHP-1 is not silenced by DNA methylation in primary lymphocytes from SS patients.
- Fas is frequently down-regulated by aberrant positional hypermethylation of the Fas CGI in SS patient lymphocytes.
- PLS3 mRNA is aberrantly expressed in 60% of SS patient lymphocytes, this may be due to aberrant positional hypomethylation of the PLS3 CGI.
- Cell lines should be used with caution in studies examining DNA methylation in SS as their methylation status may have arisen during immortalisation.
- Sézary cells display distinct heterogeneity in expression of CD45RO, CD7, CD26, CD25, CD158k, Fas and PLS3 between patients and importantly within tumour cell populations from individual patients. Therefore enrichment of CD4+ T-cells by negative selection is the best method for enriching the tumour cell population.

Future questions

This thesis successfully met its aims of determining the contribution of DNA methylation to the dysregulation of three candidate genes in SS and further allowed the exploration of the pathogenic roles of these genes. Several research tools have been developed during the course of these studies which are expected to be of value to other scientists looking to further these studies. As with any substantial body of scientific endeavour however, more questions were raised than were resolved, ranging from the molecular mechanistic dissection of how aberrant positional hypo- or hypermethylation occurs to the clinical relevance of each gene's dysregulated methylation. The most pertinent of these are discussed below along with the feasibility of instigating future studies with currently available technology and methods.

Having comprehensively ruled out loss of SHP-1 as a mechanism leading to constitutive activation of STAT3 the question remains of what causes this activation. This is a fairly major question and has been the subject of extensive study over the years. Avenues currently being pursued by others in our lab include the role of upstream cytokine receptor dysregulation and direct STAT3 methylation on arginine residues as a regulatory mechanism for STAT3 phosphorylation.

The mechanistic link between positional hypermethylation in the Fas CGI and reduced Fas mRNA expression has been conclusively demonstrated thanks to the presence of positional methylation in Sez-4 that could be reduced by 5aza treatment, with consequent re-expression of Fas mRNA (Wu & Wood, 2011). However, this has not yet been demonstrated for the positional hypomethylation observed in the PLS3 CGI of SS patients. The most straightforwards approach that could be taken would be to treat healthy CD4+ lymphocytes with 5aza to determine whether this led to a reduction

of PLS3 CGI methylation and consequent re-expression of PLS3 mRNA. 5aza treatment requires the active proliferation of cells in order to become incorporated in the DNA (Stresemann & Lyko, 2008) so it would be necessary to stimulate the healthy CD4+ lymphocytes with anti-CD3/CD28 to promote proliferation.

The loss of Fas and gain of PLS3 may have a prognostic impact, determining if this is the case will take time as patients whose Fas and PLS3 status were determined at diagnosis need to be followed through the course of treatment. If additional samples can be obtained it would also be interesting to conduct a more thorough investigation of changes in expression over time as the preliminary data presented here suggested Fas may become progressively down-regulated. Alterations in PLS3 mRNA expression has previously been followed over time in only one SS patient where it appeared to be consistent with alterations in tumour burden (Tang *et al.*, 2010). The preliminary data on the change in PLS3 mRNA expression over time in five SS patients presented in Chapter 5 was more mixed with no clear relationship to the changes in tumour burden. Following the changes in a cohort of patients over time may allow a clearer picture to be determined, particularly with respect to response to treatment and alterations in tumour burden.

So far it has only been possible to speculate on the functional role played by PLS3 when aberrantly expressed in SS lymphocytes. The optimisation of a specific and sensitive antibody for the detection of PLS3 described here should hopefully open up many avenues for analysis of the localisation and interactions of PLS3 in SS lymphocytes. Another potential approach would be to introduce PLS3 to healthy CD4+ lymphocytes by transfection of a vector containing the PLS3 gene under the control of a constitutive promoter and examine the effect upon T-cell signalling pathways. Previously it has been challenging to introduce extra DNA into primary lymphocytes as

most commercial transfection agents are ineffective or induce apoptosis (Ebert *et al.*, 1997). However, devices such as the nucleofector have reported high success rates with difficult-to-transfect cells such as primary lymphocytes so this may now be a viable option (Magg *et al.*, 2009).

Finally, since altered DNA methylation events have been shown to be so crucial to the dysregulated T-cell signalling observed in SS the question of how to therapeutically modify these effects is relevant. The most obvious way to reduce methylation is to treat with 5aza however, since hypomethylation of PLS3 has been observed this kind of broad brush approach may be inappropriate. As mentioned previously, HDIs have proven efficacious in CTCL patients and induce increased apoptosis of *ex vivo* tumour cells (Duvic *et al.*, 2007, Whittaker *et al.*, 2010). Since histone modifications and DNA methylation have been shown to exert their effects in a synergistic fashion (Cameron *et al.*, 1999) it may be that HDI induced changes in the chromatin structure lead to alterations in DNA methylation in relevant genes. Further characterisation of *ex vivo* tumour cells treated with HDIs and of lymphocytes from patients treated with HDIs should allow the elucidation of which genes and T-cell signalling pathways are influenced by HDI treatment.

References

Abrams, J.T., Lessin, S., Ghosh, S.K., Ju, W., Vonderheid, E.C., Nowell, P., Murphy, G., Elfenbein, B. & Defreitas, E. (1991). A clonal CD4-positive T-cell line established from the blood of a patient with Sézary syndrome. *The Journal of investigative dermatology*, **96**, 31–7.

Agar, N.S., Wedgeworth, E., Crichton, S., Mitchell, T.J., Cox, M., Ferreira, S., Robson, A., Calonje, E., Stefanato, C.M., Wain, E.M., Wilkins, B., Fields, P.A., Dean, A., Webb, K., Scarisbrick, J., Morris, S. & Whittaker, S.J. (2010). Survival outcomes and prognostic factors in mycosis fungoides/Sézary syndrome: validation of the revised International Society for Cutaneous Lymphomas/European Organisation for Research and Treatment of Cancer staging proposal. *J Clin Oncol*, **28**, 4730–9.

Alderson, M.R., Tough, T.W., Davis-Smith, T., Braddy, S., Falk, B., Schooley, K.A., Goodwin, R.G., Smith, C.A., Ramsdell, F. & Lynch, D.H. (1995). Fas ligand mediates activation-induced cell death in human T lymphocytes. *J Exp Med*, **181**, 71–7.

Alibert, J. (1832). Monographie des dermatoses, ou précis théorique et pratique des maladies de la peau.

Allfrey, V.G., Littau, V.C. & Mirsky, A.E. (1963). On the role of of histones in regulation ribonucleic acid synthesis in the cell nucleus. *Proceedings of the National Academy of Sciences of the United States of America*, **49**, 414–21.

Allfrey, V.G., Faulkner, R. & Mirsky, A.E. (1964). Acetylation and methylation of histones and their possible role in the regulation of RNA synthesis. *Proceedings of the National Academy of Sciences of the United States of America*, **51**, 786–94.

Amara, K., Trimeche, M., Ziadi, S., Laatiri, A., Hachana, M., Sriha, B., Mokni, M. & Korbi, S. (2007). Presence of simian virus 40 DNA sequences in diffuse large B-cell lymphomas in Tunisia correlates with aberrant promoter hypermethylation of multiple tumor suppressor genes. *Int J Cancer*, **121**, 2693–702.

Amara, K., Trimeche, M., Ziadi, S., Laatiri, A., Hachana, M. & Korbi, S. (2008). Prognostic significance of aberrant promoter hypermethylation of CpG islands in patients with diffuse large B-cell lymphomas. *Ann Oncol*, **19**, 1774–86.

Amin, H.M., Hoshino, K., Yang, H., Lin, Q., Lai, R. & Garcia-Manero, G. (2007). Decreased expression level of SH2 domain-containing protein tyrosine phosphatase-1 (Shp1) is associated with progression of chronic myeloid leukaemia. *The Journal of pathology*, **212**, 402–10.

Antequera, F. & Bird, A. (1993). Number of CpG islands and genes in human and mouse. *Proceedings of the National Academy of Sciences of the United States of America*, **90**, 11995–9.

Arányi, T., Faucheux, B.A., Khalfallah, O., Vodjdani, G., Biguet, N.F., Mallet, J. & Meloni, R. (2005). The tissue-specific methylation of the human tyrosine hydroxylase gene reveals new regulatory elements in the first exon. *J Neurochem*, **94**, 129–39.

Arpin, M., Friederich, E., Algrain, M., Vernel, F. & Louvard, D. (1994). Functional differences between L- and T-plastin isoforms. *J Cell Biol*, **127**, 1995–2008.

Bagot, M., Moretta, A., Sivori, S., Biassoni, R., Cantoni, C., Bottino, C., Boumsell, L. & Bensussan, A. (2001). CD4(+) cutaneous T-cell lymphoma cells express the p140-killer cell immunoglobulin-like receptor. *Blood*, **97**, 1388–91.

Bajic, V.B., Tan, S.L., Christoffels, A., Schönbach, C., Lipovich, L., Yang, L., Hofmann, O., Kruger, A., Hide, W., Kai, C., Kawai, J., Hume, D.A., Carninci, P. & Hayashizaki, Y. (2006). Mice and men: their promoter properties. *PLoS genetics*, **2**, e54.

Bang, K., Lund, M., Mogensen, S.C. & Thestrup-Pedersen, K. (2005). In vitro culture of skin-homing T lymphocytes from inflammatory skin diseases. *Experimental dermatology*, **14**, 391–7.

Banville, D., Stocco, R. & Shen, S.H. (1995). Human protein tyrosine phosphatase 1C (PTPN6) gene structure: alternate promoter usage and exon skipping generate multiple transcripts. *Genomics*, **27**, 165–73.

Barreto, G., Schäfer, A., Marhold, J., Stach, D., Swaminathan, S.K., Handa, V., Döderlein, G., Maltry, N., Wu, W., Lyko, F. & Niehrs, C. (2007). Gadd45a promotes epigenetic gene activation by repair-mediated DNA demethylation. *Nature*, **445**, 671–5.

Barski, A., Cuddapah, S., Cui, K., Roh, T.Y., Schones, D.E., Wang, Z., Wei, G., Chepelev, I. & Zhao, K. (2007). High-resolution profiling of histone methylations in the human genome. *Cell*, **129**, 823–37.

Batista, D.A.S., Vonderheid, E.C., Hawkins, A., Morsberger, L., Long, P., Murphy, K.M. & Griffin, C.A. (2006). Multicolor fluorescence in situ hybridization (SKY) in mycosis fungoides and Sézary syndrome: search for recurrent chromosome abnormalities. *Genes, chromosomes & cancer*, **45**, 383–91.

Baylin, S.B. & Ohm, J.E. (2006). Epigenetic gene silencing in cancer - a mechanism for early oncogenic pathway addiction? *Nat Rev Cancer*, **6**, 107–16.

Bediaga, N.G., Acha-Sagredo, A., Guerra, I., Viguri, A., Albaina, C., Diaz, I.R., Rezola, R., Alberdi, M.J., Dopazo, J., Montaner, D., de Renobales, M., Fernández, A.F., Field, J.K., Fraga, M.F., Liloglou, T. & de Pancorbo, M.M. (2010). DNA methylation epigenotypes in breast cancer molecular subtypes. *Breast Cancer Res*, **12**, R77.

Beghini, A., Ripamonti, C.B., Peterlongo, P., Roversi, G., Cairoli, R., Morra, E. & Larizza, L. (2000). RNA hyperediting and alternative splicing of hematopoietic cell phosphatase (PTPN6) gene in acute myeloid leukemia. *Human molecular genetics*, **9**, 2297–304.

Behrmann, I., Walczak, H. & Krammer, P.H. (1994). Structure of the human APO-1 gene. *Eur J Immunol*, **24**, 3057–62.

Beltinger, C., Kurz, E., Böhler, T., Schrappe, M., Ludwig, W.D. & Debatin, K.M. (1998). CD95 (APO-1/Fas) mutations in childhood T-lineage acute lymphoblastic leukemia. *Blood*, **91**, 3943–51.

Bench, A.J., Erber, W.N., Follows, G.A. & Scott, M.A. (2007). Molecular genetic analysis of haematological malignancies II: Mature lymphoid neoplasms. *International journal of laboratory hematology*, **29**, 229–60.

Benkerrou, M., Deist, F.L., de Villartay, J.P., Caillat-Zucman, S., Rieux-Laucat, F., Jabado, N., Cavazzana-Calvo, M. & Fischer, A. (1997). Correction of Fas (CD95) deficiency by haploidentical bone marrow transplantation. *Eur J Immunol*, **27**, 2043–7.

Bensussan, A., Remtoula, N., Sivori, S., Bagot, M., Moretta, A. & Marie-Cardine, A. (2011). Expression and function of the natural cytotoxicity receptor NKp46 on circulating malignant CD4+ T lymphocytes of Sézary syndrome patients. *The Journal of investigative dermatology*, **131**, 969–76.

Berger, C.L., Hanlon, D., Kanada, D., Dhodapkar, M., Lombillo, V., Wang, N., Christensen, I., Howe, G., Crouch, J., El-Fishawy, P. & Edelson, R. (2002). The growth of cutaneous T-cell lymphoma is stimulated by immature dendritic cells. *Blood*, **99**, 2929–39.

Bestor, T., Laudano, A., Mattaliano, R. & Ingram, V. (1988). Cloning and sequencing of a cDNA encoding DNA methyltransferase of mouse cells. The carboxyl-terminal domain of the mammalian enzymes is related to bacterial restriction methyltransferases. *J Mol Biol*, **203**, 971–83.

Bhattacharya, S.K., Ramchandani, S., Cervoni, N. & Szyf, M. (1999). A mammalian protein with specific demethylase activity for mCpG DNA. *Nature*, **397**, 579–83.

Bhutani, N., Brady, J.J., Damian, M., Sacco, A., Corbel, S.Y. & Blau, H.M. (2010). Reprogramming towards pluripotency requires AID-dependent DNA demethylation. *Nature*, **463**, 1042–7.

Bigler, R.D., Boselli, C.M., Foley, B. & Vonderheid, E.C. (1996). Failure of anti-T-cell receptor V beta antibodies to consistently identify a malignant T-cell clone in Sézary syndrome. *Am J Pathol*, **149**, 1477–83.

Bird, A.P. (1980). DNA methylation and the frequency of CpG in animal DNA. *Nucleic Acids Res*, **8**, 1499–504.

Bird, A.P. (1986). CpG-rich islands and the function of DNA methylation. *Nature*, **321**, 209–13.

Blake, J.A., Bult, C.J., Kadin, J.A., Richardson, J.E., Eppig, J.T. & Group, M.G.D. (2011). The Mouse Genome Database (MGD): premier model organism resource for mammalian genomics and genetics. *Nucleic Acids Res*, **39**, D842–8.

Bock, C., Walter, J., Paulsen, M. & Lengauer, T. (2007). CpG island mapping by epigenome prediction. *PLoS Comput Biol*, **3**, e110.

Bogen, S.A., Pelley, D., Charif, M., McCusker, M., Koh, H., Foss, F., Garifallou, M., Arkin, C. & Zucker-Franklin, D. (1996). Immunophenotypic identification of Sezary cells in peripheral blood. *Am J Clin Pathol*, **106**, 739–48.

Booken, N., Gratchev, A., Utikal, J., Weiss, C., Yu, X., Qadoumi, M., Schmuth, M., Sepp, N., Nashan, D., Rass, K., Tüting, T., Assaf, C., Dippel, E., Stadler, R., Klemke, C.D. & Goerdt, S. (2008). Sézary syndrome is a unique cutaneous T-cell lymphoma as identified by an expanded gene signature including diagnostic marker molecules CDO1 and DNM3. *Leukemia*, **22**, 393–9.

Borowitz, M.J., Weidner, A., Olsen, E.A. & Picker, L.J. (1993). Abnormalities of circulating T-cell subpopulations in patients with cutaneous T-cell lymphoma: cutaneous lymphocyte-associated antigen expression on T cells correlates with extent of disease. *Leukemia : official journal of the Leukemia Society of America, Leukemia Research Fund, UK*, **7**, 859–63.

Bourc'his, D., Xu, G.L., Lin, C.S., Bollman, B. & Bestor, T.H. (2001). Dnmt3L and the establishment of maternal genomic imprints. *Science*, **294**, 2536–9.

Bradford, P.T., Devesa, S.S., Anderson, W.F. & Toro, J.R. (2009). Cutaneous lymphoma incidence patterns in the United States: a population-based study of 3884 cases. *Blood*, **113**, 5064–73.

Brakensiek, K., Wingen, L.U., Länger, F., Kreipe, H. & Lehmann, U. (2007). Quantitative high-resolution CpG island mapping with Pyrosequencing reveals disease-specific methylation patterns of the CDKN2B gene in myelodysplastic syndrome and myeloid leukemia. *Clin Chem*, **53**, 17–23.

Braylan, R., Variakojis, D. & Yachnin, S. (1975). The Sézary syndrome lymphoid cell: abnormal surface properties and mitogen responsiveness. *Br J Haematol*, **31**, 553–64.

Brender, C., Nielsen, M., Kaltoft, K., Mikkelsen, G., Zhang, Q., Wasik, M., Billestrup, N. & Odum, N. (2001). STAT3-mediated constitutive expression of SOCS-3 in cutaneous T-cell lymphoma. *Blood*, **97**, 1056–62.

Brennan, E.P., Ehrich, M., Brazil, D.P., Crean, J.K., Murphy, M., Sadlier, D.M., Martin, F., Godson, C., McKnight, A.J., van den Boom, D., Maxwell, A.P. & Savage, D.A. (2009). Comparative analysis of DNA methylation profiles in peripheral blood leukocytes versus lymphoblastoid cell lines. *Epigenetics*, **4**, 159–64.

Brito-Babapulle, V., Hamoudi, R., Matutes, E., Watson, S., Kaczmarek, P., Maljaie, H. & Catovsky, D. (2000). p53 allele deletion and protein accumulation occurs in the absence of p53 gene mutation in T-prolymphocytic leukaemia and Sezary syndrome. *British journal of haematology*, **110**, 180–7.

Britten, R.J., Baron, W.F., Stout, D.B. & Davidson, E.H. (1988). Sources and evolution of human Alu repeated sequences. *Proceedings of the National Academy of Sciences of the United States of America*, **85**, 4770–4.

Brownlee, T.R. & Murad, T.M. (1970). Ultrastructure of mycosis fungoides. *Cancer*, **26**, 686–98.

Brüggemann, M., van der Velden, V.H.J., Raff, T., Droese, J., Ritgen, M., Pott, C., Wijkhuijs, A.J., Gökbuget, N., Hoelzer, D., van Wering, E.R., van Dongen, J.J.M. & Kneba, M. (2004). Rearranged T-cell receptor beta genes represent powerful targets for quantification of minimal residual disease in childhood and adult T-cell acute lymphoblastic leukemia. *Leukemia*, **18**, 709–19.

Bruniquel, D. & Schwartz, R.H. (2003). Selective, stable demethylation of the interleukin-2 gene enhances transcription by an active process. *Nat Immunol*, **4**, 235–40.

Bryksin, A.V. & Matsumura, I. (2010). Overlap extension PCR cloning: a simple and reliable way to create recombinant plasmids. *BioTechniques*, **48**, 463–5.

Bunn, P.A. & Foss, F.M. (1996). T-cell lymphoma cell lines (HUT102 and HUT78) established at the National Cancer Institute: history and importance to understanding the biology, clinical features, and therapy of cutaneous T-cell lymphomas (CTCL) and adult T-cell leukemia-lymphomas (ATLL). *J Cell Biochem Suppl*, **24**, 12–23.

Bunn, P.A., Edelson, R., Ford, S.S. & Shackney, S.E. (1981). Patterns of cell proliferation and cell migration in the Sézary syndrome. *Blood*, **57**, 452–63.

Burkhardt, J.K., Carrizosa, E. & Shaffer, M.H. (2008). The actin cytoskeleton in T cell activation. *Annu Rev Immunol*, **26**, 233–59.

Cameron, E.E., Bachman, K.E., Myöhänen, S., Herman, J.G. & Baylin, S.B. (1999). Synergy of demethylation and histone deacetylase inhibition in the re-expression of genes silenced in cancer. *Nat Genet*, **21**, 103–7.

Campanero, M.R., Armstrong, M.I. & Flemington, E.K. (2000). CpG methylation as a mechanism for the regulation of E2F activity. *Proc Natl Acad Sci USA*, **97**, 6481–6.

Campbell, J.J., Clark, R.A., Watanabe, R. & Kupper, T.S. (2010). Sezary syndrome and mycosis fungoides arise from distinct T-cell subsets: a biologic rationale for their distinct clinical behaviors. *Blood*, **116**, 767–71.

Capello, D., Deambrogi, C., Rossi, D., Lischetti, T., Piranda, D., Cerri, M., Spina, V., Rasi, S., Gaidano, G. & Lunghi, M. (2008). Epigenetic inactivation of suppressors of cytokine signalling in Philadelphia-negative chronic myeloproliferative disorders. *British journal of haematology*, **141**, 504–11.

Cappellen, D., de Medina, S.G.D., Chopin, D., Thiery, J.P. & Radvanyi, F. (1997). Frequent loss of heterozygosity on chromosome 10q in muscle-invasive transitional cell carcinomas of the bladder. *Oncogene*, **14**, 3059–66.

Caprini, E., Cristofoletti, C., Arcelli, D., Fadda, P., Citterich, M.H., Sampogna, F., Magrelli, A., Censi, F., Torreri, P., Frontani, M., Scala, E., Picchio, M.C., Temperani, P., Monopoli, A., Lombardo, G.A., Taruscio, D., Narducci, M.G. & Russo, G. (2009). Identification of key regions and genes important in the pathogenesis of sezary syndrome by combining genomic and expression microarrays. *Cancer research*, **69**, 8438–46.

Capriotti, E., Vonderheid, E.C., Thoburn, C.J., Bright, E.C. & Hess, A.D. (2007). Chemokine receptor expression by leukemic T cells of cutaneous T-cell lymphoma: clinical and histopathological correlations. *The Journal of investigative dermatology*, **127**, 2882–92.

Capriotti, E., Vonderheid, E.C., Thoburn, C.J., Wasik, M.A., Bahler, D.W. & Hess, A.D. (2008). Expression of T-plastin, FoxP3 and other tumor-associated markers by leukemic T-cells of cutaneous T-cell lymphoma. *Leuk Lymphoma*, **49**, 1190–201.

Carney, D.N., Bunn, P.A., Schechter, G.P. & Gazdar, A.F. (1980). Lymphocyte transformation in patients with cutaneous T-cell lymphomas. *Int J Cancer*, **26**, 535–42.

Cascino, I., Fiucci, G., Papoff, G. & Ruberti, G. (1995). Three functional soluble forms of the human apoptosis-inducing Fas molecule are produced by alternative splicing. *J Immunol*, **154**, 2706–13.

Chan, H., Bartos, D.P. & Owen-Schaub, L.B. (1999). Activation-dependent transcriptional regulation of the human Fas promoter requires NF-kappaB p50-p65 recruitment. *Molecular and cellular biology*, **19**, 2098–108.

Chedin, F., Lieber, M.R. & Hsieh, C.L. (2002). The DNA methyltransferase-like protein DNMT3L stimulates de novo methylation by Dnmt3a. *Proceedings of the National Academy of Sciences of the United States of America*, **99**, 16916–21.

Chen, H., Mocsai, A., Zhang, H., Ding, R.X., Morisaki, J.H., White, M., Rothfork, J.M., Heiser, P., Colucci-Guyon, E., Lowell, C.A., Gresham, H.D., Allen, P.M. & Brown, E.J. (2003). Role for plastin in host defense distinguishes integrin signaling from cell adhesion and spreading. *Immunity*, **19**, 95–104.

Chen, W., Daines, M.O. & Hershey, G.K.K. (2004). Methylation of STAT6 modulates STAT6 phosphorylation, nuclear translocation, and DNA-binding activity. *J Immunol*, **172**, 6744–50.

Cheng, J., Zhou, T., Liu, C., Shapiro, J.P., Brauer, M.J., Kiefer, M.C., Barr, P.J. & Mountz, J.D. (1994). Protection from Fas-mediated apoptosis by a soluble form of the Fas molecule. *Science*, **263**, 1759–62.

Cheng, J., Liu, C., Koopman, W.J. & Mountz, J.D. (1995). Characterization of human Fas gene. Exon/intron organization and promoter region. *J Immunol*, **154**, 1239–45.

Cheng, J., Zhang, D., Zhou, C. & Marasco, W.A. (2004). Down-regulation of SHP1 and up-regulation of negative regulators of JAK/STAT signaling in HTLV-1 transformed cell lines and freshly transformed human peripheral blood CD4+ T-cells. *Leukemia research*, **28**, 71–82.

Cheng, J., Kydd, A.R., Nakase, K., Noonan, K.M., Murakami, A., Tao, H., Dwyer, M., Xu, C., Zhu, Q. & Marasco, W.A. (2007). Negative regulation of the SH2-homology containing protein-tyrosine phosphatase-1 (SHP-1) P2 promoter by the HTLV-1 Tax oncoprotein. *Blood*, **110**, 2110–20.

Chim, C.S., Fung, T.K., Cheung, W.C., Liang, R. & Kwong, Y.L. (2004a). SOCS1 and SHP1 hypermethylation in multiple myeloma: implications for epigenetic activation of the Jak/STAT pathway. *Blood*, **103**, 4630–5.

Chim, C.S., Wong, A.S.Y. & Kwong, Y.L. (2004b). Epigenetic dysregulation of the Jak/STAT pathway by frequent aberrant methylation of SHP1 but not SOCS1 in acute leukaemias. *Ann Hematol*, **83**, 527–32.

Chim, C.S., Liang, R., Leung, M.H. & Kwong, Y.L. (2007). Aberrant gene methylation implicated in the progression of monoclonal gammopathy of undetermined significance to multiple myeloma. *J Clin Pathol*, **60**, 104–6.

Christophi, G., Hudson, C., Gruber, R., Christophi, C. & Massa, P. (2008). Promoter-specific induction of the phosphatase SHP-1 by viral infection and cytokines in CNS glia. *J Neurochem*.

Chung, C.D., Liao, J., Liu, B., Rao, X., Jay, P., Berta, P. & Shuai, K. (1997). Specific inhibition of Stat3 signal transduction by PIAS3. *Science*, **278**, 1803–5.

Clark, R.A., Shackelton, J.B., Watanabe, R., Calarese, A., ichi Yamanaka, K., Campbell, J.J., Teague, J.E., Kuo, H.P., Hijnen, D. & Kupper, T.S. (2011). High-scatter T cells: a reliable biomarker for malignant T cells in cutaneous T-cell lymphoma. *Blood*, **117**, 1966–76.

Contassot, E., Kerl, K., Roques, S., Shane, R., Gaide, O., Dupuis, M., Rook, A.H. & French, L.E. (2008). Resistance to FasL and tumor necrosis factor-related apoptosis-inducing ligand-mediated apoptosis in Sezary syndrome T-cells associated with impaired death receptor and FLICE-inhibitory protein expression. *Blood*, **111**, 4780–7.

Cooper, D.N., Taggart, M.H. & Bird, A.P. (1983). Unmethylated domains in vertebrate DNA. *Nucleic Acids Res*, **11**, 647–58.

Cornacchia, E., Golbus, J., Maybaum, J., Strahler, J., Hanash, S. & Richardson, B. (1988). Hydralazine and procainamide inhibit T cell DNA methylation and induce autoreactivity. *J Immunol*, **140**, 2197–200.

Cosgrove, M.S., Boeke, J.D. & Wolberger, C. (2004). Regulated nucleosome mobility and the histone code. *Nature structural & molecular biology*, **11**, 1037–43.

Coulondre, C., Miller, J.H., Farabaugh, P.J. & Gilbert, W. (1978). Molecular basis of base substitution hotspots in Escherichia coli. *Nature*, **274**, 775–80.

Curiel-Lewandrowski, C., Yamasaki, H., Si, C.P., Jin, X., Zhang, Y., Richmond, J., Tuzova, M., Wilson, K., Sullivan, B., Jones, D., Ryzhenko, N., Little, F., Kupper, T.S., Center, D.M. & Cruikshank, W.W. (2011). Loss of nuclear pro-IL-16 facilitates cell cycle progression in human cutaneous T cell lymphoma. *J Clin Invest*, **121**, 4838–49.

Dalloul, A., Laroche, L., Bagot, M., Mossalayi, M.D., Fourcade, C., Thacker, D.J., Hogge, D.E., Merle-Béral, H., Debré, P. & Schmitt, C. (1992). Interleukin-7 is a growth factor for Sézary lymphoma cells. *The Journal of clinical investigation*, **90**, 1054–60.

Dautigny, N., Campion, A.L. & Lucas, B. (1999). Timing and casting for actors of thymic negative selection. *J Immunol*, **162**, 1294–302.

Davis, T.H., Morton, C.C., Miller-Cassman, R., Balk, S.P. & Kadin, M.E. (1992). Hodgkin's disease, lymphomatoid papulosis, and cutaneous T-cell lymphoma derived from a common T-cell clone. *N Engl J Med*, **326**, 1115–22.

DeChiara, T.M., Robertson, E.J. & Efstratiadis, A. (1991). Parental imprinting of the mouse insulin-like growth factor II gene. *Cell*, **64**, 849–59.

Deininger, P.L. & Batzer, M.A. (1999). Alu repeats and human disease. *Mol Genet Metab*, **67**, 183–93.

Dereure, O., Portales, P., Clot, J. & Guilhou, J.J. (2000). Decreased expression of Fas (APO-1/CD95) on peripheral blood CD4+ T lymphocytes in cutaneous T-cell lymphomas. *Br J Dermatol*, **143**, 1205–10.

Dereure, O., Levi, E., Vonderheid, E.C. & Kadin, M.E. (2002). Infrequent Fas mutations but no Bax or p53 mutations in early mycosis fungoides: a possible mechanism for the accumulation of malignant T lymphocytes in the skin. *The Journal of investigative dermatology*, **118**, 949–56.

Detich, N., Bovenzi, V. & Szyf, M. (2003). Valproate induces replication-independent active DNA demethylation. *The Journal of biological chemistry*, **278**, 27586–92.

Devlin, S., Gnanadesikan, R. & Kettenring, J. (1975). Robust Estimation and Outlier Detection with Correlation Coefficients. *Biometrika*, **62**, 531–545.

Dewannieux, M., Esnault, C. & Heidmann, T. (2003). LINE-mediated retrotransposition of marked Alu sequences. *Nat Genet*, **35**, 41–8.

Dhein, J., Walczak, H., Bäumler, C., Debatin, K.M. & Krammer, P.H. (1995). Autocrine T-cell suicide mediated by APO-1/(Fas/CD95). *Nature*, **373**, 438–41.

Döbbeling, U., Dummer, R., Laine, E., Potoczna, N., Qin, J.Z. & Burg, G. (1998). Interleukin-15 is an autocrine/paracrine viability factor for cutaneous T-cell lymphoma cells. *Blood*, **92**, 252–8.

Down, T.A., Rakyan, V.K., Turner, D.J., Flicek, P., Li, H., Kulesha, E., Gräf, S., Johnson, N., Herrero, J., Tomazou, E.M., Thorne, N.P., Bäckdahl, L., Herberth, M., Howe, K.L., Jackson, D.K., Miretti, M.M., Marioni, J.C., Birney, E., Hubbard, T.J.P., Durbin, R., Tavaré, S. & Beck, S. (2008). A Bayesian deconvolution strategy for immunoprecipitation-based DNA methylome analysis. *Nat Biotechnol*, **26**, 779–85.

Drappa, J., Vaishnaw, A.K., Sullivan, K.E., Chu, J.L. & Elkon, K.B. (1996). Fas gene mutations in the Canale-Smith syndrome, an inherited lymphoproliferative disorder associated with autoimmunity. *N Engl J Med*, **335**, 1643–9.

Drummond, A., Ashton, B., Boxton, S., Cheung, M., , Cooper, A., Duran, C., Field, M., Heled, J., Kearse, M., Markowitz, S., Moir, R., Stones-Havas, S., Sturrock, S., Thierer, T. & Wilson, A. (2011). Geneious v5.4, Available from http://www.geneious.com/.

Dummer, R., Nestle, F.O., Niederer, E., Ludwig, E., Laine, E., Grundmann, H., Grob, P. & Burg, G. (1999). Genotypic, phenotypic and functional analysis of CD4+CD7+ and CD4+CD7- T lymphocyte subsets in Sézary syndrome. *Arch Dermatol Res*, **291**, 307–11.

Dutton, R.W., Bradley, L.M. & Swain, S.L. (1998). T cell memory. *Annu Rev Immunol*, **16**, 201–23.

Duvic, M., Talpur, R., Ni, X., Zhang, C., Hazarika, P., Kelly, C., Chiao, J.H., Reilly, J.F., Ricker, J.L., Richon, V.M. & Frankel, S.R. (2007). Phase 2 trial of oral vorinostat (suberoylanilide hydroxamic acid, SAHA) for refractory cutaneous T-cell lymphoma (CTCL). *Blood*, **109**, 31–9.

Ebert, O., Finke, S., Salahi, A., Herrmann, M., Trojaneck, B., Lefterova, P., Wagner, E., Kircheis, R., Huhn, D., Schriever, F. & Schmidt-Wolf, I.G. (1997). Lymphocyte apoptosis: induction by gene transfer techniques. *Gene Ther*, **4**, 296–302.

Edelman, J. & Meyerson, H.J. (2000). Diminished CD3 expression is useful for detecting and enumerating Sézary cells. *Am J Clin Pathol*, **114**, 467–77.

Ehrich, M., Turner, J., Gibbs, P., Lipton, L., Giovanneti, M., Cantor, C. & van den Boom, D. (2008). Cytosine methylation profiling of cancer cell lines. *Proceedings of the National Academy of Sciences of the United States of America*, **105**, 4844–9.

Endo, T.A., Masuhara, M., Yokouchi, M., Suzuki, R., Sakamoto, H., Mitsui, K., Matsumoto, A., Tanimura, S., Ohtsubo, M., Misawa, H., Miyazaki, T., Leonor, N., Taniguchi, T., Fujita, T., Kanakura, Y., Komiya, S. & Yoshimura, A. (1997). A new protein containing an SH2 domain that inhibits JAK kinases. *Nature*, **387**, 921–4.

Engel, N., Tront, J.S., Erinle, T., Nguyen, N., Latham, K.E., Sapienza, C., Hoffman, B. & Liebermann, D.A. (2009). Conserved DNA methylation in Gadd45a(-/-) mice. *Epigenetics*, **4**, 98–9.

Erickson, R.P. (1985). Chromosomal imprinting and the parent transmission specific variation in expressivity of Huntington disease. *Am J Hum Genet*, **37**, 827–9.

Eriksen, K.W., Kaltoft, K., Mikkelsen, G., Nielsen, M., Zhang, Q., Geisler, C., Nissen, M.H., Röpke, C., Wasik, M.A. & Odum, N. (2001). Constitutive STAT3-activation in Sezary syndrome: tyrphostin AG490 inhibits STAT3-activation, interleukin-2 receptor expression and growth of leukemic Sezary cells. *Leukemia*, **15**, 787–93.

Evavold, B.D., Sloan-Lancaster, J. & Allen, P.M. (1993). Tickling the TCR: selective T-cell functions stimulated by altered peptide ligands. *Immunol Today*, **14**, 602–9.

Ferenczi, K., Fuhlbrigge, R.C., Pinkus, J., Pinkus, G.S. & Kupper, T.S. (2002). Increased CCR4 expression in cutaneous T cell lymphoma. *The Journal of investigative dermatology*, **119**, 1405–10.

Fisher, G.H., Rosenberg, F.J., Straus, S.E., Dale, J.K., Middleton, L.A., Lin, A.Y., Strober, W., Lenardo, M.J. & Puck, J.M. (1995). Dominant interfering Fas gene mutations impair apoptosis in a human autoimmune lymphoproliferative syndrome. *Cell*, **81**, 935–46.

Fontenot, J.D., Gavin, M.A. & Rudensky, A.Y. (2003). Foxp3 programs the development and function of CD4+CD25+ regulatory T cells. *Nat Immunol*, **4**, 330–6.

Foran, E., McWilliam, P., Kelleher, D., Croke, D.T. & Long, A. (2006). The leukocyte protein L-plastin induces proliferation, invasion and loss of E-cadherin expression in colon cancer cells. *Int J Cancer*, **118**, 2098–104.

Foss, F.M., Koc, Y., Stetler-Stevenson, M.A., Nguyen, D.T., O'Brien, M.C., Turner, R. & Sausville, E.A. (1994). Costimulation of cutaneous T-cell lymphoma cells by interleukin-7 and interleukin-2: potential autocrine or paracrine effectors in the Sézary syndrome. *Journal of clinical oncology : official journal of the American Society of Clinical Oncology*, **12**, 326–35.

Fowler, C.C., Pao, L.I., Blattman, J.N. & Greenberg, P.D. (2010). SHP-1 in T cells limits the production of CD8 effector cells without impacting the formation of long-lived central memory cells. *J Immunol*, **185**, 3256–67.

Fraser-Andrews, E.A., Russell-Jones, R., Woolford, A.J., Wolstencroft, R.A., Dean, A.J. & Whittaker, S.J. (2001). Diagnostic and prognostic importance of T-cell receptor gene analysis in patients with Sézary syndrome. *Cancer*, **92**, 1745–52.

Frommer, M., McDonald, L.E., Millar, D.S., Collis, C.M., Watt, F., Grigg, G.W., Molloy, P.L. & Paul, C.L. (1992). A genomic sequencing protocol that yields a positive display of 5-methylcytosine residues in individual DNA strands. *Proceedings of the National Academy of Sciences of the United States of America*, **89**, 1827–31.

Füllgrabe, J., Kavanagh, E. & Joseph, B. (2011). Histone onco-modifications. *Oncogene*, **30**, 3391–403.

Gallardo, F., Esteller, M., Pujol, R.M., Costa, C., Estrach, T. & Servitje, O. (2004). Methylation status of the p15, p16 and MGMT promoter genes in primary cutaneous T-cell lymphomas. *Haematologica*, **89**, 1401–3.

Gardiner-Garden, M. & Frommer, M. (1987). CpG islands in vertebrate genomes. *J Mol Biol*, **196**, 261–82.

Gautier, F., Bünemann, H. & Grotjahn, L. (1977). Analysis of calf-thymus satellite DNA: evidence for specific methylation of cytosine in C-G sequences. *Eur J Biochem*, **80**, 175–83.

Gazdar, A.F., Carney, D.N., Bunn, P.A., Russell, E.K., Jaffe, E.S., Schechter, G.P. & Guccion, J.G. (1980). Mitogen requirements for the in vitro propagation of cutaneous T-cell lymphomas. *Blood*, **55**, 409–17.

Gebhard, C., Schwarzfischer, L., Pham, T.H., Schilling, E., Klug, M., Andreesen, R. & Rehli, M. (2006). Genome-wide profiling of CpG methylation identifies novel targets of aberrant hypermethylation in myeloid leukemia. *Cancer research*, **66**, 6118–28.

Giannoukakis, N., Deal, C., Paquette, J., Goodyer, C.G. & Polychronakos, C. (1993). Parental genomic imprinting of the human IGF2 gene. *Nature genetics*, **4**, 98–101.

Giganti, A., Plastino, J., Janji, B., Troys, M.V., Lentz, D., Ampe, C., Sykes, C. & Friederich, E. (2005). Actin-filament cross-linking protein T-plastin increases Arp2/3-mediated actin-based movement. *J Cell Sci*, **118**, 1255–65.

Glenn, C.C., Porter, K.A., Jong, M.T., Nicholls, R.D. & Driscoll, D.J. (1993). Functional imprinting and epigenetic modification of the human SNRPN gene. *Hum Mol Genet*, **2**, 2001–5.

Golbus, J., Palella, T.D. & Richardson, B.C. (1990). Quantitative changes in T cell DNA methylation occur during differentiation and ageing. *Eur J Immunol*, **20**, 1869–72.

Gomez, T.S. & Billadeau, D.D. (2008). T cell activation and the cytoskeleton: you can't have one without the other. *Adv Immunol*, **97**, 1–64.

Gorochov, G., Bachelez, H., Cayuela, J.M., Legac, E., Laroche, L., Dubertret, L. & Sigaux, F. (1995). Expression of V beta gene segments by Sezary cells. *The Journal of investigative dermatology*, **105**, 56–61.

Goto, T. & Monk, M. (1998). Regulation of X-chromosome inactivation in development in mice and humans. *Microbiol Mol Biol Rev*, **62**, 362–78.

Grimm-Günter, E.M.S., Revenu, C., Ramos, S., Hurbain, I., Smyth, N., Ferrary, E., Louvard, D., Robine, S. & Rivero, F. (2009). Plastin 1 binds to keratin and is required for terminal web assembly in the intestinal epithelium. *Mol Biol Cell*, **20**, 2549–62.

Gruenbaum, Y., Cedar, H. & Razin, A. (1982). Substrate and sequence specificity of a eukaryotic DNA methylase. *Nature*, **295**, 620–2.

Guillemot, F., Caspary, T., Tilghman, S.M., Copeland, N.G., Gilbert, D.J., Jenkins, N.A., Anderson, D.J., Joyner, A.L., Rossant, J. & Nagy, A. (1995). Genomic imprinting of Mash2, a mouse gene required for trophoblast development. *Nature genetics*, **9**, 235–42.

Hahtola, S., Tuomela, S., Elo, L., Häkkinen, T., Karenko, L., Nedoszytko, B., Heikkilä, H., Saarialho-Kere, U., Roszkiewicz, J., Aittokallio, T., Lahesmaa, R. & Ranki, A. (2006). Th1 response and cytotoxicity genes are down-regulated in cutaneous T-cell lymphoma. *Clinical cancer research : an official journal of the American Association for Cancer Research*, **12**, 4812–21.

Hajkova, P., Erhardt, S., Lane, N., Haaf, T., El-Maarri, O., Reik, W., Walter, J. & Surani, M.A. (2002). Epigenetic reprogramming in mouse primordial germ cells. *Mech Dev*, **117**, 15–23.

Han, Y., Amin, H.M., Frantz, C., Franko, B., Lee, J., Lin, Q. & Lai, R. (2006). Restoration of shp1 expression by 5-AZA-2'-deoxycytidine is associated with downregulation of JAK3/STAT3 signaling in ALK-positive anaplastic large cell lymphoma. *Leukemia*, **20**, 1602–9.

Harmon, C.B., Witzig, T.E., Katzmann, J.A. & Pittelkow, M.R. (1996). Detection of circulating T cells with CD4+CD7- immunophenotype in patients with benign and malignant lymphoproliferative dermatoses. *J Am Acad Dermatol*, **35**, 404–10.

Hata, K., Okano, M., Lei, H. & Li, E. (2002). Dnmt3L cooperates with the Dnmt3 family of de novo DNA methyltransferases to establish maternal imprints in mice. *Development*, **129**, 1983–93.

Hattori, N., Nishino, K., Ko, Y.G., Hattori, N., Ohgane, J., Tanaka, S. & Shiota, K. (2004). Epigenetic control of mouse Oct-4 gene expression in embryonic stem cells and trophoblast stem cells. *The Journal of biological chemistry*, **279**, 17063–9.

Hattori, N., Imao, Y., Nishino, K., Hattori, N., Ohgane, J., Yagi, S., Tanaka, S. & Shiota, K. (2007). Epigenetic regulation of Nanog gene in embryonic stem and trophoblast stem cells. *Genes Cells*, **12**, 387–96.

Haynes, B.F., Metzgar, R.S., Minna, J.D. & Bunn, P.A. (1981). Phenotypic characterization of cutaneous T-cell lymphoma. Use of monoclonal antibodies to compare with other malignant T cells. *N Engl J Med*, **304**, 1319–23, download.

Heald, P.W., Yan, S.L., Edelson, R.L., Tigelaar, R. & Picker, L.J. (1993). Skin-selective lymphocyte homing mechanisms in the pathogenesis of leukemic cutaneous T-cell lymphoma. *The Journal of investigative dermatology*, **101**, 222–6.

Heisler, L.E., Torti, D., Boutros, P.C., Watson, J., Chan, C., Winegarden, N., Takahashi, M., Yau, P., Huang, T.H.M., Farnham, P.J., Jurisica, I., Woodgett, J.R., Bremner, R., Penn, L.Z. & Der, S.D. (2005). CpG Island microarray probe sequences derived from a physical library are representative of CpG Islands annotated on the human genome. *Nucleic acids research*, **33**, 2952–61.

Herman, J.G., Graff, J.R., Myöhänen, S., Nelkin, B.D. & Baylin, S.B. (1996). Methylation-specific PCR: a novel PCR assay for methylation status of CpG islands. *Proceedings of the National Academy of Sciences of the United States of America*, **93**, 9821–6.

Herman, J.G., Civin, C.I., Issa, J.P., Collector, M.I., Sharkis, S.J. & Baylin, S.B. (1997). Distinct patterns of inactivation of p15INK4B and p16INK4A characterize the major types of hematological malignancies. *Cancer research*, **57**, 837–41.

Higuchi, Y., Kita, K., Nakanishi, H., Wang, X.L., Sugaya, S., Tanzawa, H., Yamamori, H., Sugita, K., Yamaura, A. & Suzuki, N. (1998). Search for genes involved in UV-resistance in human cells by mRNA differential display: increased transcriptional

expression of nucleophosmin and T-plastin genes in association with the resistance. *Biochem Biophys Res Commun*, **248**, 597–602.

Hillman, R.T., Green, R.E. & Brenner, S.E. (2004). An unappreciated role for RNA surveillance. *Genome Biol*, **5**, R8.

Hisano, T., Ono, M., Nakayama, M., Naito, S., Kuwano, M. & Wada, M. (1996). Increased expression of T-plastin gene in cisplatin-resistant human cancer cells: identification by mRNA differential display. *FEBS Lett*, **397**, 101–7.

Holliday, R. & Pugh, J.E. (1975). DNA modification mechanisms and gene activity during development. *Science*, **187**, 226–32.

Hopkins-Donaldson, S., Ziegler, A., Kurtz, S., Bigosch, C., Kandioler, D., Ludwig, C., Zangemeister-Wittke, U. & Stahel, R. (2003). Silencing of death receptor and caspase-8 expression in small cell lung carcinoma cell lines and tumors by DNA methylation. *Cell Death Differ*, **10**, 356–64.

Howlett, S.K. & Reik, W. (1991). Methylation levels of maternal and paternal genomes during preimplantation development. *Development*, **113**, 119–27.

Hristov, A.C., Vonderheid, E.C. & Borowitz, M.J. (2011). Simplified flow cytometric assessment in mycosis fungoides and sezary syndrome. *Am J Clin Pathol*, **136**, 944–53.

Hu, X.V., Rodrigues, T.M.A., Tao, H., Baker, R.K., Miraglia, L., Orth, A.P., Lyons, G.E., Schultz, P.G. & Wu, X. (2010). Identification of RING finger protein 4 (RNF4) as a modulator of DNA demethylation through a functional genomics screen. *Proceedings of the National Academy of Sciences of the United States of America*, **107**, 15087–92.

Huang, J., Fan, T., Yan, Q., Zhu, H., Fox, S., Issaq, H.J., Best, L., Gangi, L., Munroe, D. & Muegge, K. (2004). Lsh, an epigenetic guardian of repetitive elements. *Nucleic acids research*, **32**, 5019–28.

Hughes, T., Webb, R., Fei, Y., Wren, J.D. & Sawalha, A.H. (2010). DNA methylome in human CD4+ T cells identifies transcriptionally repressive and non-repressive methylation peaks. *Genes Immun*, **11**, 554–60.

Ikeda, H., Sasaki, Y., Kobayashi, T., Suzuki, H., Mita, H., Toyota, M., Itoh, F., Shinomura, Y., Tokino, T. & Imai, K. (2005). The role of T-fimbrin in the response to DNA damage: silencing of T-fimbrin by small interfering RNA sensitizes human liver cancer cells to DNA-damaging agents. *Int J Oncol*, **27**, 933–40.

Illingworth, R., Kerr, A., Desousa, D., Jørgensen, H., Ellis, P., Stalker, J., Jackson, D., Clee, C., Plumb, R., Rogers, J., Humphray, S., Cox, T., Langford, C. & Bird, A. (2008). A novel CpG island set identifies tissue-specific methylation at developmental gene loci. *PLoS Biol*, **6**, e22.

Iwasaki, H., Kovacic, J.C., Olive, M., Beers, J.K., Yoshimoto, T., Crook, M.F., Tonelli, L.H. & Nabel, E.G. (2010). Disruption of protein arginine N-methyltransferase 2 regulates leptin signaling and produces leanness in vivo through loss of STAT3 methylation. *Circ Res*, **107**, 992–1001.

Izban, K.F., Ergin, M., Qin, J.Z., Martinez, R.L., RJ, J.R.P., Saeed, S. & Alkan, S. (2000). Constitutive expression of NF-kappa B is a characteristic feature of mycosis fungoides: implications for apoptosis resistance and pathogenesis. *Human pathology*, **31**, 1482–90.

Jiao, H., Berrada, K., Yang, W., Tabrizi, M., Platanias, L.C. & Yi, T. (1996). Direct association with and dephosphorylation of Jak2 kinase by the SH2-domain-containing protein tyrosine phosphatase SHP-1. *Mol Cell Biol*, **16**, 6985–92.

Jin, S.G., Guo, C. & Pfeifer, G.P. (2008). GADD45A does not promote DNA demethylation. *PLoS Genet*, **4**, e1000013.

Jin, Y.J., Yu, C.L. & Burakoff, S.J. (1999). Human 70-kDa SHP-1L differs from 68-kDa SHP-1 in its C-terminal structure and catalytic activity. *The Journal of biological chemistry*, **274**, 28301–7.

Johan, M.F., Bowen, D.T., Frew, M.E., Goodeve, A.C. & Reilly, J.T. (2005). Aberrant methylation of the negative regulators RASSFIA, SHP-1 and SOCS-1 in myelodysplastic syndromes and acute myeloid leukaemia. *British journal of haematology*, **129**, 60–5.

Johnson, G.A., Dewald, G.W., Strand, W.R. & Winkelmann, R.K. (1985). Chromosome studies in 17 patients with the Sézary syndrome. *Cancer*, **55**, 2426–33.

Johnson, T. & Coghill, R. (1925). Researches on pyrimidines. C111. The discovery of 5-methyl-cytosine in tuberculin acid, the nucleic acid of the tubercle bacillus. *Journal of the American Chemical Society*, **47**, 2838–2844

Jones, C.L., Wain, E.M., Chu, C.C., Tosi, I., Foster, R., McKenzie, R.C.T., Whittaker, S.J. & Mitchell, T.J. (2010). Downregulation of Fas gene expression in Sézary syndrome is associated with promoter hypermethylation. *The Journal of investigative dermatology*, **130**, 1116–25.

Jones, C.L., Ferreira, S., McKenzie, R.C.T., Tosi, I., Caesar, J.A., Bagot, M., Whittaker, S.J. & Mitchell, T.J. (2012). Regulation of T-plastin expression by promoter hypomethylation in primary cutaneous T-cell lymphoma. *The Journal of investigative dermatology*, **132**, 2042–9.

Jones, D., Dang, N.H., Duvic, M., Washington, L.T. & Huh, Y.O. (2001). Absence of CD26 expression is a useful marker for diagnosis of T-cell lymphoma in peripheral blood. *Am J Clin Pathol*, **115**, 885–92.

Jones, P.A. & Baylin, S.B. (2002). The fundamental role of epigenetic events in cancer. *Nat Rev Genet*, **3**, 415–28.

Jones, P.A., Wolkowicz, M.J., Rideout, W.M., Gonzales, F.A., Marziasz, C.M., Coetzee, G.A. & Tapscott, S.J. (1990). De novo methylation of the MyoD1 CpG island during the establishment of immortal cell lines. *Proceedings of the National Academy of Sciences of the United States of America*, **87**, 6117–21.

Jordan, C.T., Guzman, M.L. & Noble, M. (2006). Cancer stem cells. *N Engl J Med*, **355**, 1253–61.

Josse, J., Kaiser, A. & Kornberg, A. (1961). Enzymatic synthesis of deoxyribonucleic acid. VIII. Frequencies of nearest neighbor base sequences in deoxyribonucleic acid. *J Biol Chem*, **236**, 864–75.

Jost, E., do O, N., Dahl, E., Maintz, C.E., Jousten, P., Habets, L., Wilop, S., Herman, J.G., Osieka, R. & Galm, O. (2007). Epigenetic alterations complement mutation of JAK2 tyrosine kinase in patients with BCR/ABL-negative myeloproliferative disorders. *Leukemia*, **21**, 505–10.

Ju, S.T., Panka, D.J., Cui, H., Ettinger, R., el Khatib, M., Sherr, D.H., Stanger, B.Z. & Marshak-Rothstein, A. (1995). Fas(CD95)/FasL interactions required for programmed cell death after T-cell activation. *Nature*, **373**, 444–8.

Jurka, J. & Smith, T. (1988). A fundamental division in the Alu family of repeated sequences. *Proceedings of the National Academy of Sciences of the United States of America*, **85**, 4775–8.

Kahwash, S.B., Fung, B., Savelli, S., Bleesing, J.J. & Qualman, S.J. (2007). Autoimmune lymphoproliferative syndrome (ALPS): a case with congenital onset. *Pediatr Dev Pathol*, **10**, 315–9.

Kaltoft, K., Thestrup-Pedersen, K., Jensen, J.R., Bisballe, S. & Zachariae, H. (1984). Establishment of T and B cell lines from patients with mycosis fungoides. *The British journal of dermatology*, **111**, 303–8.

Kaltoft, K., Bisballe, S., Rasmussen, H.F., Thestrup-Pedersen, K., Thomsen, K. & Sterry, W. (1987). A continuous T-cell line from a patient with Sézary syndrome. *Arch Dermatol Res*, **279**, 293–8, download.

Kaltoft, K., Bisballe, S., Dyrberg, T., Boel, E., Rasmussen, P.B. & Thestrup-Pedersen, K. (1992). Establishment of two continuous T-cell strains from a single plaque of a patient with mycosis fungoides. *In Vitro Cell Dev Biol*, **28A**, 161–7.

Kaltoft, K., Hansen, B.H. & Thestrup-Pedersen, K. (1994). Cytogenetic findings in cell lines from cutaneous T-cell lymphoma. *Dermatol Clin*, **12**, 295–304, ordered from library.

Kamiyama, H., Suzuki, K., Maeda, T., Koizumi, K., Miyaki, Y., Okada, S., Kawamura, Y.J., Samuelsson, J.K., Alonso, S., Konishi, F. & Perucho, M. (2012). DNA demethylation in normal colon tissue predicts predisposition to multiple cancers. *Oncogene*.

Kaneda, M., Okano, M., Hata, K., Sado, T., Tsujimoto, N., Li, E. & Sasaki, H. (2004). Essential role for de novo DNA methyltransferase Dnmt3a in paternal and maternal imprinting. *Nature*, **429**, 900–3.

Kappler, J.W. (1971). The 5-methylcytosine content of DNA: tissue specificity. *J Cell Physiol*, **78**, 33–6.

Kapsenberg, M.L. (2003). Dendritic-cell control of pathogen-driven T-cell polarization. *Nat Rev Immunol*, **3**, 984–93.

Karenko, L., Hahtola, S., Päivinen, S., Karhu, R., Syrjä, S., Kähkönen, M., Nedoszytko, B., Kytölä, S., Zhou, Y., Blazevic, V., Pesonen, M., Nevala, H., Nupponen, N., Sihto, H., Krebs, I., Poustka, A., Roszkiewicz, J., Saksela, K., Peterson, P., Visakorpi, T. & Ranki, A. (2005). Primary cutaneous T-cell lymphomas show a deletion or translocation affecting NAV3, the human UNC-53 homologue. *Cancer research*, **65**, 8101–10.

Kari, L., Loboda, A., Nebozhyn, M., Rook, A.H., Vonderheid, E.C., Nichols, C., Virok, D., Chang, C., Horng, W.H., Johnston, J., Wysocka, M., Showe, M.K. & Showe, L.C. (2003). Classification and prediction of survival in patients with the leukemic phase of cutaneous T cell lymphoma. *J Exp Med*, **197**, 1477–88.

Kelemen, K., Guitart, J., Kuzel, T.M., Goolsby, C.L. & Peterson, L.C. (2008). The usefulness of CD26 in flow cytometric analysis of peripheral blood in Sézary syndrome. *Am J Clin Pathol*, **129**, 146–56.

Khoury, J.D., Rassidakis, G.Z., Medeiros, L.J., Amin, H.M. & Lai, R. (2004). Methylation of SHP1 gene and loss of SHP1 protein expression are frequent in systemic anaplastic large cell lymphoma. *Blood*, **104**, 1580–1.

Khulan, B., Thompson, R.F., Ye, K., Fazzari, M.J., Suzuki, M., Stasiek, E., Figueroa, M.E., Glass, J.L., Chen, Q., Montagna, C., Hatchwell, E., Selzer, R.R., Richmond, T.A., Green, R.D., Melnick, A. & Greally, J.M. (2006). Comparative isoschizomer profiling of cytosine methylation: the HELP assay. *Genome Res*, **16**, 1046–55.

Kilgore, N.E., Carter, J.D., Lorenz, U. & Evavold, B.D. (2003). Cutting edge: dependence of TCR antagonism on Src homology 2 domain-containing protein tyrosine phosphatase activity. *J Immunol*, **170**, 4891–5.

Kirchhoff, S., Müller, W.W., Krueger, A., Schmitz, I. & Krammer, P.H. (2000). TCR-mediated up-regulation of c-FLIPshort correlates with resistance toward CD95-mediated apoptosis by blocking death-inducing signaling complex activity. *J Immunol*, **165**, 6293–300.

Kitazawa, R. & Kitazawa, S. (2007). Methylation status of a single CpG locus 3 bases upstream of TATA-box of receptor activator of nuclear factor-kappaB ligand (RANKL) gene promoter modulates cell- and tissue-specific RANKL expression and osteoclastogenesis. *Mol Endocrinol*, **21**, 148–58.

Klas, C., Debatin, K.M., Jonker, R.R. & Krammer, P.H. (1993). Activation interferes with the APO-1 pathway in mature human T cells. *Int Immunol*, **5**, 625–30.

Klemke, C.D., Brade, J., Weckesser, S., Sachse, M.M., Booken, N., Neumaier, M., Goerdt, S. & Nebe, T.C. (2008). The diagnosis of Sézary syndrome on peripheral blood by flow cytometry requires the use of multiple markers. *Br J Dermatol*, **159**, 871–80.

Klemke, C.D., Brenner, D., Weiss, E.M., Schmidt, M., Leverkus, M., Gülow, K. & Krammer, P.H. (2009). Lack of T-cell receptor-induced signaling is crucial for CD95 ligand up-regulation and protects cutaneous T-cell lymphoma cells from activation-induced cell death. *Cancer research*, **69**, 4175–83.

Klemke, M., Rafael, M.T., Wabnitz, G.H., Weschenfelder, T., Konstandin, M.H., Garbi, N., Autschbach, F., Hartschuh, W. & Samstag, Y. (2007). Phosphorylation of ectopically expressed L-plastin enhances invasiveness of human melanoma cells. *Int J Cancer*, **120**, 2590–9.

Klose, R.J. & Bird, A.P. (2006). Genomic DNA methylation: the mark and its mediators. *Trends Biochem Sci*, **31**, 89–97.

Knoll, J.H., Nicholls, R.D., Magenis, R.E., Graham, J.M., Lalande, M. & Latt, S.A. (1989). Angelman and Prader-Willi syndromes share a common chromosome 15 deletion but differ in parental origin of the deletion. *Am J Med Genet*, **32**, 285–90.

Komiya, A., Suzuki, H., Ueda, T., Yatani, R., Emi, M., Ito, H. & Shimazaki, J. (1996). Allelic losses at loci on chromosome 10 are associated with metastasis and progression of human prostate cancer. *Genes, chromosomes & cancer*, **17**, 245–53.

Komyod, W., Bauer, U.M., Heinrich, P.C., Haan, S. & Behrmann, I. (2005). Are STATS arginine-methylated? *J Biol Chem*, **280**, 21700–5.

Kowalski, C. (1972). On the Effects of Non-Normality on the Distribution of the Sample Product-Moment Correlation Coefficient. *Journal of the Royal Statistical Society. Series C (Applied Statistics)*, **21**, 1–12.

Koyama, M., Oka, T., Ouchida, M., Nakatani, Y., Nishiuchi, R., Yoshino, T., Hayashi, K., Akagi, T. & Seino, Y. (2003). Activated proliferation of B-cell lymphomas/leukemias with the SHP1 gene silencing by aberrant CpG methylation. *Lab Invest*, **83**, 1849–58.

Krammer, P.H., Arnold, R. & Lavrik, I.N. (2007). Life and death in peripheral T cells. *Nat Rev Immunol*, **7**, 532–42.

Kunnumakkara, A.B., Nair, A.S., Sung, B., Pandey, M.K. & Aggarwal, B.B. (2009). Boswellic acid blocks signal transducers and activators of transcription 3 signaling, proliferation, and survival of multiple myeloma via the protein tyrosine phosphatase SHP-1. *Mol Cancer Res*, **7**, 118–28.

Laetsch, B., Häffner, A.C., Döbbeling, U., Seifert, B., Ludwig, E., Burg, G. & Dummer, R. (2000). CD4 + /CD7- T cell frequency and polymerase chain reaction-based clonality assay correlate with stage in cutaneous T cell lymphomas. *The Journal of investigative dermatology*, **114**, 107–11.

Laharanne, E., Chevret, E., Idrissi, Y., Gentil, C., Longy, M., Ferrer, J., Dubus, P., Jouary, T., Vergier, B., Beylot-Barry, M. & Merlio, J.P. (2010a). CDKN2A-CDKN2B deletion defines an aggressive subset of cutaneous T-cell lymphoma. *Mod Pathol*, **23**, 547–58.

Laharanne, E., Oumouhou, N., Bonnet, F., Carlotti, M., Gentil, C., Chevret, E., Jouary, T., Longy, M., Vergier, B., Beylot-Barry, M. & Merlio, J.P. (2010b). Genome-wide analysis of cutaneous T-cell lymphomas identifies three clinically relevant classes. *The Journal of investigative dermatology*, **130**, 1707–18.

Lander, E.S., Linton, L.M., Birren, B., Nusbaum, C., Zody, M.C., Baldwin, J., Devon, K., Dewar, K., Doyle, M., FitzHugh, W., Funke, R., Gage, D., Harris, K., Heaford, A., Howland, J., Kann, L., Lehoczky, J., LeVine, R., McEwan, P., McKernan, K., Meldrim, J., Mesirov, J.P., Miranda, C., Morris, W., Naylor, J., Raymond, C., Rosetti, M., Santos, R., Sheridan, A., Sougnez, C., Stange-Thomann, N., Stojanovic, N., Subramanian, A., Wyman, D., Rogers, J., Sulston, J., Ainscough, R., Beck, S., Bentley, D., Burton, J., Clee, C., Carter, N., Coulson, A., Deadman, R., Deloukas, P., Dunham, A., Dunham, I., Durbin, R., French, L., Grafham, D., Gregory, S., Hubbard, T., Humphray, S., Hunt, A., Jones, M., Lloyd, C., McMurray, A., Matthews, L., Mercer, S., Milne, S., Mullikin, J.C., Mungall, A., Plumb, R., Ross, M., Shownkeen, R., Sims, S., Waterston, R.H., Wilson, R.K., Hillier, L.W., McPherson, J.D., Marra, M.A., Mardis, E.R., Fulton, L.A., Chinwalla, A.T., Pepin, K.H., Gish, W.R., Chissoe, S.L., Wendl, M.C., Delehaunty, K.D., Miner, T.L., Delehaunty, A., Kramer, J.B., Cook, L.L., Fulton, R.S., Johnson, D.L., Minx, P.J., Clifton, S.W., Hawkins, T., Branscomb, E., Predki, P., Richardson, P., Wenning, S., Slezak, T., Doggett, N., Cheng, J.F., Olsen, A., Lucas, S., Elkin, C., Uberbacher, E., Frazier, M., Gibbs, R.A., Muzny, D.M., Scherer, S.E., Bouck, J.B., Sodergren, E.J., Worley, K.C., Rives, C.M., Gorrell, J.H., Metzker, M.L., Naylor, S.L., Kucherlapati, R.S., Nelson, D.L., Weinstock, G.M., Sakaki, Y., Fujiyama, A., Hattori, M., Yada, T., Toyoda, A., Itoh, T., Kawagoe, C., Watanabe, H., Totoki, Y., Taylor, T., Weissenbach, J., Heilig, R., Saurin, W., Artiguenave, F., Brottier, P., Bruls, T., Pelletier, E., Robert, C., Wincker, P., Smith, D.R., Doucette-Stamm, L., Rubenfield, M., Weinstock, K., Lee, H.M., Dubois, J., Rosenthal, A., Platzer, M., Nyakatura, G., Taudien, S., Rump, A., Yang, H., Yu, J., Wang, J., Huang, G., Gu, J., Hood, L., Rowen, L., Madan, A., Qin, S., Davis, R.W., Federspiel, N.A., Abola, A.P., Proctor, M.J., Myers, R.M.,

Schmutz, J., Dickson, M., Grimwood, J., Cox, D.R., Olson, M.V., Kaul, R., Raymond, C., Shimizu, N., Kawasaki, K., Minoshima, S., Evans, G.A., Athanasiou, M., Schultz, R., Roe, B.A., Chen, F., Pan, H., Ramser, J., Lehrach, H., Reinhardt, R., McCombie, W.R., de la Bastide, M., Dedhia, N., Blöcker, H., Hornischer, K., Nordsiek, G., Agarwala, R., Aravind, L., Bailey, J.A., Bateman, A., Batzoglou, S., Birney, E., Bork, P., Brown, D.G., Burge, C.B., Cerutti, L., Chen, H.C., Church, D., Clamp, M., Copley, R.R., Doerks, T., Eddy, S.R., Eichler, E.E., Furey, T.S., Galagan, J., Gilbert, J.G., Harmon, C., Hayashizaki, Y., Haussler, D., Hermjakob, H., Hokamp, K., Jang, W., Johnson, L.S., Jones, T.A., Kasif, S., Kaspryzk, A., Kennedy, S., Kent, W.J., Kitts, P., Koonin, E.V., Korf, I., Kulp, D., Lancet, D., Lowe, T.M., McLysaght, A., Mikkelsen, T., Moran, J.V., Mulder, N., Pollara, V.J., Ponting, C.P., Schuler, G., Schultz, J., Slater, G., Smit, A.F., Stupka, E., Szustakowski, J., Thierry-Mieg, D., Thierry-Mieg, J., Wagner, L., Wallis, J., Wheeler, R., Williams, A., Wolf, Y.I., Wolfe, K.H., Yang, S.P., Yeh, R.F., Collins, F., Guyer, M.S., Peterson, J., Felsenfeld, A., Wetterstrand, K.A., Patrinos, A., Morgan, M.J., de Jong, P., Catanese, J.J., Osoegawa, K., Shizuya, H., Choi, S., Chen, Y.J., Szustakowki, J. & Consortium, I.H.G.S. (2001). Initial sequencing and analysis of the human genome. *Nature*, **409**, 860–921.

Larsen, F., Gundersen, G., Lopez, R. & Prydz, H. (1992). CpG islands as gene markers in the human genome. *Genomics*, **13**, 1095–107.

Lee, D.U., Agarwal, S. & Rao, A. (2002). Th2 lineage commitment and efficient IL-4 production involves extended demethylation of the IL-4 gene. *Immunity*, **16**, 649–60.

Lee, P.P., Fitzpatrick, D.R., Beard, C., Jessup, H.K., Lehar, S., Makar, K.W., Pérez-Melgosa, M., Sweetser, M.T., Schlissel, M.S., Nguyen, S., Cherry, S.R., Tsai, J.H., Tucker, S.M., Weaver, W.M., Kelso, A., Jaenisch, R. & Wilson, C.B. (2001). A critical role for Dnmt1 and DNA methylation in T cell development, function, and survival. *Immunity*, **15**, 763–74.

Lee, S.H., Shin, M.S., Park, W.S., Kim, S.Y., Dong, S.M., Pi, J.H., Lee, H.K., Kim, H.S., Jang, J.J., Kim, C.S., Kim, S.H., Lee, J.Y. & Yoo, N.J. (1999). Alterations of Fas (APO-1/CD95) gene in transitional cell carcinomas of urinary bladder. *Cancer research*, **59**, 3068–72.

León, F., Cespón, C., Franco, A., Lombardía, M., Roldán, E., Escribano, L., Harto, A., González-Porqué, P. & Roy, G. (2002). SHP-1 expression in peripheral T cells from patients with Sezary syndrome and in the T cell line HUT-78: implications in JAK3-mediated signaling. *Leukemia*, **16**, 1470–7.

Li, E., Bestor, T.H. & Jaenisch, R. (1992). Targeted mutation of the DNA methyltransferase gene results in embryonic lethality. *Cell*, **69**, 915–26.

Limon, J., Nedoszytko, B., Brozek, I., Hellmann, A., Zajaczek, S., Lubiński, J. & Mrózek, K. (1995). Chromosome aberrations, spontaneous SCE, and growth kinetics in PHA-stimulated lymphocytes of five cases with Sézary syndrome. *Cancer Genet Cytogenet*, **83**, 75–81.

Lin, C., Lau, A., Huynh, T. & Lue, T. (1999). Differential regulation of human T-plastin gene in leukocytes and non-leukocytes: identification of the promoter, enhancer, and CpG island. *DNA and cell biology.*, **18**, 27–37.

Lin, C.S., Aebersold, R.H., Kent, S.B., Varma, M. & Leavitt, J. (1988). Molecular cloning and characterization of plastin, a human leukocyte protein expressed in transformed human fibroblasts. *Molecular and cellular biology*, **8**, 4659–68.

Lin, C.S., Aebersold, R.H. & Leavitt, J. (1990). Correction of the N-terminal sequences of the human plastin isoforms by using anchored polymerase chain reaction: identification of a potential calcium-binding domain. *Molecular and cellular biology*, **10**, 1818–21.

Lin, C.S., Chen, Z.P., Park, T., Ghosh, K. & Leavitt, J. (1993a). Characterization of the human L-plastin gene promoter in normal and neoplastic cells. *J Biol Chem*, **268**, 2793–801.

Lin, C.S., Park, T., Chen, Z.P. & Leavitt, J. (1993b). Human plastin genes. Comparative gene structure, chromosome location, and differential expression in normal and neoplastic cells. *The Journal of biological chemistry*, **268**, 2781–92.

Lin, C.S., Shen, W., Chen, Z.P., Tu, Y.H. & Matsudaira, P. (1994). Identification of I-plastin, a human fimbrin isoform expressed in intestine and kidney. *Mol Cell Biol*, **14**, 2457–67.

Lin, W.M., Lewis, J.M., Filler, R.B., Modi, B.G., Carlson, K.R., Reddy, S., Thornberg, A., Saksena, G., Umlauf, S., Oberholzer, P.A., Karpova, M., Getz, G., Mane, S., Garraway, L.A., Dummer, R., Berger, C.L., Edelson, R.L. & Girardi, M. (2012). Characterization of the DNA copy-number genome in the blood of cutaneous T-cell lymphoma patients. *The Journal of investigative dermatology*, **132**, 188–97.

Liu, C., Cheng, J. & Mountz, J.D. (1995). Differential expression of human Fas mRNA species upon peripheral blood mononuclear cell activation. *Biochem J*, **310 (Pt 3)**, 957–63.

Loots, G.G., Locksley, R.M., Blankespoor, C.M., Wang, Z.E., Miller, W., Rubin, E.M. & Frazer, K.A. (2000). Identification of a coordinate regulator of interleukins 4, 13, and 5 by cross-species sequence comparisons. *Science*, **288**, 136–40.

Lorenz, U., Ravichandran, K.S., Burakoff, S.J. & Neel, B.G. (1996). Lack of SHPTP1 results in src-family kinase hyperactivation and thymocyte hyperresponsiveness. *Proc Natl Acad Sci USA*, **93**, 9624–9.

Lubin, F.D., Roth, T.L. & Sweatt, J.D. (2008). Epigenetic regulation of BDNF gene transcription in the consolidation of fear memory. *J Neurosci*, **28**, 10576–86.

Lutzner, M.A., Hobbs, J.W. & Horvath, P. (1971). Ultrastructure of abnormal cells in Sezary syndrome, mycosis fungoides, and parapsoriasis en plaque. *Archives of dermatology*, **103**, 375–86.

Lutzner, M.A., Emerit, I., Durepaire, R., Flandrin, G., Grupper, C. & Prunieras, M. (1973). Cytogenetic, cytophotometric, and ultrastructural study of large cerebriform cells of the Sézary syndrome and description of a small-cell variant. *J Natl Cancer Inst*, **50**, 1145–62.

Lyon, M.F. (1961). Gene action in the X-chromosome of the mouse (Mus musculus L.). *Nature*, **190**, 372–3.

Ma, X.Z., Jin, T., Sakac, D., Fahim, S., Zhang, X., Katsman, Y., Bali, M. & Branch, D.R. (2003). Abnormal splicing of SHP-1 protein tyrosine phosphatase in human T cells. Implications for lymphomagenesis. *Exp Hematol*, **31**, 131–42.

MacDonald, H.R. & Wevrick, R. (1997). The necdin gene is deleted in Prader-Willi syndrome and is imprinted in human and mouse. *Hum Mol Genet*, **6**, 1873–8.

Magg, T., Hartrampf, S. & Albert, M.H. (2009). Stable nonviral gene transfer into primary human T cells. *Hum Gene Ther*, **20**, 989–98.

Makar, K.W., Pérez-Melgosa, M., Shnyreva, M., Weaver, W.M., Fitzpatrick, D.R. & Wilson, C.B. (2003). Active recruitment of DNA methyltransferases regulates interleukin 4 in thymocytes and T cells. *Nat Immunol*, **4**, 1183–90.

Mao, X. & McElwaine, S. (2008). Functional copy number changes in Sézary syndrome: toward an integrated molecular cytogenetic map III. *Cancer Genet Cytogenet*, **185**, 86–94.

Mao, X., Lillington, D., Child, F., Russell-Jones, R., Young, B. & Whittaker, S. (2002a). Comparative genomic hybridization analysis of primary cutaneous B-cell lymphomas: identification of common genomic alterations in disease pathogenesis. *Genes Chromosomes Cancer*, **35**, 144–55.

Mao, X., Lillington, D., Scarisbrick, J.J., Mitchell, T., Czepulkowski, B., Russell-Jones, R., Young, B. & Whittaker, S.J. (2002b). Molecular cytogenetic analysis of cutaneous T-cell lymphomas: identification of common genetic alterations in Sézary syndrome and mycosis fungoides. *The British journal of dermatology*, **147**, 464–75.

Mao, X., Lillington, D.M., Czepulkowski, B., Russell-Jones, R., Young, B.D. & Whittaker, S. (2003a). Molecular cytogenetic characterization of Sézary syndrome. *Genes, chromosomes & cancer*, **36**, 250–60.

Mao, X., Orchard, G., Lillington, D.M., Russell-Jones, R., Young, B.D. & Whittaker, S.J. (2003b). Amplification and overexpression of JUNB is associated with primary cutaneous T-cell lymphomas. *Blood*, **101**, 1513–9.

Mao, X., Orchard, G., Lillington, D.M., Child, F.J., Vonderheid, E.C., Nowell, P.C., Bagot, M., Bensussan, A., Russell-Jones, R., Young, B.D. & Whittaker, S.J. (2004). BCL2 and JUNB abnormalities in primary cutaneous lymphomas. *The British journal of dermatology*, **151**, 546–56.

Marks, D.I., Vonderheid, E.C., Kurz, B.W., Bigler, R.D., Sinha, K., Morgan, D.A., Sukman, A., Nowell, P.C. & Haines, D.S. (1996). Analysis of p53 and mdm-2 expression in 18 patients with Sézary syndrome. *Br J Haematol*, **92**, 890–9.

Marrogi, A.J., Khan, M.A., Vonderheid, E.C., Wood, G.S. & McBurney, E. (1999). p53 tumor suppressor gene mutations in transformed cutaneous T-cell lymphoma: a study of 12 cases. *J Cutan Pathol*, **26**, 369–78.

Martin-Subero, J.I., Ammerpohl, O., Bibikova, M., Wickham-Garcia, E., Agirre, X., Alvarez, S., Brüggemann, M., Bug, S., Calasanz, M.J., Deckert, M., Dreyling, M., Du, M.Q., Dürig, J., Dyer, M.J.S., Fan, J.B., Gesk, S., Hansmann, M.L., Harder, L., Hartmann, S., Klapper, W., Küppers, R., Montesinos-Rongen, M., Nagel, I., Pott, C., Richter, J., Román-Gómez, J., Seifert, M., Stein, H., Suela, J., Trümper, L., Vater, I., Prosper, F., Haferlach, C., Cigudosa, J.C. & Siebert, R. (2009). A comprehensive microarray-based DNA methylation study of 367 hematological neoplasms. *PLoS ONE*, **4**, e6986.

Martínez-Delgado, B., Cuadros, M., Honrado, E., de la Parte, A.R., Roncador, G., Alves, J., Castrillo, J.M., Rivas, C. & Benítez, J. (2005). Differential expression of NF-kappaB pathway genes among peripheral T-cell lymphomas. *Leukemia*, **19**, 2254–63.

Marty, M., Prochazkova, M., Laharanne, E., Chevret, E., Longy, M., Jouary, T., Vergier, B., Beylot-Barry, M., Merlio, J.P. & Philippe, M.J. (2008). Primary cutaneous T-cell lymphomas do not show specific NAV3 gene deletion or translocation. *The Journal of investigative dermatology*, **128**, 2458–66.

Mayer, W., Niveleau, A., Walter, J., Fundele, R. & Haaf, T. (2000). Demethylation of the zygotic paternal genome. *Nature*, **403**, 501–2.

McCusker, M.E., Garifallou, M. & Bogen, S.A. (1997). Sezary lineage cells can be induced to proliferate via CD28-mediated costimulation. *J Immunol*, **158**, 4984–91.

McGrath, J. & Solter, D. (1984). Completion of mouse embryogenesis requires both the maternal and paternal genomes. *Cell*, **37**, 179–83.

McGregor, J.M., Crook, T., Fraser-Andrews, E.A., Rozycka, M., Crossland, S., Brooks, L. & Whittaker, S.J. (1999). Spectrum of p53 gene mutations suggests a

possible role for ultraviolet radiation in the pathogenesis of advanced cutaneous lymphomas. *The Journal of investigative dermatology*, **112**, 317–21.

McKenzie, R.C.T., Jones, C.L., Tosi, I., Caesar, J.A., Whittaker, S.J. & Mitchell, T.J. (2011). Constitutive activation of STAT3 in Sézary syndrome is independent of SHP-1. *Leukemia : official journal of the Leukemia Society of America, Leukemia Research Fund, UK*.

Meech, S.J., Edelson, R., Walsh, P., Norris, D.A. & Duke, R.C. (2001). Reversible resistance to apoptosis in cutaneous T cell lymphoma. *Ann N Y Acad Sci*, **941**, 46–58.

Meister, G.E., Chandrasegaran, S. & Ostermeier, M. (2010). Heterodimeric DNA methyltransferases as a platform for creating designer zinc finger methyltransferases for targeted DNA methylation in cells. *Nucleic acids research*, **38**, 1749–59.

Mitchell, T.J. & John, S. (2005). Signal transducer and activator of transcription (STAT) signalling and T-cell lymphomas. *Immunology*, **114**, 301–12.

Mitchell, T.J., Whittaker, S.J. & John, S. (2003). Dysregulated expression of COOH-terminally truncated Stat5 and loss of IL2-inducible Stat5-dependent gene expression in Sezary Syndrome. *Cancer research*, **63**, 9048–54.

Miyamoto, T., Hasuike, S., Jinno, Y., Soejima, H., Yun, K., Miura, K., Ishikawa, M. & Niikawa, N. (2002). The human ASCL2 gene escaping genomic imprinting and its expression pattern. *J Assist Reprod Genet*, **19**, 240–4.

Miyawaki, T., Uehara, T., Nibu, R., Tsuji, T., Yachie, A., Yonehara, S. & Taniguchi, N. (1992). Differential expression of apoptosis-related Fas antigen on lymphocyte subpopulations in human peripheral blood. *J Immunol*, **149**, 3753–8.

Monk, M., Boubelik, M. & Lehnert, S. (1987). Temporal and regional changes in DNA methylation in the embryonic, extraembryonic and germ cell lineages during mouse embryo development. *Development*, **99**, 371–82.

Morimoto, C. & Schlossman, S.F. (1998). The structure and function of CD26 in the T-cell immune response. *Immunol Rev*, **161**, 55–70.

Mowen, K.A., Tang, J., Zhu, W., Schurter, B.T., Shuai, K., Herschman, H.R. & David, M. (2001). Arginine methylation of STAT1 modulates IFNalpha/beta-induced transcription. *Cell*, **104**, 731–41.

Muench, M.O., Bärtsch, E.M.P., Chen, J.C., Lopoo, J.B. & Bárcena, A. (2003). Ontogenic changes in CD95 expression on human leukocytes: prevalence of T-cells expressing activation markers and identification of CD95-CD45RO+ T-cells in the fetus. *Dev Comp Immunol*, **27**, 899–914.

Muramatsu, M., Kinoshita, K., Fagarasan, S., Yamada, S., Shinkai, Y. & Honjo, T. (2000). Class switch recombination and hypermutation require activation-induced cytidine deaminase (AID), a potential RNA editing enzyme. *Cell*, **102**, 553–63.

Murray, P.J. (2007). The JAK-STAT signaling pathway: input and output integration. *J Immunol*, **178**, 2623–9.

Nagasawa, T., Takakuwa, T., Takayama, H., Dong, Z., Miyagawa, S., Itami, S., Yoshikawa, K. & Aozasa, K. (2004). Fas gene mutations in mycosis fungoides: analysis of laser capture-microdissected specimens from cutaneous lesions. *Oncology*, **67**, 130–4.

Naka, T., Narazaki, M., Hirata, M., Matsumoto, T., Minamoto, S., Aono, A., Nishimoto, N., Kajita, T., Taga, T., Yoshizaki, K., Akira, S. & Kishimoto, T. (1997). Structure and function of a new STAT-induced STAT inhibitor. *Nature*, **387**, 924–9.

Nakase, K., Cheng, J., Zhu, Q. & Marasco, W.A. (2009). Mechanisms of SHP-1 P2 promoter regulation in hematopoietic cells and its silencing in HTLV-1-transformed T cells. *Journal of leukocyte biology*, **85**, 165–74.

Navas, I.C., Ortiz-Romero, P.L., Villuendas, R., Martínez, P., García, C., Gómez, E., Rodriguez, J.L., García, D., Vanaclocha, F., Iglesias, L., Piris, M.A. & Algara, P. (2000). p16(INK4a) gene alterations are frequent in lesions of mycosis fungoides. *Am J Pathol*, **156**, 1565–72.

Nebozhyn, M., Loboda, A., Kari, L., Rook, A.H., Vonderheid, E.C., Lessin, S., Berger, C., Edelson, R., Nichols, C., Yousef, M., Gudipati, L., Shang, M., Showe, M.K. & Showe, L.C. (2006). Quantitative PCR on 5 genes reliably identifies CTCL patients with 5accuracy. *Blood*, **107**, 3189–96.

Negrini, S., Gorgoulis, V.G. & Halazonetis, T.D. (2010). Genomic instability–an evolving hallmark of cancer. *Nat Rev Mol Cell Biol*, **11**, 220–8.

Newell-Price, J., Clark, A.J. & King, P. (2000). DNA methylation and silencing of gene expression. *Trends Endocrinol Metab*, **11**, 142–8.

Ng, H.H., Zhang, Y., Hendrich, B., Johnson, C.A., Turner, B.M., Erdjument-Bromage, H., Tempst, P., Reinberg, D. & Bird, A. (1999). MBD2 is a transcriptional repressor belonging to the MeCP1 histone deacetylase complex. *Nature genetics*, **23**, 58–61.

Nielsen, M., Kaestel, C.G., Eriksen, K.W., Woetmann, A., Stokkedal, T., Kaltoft, K., Geisler, C., Röpke, C. & Odum, N. (1999). Inhibition of constitutively activated Stat3 correlates with altered Bcl-2/Bax expression and induction of apoptosis in mycosis fungoides tumor cells. *Leukemia*, **13**, 735–8.

Norris, D.P., Patel, D., Kay, G.F., Penny, G.D., Brockdorff, N., Sheardown, S.A. & Rastan, S. (1994). Evidence that random and imprinted Xist expression is controlled by preemptive methylation. *Cell*, **77**, 41–51.

Nowell, P.C. (1976). The clonal evolution of tumor cell populations. *Science*, **194**, 23–8.

Ohno, S., Kaplan, W. & Kinosita, R. (1959). Formation of the sex chromatin by a single X-chromosome in liver cells of Rattus norvegicus. *Exp Cell Res*, **18**, 415–8.

Oie, H.K., Russell, E.K., Carney, D.N. & Gazdar, A.F. (1996). Cell culture methods for the establishment of the NCI series of lung cancer cell lines. *J Cell Biochem Suppl*, **24**, 24–31.

Oka, T., Yoshino, T., Hayashi, K., Ohara, N., Nakanishi, T., Yamaai, Y., Hiraki, A., Sogawa, C.A., Kondo, E., Teramoto, N., Takahashi, K., Tsuchiyama, J. & Akagi, T. (2001). Reduction of hematopoietic cell-specific tyrosine phosphatase SHP-1 gene expression in natural killer cell lymphoma and various types of lymphomas/leukemias : combination analysis with cDNA expression array and tissue microarray. *Am J Pathol*, **159**, 1495–505.

Oka, T., Ouchida, M., Koyama, M., Ogama, Y., Takada, S., Nakatani, Y., Tanaka, T., Yoshino, T., Hayashi, K., Ohara, N., Kondo, E., Takahashi, K., Tsuchiyama, J., Tanimoto, M., Shimizu, K. & Akagi, T. (2002). Gene silencing of the tyrosine phosphatase SHP1 gene by aberrant methylation in leukemias/lymphomas. *Cancer research*, **62**, 6390–4.

Okano, M., Xie, S. & Li, E. (1998). Cloning and characterization of a family of novel mammalian DNA (cytosine-5) methyltransferases. *Nature genetics*, **19**, 219–20.

Okano, M., Bell, D.W., Haber, D.A. & Li, E. (1999). DNA methyltransferases Dnmt3a and Dnmt3b are essential for de novo methylation and mammalian development. *Cell*, **99**, 247–57.

Olsen, E.A., Whittaker, S., Kim, Y.H., Duvic, M., Prince, H.M., Lessin, S.R., Wood, G.S., Willemze, R., Demierre, M.F., Pimpinelli, N., Bernengo, M.G., Ortiz-Romero, P.L., Bagot, M., Estrach, T., Guitart, J., Knobler, R., Sanches, J.A., Iwatsuki, K., Sugaya, M., Dummer, R., Pittelkow, M., Hoppe, R., Parker, S., Geskin, L., Pinter-Brown, L., Girardi, M., Burg, G., Ranki, A., Vermeer, M., Horwitz, S., Heald, P., Rosen, S., Cerroni, L., Dreno, B., Vonderheid, E.C., for Cutaneous Lymphomas, I.S., Consortium, U.S.C.L., of the European Organisation for Research, C.L.T.F. & of Cancer, T. (2011). Clinical end points and response criteria in mycosis fungoides and Sézary syndrome: a consensus statement of the International Society for Cutaneous Lymphomas, the United States Cutaneous Lymphoma Consortium, and the Cutaneous Lymphoma Task Force of the European Organisation for Research and Treatment of Cancer. *J Clin Oncol*, **29**, 2598–607.

Oprea, G.E., Kröber, S., McWhorter, M.L., Rossoll, W., Müller, S., Krawczak, M., Bassell, G.J., Beattie, C.E. & Wirth, B. (2008). Plastin 3 is a protective modifier of autosomal recessive spinal muscular atrophy. *Science*, **320**, 524–7.

Osella-Abate, S., Zaccagna, A., Savoia, P., Quaglino, P., Salomone, B. & Bernengo, M.G. (2001). Expression of apoptosis markers on peripheral blood lymphocytes from patients with cutaneous T-cell lymphoma during extracorporeal photochemotherapy. *J Am Acad Dermatol*, **44**, 40–7.

Pandey, M.K., Sung, B., Ahn, K.S. & Aggarwal, B.B. (2009). Butein suppresses constitutive and inducible signal transducer and activator of transcription (STAT) 3 activation and STAT3-regulated gene products through the induction of a protein tyrosine phosphatase SHP-1. *Mol Pharmacol*, **75**, 525–33.

Papadavid, E., Economidou, J., Psarra, A., Kapsimali, V., Mantzana, V., Antoniou, C., Limas, K., Stratigos, A., Stavrianeas, N., Avgerinou, G. & Katsambas, A. (2003). The relevance of peripheral blood T-helper 1 and 2 cytokine pattern in the evaluation of patients with mycosis fungoides and Sézary syndrome. *The British journal of dermatology*, **148**, 709–18.

Papoff, G., Cascino, I., Eramo, A., Starace, G., Lynch, D.H. & Ruberti, G. (1996). An N-terminal domain shared by Fas/Apo-1 (CD95) soluble variants prevents cell death in vitro. *J Immunol*, **156**, 4622–30.

Park, W.S., Oh, R.R., Kim, Y.S., Park, J.Y., Lee, S.H., Shin, M.S., Kim, S.Y., Kim, P.J., Lee, H.K., Yoo, N.Y. & Lee, J.Y. (2001). Somatic mutations in the death domain of the Fas (Apo-1/CD95) gene in gastric cancer. *J Pathol*, **193**, 162–8.

Paz, M.F., Fraga, M.F., Avila, S., Guo, M., Pollan, M., Herman, J.G. & Esteller, M. (2003). A systematic profile of DNA methylation in human cancer cell lines. *Cancer research*, **63**, 1114–21.

Petak, I., Danam, R.P., Tillman, D.M., Vernes, R., Howell, S.R., Berczi, L., Kopper, L., Brent, T.P. & Houghton, J.A. (2003). Hypermethylation of the gene promoter and enhancer region can regulate Fas expression and sensitivity in colon carcinoma. *Cell death and differentiation*, **10**, 211–7.

Piekarz, R.L., Robey, R.W., Zhan, Z., Kayastha, G., Sayah, A., Abdeldaim, A.H., Torrico, S. & Bates, S.E. (2004). T-cell lymphoma as a model for the use of histone deacetylase inhibitors in cancer therapy: impact of depsipeptide on molecular markers, therapeutic targets, and mechanisms of resistance. *Blood*, **103**, 4636–43.

Poiesz, B.J., Ruscetti, F.W., Mier, J.W., Woods, A.M. & Gallo, R.C. (1980). T-cell lines established from human T-lymphocytic neoplasias by direct response to T-cell growth factor. *Proceedings of the National Academy of Sciences of the United States of America*, **77**, 6815–9.

Popovic, M., Sarin, P.S., Robert-Gurroff, M., Kalyanaraman, V.S., Mann, D., Minowada, J. & Gallo, R.C. (1983). Isolation and transmission of human retrovirus (human t-cell leukemia virus). *Science*, **219**, 856–9, download.

Popp, C., Dean, W., Feng, S., Cokus, S.J., Andrews, S., Pellegrini, M., Jacobsen, S.E. & Reik, W. (2010). Genome-wide erasure of DNA methylation in mouse primordial germ cells is affected by AID deficiency. *Nature*, **463**, 1101–5.

Poszepczynska-Guigné, E., Schiavon, V., D'Incan, M., Echchakir, H., Musette, P., Ortonne, N., Boumsell, L., Moretta, A., Bensussan, A. & Bagot, M. (2004). CD158k/KIR3DL2 is a new phenotypic marker of Sezary cells: relevance for the diagnosis and follow-up of Sezary syndrome. *The Journal of investigative dermatology*, **122**, 820–3.

Preter, K.D., Speleman, F., Combaret, V., Lunec, J., Laureys, G., Eussen, B.H.J., Francotte, N., Board, J., Pearson, A.D.J., Paepe, A.D., Roy, N.V. & Vandesompele, J. (2002). Quantification of MYCN, DDX1, and NAG gene copy number in neuroblastoma using a real-time quantitative PCR assay. *Mod Pathol*, **15**, 159–66.

Prochazkova, M., Chevret, E., Mainhaguiet, G., Sobotka, J., Vergier, B., Belaud-Rotureau, M.A., Beylot-Barry, M. & Merlio, J.P. (2007). Common chromosomal abnormalities in mycosis fungoides transformation. *Genes Chromosomes Cancer*, **46**, 828–38.

Quddus, J., Johnson, K.J., Gavalchin, J., Amento, E.P., Chrisp, C.E., Yung, R.L. & Richardson, B.C. (1993). Treating activated CD4+ T cells with either of two distinct DNA methyltransferase inhibitors, 5-azacytidine or procainamide, is sufficient to cause a lupus-like disease in syngeneic mice. *J Clin Invest*, **92**, 38–53.

Ralfkiaer, E., O'Connor, N.T., Crick, J., Wantzin, G.L. & Mason, D.Y. (1987). Genotypic analysis of cutaneous T-cell lymphomas. *The Journal of investigative dermatology*, **88**, 762–5.

Rappl, G., Muche, J.M., Abken, H., Sterry, W., Tilgen, W., Ugurel, S. & Reinhold, U. (2001). CD4(+)CD7(-) T cells compose the dominant T-cell clone in the peripheral blood of patients with Sézary syndrome. *J Am Acad Dermatol*, **44**, 456–61.

Rayet, B. & Gélinas, C. (1999). Aberrant rel/nfkb genes and activity in human cancer. *Oncogene*, **18**, 6938–47.

Reddy, J., Shivapurkar, N., Takahashi, T., Parikh, G., Stastny, V., Echebiri, C., Crumrine, K., Zöchbauer-Müller, S., Drach, J., Zheng, Y., Feng, Z., Kroft, S.H., McKenna, R.W. & Gazdar, A.F. (2005). Differential methylation of genes that regulate cytokine signaling in lymphoid and hematopoietic tumors. *Oncogene*, **24**, 732–6.

Reinhold, U., Liu, L., Sesterhenn, J. & Abken, H. (1996). CD7-negative T cells represent a separate differentiation pathway in a subset of post-thymic helper T cells. *Immunology*, **89**, 391–6.

Revy, P., Muto, T., Levy, Y., Geissmann, F., Plebani, A., Sanal, O., Catalan, N., Forveille, M., Dufourcq-Labelouse, R., Gennery, A., Tezcan, I., Ersoy, F., Kayserili, H., Ugazio, A.G., Brousse, N., Muramatsu, M., Notarangelo, L.D., Kinoshita, K., Honjo, T., Fischer, A. & Durandy, A. (2000). Activation-induced cytidine deaminase (AID) deficiency causes the autosomal recessive form of the Hyper-IgM syndrome (HIGM2). *Cell*, **102**, 565–75.

Rho, H.M., Poiesz, B., Ruscetti, F.W. & Gallo, R.C. (1981). Characterization of the reverse transcriptase from a new retrovirus (HTLV) produced by a human cutaneous T-cell lymphoma cell line. *Virology*, **112**, 355–60.

Rho, J., Choi, S., Seong, Y.R., Choi, J. & Im, D.S. (2001). The arginine-1493 residue in QRRGRTGR1493G motif IV of the hepatitis C virus NS3 helicase domain is essential for NS3 protein methylation by the protein arginine methyltransferase 1. *J Virol*, **75**, 8031–44.

Richardson, B. (1986). Effect of an inhibitor of DNA methylation on T cells. II. 5-Azacytidine induces self-reactivity in antigen-specific T4+ cells. *Hum Immunol*, **17**, 456–70.

Richardson, B., Kahn, L., Lovett, E.J. & Hudson, J. (1986). Effect of an inhibitor of DNA methylation on T cells. I. 5-Azacytidine induces T4 expression on T8+ T cells. *J Immunol*, **137**, 35–9.

Richardson, B., Scheinbart, L., Strahler, J., Gross, L., Hanash, S. & Johnson, M. (1990). Evidence for impaired T cell DNA methylation in systemic lupus erythematosus and rheumatoid arthritis. *Arthritis Rheum*, **33**, 1665–73.

Riggs, A.D. (1975). X inactivation, differentiation, and DNA methylation. *Cytogenet Cell Genet*, **14**, 9–25.

Robinson, M.D., Stirzaker, C., Statham, A.L., Coolen, M.W., Song, J.Z., Nair, S.S., Strbenac, D., Speed, T.P. & Clark, S.J. (2010). Evaluation of affinity-based genome-wide DNA methylation data: effects of CpG density, amplification bias, and copy number variation. *Genome Res*, **20**, 1719–29.

Roman-Gomez, J., Jimenez-Velasco, A., Agirre, X., Prosper, F., Heiniger, A. & Torres, A. (2005). Lack of CpG island methylator phenotype defines a clinical subtype of T-cell acute lymphoblastic leukemia associated with good prognosis. *Journal of clinical oncology : official journal of the American Society of Clinical Oncology*, **23**, 7043–9.

Rouvier, E., Luciani, M.F. & Golstein, P. (1993). Fas involvement in Ca(2+)-independent T cell-mediated cytotoxicity. *J Exp Med*, **177**, 195–200.

Ruchusatsawat, K., Wongpiyabovorn, J., Shuangshoti, S., Hirankarn, N. & Mutirangura, A. (2006). SHP-1 promoter 2 methylation in normal epithelial tissues and demethylation in psoriasis. *J Mol Med*, **84**, 175–82.

Ruike, Y., Imanaka, Y., Sato, F., Shimizu, K. & Tsujimoto, G. (2010). Genome-wide analysis of aberrant methylation in human breast cancer cells using methyl-DNA immunoprecipitation combined with high-throughput sequencing. *BMC Genomics*, **11**, 137.

Russell, G.J., Walker, P.M., Elton, R.A. & Subak-Sharpe, J.H. (1976). Doublet frequency analysis of fractionated vertebrate nuclear DNA. *J Mol Biol*, **108**, 1–23.

Sandur, S.K., Pandey, M.K., Sung, B. & Aggarwal, B.B. (2010). 5-hydroxy-2-methyl-1,4-naphthoquinone, a vitamin K3 analogue, suppresses STAT3 activation pathway through induction of protein tyrosine phosphatase, SHP-1: potential role in chemosensitization. *Mol Cancer Res*, **8**, 107–18.

Santos, F., Hendrich, B., Reik, W. & Dean, W. (2002). Dynamic reprogramming of DNA methylation in the early mouse embryo. *Dev Biol*, **241**, 172–82.

Santourlidis, S., Warskulat, U., Florl, A.R., Maas, S., Pulte, T., Fischer, J., Müller, W. & Schulz, W.A. (2001). Hypermethylation of the tumor necrosis factor receptor superfamily 6 (APT1, Fas, CD95/Apo-1) gene promoter at rel/nuclear factor kappaB sites in prostatic carcinoma. *Molecular carcinogenesis*, **32**, 36–43.

Sasaki, Y., Itoh, F., Kobayashi, T., Kikuchi, T., Suzuki, H., Toyota, M. & Imai, K. (2002). Increased expression of T-fimbrin gene after DNA damage in CHO cells and inactivation of T-fimbrin by CpG methylation in human colorectal cancer cells. *Int J Cancer*, **97**, 211–6.

Scala, E., Russo, G., Cadoni, S., Narducci, M.G., Girardelli, C.R., Pità, O.D. & Puddu, P. (1999). Skewed expression of activation, differentiation and homing-related antigens in circulating cells from patients with cutaneous T cell lymphoma associated with CD7- T helper lymphocytes expansion. *The Journal of investigative dermatology*, **113**, 622–7.

Scarisbrick, J.J., Woolford, A.J., Russell-Jones, R. & Whittaker, S.J. (2001). Allelotyping in mycosis fungoides and Sézary syndrome: common regions of allelic loss identified on 9p, 10q, and 17p. *The Journal of investigative dermatology*, **117**, 663–70.

Scarisbrick, J.J., Woolford, A.J., Calonje, E., Photiou, A., Ferreira, S., Orchard, G., Russell-Jones, R. & Whittaker, S.J. (2002). Frequent abnormalities of the p15 and p16 genes in mycosis fungoides and sezary syndrome. *The Journal of investigative dermatology*, **118**, 493–9.

Scarisbrick, J.J., Mitchell, T.J., Calonje, E., Orchard, G., Russell-Jones, R. & Whittaker, S.J. (2003). Microsatellite instability is associated with hypermethylation of the hMLH1 gene and reduced gene expression in mycosis fungoides. *The Journal of investigative dermatology*, **121**, 894–901.

Schadt, E.E., Turner, S. & Kasarskis, A. (2010). A window into third-generation sequencing. *Hum Mol Genet*, **19**, R227–40.

Schilling, T., Schleithoff, E.S., Kairat, A., Melino, G., Stremmel, W., Oren, M., Krammer, P.H. & Müller, M. (2009). Active transcription of the human FAS/CD95/TNFRSF6 gene involves the p53 family. *Biochem Biophys Res Commun*, **387**, 399–404.

Schmid, C.W. (1991). Human Alu subfamilies and their methylation revealed by blot hybridization. *Nucleic Acids Res*, **19**, 5613–7.

Schmidl, C., Klug, M., Boeld, T.J., Andreesen, R., Hoffmann, P., Edinger, M. & Rehli, M. (2009). Lineage-specific DNA methylation in T cells correlates with histone methylation and enhancer activity. *Genome Res*, **19**, 1165–74.

Schmidt-Skrabs, C.C. (2000). Pautrier microabscesses (PA): a historical note. *Am J Dermatopathol*, **22**, 555.

Schmitz, I., Weyd, H., Krueger, A., Baumann, S., Fas, S.C., Krammer, P.H. & Kirchhoff, S. (2004). Resistance of short term activated T cells to CD95-mediated apoptosis correlates with de novo protein synthesis of c-FLIPshort. *J Immunol*, **172**, 2194–200.

Schmitz, K.M., Schmitt, N., Hoffmann-Rohrer, U., Schäfer, A., Grummt, I. & Mayer, C. (2009). TAF12 recruits Gadd45a and the nucleotide excision repair complex to the promoter of rRNA genes leading to active DNA demethylation. *Mol Cell*, **33**, 344–53.

Schones, D.E., Cui, K., Cuddapah, S., Roh, T.Y., Barski, A., Wang, Z., Wei, G. & Zhao, K. (2008). Dynamic regulation of nucleosome positioning in the human genome. *Cell*, **132**, 887–98.

Scott, F.L., Stec, B., Pop, C., Dobaczewska, M.K., Lee, J.J., Monosov, E., Robinson, H., Salvesen, G.S., Schwarzenbacher, R. & Riedl, S.J. (2009). The Fas-FADD death domain complex structure unravels signalling by receptor clustering. *Nature*, **457**, 1019–22.

Sézary, A. & Bouvrain, J. (1938). Erythrodermie avec presence de cellules monstrueuses dans le derme et le sang circulant. *Bulletin de la Société Francaise de Dermatologie et de Syphiligraphie*, **45**, 254–60.

Shackleton, M., Quintana, E., Fearon, E.R. & Morrison, S.J. (2009). Heterogeneity in cancer: cancer stem cells versus clonal evolution. *Cell*, **138**, 822–9.

Shackney, S.E. & Schuette, W.H. (1983). Multicompartment analysis of cell proliferation and cell migration in the Sezary syndrome. *Hematol Oncol*, **1**, 31–48.

Shemer, R., Walsh, A., Eisenberg, S., Breslow, J.L. & Razin, A. (1990). Tissue-specific methylation patterns and expression of the human apolipoprotein AI gene. *The Journal of biological chemistry*, **265**, 1010–5.

Shen, C.K. & Maniatis, T. (1980). Tissue-specific DNA methylation in a cluster of rabbit beta-like globin genes. *Proc Natl Acad Sci USA*, **77**, 6634–8.

Shin, J., Monti, S., Aires, D.J., Duvic, M., Golub, T., Jones, D.A. & Kupper, T.S. (2007). Lesional gene expression profiling in cutaneous T-cell lymphoma reveals natural clusters associated with disease outcome. *Blood*, **110**, 3015–27.

Shivapurkar, N., Takahashi, T., Reddy, J., Zheng, Y., Stastny, V., Collins, R., Toyooka, S., Suzuki, M., Parikh, G., Asplund, S., Kroft, S.H., Timmons, C., McKenna, R.W., Feng, Z. & Gazdar, A.F. (2004). Presence of simian virus 40 DNA sequences in human lymphoid and hematopoietic malignancies and their relationship to aberrant promoter methylation of multiple genes. *Cancer research*, **64**, 3757–60.

Singer, J., Roberts-Ems, J. & Riggs, A.D. (1979). Methylation of mouse liver DNA studied by means of the restriction enzymes msp I and hpa II. *Science*, **203**, 1019–21.

Sleight, B.J., Prasad, V.S., DeLaat, C., Steele, P., Ballard, E., Arceci, R.J. & Sidman, C.L. (1998). Correction of autoimmune lymphoproliferative syndrome by bone marrow transplantation. *Bone Marrow Transplant*, **22**, 375–80.

Smith, K.A. (1984). Interleukin 2. *Annu Rev Immunol*, **2**, 319–33.

Sokolowska-Wojdylo, M., Wenzel, J., Gaffal, E., Lenz, J., Speuser, P., Erdmann, S., Abuzahra, F., Bowman, E., Roszkiewicz, J., Bieber, T. & Tüting, T. (2005a). Circulating clonal CLA(+) and CD4(+) T cells in Sezary syndrome express the skin-homing chemokine receptors CCR4 and CCR10 as well as the lymph node-homing chemokine receptor CCR7. *The British journal of dermatology*, **152**, 258–64.

Sokolowska-Wojdylo, M., Wenzel, J., Gaffal, E., Steitz, J., Roszkiewicz, J., Bieber, T. & Tüting, T. (2005b). Absence of CD26 expression on skin-homing CLA+ CD4+ T lymphocytes in peripheral blood is a highly sensitive marker for early diagnosis and therapeutic monitoring of patients with Sézary syndrome. *Clinical and experimental dermatology*, **30**, 702–6.

Sommer, V.H., Clemmensen, O.J., Nielsen, O., Wasik, M., Lovato, P., Brender, C., Eriksen, K.W., Woetmann, A., Kaestel, C.G., Nissen, M.H., Ropke, C., Skov, S. & Ødum, N. (2004). In vivo activation of STAT3 in cutaneous T-cell lymphoma. Evidence for an antiapoptotic function of STAT3. *Leukemia*, **18**, 1288–95.

Sors, A., Jean-Louis, F., Pellet, C., Laroche, L., Dubertret, L., Courtois, G., Bachelez, H. & Michel, L. (2006). Down-regulating constitutive activation of the NF-kappaB canonical pathway overcomes the resistance of cutaneous T-cell lymphoma to apoptosis. *Blood*, **107**, 2354–63.

Starkebaum, G., Loughran, T.P., Waters, C.A. & Ruscetti, F.W. (1991). Establishment of an IL-2 independent, human T-cell line possessing only the p70 IL-2 receptor. *Int J Cancer*, **49**, 246–53.

Starr, R., Willson, T.A., Viney, E.M., Murray, L.J., Rayner, J.R., Jenkins, B.J., Gonda, T.J., Alexander, W.S., Metcalf, D., Nicola, N.A. & Hilton, D.J. (1997). A family of cytokine-inducible inhibitors of signalling. *Nature*, **387**, 917–21.

Stein, R., Gruenbaum, Y., Pollack, Y., Razin, A. & Cedar, H. (1982). Clonal inheritance of the pattern of DNA methylation in mouse cells. *Proceedings of the National Academy of Sciences of the United States of America*, **79**, 61–5.

Steinhoff, M., Schöpp, S., Assaf, C., Muche, M., Beyer, M., Sterry, W. & Lukowsky, A. (2009). Prevalence of genetically defined tumor cells in CD7 as well as CD26 positive and negative circulating T-cell subsets in Sézary syndrome. *Leukemia research*, **33**, 88–99.

Stillwell, R. & Bierer, B.E. (2001). T cell signal transduction and the role of CD7 in costimulation. *Immunol Res*, **24**, 31–52.

Straus, S.E., Jaffe, E.S., Puck, J.M., Dale, J.K., Elkon, K.B., Rösen-Wolff, A., Peters, A.M., Sneller, M.C., Hallahan, C.W., Wang, J., Fischer, R.E., Jackson, C.M., Lin, A.Y., Bäumler, C., Siegert, E., Marx, A., Vaishnaw, A.K., Grodzicky, T., Fleisher, T.A. & Lenardo, M.J. (2001). The development of lymphomas in families with autoimmune lymphoproliferative syndrome with germline Fas mutations and defective lymphocyte apoptosis. *Blood*, **98**, 194–200.

Stresemann, C. & Lyko, F. (2008). Modes of action of the DNA methyltransferase inhibitors azacytidine and decitabine. *Int J Cancer*, **123**, 8–13.

Su, M., Dorocicz, I., Dragowska, W.H., Ho, V., Li, G., Voss, N., Gascoyne, R. & Zhou, Y. (2003). Aberrant expression of T-plastin in Sezary cells. *Cancer Res*, **63**, 7122–7.

Swartz, M., Trautner, T. & Kornberg, A. (1962). Enzymatic synthesis of deoxyribonucleic acid. XI. Further studies on nearest neighbor base sequences in deoxyribonucleic acids. *The Journal of biological chemistry*, **237**, 1961–7.

Szabo, S.J., Kim, S.T., Costa, G.L., Zhang, X., Fathman, C.G. & Glimcher, L.H. (2000). A novel transcription factor, T-bet, directs Th1 lineage commitment. *Cell*, **100**, 655–69.

Takai, D. & Jones, P.A. (2002). Comprehensive analysis of CpG islands in human chromosomes 21 and 22. *Proc Natl Acad Sci USA*, **99**, 3740–5.

Takakuwa, T., Dong, Z., Nakatsuka, S., Kojya, S., Harabuchi, Y., Yang, W.I., Nagata, S. & Aozasa, K. (2002). Frequent mutations of Fas gene in nasal NK/T cell lymphoma. *Oncogene*, **21**, 4702–5.

Takamiya, T., Hosobuchi, S., Asai, K., Nakamura, E., Tomioka, K., Kawase, M., Kakutani, T., Paterson, A.H., Murakami, Y. & Okuizumi, H. (2006). Restriction landmark genome scanning method using isoschizomers (MspI/HpaII) for DNA methylation analysis. *Electrophoresis*, **27**, 2846–56.

Takayama, H., Takakuwa, T., Tsujimoto, Y., Tani, Y., Nonomura, N., Okuyama, A., Nagata, S. & Aozasa, K. (2002). Frequent Fas gene mutations in testicular germ cell tumors. *Am J Pathol*, **161**, 635–41.

Takeshima, H., Yamashita, S., Shimazu, T., Niwa, T. & Ushijima, T. (2009). The presence of RNA polymerase II, active or stalled, predicts epigenetic fate of promoter CpG islands. *Genome Res*, **19**, 1974–82.

Tang, N., Gibson, H., Germeroth, T., Porcu, P., Lim, H.W. & Wong, H.K. (2010). T-plastin (PLS3) gene expression differentiates Sézary syndrome from mycosis fungoides and inflammatory skin diseases and can serve as a biomarker to monitor disease progression. *Br J Dermatol*, **162**, 463–6.

Taswell, H. & Winkelmann, R.K. (1961). Sezary syndrome–a malignant reticulemic erythroderma. *JAMA*, **177**, 465–72.

Taylor, A., Verhagen, J., Akkoç, T., Wenig, R., Flory, E., Blaser, K., Akdis, M. & Akdis, C.A. (2009). IL-10 suppresses CD2-mediated T cell activation via SHP-1. *Mol Immunol*, **46**, 622–9.

Tiemessen, M.M., Mitchell, T.J., Hendry, L., Whittaker, S.J., Taams, L.S. & John, S. (2006). Lack of suppressive CD4+CD25+FOXP3+ T cells in advanced stages of primary cutaneous T-cell lymphoma. *The Journal of investigative dermatology*, **126**, 2217–23.

Tiffon, C., Adams, J., van der Fits, L., Wen, S., Townsend, P., Ganesan, A., Hodges, E., Vermeer, M. & Packham, G. (2011). The histone deacetylase inhibitors vorinostat and romidepsin downmodulate IL-10 expression in cutaneous T-cell lymphoma cells. *Br J Pharmacol*, **162**, 1590–602.

Tost, J., Dunker, J. & Gut, I.G. (2003). Analysis and quantification of multiple methylation variable positions in CpG islands by Pyrosequencing. *BioTechniques*, **35**, 152–6.

Tost, J., abdalaoui, H.E. & Gut, I.G. (2006). Serial pyrosequencing for quantitative DNA methylation analysis. *BioTechniques*, **40**, 721–2, 724, 726.

Toyooka, S., Toyooka, K.O., Maruyama, R., Virmani, A.K., Girard, L., Miyajima, K., Harada, K., Ariyoshi, Y., Takahashi, T., Sugio, K., Brambilla, E., Gilcrease, M., Minna, J.D. & Gazdar, A.F. (2001). DNA methylation profiles of lung tumors. *Mol Cancer Ther*, **1**, 61–7.

Toyota, M., Suzuki, H., Yamashita, T., Hirata, K., Imai, K., Tokino, T. & Shinomura, Y. (2009). Cancer epigenomics: implications of DNA methylation in personalized cancer therapy. *Cancer Sci*, **100**, 787–91.

Tracey, L., Villuendas, R., Dotor, A.M., Spiteri, I., Ortiz, P., Garcia, J.F., Peralto, J.L.R., Lawler, M. & Piris, M.A. (2003). Mycosis fungoides shows concurrent deregulation of multiple genes involved in the TNF signaling pathway: an expression profile study. *Blood*, **102**, 1042–50.

Tsui, F.W.L., Martin, A., Wang, J. & Tsui, H.W. (2006). Investigations into the regulation and function of the SH2 domain-containing protein-tyrosine phosphatase, SHP-1. *Immunol Res*, **35**, 127–36.

Tsui, H.W., Hasselblatt, K., Martin, A., ho Mok, S.C. & Tsui, F.W.L. (2002). Molecular mechanisms underlying SHP-1 gene expression. *Eur J Biochem*, **269**, 3057–64.

Ueki, T., Walter, K.M., Skinner, H., Jaffee, E., Hruban, R.H. & Goggins, M. (2002). Aberrant CpG island methylation in cancer cell lines arises in the primary cancers from which they were derived. *Oncogene*, **21**, 2114–7.

Utikal, J., Poenitz, N., Gratchev, A., Klemke, C.D., Nashan, D., Tüting, T. & Goerdt, S. (2006). Additional Her 2/neu gene copies in patients with Sézary syndrome. *Leukemia research*, **30**, 755–60.

van der Fits, L., van Kester, M.S., Qin, Y., Out-Luiting, J.J., Smit, F., Zoutman, W.H., Willemze, R., Tensen, C.P. & Vermeer, M.H. (2011). MicroRNA-21 expression in CD4+ T cells is regulated by STAT3 and is pathologically involved in Sézary syndrome. *The Journal of investigative dermatology*, **131**, 762–8.

van der Loo, E.M., Cnossen, J. & Meijer, C.J. (1981). Morphological aspects of T cell subpopulations in human blood: characterization of the cerebriform mononuclear cells in healthy individuals. *Clin Exp Immunol*, **43**, 506–16.

van der Ploeg, L.H. & Flavell, R.A. (1980). DNA methylation in the human gamma delta beta-globin locus in erythroid and nonerythroid tissues. *Cell*, **19**, 947–58.

van der Velden, V.H.J. & van Dongen, J.J.M. (2009). MRD detection in acute lymphoblastic leukemia patients using Ig/TCR gene rearrangements as targets for real-time quantitative PCR. *Methods Mol Biol*, **538**, 115–50.

van Doorn, R., Dijkman, R., Vermeer, M.H., Starink, T.M., Willemze, R. & Tensen, C.P. (2002). A novel splice variant of the Fas gene in patients with cutaneous T-cell lymphoma. *Cancer research*, **62**, 5389–92.

van Doorn, R., Dijkman, R., Vermeer, M.H., Out-Luiting, J.J., van der Raaij-Helmer, E.M.H., Willemze, R. & Tensen, C.P. (2004). Aberrant expression of the tyrosine kinase receptor EphA4 and the transcription factor twist in Sézary syndrome identified by gene expression analysis. *Cancer research*, **64**, 5578–86.

van Doorn, R., Zoutman, W.H., Dijkman, R., de Menezes, R.X., Commandeur, S., Mulder, A.A., van der Velden, P.A., Vermeer, M.H., Willemze, R., Yan, P.S., Huang, T.H. & Tensen, C.P. (2005). Epigenetic profiling of cutaneous T-cell lymphoma: promoter hypermethylation of multiple tumor suppressor genes including BCL7a, PTPRG, and p73. *J Clin Oncol*, **23**, 3886–96.

van Doorn, R., van Kester, M.S., Dijkman, R., Vermeer, M.H., Mulder, A.A., Szuhai, K., Knijnenburg, J., Boer, J.M., Willemze, R. & Tensen, C.P. (2009). Oncogenomic analysis of mycosis fungoides reveals major differences with Sezary syndrome. *Blood*, **113**, 127–36.

van Kester, M.S., Out-Luiting, J.J., von dem Borne, P.A., Willemze, R., Tensen, C.P. & Vermeer, M.H. (2008). Cucurbitacin I inhibits Stat3 and induces apoptosis in Sézary cells. *The Journal of investigative dermatology*, **128**, 1691–5.

van Krieken, J.H.J.M., Langerak, A.W., Macintyre, E.A., Kneba, M., Hodges, E., Sanz, R.G., Morgan, G.J., Parreira, A., Molina, T.J., Cabeçadas, J., Gaulard, P., Jasani, B., Garcia, J.F., Ott, M., Hannsmann, M.L., Berger, F., Hummel, M., Davi, F., Brüggemann, M., Lavender, F.L., Schuuring, E., Evans, P.A.S., White, H., Salles, G., Groenen, P.J.T.A., Gameiro, P., Pott, C. & van Dongen, J.J.M. (2007). Improved reliability of lymphoma diagnostics via PCR-based clonality testing: report of the BIOMED-2 Concerted Action BHM4-CT98-3936. *Leukemia*, **21**, 201–6.

Vanyushin, B.F., Mazin, A.L., Vasilyev, V.K. & Belozersky, A.N. (1973). The content of 5-methylcytosine in animal DNA: the species and tissue specificity. *Biochim Biophys Acta*, **299**, 397–403.

Varrault, A., Bilanges, B., Mackay, D.J., Basyuk, E., Ahr, B., Fernandez, C., Robinson, D.O., Bockaert, J. & Journot, L. (2001). Characterization of the methylation-sensitive promoter of the imprinted ZAC gene supports its role in transient neonatal diabetes mellitus. *The Journal of biological chemistry*, **276**, 18653–6.

Vermeer, M.H., van Doorn, R., Dijkman, R., Mao, X., Whittaker, S., van Voorst Vader, P.C., Gerritsen, M.J.P., Geerts, M.L., Gellrich, S., Söderberg, O., Leuchowius, K.J., Landegren, U., Out-Luiting, J.J., Knijnenburg, J., Ijszenga, M., Szuhai, K., Willemze, R. & Tensen, C.P. (2008). Novel and highly recurrent chromosomal alterations in Sézary syndrome. *Cancer research*, **68**, 2689–98.

Vonderheid, E.C., Bernengo, M.G., Burg, G., Duvic, M., Heald, P., Laroche, L., Olsen, E., Pittelkow, M., Russell-Jones, R., Takigawa, M., Willemze, R. & ISCL (2002). Update on erythrodermic cutaneous T-cell lymphoma: report of the International Society for Cutaneous Lymphomas. *J Am Acad Dermatol*, **46**, 95–106.

Vonderheid, E.C., Boselli, C.M., Conroy, M., Casaus, L., Espinoza, L.C., Venkataramani, P., Bigler, R.D. & Hou, J.S. (2005). Evidence for restricted Vbeta usage in the leukemic phase of cutaneous T cell lymphoma. *The Journal of investigative dermatology*, **124**, 651–61.

Vowels, B.R., Cassin, M., Vonderheid, E.C. & Rook, A.H. (1992). Aberrant cytokine production by Sezary syndrome patients: cytokine secretion pattern resembles murine Th2 cells. *The Journal of investigative dermatology*, **99**, 90–4.

Wabnitz, G.H., Köcher, T., Lohneis, P., Stober, C., Konstandin, M.H., Funk, B., Sester, U., Wilm, M., Klemke, M. & Samstag, Y. (2007). Costimulation induced phosphorylation of L-plastin facilitates surface transport of the T cell activation molecules CD69 and CD25. *Eur J Immunol*, **37**, 649–62.

Wain, E.M., Mitchell, T.J., Russell-Jones, R. & Whittaker, S.J. (2005). Fine mapping of chromosome 10q deletions in mycosis fungoides and sezary syndrome: identification of two discrete regions of deletion at 10q23.33-24.1 and 10q24.33-25.1. *Genes, chromosomes & cancer*, **42**, 184–92.

Wallace, E.V.B., Stoddart, D., Heron, A.J., Mikhailova, E., Maglia, G., Donohoe, T.J. & Bayley, H. (2010). Identification of epigenetic DNA modifications with a protein nanopore. *Chem Commun (Camb)*, **46**, 8195–7.

Walton, K.M. & Dixon, J.E. (1993). Protein tyrosine phosphatases. *Annu Rev Biochem*, **62**, 101–20.

Wang, C., Morley, S.C., Donermeyer, D., Peng, I., Lee, W.P., Devoss, J., Danilenko, D.M., Lin, Z., Zhang, J., Zhou, J., Allen, P.M. & Brown, E.J. (2010). Actin-bundling protein L-plastin regulates T cell activation. *J Immunol*, **185**, 7487–97.

Wang, Z., Zang, C., Rosenfeld, J.A., Schones, D.E., Barski, A., Cuddapah, S., Cui, K., Roh, T.Y., Peng, W., Zhang, M.Q. & Zhao, K. (2008). Combinatorial patterns of histone acetylations and methylations in the human genome. *Nature genetics*, **40**, 897–903.

Warnecke, P.M., Stirzaker, C., Song, J., Grunau, C., Melki, J.R. & Clark, S.J. (2002). Identification and resolution of artifacts in bisulfite sequencing. *Methods*, **27**, 101–7.

Washington, L., Huh, Y., Powers, L., Duvic, M. & Jones, D. (2002). A stable aberrant immunophenotype characterizes nearly all cases of cutaneous T-cell lymphoma in blood and can be used to monitor response to therapy. *BMC clinical pathology*, **2**, 5.

Weber, M., Davies, J.J., Wittig, D., Oakeley, E.J., Haase, M., Lam, W.L. & Schübeler, D. (2005). Chromosome-wide and promoter-specific analyses identify sites of differential DNA methylation in normal and transformed human cells. *Nature genetics*, **37**, 853–62.

Weiss, L.M., Hu, E., Wood, G.S., Moulds, C., Cleary, M.L., Warnke, R. & Sklar, J. (1985). Clonal rearrangements of T-cell receptor genes in mycosis fungoides and dermatopathic lymphadenopathy. *N Engl J Med*, **313**, 539–44, weston Education Centre has coppies.

Whang-Peng, J., Lutzner, M., Edelson, R. & Knutsen, T. (1976). Cytogenetic studies and clinical implications in patients with Sézary syndrome. *Cancer*, **38**, 861–7.

Whittaker, S.J., Demierre, M.F., Kim, E.J., Rook, A.H., Lerner, A., Duvic, M., Scarisbrick, J., Reddy, S., Robak, T., Becker, J.C., Samtsov, A., McCulloch, W. & Kim, Y.H. (2010). Final results from a multicenter, international, pivotal study of romidepsin in refractory cutaneous T-cell lymphoma. *Journal of clinical oncology : official journal of the American Society of Clinical Oncology*, **28**, 4485–91.

Wigler, M., Levy, D. & Perucho, M. (1981). The somatic replication of DNA methylation. *Cell*, **24**, 33–40.

Willemze, R., Jaffe, E.S., Burg, G., Cerroni, L., Berti, E., Swerdlow, S.H., Ralfkiaer, E., Chimenti, S., Diaz-Perez, J.L., Duncan, L.M., Grange, F., Harris, N.L., Kempf, W., Kerl, H., Kurrer, M., Knobler, R., Pimpinelli, N., Sander, C., Santucci, M., Sterry, W., Vermeer, M.H., Wechsler, J., Whittaker, S. & Meijer, C.J.L.M. (2005). WHO-EORTC classification for cutaneous lymphomas. *Blood*, **105**, 3768–85.

Wilson, I.M., Davies, J.J., Weber, M., Brown, C.J., Alvarez, C.E., MacAulay, C., Schübeler, D. & Lam, W.L. (2006). Epigenomics: mapping the methylome. *Cell Cycle*, **5**, 155–8.

Wlodarski, P., Zhang, Q., Liu, X., Kasprzycka, M., Marzec, M. & Wasik, M.A. (2007). PU.1 activates transcription of SHP-1 gene in hematopoietic cells. *The Journal of biological chemistry*, **282**, 6316–23.

Wohlfart, S., Sebinger, D., Gruber, P., Buch, J., Polgar, D., Krupitza, G., Rosner, M., Hengstschläger, M., Raderer, M., Chott, A. & Müllauer, L. (2004). FAS (CD95) mutations are rare in gastric MALT lymphoma but occur more frequently in primary gastric diffuse large B-cell lymphoma. *Am J Pathol*, **164**, 1081–9.

Wojdacz, T.K. & Dobrovic, A. (2007). Methylation-sensitive high resolution melting (MS-HRM): a new approach for sensitive and high-throughput assessment of methylation. *Nucleic acids research*, **35**, e41.

Wu, C., Sun, M., Liu, L. & Zhou, G.W. (2003). The function of the protein tyrosine phosphatase SHP-1 in cancer. *Gene*, **306**, 1–12.

Wu, J. & Wood, G.S. (2011). Reduction of Fas/CD95 Promoter Methylation, Upregulation of Fas Protein, and Enhancement of Sensitivity to Apoptosis in Cutaneous T-Cell Lymphoma. *Archives of dermatology*.

Wu, J., Nihal, M., Siddiqui, J., Vonderheid, E.C. & Wood, G.S. (2009). Low FAS/CD95 expression by CTCL correlates with reduced sensitivity to apoptosis that can be restored by FAS upregulation. *The Journal of investigative dermatology*, **129**, 1165–73.

Wu, J., Siddiqui, J., Nihal, M., Vonderheid, E.C. & Wood, G.S. (2011). Structural alterations of the FAS gene in cutaneous T-cell lymphoma (CTCL). *Arch Biochem Biophys*, **508**, 185–91.

Xerri, L., Carbuccia, N., Parc, P. & Birg, F. (1995). Search for rearrangements and/or allelic loss of the fas/APO-1 gene in 101 human lymphomas. *Am J Clin Pathol*, **104**, 424–30.

Xi, Y. & Li, W. (2009). BSMAP: whole genome bisulfite sequence MAPping program. *BMC Bioinformatics*, **10**, 232.

Xu, G.L., Bestor, T.H., Bourc'his, D., Hsieh, C.L., Tommerup, N., Bugge, M., Hulten, M., Qu, X., Russo, J.J. & Viegas-Péquignot, E. (1999). Chromosome instability and immunodeficiency syndrome caused by mutations in a DNA methyltransferase gene. *Nature*, **402**, 187–91.

Xu, Y., Banville, D., Zhao, H.F., Zhao, X. & Shen, S.H. (2001). Transcriptional activity of the SHP-1 gene in MCF7 cells is differentially regulated by binding of NF-Y factor to two distinct CCAAT-elements. *Gene*, **269**, 141–53.

Yagi, H., Tokura, Y., Furukawa, F. & Takigawa, M. (1996). CD7-positive Sézary syndrome with a Th1 cytokine profile. *J Am Acad Dermatol*, **34**, 368–74.

Yagil, Z., Nechushtan, H., Kay, G., Yang, C.M., Kemeny, D.M. & Razin, E. (2010). The enigma of the role of protein inhibitor of activated STAT3 (PIAS3) in the immune response. *Trends Immunol*, **31**, 199–204.

Yamada, Y., Watanabe, H., Miura, F., Soejima, H., Uchiyama, M., Iwasaka, T., Mukai, T., Sakaki, Y. & Ito, T. (2004). A comprehensive analysis of allelic methylation status of CpG islands on human chromosome 21q. *Genome research*, **14**, 247–66.

Yoon, J.S., Newton, S.M., Wysocka, M., Troxel, A.B., Hess, S.D., Richardson, S.K., Lin, J.H., Benoit, B.M., Kasprzycka, M., Wasik, M.A. & Rook, A.H. (2008). IL-21 enhances antitumor responses without stimulating proliferation of malignant T cells of patients with Sézary syndrome. *The Journal of investigative dermatology*, **128**, 473–80.

Yu, H., Kortylewski, M. & Pardoll, D. (2007). Crosstalk between cancer and immune cells: role of STAT3 in the tumour microenvironment. *Nat Rev Immunol*, **7**, 41–51.

Zhang, C., Richon, V., Ni, X., Talpur, R. & Duvic, M. (2005a). Selective induction of apoptosis by histone deacetylase inhibitor SAHA in cutaneous T-cell lymphoma cells: relevance to mechanism of therapeutic action. *The Journal of investigative dermatology*, **125**, 1045–52.

Zhang, C., Li, B., Zhang, X., Hazarika, P., Aggarwal, B.B. & Duvic, M. (2010). Curcumin selectively induces apoptosis in cutaneous T-cell lymphoma cell lines and

patients' PBMCs: potential role for STAT-3 and NF-kappaB signaling. *The Journal of investigative dermatology*, **130**, 2110–9.

Zhang, J., Chang, C.C., Lombardi, L. & Dalla-Favera, R. (1994). Rearranged NFKB2 gene in the HUT78 T-lymphoma cell line codes for a constitutively nuclear factor lacking transcriptional repressor functions. *Oncogene*, **9**, 1931–7.

Zhang, Q., Nowak, I., Vonderheid, E.C., Rook, A.H., Kadin, M.E., Nowell, P.C., Shaw, L.M. & Wasik, M.A. (1996). Activation of Jak/STAT proteins involved in signal transduction pathway mediated by receptor for interleukin 2 in malignant T lymphocytes derived from cutaneous anaplastic large T-cell lymphoma and Sezary syndrome. *Proceedings of the National Academy of Sciences of the United States of America*, **93**, 9148–53.

Zhang, Q., Raghunath, P.N., Vonderheid, E., Odum, N. & Wasik, M.A. (2000). Lack of phosphotyrosine phosphatase SHP-1 expression in malignant T-cell lymphoma cells results from methylation of the SHP-1 promoter. *Am J Pathol*, **157**, 1137–46.

Zhang, Q., Wang, H.Y., Marzec, M., Raghunath, P.N., Nagasawa, T. & Wasik, M.A. (2005b). STAT3- and DNA methyltransferase 1-mediated epigenetic silencing of SHP-1 tyrosine phosphatase tumor suppressor gene in malignant T lymphocytes. *Proc Natl Acad Sci USA*, **102**, 6948–53.

Zhao, S., Wang, Y., Liang, Y., Zhao, M., Long, H., Ding, S., Yin, H. & Lu, Q. (2011). MicroRNA-126 regulates DNA methylation in CD4+ T cells and contributes to systemic lupus erythematosus by targeting DNA methyltransferase 1. *Arthritis Rheum*, **63**, 1376–86.

Zheng, W. & Flavell, R.A. (1997). The transcription factor GATA-3 is necessary and sufficient for Th2 cytokine gene expression in CD4 T cells. *Cell*, **89**, 587–96.

Zhu, J.K. (2009). Active DNA demethylation mediated by DNA glycosylases. *Annu Rev Genet*, **43**, 143–66.

Zhu, W., Mustelin, T. & David, M. (2002). Arginine methylation of STAT1 regulates its dephosphorylation by T cell protein tyrosine phosphatase. *J Biol Chem*, **277**, 35787–90.

Zoi-Toli, O., Vermeer, M.H., Vries, E.D., Beek, P.V., Meijer, C.J. & Willemze, R. (2000). Expression of Fas and Fas-ligand in primary cutaneous T-cell lymphoma (CTCL): association between lack of Fas expression and aggressive types of CTCL. *The British journal of dermatology*, **143**, 313–9.

Zou, B., Chim, C.S., Zeng, H., Leung, S.Y., Yang, Y., Tu, S.P., Lin, M.C.M., Wang, J., He, H., Jiang, S.H., Sun, Y.W., Yu, L.F., Yuen, S.T., Kung, H.F. & Wong, B.C.Y. (2006). Correlation between the single-site CpG methylation and expression silencing of the XAF1 gene in human gastric and colon cancers. *Gastroenterology*, **131**, 1835–43.

Zu, Y., Kohno, M., Kubota, I., Nishida, E., Hanaoka, M. & Namba, Y. (1990). Characterization of interleukin 2 stimulated 65-kilodalton phosphoprotein in human T cells. *Biochemistry*, **29**, 1055–62.

Appendices

ORIGINAL ARTICLE

See related commentary on pg 922

Downregulation of Fas Gene Expression in Sézary Syndrome Is Associated with Promoter Hypermethylation

Christine L. Jones[1], E. Mary Wain[1], Chung-Ching Chu[2], Isabella Tosi[3], Rosalind Foster[4], Robert C.T. McKenzie[1], Sean J. Whittaker[1] and Tracey J. Mitchell[1]

Sézary Syndrome (SS) is an aggressive leukemic variant of primary cutaneous T-cell lymphoma characterized by the presence of tumor or Sézary cells that generally display a mature memory T-cell immunophenotype. Sézary cells proliferate poorly and therefore their accumulation may be due to defective T-cell homeostasis involving resistance to apoptosis. In this study, we analyzed Fas expression in CD4+ lymphocytes at the mRNA and protein levels in a large cohort of SS patients as compared with healthy controls. Fas mRNA expression was dysregulated in 34/47 patients, with significant under- and overexpression of Fas mRNA detected in 21 and 13 patients respectively ($P<0.01$). Examination of cell-surface Fas expression showed correlation with the observed downregulation of mRNA in CD4+ T cells. Mutational analysis demonstrated that functional *FAS* gene mutations are rare. Moreover, 16 SS patients who showed significant under-expression of Fas mRNA also showed significant positional hypermethylation within the *FAS* CpG island, which was not present in healthy controls or SS patients determined to have normal or overexpression of Fas mRNA. These data demonstrate that dysregulation of Fas expression is a common feature of SS, and provide a rationale for targeted therapies to restore the extrinsic Fas-dependent apoptotic pathway in this malignancy.

Journal of Investigative Dermatology (2010) **130,** 1116–1125; doi:10.1038/jid.2009.301; published online 17 September 2009

INTRODUCTION

Sézary Syndrome (SS) is an aggressive, leukemic variant of primary cutaneous T-cell lymphoma (CTCL). Clinically SS is characterized by erythroderma, lymphadenopathy, pruritus, and presence in the peripheral blood of a clonal population of malignant T cells with hyper-convoluted, cerebriform nuclei, known as Sézary cells (Willemze *et al.*, 2005). The immunophenotype of Sézary cells is typically that of a mature memory T-cell (CD4+/CD45RO+) expressing the skin-homing marker cutaneous lymphocyte antigen and the chemokine receptor CCR4, but frequently lacking expression of other T-cell surface markers such as CD7 and CD26 (Burg *et al.*, 2005).

Unlike other T-cell lymphomas/leukemias such as adult and childhood T-cell acute lymphoblastic leukemia, which are commonly associated with balanced chromosomal translocations, no specific karyotype is associated with SS, although genetic instability with recurrent ''hotspots'' of chromosomal abnormalities are a common feature of the disease. Of note are frequent deletions within the long arm of chromosome 10, which harbors the *FAS* gene. Loss of heterozygosity at microsatellite markers in 10q23.31 has been reported by two independent studies in up to 50% of SS patients (Wain *et al.*, 2005; Vermeer *et al.*, 2008). Loss of 10q has also been described in several other malignancies and is associated with tumor progression in prostatic and bladder carcinomas (Cappellen *et al.*, 1997; Komiya *et al.*, 1996).

The *FAS* gene, which encodes the death receptor Fas (CD95/APO-1), is activated by its natural ligand (FasL/CD95 L) and plays a key role in regulating T-cell homeostasis, primarily through induction of apoptosis via activation-induced cell death (AICD). Fas signaling leads to the formation of a multi-molecular complex called the death-inducing signaling complex, which in turn triggers a cascade of caspase activation that constitutes the activation phase of apoptosis. Induction of an immune response following antigen challenge leads to rapid clonal expansion and differentiation of naïve T cells resulting in a large pool of

[1]*King's College London, Skin Tumour Unit, St. John's Institute of Dermatology, Division of Genetics and Molecular Medicine, London, UK;* [2]*King's College London, Cutaneous Medicine and Immunotherapy Unit, St. John's Institute of Dermatology, Division of Genetics and Molecular Medicine, London, UK;* [3]*Cutaneous Medicine Theme, NIHR Biomedical Research Centre, Guy's and St Thomas' NHS Foundation Trust and King's College London, London, UK and* [4]*Jefferiss Trust Laboratories, Imperial College, Norfolk Place, London, UK*

Correspondence: Dr Tracey J. Mitchell, King's College London, Skin Tumour Unit, St. John's Institute of Dermatology, Division of Genetics and Molecular Medicine, 9th Floor, Tower Wing, Guy's Hospital, London SE1 9RT, UK. E mail: tracey.mitchell@kcl.ac.uk

Abbreviations: AICD, activation induced cell death; CTCL, cutaneous T-cell lymphoma; PBLs, peripheral blood lymphocytes; qPCR, quantitative reverse transcription PCR; SS, Sézary Syndrome; SSCP, single strand conformational polymorphism

Received 11 March 2009; revised 29 July 2009; accepted 2 August 2009; published online 17 September 2009

effector T cells. During the termination phase of the immune response, the vast majority of effector T cells are eliminated by AICD, with only a small proportion surviving AICD and entering the memory T-cell pool (reviewed by Krammer *et al.*, 2007). Several studies have revealed that the Fas system is highly regulated during the phases of a T-cell immune response. Resting T cells express marginal amounts of Fas and are resistant to apoptosis (Klas *et al.*, 1993). During the activation phase, Fas is upregulated (Ju *et al.*, 1995) although short-term activated effector T cells remain resistant to AICD (Klas *et al.*, 1993), which is thought to be due to incomplete death-inducing signaling complex formation and the presence of high levels of the apoptosis inhibitor c-FLIP (Kirchhoff *et al.*, 2000; Schmitz *et al.*, 2004). Long-term activated T cells express comparable levels of Fas to short-term activated T cells, but have complete death-inducing signaling complex formation with concomitant downregulation of c-FLIP expression, and are therefore sensitive to Fas-mediated AICD (Dhein *et al.*, 1995).

Given the high frequency of deletion within the *FAS* gene locus in SS and the fundamental role of the Fas system in T-cell homeostasis, Fas is an attractive candidate for a pivotal role in the pathogenesis of this disease. Studies determining the molecular basis of Canale–Smith syndrome have shown that heterozygous *FAS* mutations are sufficient to compromise Fas function (Drappa *et al.*, 1996). Somatic *FAS* gene mutations have been described in several malignancies, including multiple myeloma and non-Hodgkin's lymphoma (Lee *et al.*, 1999; Park *et al.*, 2001; Takakuwa *et al.*, 2002; Wohlfart *et al.*, 2004). Somatic *FAS* gene mutations have been described rarely in tumor cells isolated from skin lesions of mycosis fungoides (Dereure *et al.*, 2002; Nagasawa *et al.*, 2004), which is an indolent form of CTCL. However, it remains to be determined if these mutations result in loss of function. To date there are no reports of mutational analysis of the *FAS* gene in SS. A recent report has demonstrated frequent resistance (9/16 cases) to Fas-mediated apoptosis in freshly isolated primary Sézary cells (Contassot *et al.*, 2008). Heterogeneity of Fas expression levels was observed with five cases showing normal or increased Fas expression, and four cases showing reduced Fas expression. In cases with normal or enhanced Fas expression, resistance to apoptosis was attributed to increased expression of the apoptosis inhibitor c-FLIP. However, the mechanism mediating reduced Fas expression was not addressed.

Epigenetic gene silencing through promoter hypermethylation of CpG islands is recognized as an important mechanism regulating transcriptional silencing of genes, expression of imprinted genes, and in tumorigenesis (Jones and Baylin, 2002; Schaefer *et al.*, 2007). Tumor suppressor genes involved in DNA repair, cell cycling, proliferation, and apoptotic pathways are commonly inactivated through hypermethylation in malignancy. The *FAS* gene contains a 1,072 bp CpG island, which spans the transcriptional start site and exon 1. Hypermethylation of the *FAS* gene promoter has been described in colon, prostatic, and small-cell lung carcinoma (Santourlidis *et al.*, 2001; Hopkins-Donaldson *et al.*, 2003; Petak *et al.*, 2003), and associated with decreased Fas gene expression in these malignancies.

In this study we investigated Fas expression status in tumor cell populations from patients with SS. We demonstrate that reduced Fas mRNA and protein expression is common in SS and can be attributed to a specific pattern of methylation within the *FAS* CpG island.

RESULTS

Heterogeneity in tumor cell surface markers

We enriched for tumor cells using negative selection to remove all non-CD4+ cells from the PBL population. This was justified by experiments we performed on a subset of patients to identify the cell subset which included the whole tumor cell population while excluding as many reactive cells as possible. We examined CD26 as a potential marker to further isolate the tumor cell population (Jones *et al.*, 2001). Fluorescence-activated cell sorting was used to isolate the CD3+CD4+/CD45RO+/CD26− and CD3+CD4+/CD45RO+/CD26+ cell populations from five patients, and T-plastin mRNA expression levels were used to identify those populations that contained Sézary cells (Su *et al.*, 2003). We detected T-plastin mRNA in both CD26− and CD26+ subsets, with no significant difference in expression between the two groups (Figure 1).

Decreased Fas mRNA expression in CD4+ cells from SS patients

Quantitative reverse transcription PCR (qPCR) was used to determine Fas mRNA expression levels in CD4+ T cells isolated from peripheral blood. The expression of Fas mRNA was measured in 47 SS patients and compared to average expression levels from 16 healthy controls (Figure 2a). Fas mRNA expression in the healthy control samples showed little variation, whereas expression in SS patients was highly heterogeneous, ranging from a three-fold increase to a 30-fold reduction as compared with healthy controls. Overall, 21 samples showed significant underexpression ($P=0.01$) and 13 showed significant overexpression ($P=0.01$) of Fas

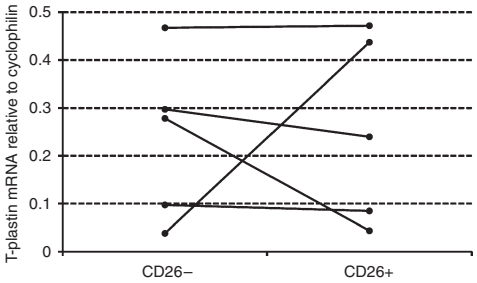

Figure 1. Expression of T-plastin mRNA in sorted patient-cell subsets. PBL's from five SS patients were sorted into CD3+CD4+/CD45RO+/CD26− and CD3+CD4+/CD45RO+/CD26+ subsets then expression of T-plastin mRNA was quantitated in each subset using qPCR and expressed relative to the housekeeping gene cyclophilin.

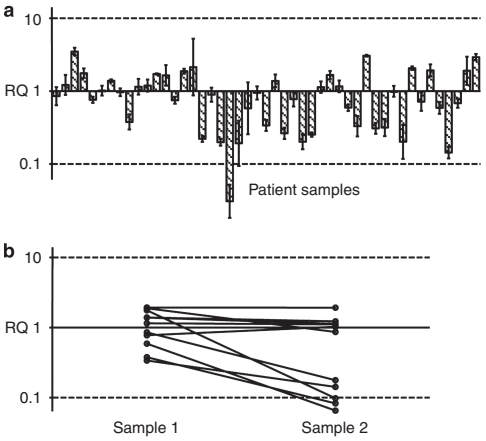

Figure 2. Expression of Fas mRNA in SS patient samples. Quantitative reverse transcription-PCR analysis of Fas mRNA expression in SS samples expressed as a fold difference in amount of mRNA relative to the mean of 16 healthy controls (RQ). Measurements were performed in triplicate and normalized against cyclophilin A. (**a**) Means ± 99% confidence interval for 47 patient samples. (**b**) Sequential samples taken from 12 patients between six months and two years apart to assess the change in Fas mRNA expression over time.

Table 1. Lymphocyte counts for the 12 SS patients from whom two sequential samples were obtained

Sample	Total lymphocytes ($\times 10^3\,\mu l^{-1}$)	CD4+ count ($\times 10^3\,\mu l^{-1}$)	CD4:CD8 ratio
SS5a	NA	1.12	8.00
SS5b	8.57	6.74	38.58
SS14a	NA	2.27	22.00
SS14b	2.02	1.51	124.33
SS16a	NA	0.32	11.00
SS16b	6.65	6.28	108.39
SS18a	NA	1.22	11.00
SS18b	3.04	2.34	19.65
SS20a	4.07	3.62	40.41
SS20b	3.21	2.78	24.53
SS21a	6.57	5.89	16.02
SS21b	9.26	8.77	342.00
SS23a	0.61	0.43	9.86
SS23b	1.59	1.33	26.57
SS28a	4.19	3.70	55.25
SS28b	7.79	7.12	53.76
SS31a	6.44	6.08	42.91
SS31b	31.67	31.41	119.48
SS33a	5.04	4.77	80.85
SS33b	5.22	4.92	84.20
SS34a	25.06	24.71	164.33
SS34b	24.85	24.63	198.20
SS46a	1.33	0.67	1.56
SS46b	1.65	0.79	1.61

NA, not available; SS, Sézary Syndrome.

mRNA. Total lymphocyte count, CD4+ count, and CD4:CD8 ratio were used to assess tumor burden in all patients. No correlation between the expression of Fas and tumor burden or survival was found.

Sequential samples taken at least six months apart were available from 12 patients, which allowed us to investigate any changes in Fas mRNA expression over time. Figure 2b shows the change in expression for each patient between their first and second samples. The general trend is toward a decrease in Fas expression over time, which was shown to be significant using a pairwise *t*-test ($P=0.021$); however, there is a notable subset of patients who maintained a consistent level of Fas expression. Total lymphocyte count, CD4+ count, and CD4:CD8 ratio were recorded at the time of sampling and are presented in Table 1. There was no association between the observed decrease in Fas expression and changes in CD4+ lymphocytes, suggesting that this decrease is not simply due to an increase in tumor burden.

Loss of cell surface Fas protein in memory T cells from SS patients

To validate the Fas mRNA expression data, we determined the level of cell surface protein expression of Fas on the CD3+CD4+/CD45RO+ T-cell population by flow cytometry using peripheral blood lymphocytes (PBLs) from 10 SS patients and six healthy controls. We also examined the cell surface Fas expression on the Sézary cell lines SeAx and HuT78, and the mycosis fungoides cell line MyLa. Figure 3a shows representative Fas histogram plots for one healthy individual (H6), two SS patients (P2, P7), and the cell lines. Whereas HuT78 and MyLa expressed Fas, SeAx displayed complete absence of cell surface Fas protein.

The proportion of Fas-positive cells within the CD3+CD4+/CD45RO+ population was calculated for each sample (Figure 3b). As expected, nearly all of the memory T cells in healthy control samples expressed Fas protein on their cell surface (range: 95.2–99.4% Fas+). Patient samples, however, showed loss of cell surface Fas expression in a proportion of their memory T cells (range: 1.5–96% Fas+). Patient samples were considered significantly different to healthy if the proportion of Fas-positive cells within the CD3+CD4+/CD45RO+ cell population was less than 80.7% (mean healthy proportion−10 standard deviations). Overall, 7/10 SS patients showed significant loss of Fas cell surface expression on the memory T-cell population.

To determine whether loss of Fas expression could be used to identify the tumor cells, we isolated the CD3+CD4+/CD45RO+/Fas- and CD3+CD4+/CD45RO+/Fas+ subsets from four patient samples. RNA was extracted and qPCR

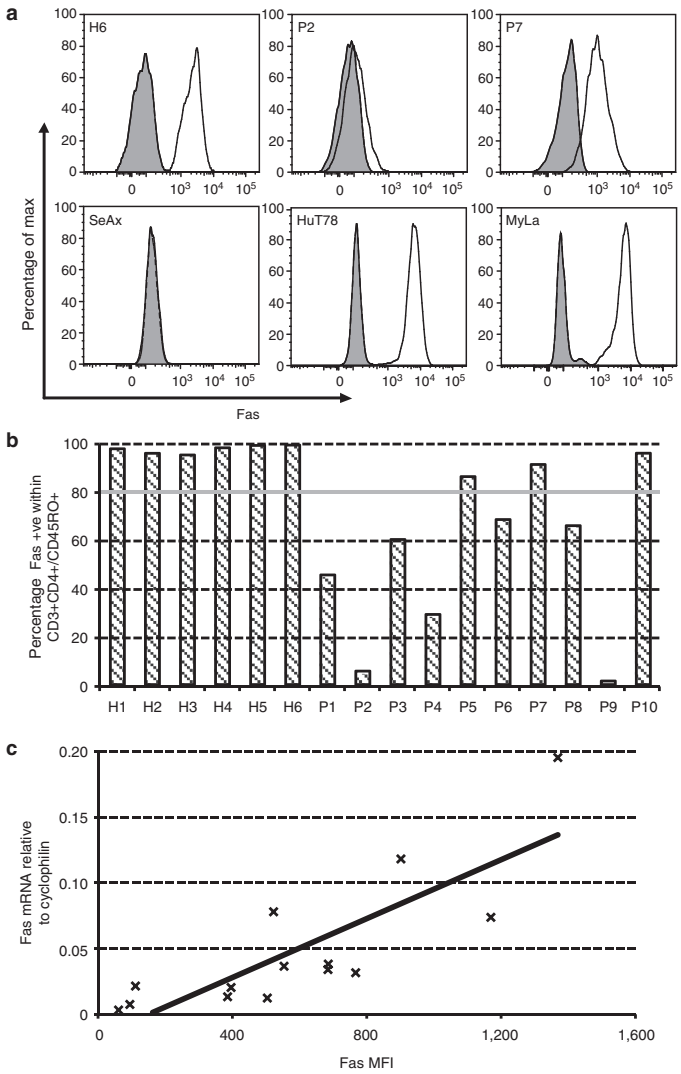

Figure 3. Flow cytometry analysis of Fas on Sézary patient cells and cell lines. (**a**) Histogram plots showing the expression of Fas by one healthy control (H6), two patients (P2 and P7), and the SeAx, HuT78, and MyLa cell lines. The isotype control is shown with the curve filled in grey. (**b**) PBLs from six healthy controls (H1–H6) and 10 patients (P1–P10) were gated on CD3+, CD4+, and CD45RO+ and the proportion of Fas-positive cells measured within this population. The gray line represents the average healthy proportion−10 standard deviations. (**c**) Scatter plot to show the relationship between Fas mean fluorescent intensity (MFI) and Fas mRNA expression level relative to cyclophilin, the line of best fit is also shown.

used to detect the expression of T-plastin in each subset. Both subsets had detectable T-plastin expression and there was no significant difference between the two subsets (data not shown). We also used RNA from the sorted cell populations in Figure 1 to determine Fas mRNA expression by qPCR. This was used to demonstrate the correlation between Fas mRNA expression and cell surface protein ($r=0.816$ and $P=0.00019$), which is shown in Figure 3c.

Absence of functional mutations within the *FAS* coding region in SS

To establish whether the observed decrease in Fas expression was due to a genomic mutation, we performed single-strand conformational polymorphism (SSCP) spanning nine exons and the 3′ end of the promoter of the *FAS* gene. Abnormal banding patterns with SSCP as seen in Figure 4a were identified in 4/20 SS samples. Sequencing of these bands revealed that one corresponded to a previously reported silent polymorphism of exon 3 (250A→G), while the other three anomalies were found to be single-base substitutions within the promoter region (one −274C→A and two −34A→G).

Single-strand conformational polymorphism analysis of the promoter and exon 3 was then performed on DNA extracted from the PBLs of 20 healthy controls to investigate if the observed substitutions were unique to SS patients. This revealed a similar rate of detection of the exon 3 polymorphism (1/20) and of promoter region band shifts (2/20). Sequencing established that the healthy promoter region band shifts also represented single-base substitutions consisting of one −373C→T and one −295G→A.

Single-strand conformational polymorphism was also performed on DNA from the SeAx cell line since this had demonstrated a lack of Fas protein (Figure 3a). Failure to amplify any of the exons using PCR revealed that the *FAS* gene has been deleted in this cell line and further investigation revealed a complete absence of Fas mRNA (data not shown). In the two patients who showed minimal cell surface Fas expression, SSCP analysis revealed loss of some bands using primer pairs 1.1 (P2a, P2b, and P9), 2 (P2a, P2b and P9), and 3 (P9). This suggests that allelic loss of some exons may have occurred in the malignant cells of these patients (Figure 4b).

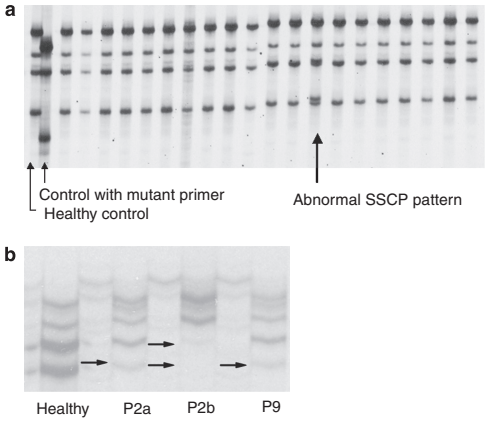

Figure 4. SSCP analysis of the *FAS* gene in SS patients. (**a**) Patient samples analyzed using primer pair 1.1 for the promoter region demonstrating an abnormal band shift in one SS patient sample. (**b**) Sequential samples from Patient 2 and one sample from Patient 9 who showed minimal cell surface protein expression of Fas by fluorescence-activated cell sorting; arrows indicate the decreased intensity of bands in exon two consistent with allelic loss.

Downregulation of Fas mRNA expression in Sézary patients is associated with promoter hypermethylation

The *FAS* gene contains a 1,072 bp CpG island, which spans the transcriptional start site and first exon of the gene. Pyrosequencing of bisulfite-converted DNA was used to assess the methylation status of each of the 74 CpG dinucleotides in the *FAS* CpG island. Pyrosequencing is a quantitative sequencing by synthesis technique (Tost *et al.*, 2003) and facilitates the analysis of mixed cell populations, circumventing the need for a specific tumor-cell marker.

We first demonstrated the highly quantitative nature of the pyrosequencing assays using artificially methylated DNA mixed in varying proportions with unmethylated DNA. Average methylation across the CpG island was plotted for each of these mixtures (Figure 5a); this shows a linear relationship across the entire range of measurements ($r^2 = 0.99$). However, the graph achieved a maximum methylation measurement of only 80%. We believe this is due to the CpG methyltransferase reaction not proceeding to completion rather than any deficiency in the actual measurement. This data suggested that a minimum of 5% tumor cells displaying methylation could be detected within the reactive T-cell background.

Methylation of each CpG dinucleotide was then measured in DNA from 10 healthy control samples and 35 patient samples comprising 16 who showed downregulation of Fas mRNA expression, nine who showed normal Fas mRNA expression, and 10 who showed upregulation of Fas mRNA expression. Wilcoxon unpaired *U*-test was used to compare the methylation in each group of patients with that in healthy controls at each CpG dinucleotide. In the 16 patients showing downregulation of Fas mRNA expression, five CpG dinucleotides (1, 2, 3, 31, and 51 numbered from the start of the CpG island) were found to have significantly greater methylation than in healthy controls (Figure 5b). No significant differences were seen between patients with normal Fas mRNA expression and healthy controls, or between patients with upregulation of Fas mRNA expression and healthy controls in these CpG dinucleotides (data not shown).

The CpG dinucleotides which showed hypermethylation in patients with downregulated Fas mRNA expression have been highlighted on the schematic diagram of the *FAS* CpG island shown in Figure 5c. Also highlighted are the NF-κB- and p53 transcription factor binding sites, which have been experimentally validated, and the transcriptional start site and first exon of the gene.

DISCUSSION

This study of a large cohort of SS patients demonstrates that downregulation of Fas gene expression, associated with positional methylation of the *FAS* CpG island, is a common feature of Sézary cells.

Our results show a distinct heterogeneity in Fas mRNA levels with significant underexpression in 21/47 (∼45%) and overexpression in 13/47 (∼28%) of patient-derived CD4+ T cells as compared with healthy controls. These data are similar to those of a recently published study that reported

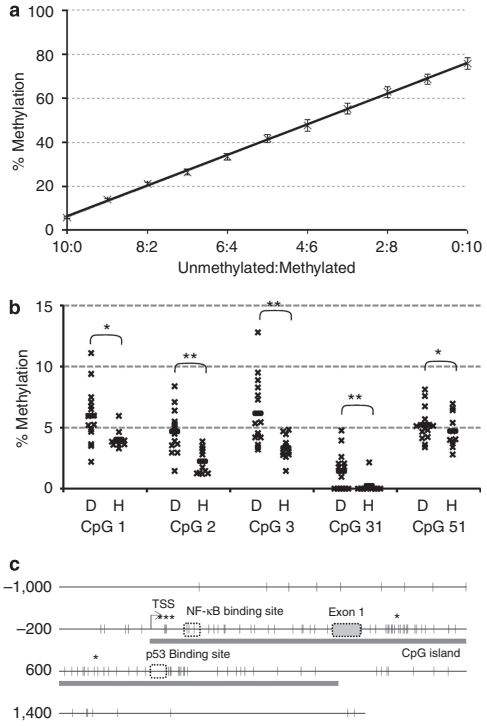

Figure 5. Quantification of methylation in the *FAS* CpG island. (**a**) Mixtures of artificially methylated and unmethylated DNA were quantified at each CpG dinucleotide. Data represent the mean methylation across all CpG dinucleotides ± SEM. (**b**) Methylation in each sample at five CpG dinucleotides showing significantly increased methylation in the patients with downregulation of Fas mRNA (D) when compared to the healthy samples (H). The mean value for each group is shown as a horizontal bar; $*P<0.05$ and $**P<0.01$. (**c**) Diagram of the region around the *FAS* promoter numbered relative to the transcriptional start site (TSS). CpG dinucleotides are marked by a vertical dash, the five hypermethylated CpG dinucleotides are highlighted by *, and important gene regulatory elements within the CpG island are marked.

disparity in the levels of Fas expression in a cohort of 16 SS patients (Contassot *et al.*, 2008). The study by Contassot *et al.* focused on the group of patients in whom overexpression of Fas was demonstrated and showed that resistance to apoptosis in this group was due to overexpression of c-FLIP. In addition, those patients with downregulation of Fas expression also showed resistance to apoptosis, but the mechanism was not addressed. We sought to investigate the patient group exhibiting downregulation of Fas as this was the dominant mode of Fas dysregulation in our patient cohort.

Follow-up analysis of samples taken at least six months apart demonstrated a trend for decreased Fas mRNA expression over time, with the most significant reduction observed in patients showing increase in disease severity over time. These findings are consistent with a study demonstrating an association between loss of Fas protein expression and aggressive types of CTCL (Zoi-Toli *et al.*, 2000).

Examining cell surface expression of Fas validated the observed downregulation of Fas mRNA expression in Sézary cells. Sézary cells are generally derived from CD3 + CD4 + /CD45RO + memory T cells and show variable loss of expression of CD7 and CD26 (Steinhoff *et al.*, 2008). At present there are no tumor-specific cell surface biomarkers available. We found that loss of CD26 does not clearly distinguish between Sézary and reactive cell populations since both CD26− and CD26 + populations contain detectable T-plastin, a Sézary-cell-specific mRNA. In healthy individuals, a large proportion of the CD4 + /CD45RO + T-cell population show cell surface Fas expression (Miyawaki *et al.*, 1992; Muench *et al.*, 2003), which is consistent with the findings reported here demonstrating Fas expression in at least 95% of the CD3 + CD4 + /CD45RO + T cells. In contrast, loss of Fas expression in 7/10 SS patients affected between 32 and 94% of CD3 + CD4 + /CD45RO + cells (shown in Figure 3b) and was associated with downregulation at the mRNA level. The detection of tumor cells within both the Fas− and Fas + subsets (data not shown) and the CD26− and CD26 + subsets (Figure 1) highlights the marked heterogeneity present within the tumor cell population, which we have previously observed in relation to CD25 expression (Tiemessen *et al.*, 2006). Fas expression was also examined in three CTCL cell lines HuT78, MyLa, and SeAx. Whereas HuT78 and MyLa cells displayed cell surface Fas expression, SeAx cells were found to have loss of expression, which is consistent with the absence of Fas mRNA expression in this cell line. Loss of cell surface Fas expression has been reported in several previous studies of SS, although the underlying mechanism has not established (Dereure *et al.*, 2000; Osella-Abate *et al.*, 2001; Wu *et al.*, 2009).

To address putative molecular mechanisms that may mediate the observed downregulation of Fas in Sézary cells, we performed comprehensive mutational scan of the *FAS* gene and analyzed the CpG island around the *FAS* promoter region for methylation events. Promoter polymorphisms were identified in 3/20 SS patients and also in some healthy controls, suggesting that, while the functional relevance of these polymorphisms are unknown, they are unlikely to contribute to the downregulation of Fas in SS. The Sézary cell line SeAx was found to have a deletion of all exons of the *FAS* gene, resulting in complete absence of Fas protein and mRNA. Loss of multiple exons was also observed in two SS patients, in whom we found less than 10% of CD4 + /CD45RO + T cells displaying surface Fas expression. However, the commonest finding was the demonstration of hypermethylation of five specific CpG dinucleotide repeats in the *FAS* promoter, which was associated with downregulation of Fas expression.

As a mediator of apoptosis, Fas plays a critical role in regulating T-cell homeostasis. Heterozygous germ-line mutations of the *FAS* gene are implicated in the etiology of

Canale–Smith Syndrome (Drappa *et al.*, 1996), which is characterized by marked lymphoproliferation and autoimmunity. *FAS* is located on chromosome 10q23.31 and 10q is a frequent region of genomic loss in many malignancies (Cappellen *et al.*, 1997; Komiya *et al.*, 1996) including CTCL (Wain *et al.*, 2005; Vermeer *et al.*, 2008). Somatic loss of function *FAS* mutations have been described in both lymphoid (Takakuwa *et al.*, 2002) and non-lymphoid (Takayama *et al.*, 2002) malignancies, and in some cases have been found to inhibit Fas ligand induced apoptosis in a dominant-negative mode (Wohlfart *et al.*, 2004). Two mutational studies have been performed in mycosis fungoides, reporting mutations in 14 and 18% of cases respectively (Dereure *et al.*, 2002; Nagasawa *et al.*, 2004). Our study suggests that specific *FAS* mutations are uncommon in SS, but given that loss of heterozygosity in the region of 10q23.31 spanning the *FAS* gene has been detected in 50% of SS patients (Wain *et al.*, 2005; Vermeer *et al.*, 2008), it is likely that chromosomal deletion/loss may also contribute to loss of Fas protein expression in SS.

Epigenetic events are known to be a critical mechanism of gene dysregulation in malignancy, and aberrant *FAS* promoter methylation with associated loss of Fas expression has previously been described in colon, prostatic, and small-cell lung carcinoma (Santourlidis *et al.*, 2001; Hopkins-Donaldson *et al.*, 2003; Petak *et al.*, 2003). Recent studies of disease-specific methylation events have demonstrated that complex methylation patterns exist within CpG islands (Brakensiek *et al.*, 2007). Pyrosequencing of bisulfite-converted DNA facilitates examination of individual CpG dinucleotides within a CpG island to allow thorough evaluation of the methylation status across the whole island (Tost *et al.*, 2003; Brakensiek *et al.*, 2007; Oprea *et al.*, 2008). In addition, this technique allows quantitative detection of changes in methylation in a mixed cell population, and, therefore, is ideally applicable to the study of SS cells, overcoming the problems of analysis of a heterogeneous population of tumor cells admixed with non-malignant cells. Five hypermethylated CpG dinucleotides within the *FAS* CpG island were significantly associated with reduced Fas expression in SS patients. It is well recognized that the methylation status of even a single CpG within a CpG island can be responsible for the control of tissue-specific gene expression (Aranyi *et al.*, 2005; Kitazawa and Kitazawa, 2007) and for aberrant gene silencing in cancer (Zou *et al.*, 2006). Three of the hypermethylated CpG dinucleotides in the *FAS* promoter are clustered around the transcriptional start site and, therefore, could be directly responsible for preventing the binding of the transcriptional machinery. Furthermore, other studies of the *FAS* CpG island have identified hypermethylation of CpG dinucleotides located at or near transcription factor binding sites, namely the p53-binding site in colon carcinoma (Petak *et al.*, 2003) and the NF-κB-binding site in prostatic carcinoma (Santourlidis *et al.*, 2001). Other mechanisms by which DNA methylation affects gene expression include recruitment of methylation binding domain proteins, which impairs binding of transcriptional machinery, and recruitment of histone-modifying factors inducing condensation of the local chromatin structure (Newell-Price *et al.*, 2000).

At present there is no direct functional evidence to provide a link between hypermethylation, Fas expression, and resistance to apoptosis in SS. Such studies require the availability of suitable cell lines since the demethylating effect of 5′-azacytidine requires cellular proliferation in order to become incorporated into DNA and prevent maintenance of methylation. Primary cultures of Sézary cells do not proliferate to any significant degree (Berger *et al.*, 2002; Tiemessen *et al.*, 2006) and, therefore, cannot be used for such studies. We show that the commonest SS cell lines SeAx and Hut78, respectively, exhibit homozygous deletion of the *FAS* gene and absence of methylation of the FAS CpG island. However, studies of human colon carcinoma cell lines in which hypermethylation of Fas and reduced expression has been found, demonstrate that Fas expression and Fas-mediated apoptosis can be restored by treatment with demethylating agents (Petak *et al.*, 2003).

It is now apparent that in addition to loss of heterozygosity in the FAS gene locus, multiple molecular mechanisms can mediate Fas dysregulation and resistance to apoptosis in SS. A recent study (Wu *et al.*, 2009) reported some findings similar to those reported here, identifying reduced Fas expression in SS and in CTCL cells from lesional skin of mycosis fungoides patients. Reduced Fas expression was shown to correlate with loss of sensitivity to Fas-mediated apoptosis. Contassot *et al.* have demonstrated that in SS patients with overexpression of Fas, resistance to Fas-mediated apoptosis is still observed and can be attributed to a concomitant increase in expression of the apoptosis inhibitory protein c-FLIP. Another study (Klemke *et al.*, 2009) suggests that attenuated T-cell receptor signaling leading to loss of FasL upregulation also contributes to apoptosis resistance in patients with normal expression of Fas. Fas-mediated apoptosis represents a key mechanism underlying activation induced T-cell death. Therefore, these findings suggest that dysregulation of T-cell homeostasis may play a pivotal role in the pathogenesis of SS.

In summary, we have identified that loss of Fas receptor on the surface of malignant T cells is a common feature of SS. Our data suggest that mutational events are uncommon and are not linked to the observed loss of Fas expression in the majority of patients. Significantly, aberrant promoter hypermethylation appears to be the most frequent mechanism that is associated with loss of Fas expression in SS.

MATERIALS AND METHODS

Patient material and cell lines

DNA and cDNA samples derived from Sézary Syndrome patients were obtained from a nationally approved research tissue bank (07/H10712/106), while flow cytometry studies were performed on freshly isolated PBLs with the approval of the Guy's and St. Thomas' Hospital Research Ethics Committee (EC01/301). SS patient blood samples were obtained during the course of standard clinical procedures, whereas those from 20 healthy volunteers were obtained by venepuncture. For all samples, informed consent was obtained in accordance with the Declaration of Helsinki Principles,

1975, as revised in 2005. Lymphoprep (Axis-Shield, Kimbolton, UK) gradient centrifugation was used either directly to isolate PBLs or following incubation with RosetteSep CD4+ T-cell enrichment cocktail (Stem Cell Technologies, London, UK) to isolate CD4+ T cells. We chose to use negative selection in order to avoid activating the cells and causing any changes in gene expression due to processing.

All patients had a T-cell clone detected in the peripheral blood as demonstrated by T-cell receptor V beta and gamma gene rearrangement studies using BIOMED-2 primer sets and fulfilled the WHO–EORTC diagnostic criteria for SS (Willemze *et al.*, 2005). Sézary cell counts were determined at the time of diagnosis and all patients included in the study had a Sézary count of greater than 1000 cells/mm^3. However, we did not routinely determine Sézary counts at the time of patient sampling for our research study, but relied on measuring total lymphocyte and lymphocyte subset counts, and using total CD4+ T-cell count and CD4:CD8 ratio as an indicator of tumor burden.

The cell lines HuT78 and HEK293 were kind gifts from Dr S. John (King's College London); SeAx was a kind gift from Dr M. Vermeer (Leiden University Medical Centre); and MyLa was obtained from the ECACC (Salisbury, UK). All cultures were maintained in Roswell's Park Memorial Institute medium containing 10% fetal calf serum and 1% penicillin/streptomycin (Invitrogen, Paisley, UK); SeAx cells were supplemented with 25 U ml^{-1} interleukin-2.

Quantitative RT-PCR

Total RNA was extracted from CD4+ T cells (RNeasy minikit; Qiagen Ltd, Crawley, UK) and the high-capacity cDNA archive kit (Applied Biosystems, Warrington, UK) was used to generate randomly primed cDNA. Quantitative RT-PCR was performed on the ABI Prism 7000 sequence detection system (Applied Biosystems) with the following optimized TaqMan probe/primer sets: Hs00236330 m1–Fas and Hs99999904 m1–cyclophilin A. Each sample was analyzed in triplicate for both the target gene (Fas) and an endogenous control (cyclophilin A). The $\Delta\Delta C_t$ method was used to compare the C_t of each patient sample to the mean C_t of 16 healthy control samples after ascertaining that the PCR reactions for Fas and cyclophilin A proceeded with equal amplification efficiency.

Flow cytometry

Peripheral blood lymphocytes were incubated with monoclonal antibodies APC-αCD3 (eBioscience, San Diego, CA), PerCp-αCD4 (BD Biosciences, Erembodegem, Belgium), FITC-αCD45RO (DAKO, Ely, UK), and PE-αFas (BD Biosciences) or the appropriate isotype controls (BD Biosciences). Flow cytometry analysis was performed on a FACSAria II (BD Biosciences) and data were analyzed using FlowJo software (Tree Star Inc., Ashland, OR). Fluorescence-activated cell sorting was performed on a FACSAria II (BD Biosciences) and used the additional antibodies APC-αCD26 (Miltenyi Biotech, Bisley, UK) and PE-Cy7-αCD3 (eBioscience).

SSCP

DNA was isolated from PBLs using standard procedures. PCR was performed with primer pairs (as described by Beltinger *et al.* (1998)) designed to amplify all nine exons and the 3′ end of the promoter. PCR products were labeled using α-^{33}PdCTP as previously described (Scarisbrick *et al.*, 2000). Denatured PCR products were separated by electrophoresis through polyacrylamide gels containing both 5% glycerol and no glycerol. A negative control (deionized water) was performed for each primer pair. DNA from healthy individuals was used as a positive control.

Sequencing

Abnormal bands were excised from the SSCP polyacrylamide gels. DNA was eluted, re-amplified, and sequenced using the *fmol* DNA Cycle Sequencing System (Promega, Southampton, UK). DNA from a healthy control was subjected to the same technique and run simultaneously to ensure reproduction of the published sequence.

Preparation of methylated and unmethylated DNA standards

DNA from the HEK293 cell line was used as completely unmethylated DNA. An aliquot was subjected to *in vitro* methylation using the M. SssI CpG methyltransferase enzyme (NEB, Hitchin, UK) followed by purification using the MinElute reaction cleanup kit (Qiagen) to generate completely methylated DNA. Mixtures of methylated and unmethylated DNA were then prepared prior to bisulfite treatment.

Bisulfite conversion of DNA

Methylated and unmethylated DNA standards and PBL-derived genomic DNA from SS patients and healthy controls were bisulfite treated in 20 µl aliquots containing 1 µg DNA using the EZ DNA methylation kit (Zymo Research, Orange, CA) according to the manufacturer's instructions.

Pyrosequencing

A set of PCR primers specific to bisulfite-treated DNA were designed to cover the *FAS* CpG island (available on request). After PCR with one biotinylated primer, 20 µl of PCR product were immobilized onto 4 µl of streptavidin Sepharose HP beads (GE Healthcare, Chalfont St Giles, UK) and a vacuum prep workstation (Biotage AB, Uppsala, Sweden) was used to isolate and wash the beads with bound single-stranded PCR product. These were deposited into a pyrosequencing plate (Biotage) and the sequencing primer annealed. The pyrosequencing reaction was carried out using a PSQ HS 96 machine (Biotage) following the manufacturer's instructions for methylation analysis. The PSQ HS 96 software was used to analyze the success of each reaction and to calculate the corresponding percentage methylation. Data were exported into an Excel spreadsheet and summarized using a pivot table. For each of the standards with known methylation, an average was taken across all the positions measured.

Statistics

All statistical tests were performed using the R statistical software package (http://www.r-project.org/).

CONFLICT OF INTEREST

The authors state no conflict of interest.

ACKNOWLEDGMENTS

We are grateful to Dr Rebecca Oakey for thoughtful discussion and helpful comments on the manuscript. This work was supported by grants from the Guy's and St. Thomas' Charitable Foundation and includes support from the ''Skin Matters'' fund (E.M.W., C.L.J.). Support from Guy's & St Thomas' NHS Foundation Trust (T.J.M.) is gratefully acknowledged. We acknowledge

financial support from the Department of Health via the National Institute for Health Research (NIHR) comprehensive Biomedical Research Centre award to Guy's & St Thomas' NHS Foundation Trust in partnership with King's College London and King's College Hospital NHS Foundation Trust.

REFERENCES

Aranyi T, Faucheux BA, Khalfallah O, Vodjdani G, Biguet NF, Mallet J *et al.* (2005) The tissue-specific methylation of the human tyrosine hydroxylase gene reveals new regulatory elements in the first exon. *J Neurochem* 94:129–39

Beltinger C, Kurz E, Bohler T, Schrappe M, Ludwig WD, Debatin KM (1998) CD95 (APO-1/Fas) mutations in childhood T-lineage acute lymphoblastic leukemia. *Blood* 91:3943–51

Berger CL, Hanlon D, Kanada D, Dhodapkar M, Lombillo V, Wang N *et al.* (2002) The growth of cutaneous T-cell lymphoma is stimulated by immature dendritic cells. *Blood* 99:2929–39

Brakensiek K, Wingen LU, Langer F, Kreipe H, Lehmann U (2007) Quantitative high-resolution CpG island mapping with pyrosequencing reveals disease-specific methylation patterns of the CDKN2B gene in myelodysplastic syndrome and myeloid leukemia. *Clin Chem* 53:17–23

Burg G, Kempf W, Cozzio A, Feit J, Willemze R, Jaffe E *et al.* (2005) WHO/EORTC classification of cutaneous lymphomas 2005: histological and molecular aspects. *J Cutan Pathol* 32:647–74

Cappellen D, Gil Diez de Medina S, Chopin D, Thiery JP, Radvanyi F (1997) Frequent loss of heterozygosity on chromosome 10q in muscle-invasive transitional cell carcinomas of the bladder. *Oncogene* 14:3059–66

Contassot E, Kerl K, Roques S, Shane R, Gaide O, Dupuis M *et al.* (2008) Resistance to FasL and tumor necrosis factor-related apoptosis-inducing ligand-mediated apoptosis in Sezary Syndrome T-cells associated with impaired death receptor and FLICE-inhibitory protein expression. *Blood* 111:4780–7

Dereure O, Levi E, Vonderheid E, Kadin M (2002) Infrequent Fas mutations but no Bax or p53 mutations in early mycosis fungoides: a possible mechanism for the accumulation of malignant T lymphocytes in the skin. *J Invest Dermatol* 118:949–56

Dhein J, Walczak H, Baumler C, Debatin KM, Krammer PH (1995) Autocrine T-cell suicide mediated by APO-1/(Fas/CD95). *Nature* 373:438–41

Drappa J, Vaishnaw AK, Sullivan KE, Chu JL, Elkon KB (1996) Fas gene mutations in the Canale-Smith syndrome, an inherited lymphoproliferative disorder associated with autoimmunity. *N Engl J Med* 335:1643–9

Hopkins-Donaldson S, Ziegler A, Kurtz S, Bigosch C, Kandioler D, Ludwig C *et al.* (2003) Silencing of death receptor and caspase-8 expression in small cell lung carcinoma cell lines and tumors by DNA methylation. *Cell Death Differ* 10:356–64

Jones D, Dang NH, Duvic M, Washington LT, Huh YO (2001) Absence of CD26 expression is a useful marker for diagnosis of T-cell lymphoma in peripheral blood. *Am J Clin Pathol* 115:885–92

Jones PA, Baylin SB (2002) The fundamental role of epigenetic events in cancer. *Nat Rev Genet* 3:415–28

Ju ST, Panka DJ, Cui H, Ettinger R, el-Khatib M, Sherr DH *et al.* (1995) Fas(CD95)/FasL interactions required for programmed cell death after T-cell activation. *Nature* 373:444–8

Kirchhoff S, Muller WW, Krueger A, Schmitz I, Krammer PH (2000) TCR-mediated up-regulation of c-FLIPshort correlates with resistance toward CD95-mediated apoptosis by blocking death-inducing signaling complex activity. *J Immunol* 165:6293–300

Kitazawa R, Kitazawa S (2007) Methylation status of a single CpG locus 3 bases upstream of TATA-box of receptor activator of nuclear factor-kappaB ligand (RANKL) gene promoter modulates cell- and tissue-specific RANKL expression and osteoclastogenesis. *Mol Endocrinol* 21:148–58

Klas C, Debatin KM, Jonker RR, Krammer PH (1993) Activation interferes with the APO-1 pathway in mature human T cells. *Int Immunol* 5: 625–30

Klemke CD, Brenner D, Weiss EM, Schmidt M, Leverkus M, Gulow K *et al.* (2009) Lack of T-cell receptor-induced signaling is crucial for CD95 ligand upregulation and protects cutaneous T-cell lymphoma cells from activation-induced cell death. *Cancer Res* 69:4175–83

Komiya A, Suzuki H, Ueda T, Yatani R, Emi M, Ito H *et al.* (1996) Allelic losses at loci on chromosome 10 are associated with metastasis and progression of human prostate cancer. *Genes Chromosomes Cancer* 17:245–53

Krammer PH, Arnold R, Lavrik IN (2007) Life and death in peripheral T cells. *Nat Rev Immunol* 7:532–42

Lee SH, Shin MS, Park WS, Kim SY, Dong SM, Pi JH *et al.* (1999) Alterations of Fas (APO-1/CD95) gene in transitional cell carcinomas of urinary bladder. *Cancer Res* 59:3068–72

Miyawaki T, Uehara T, Nibu R, Tsuji T, Yachie A, Yonehara S *et al.* (1992) Differential expression of apoptosis-related Fas antigen on lymphocyte subpopulations in human peripheral blood. *J Immunol* 149:3753–8

Muench MO, Pott Bartsch EM, Chen JC, Lopoo JB, Barcena A (2003) Ontogenic changes in CD95 expression on human leukocytes: prevalence of T-cells expressing activation markers and identification of CD95−CD45RO+ T-cells in the fetus. *Dev Comp Immunol* 27:899–914

Nagasawa T, Takakuwa T, Takayama H, Dong Z, Miyagawa S, Itami S *et al.* (2004) Fas gene mutations in mycosis fungoides: analysis of laser capture-microdissected specimens from cutaneous lesions. *Oncology* 67:130–4

Newell-Price J, Clark AJ, King P (2000) DNA methylation and silencing of gene expression. *Trends Endocrinol Metab* 11:142–8

Oprea GE, Krober S, McWhorter ML, Rossoll W, Muller S, Krawczak M *et al.* (2008) Plastin 3 is a protective modifier of autosomal recessive spinal muscular atrophy. *Science* 320:524–7

Osella-Abate S, Zaccagna A, Savoia P, Quaglino P, Salomone B, Bernengo MG (2001) Expression of apoptosis markers on peripheral blood lymphocytes from patients with cutaneous T-cell lymphoma during extracorporeal photochemotherapy. *J Am Acad Dermatol* 44:40–7

Park WS, Oh RR, Kim YS, Park JY, Lee SH, Shin MS *et al.* (2001) Somatic mutations in the death domain of the Fas (Apo-1/CD95) gene in gastric cancer. *J Pathol* 193:162–8

Petak I, Danam RP, Tillman DM, Vernes R, Howell SR, Berczi L *et al.* (2003) Hypermethylation of the gene promoter and enhancer region can regulate Fas expression and sensitivity in colon carcinoma. *Cell Death Differ* 10:211–7

Santourlidis S, Warskulat U, Florl AR, Maas S, Pulte T, Fischer J *et al.* (2001) Hypermethylation of the tumor necrosis factor receptor superfamily 6 (APT1, Fas, CD95/Apo-1) gene promoter at rel/nuclear factor kappaB sites in prostatic carcinoma. *Mol Carcinog* 32:36–43

Scarisbrick JJ, Woolford AJ, Russell-Jones R, Whittaker SJ (2000) Loss of heterozygosity on 10q and microsatellite instability in advanced stages of primary cutaneous T-cell lymphoma and possible association with homozygous deletion of PTEN. *Blood* 95:2937–42

Schaefer CB, Ooi SK, Bestor TH, Bourc'his D (2007) Epigenetic decisions in mammalian germ cells. *Science* 316:398–9

Schmitz I, Weyd H, Krueger A, Baumann S, Fas SC, Krammer PH *et al.* (2004) Resistance of short term activated T cells to CD95-mediated apoptosis correlates with de novo protein synthesis of c-FLIPshort. *J Immunol* 172:2194–200.

Steinhoff M, Schopp S, Assaf C, Muche M, Beyer M, Sterry W *et al.* (2008) Prevalence of genetically defined tumor cells in CD7 as well as CD26 positive and negative circulating T-cell subsets in Sezary Syndrome. *Leuk Res* 33:88–99

Su MW, Dorocicz I, Dragowska WH, Ho V, Li G, Voss N *et al.* (2003) Aberrant expression of T-plastin in Sezary cells. *Cancer Res* 63:7122–7

Takakuwa T, Dong Z, Nakatsuka S, Kojya S, Harabuchi Y, Yang WI *et al.* (2002) Frequent mutations of Fas gene in nasal NK/T cell lymphoma. *Oncogene* 21:4702–5

Takayama H, Takakuwa T, Tsujimoto Y, Tani Y, Nonomura N, Okuyama A *et al.* (2002) Frequent Fas gene mutations in testicular germ cell tumors. *Am J Pathol* 161:635–41

Tiemessen M, Mitchell T, Hendry L, Whittaker S, Taams L, John S (2006) Lack of suppressive CD4+CD25+FOXP3+ T cells in advanced stages of primary cutaneous T-cell lymphoma. *J Invest Dermatol* 126:2217–23

Tost J, Dunker J, Gut IG (2003) Analysis and quantification of multiple methylation variable positions in CpG islands by pyrosequencing. *BioTechniques* 35:152–6

Vermeer MH, van Doorn R, Dijkman R, Mao X, Whittaker S, van Voorst Vader PC *et al.* (2008) Novel and highly recurrent chromosomal alterations in Sezary Syndrome. *Cancer Res* 68:2689–98

Wain E, Mitchell T, Russell-Jones R, Whittaker S (2005) Fine mapping of chromosome 10q deletions in mycosis fungoides and Sezary Syndrome: identification of two discrete regions of deletion at 10q23.33–24.1 and 10q24.33–25.1. *Genes Chromosomes Cancer* 42:184–92

Willemze R, Jaffe ES, Burg G, Cerroni L, Berti E, Swerdlow SH *et al.* (2005) WHO–EORTC classification for cutaneous lymphomas. *Blood* 105:3768–85

Wohlfart S, Sebinger D, Gruber P, Buch J, Polgar D, Krupitza G *et al.* (2004) FAS (CD95) mutations are rare in gastric MALT lymphoma but occur more frequently in primary gastric diffuse large B-cell lymphoma. *Am J Pathol* 164:1081–9

Wu J, Nihal M, Siddiqui J, Vonderheid EC, Wood GS (2009) Low FAS/CD95 expression by CTCL correlates with reduced sensitivity to apoptosis that can be restored by FAS upregulation. *J Invest Dermatol* 129: 1165–1173

Zoi-Toli O, Vermeer M, de Vries E, van Beek P, Meijer C, Willemze R (2000) Expression of Fas and Fas-ligand in primary cutaneous T-cell lymphoma (CTCL): association between lack of Fas expression and aggressive types of CTCL. *Br J Dermatol* 143:313–9

Zou B, Chim CS, Zeng H, Leung SY, Yang Y, Tu SP *et al.* (2006) Correlation between the single-site CpG methylation and expression silencing of the XAF1 gene in human gastric and colon cancers. *Gastroenterology* 131:1835–43

Leukemia (2011), 1–9

www.nature.com/leu

ORIGINAL ARTICLE

Constitutive activation of STAT3 in Sézary syndrome is independent of SHP-1

RCT McKenzie, CL Jones, I Tosi, JA Caesar, SJ Whittaker and TJ Mitchell

Skin Tumour Unit, St John's Institute of Dermatology, Division of Genetics and Molecular Medicine, King's College London, London, UK

Constitutive and persistent activation of STAT3 has been implicated in the pathogenesis of many malignancies. Studies of CTCL cell lines have previously suggested that aberrant activation of STAT3 is mediated via silencing of the negative regulator SHP-1 by promoter methylation. In this study of *ex vivo* tumour cell populations from 18 Sézary syndrome (SS) patients, constitutive phosphorylation of STAT3, JAK1 and JAK2 was present in all patients, but was absent in comparative CD4+ T-cells from healthy controls. Furthermore, no loss or significant difference in SHP-1 expression was observed between patients and healthy control samples. Methylation-specific PCR analysis of the SHP-1 CpG island in 47 SS patients and 11 healthy controls did not detect any evidence of methylation. Moreover, small interfering RNA knockdown of SHP-1 had no effect on phosphorylation of STAT3. In contrast, treatment of SS tumour cells with the pan-JAK inhibitor pyridone 6 led to downregulation of phosphorylated STAT3 (pSTAT3), its target genes and induction of apoptosis. No evidence for common JAK1/JAK2-activating mutations was found. These data demonstrate that constitutive activation of STAT3 in SS is not due to the loss of SHP-1, but is mediated by constitutive aberrant activation of JAK family members.
Leukemia advance online publication, 5 August 2011;
doi:10.1038/leu.2011.198
Keywords: Sézary syndrome; cutaneous T-cell lymphoma; STAT3; SHP-1; JAK

Introduction

Sézary syndrome (SS) is the leukaemic variant of primary cutaneous T-cell lymphoma (CTCL) with an aggressive clinical course, poor prognosis and median survival of 3.13 years.[1] The aetiology of SS is not well understood, but in common with other types of CTCL, it is characterised by a clonal proliferation of malignant mature T-cells (Sézary cells) that display skin-homing properties mediated via expression of the receptors CLA and CCR4. A recent immunophenotypic study suggests that the origin of Sézary cells is the central memory T-cell pool, while skin-restricted mycosis fungoides (MF) is derived from skin-resident effector memory T-cells.[2] Sézary cells can also be further differentiated from MF cells, based on high level co-expression of the lymph node homing markers CCR7 and L-selectin.

Sézary cells have a low proliferative potential and their accumulation appears to be due to defective T-cell homeostatic mechanisms mediated by dysregulation of key signalling pathways controlling apoptosis and survival.[3] The signal transducers and activators of transcription (STATs) are a pleiotropic family of transcription factors that have a pivotal role regulating many gene networks, including those involved in cell survival and proliferation.[4] There are seven STAT family gene members that show a high degree of sequence identity at the amino-acid level. Phosphorylation of STATs is normally a rapid and transient process mediated via protein ligand binding of cell-surface cytokine and growth factor receptors that trigger a cascade of phosphorylation events involving the JAK kinases and culminating in the phosphorylation of STATs on a single tyrosine residue.[5] Phosphorylated STATs (pSTATs) dimerise and are transported to the nucleus where they activate transcription of target genes. Until recently it was thought that only pSTATs could function as transcription factors, but it is now clear that unphosphorylated monomeric STATs have a distinct set of target genes to their phosphorylated counterparts and can shuttle between the cytoplasm and nucleus in the absence of cytokine activation.[6,7]

The most strongly implicated STAT in oncogenesis is STAT3, which is considered an oncogene through its ability to transform cultured cells.[8] Persistent or constitutive JAK–STAT3 activation is common in many solid and haematological malignancies, and is recognised as a significant driver of pathways mediating tumour initiation, development and progression.[9] Constitutive activation of STAT3 has been demonstrated in studies of cell lines derived from MF and SS patients and anaplastic large cell lymphoma.[10–19] In lesional patient-derived material, strong expression of pSTAT3 has been identified by immunohistochemistry in tumour biopsy samples from advanced stage MF patients, but only weak expression was detected in early patch/plaque lesions.[11] In SS patients, the activation status of STAT3 is less clear, with one study demonstrating the strong expression of pSTAT3 in peripheral blood mononuclear cells (PBMCs) from only 2 of 14 patients.[10] Another study of six SS patients suggested that activation of STAT3 is not constitutive, but is cytokine dependent.[17] However, a recent report demonstrated persistent and constitutive activation of STAT3 in PBMCs from 4/4 SS/MF patients.[18]

STAT3 activation may be a key abnormality in CTCL because abrogation of constitutive STAT3 activity by dominant-negative STAT3 mutant proteins or STAT3 knockdown by small interfering RNA (siRNA) induces apoptosis in CTCL cell lines.[11,12] The downstream effects of STAT3 knockdown are downregulation of expression of key pSTAT3 target genes including the prosurvival genes *Bcl-XL*, *Mcl-1* and *Survivin* and the regulators of cell growth *cyclin D1*, *cyclin D2* and *cMyc*.[20]

No activating mutations of *STAT3* have been reported, and persistent or constitutive STAT3 activation has been attributed to a variety of upstream events in different malignancies based on both studies, *in vitro* using cell lines and *ex vivo* using primary cancer cells. In the chronic myeloproliferative disorders, essential thrombocythemia, primary myelofibrosis and

Correspondence: Dr TJ Mitchell, Skin Tumour Unit, St John's Institute of Dermatology, Division of Genetics and Molecular Medicine, Kings College London, 9th Floor, Tower Wing, Guys Hospital, London, SE1 9RT, UK.
E-mail: tracey.mitchell@kcl.ac.uk
Received 14 February 2011; revised 19 April 2011; accepted 24 May 2011

polycythemia vera, the activating *JAK2* mutation, *JAK2* V617F has been detected at a very high frequency.[21] In contrast, activating *JAK* mutations appear to be much less frequent in lymphoid malignancies, and alternative mechanisms of STAT3 activation includes the anaplastic lymphoma kinase (*ALK*) gene fusion with nucleophosmin found in a subset of anaplastic large cell lymphoma patients,[22] and the nuclear pore protein NUP214–ABL1 kinase fusion protein in a small proportion of T-cell acute lymphoblastic leukaemia cases.[23] Gain-of-function mutations in *JAK1* and *JAK3* are notably absent in adult T-cell leukaemia/lymphoma.[24] To date, only *JAK3* mutations have been investigated in CTCL, and a study of 30 patients found the *JAK3* A572V mutation in only one patient with MF and large cell transformation.[25]

In normal cells, the JAK–STAT3 pathway is tightly regulated, primarily by negative feedback mechanisms involving the protein inhibitors of activated STATs, the suppressors of cytokine signalling (SOCS) and the SH2-containing phosphatases (SHPs). Loss of SHP-1 expression has been linked to aberrant JAK–STAT3 activation in several malignancies, including multiple myeloma,[26] adult T-cell leukaemia/lymphoma[27] and in a subset of MF patients with large cell transformation[28,29] or advanced tumour stage disease.[30] The mechanism of SHP-1 inactivation has been attributed to epigenetic silencing by aberrant promoter hypermethylation, demonstrated by methylation-specific PCR (MSP) in CTCL-derived cell lines,[28] and in diagnostic samples from myeloma[26] and adult T-cell leukaemia/lymphoma[27] rather than due to inactivating mutations. To date, the role of SHP-1 in the persistent activation of the JAK–STAT3 pathway in SS patients has not been investigated.

The aim of this study was to examine the frequency of JAK–STAT3 activation in *ex vivo*-enriched primary tumour cell populations derived from the peripheral blood of SS patients and to determine whether this is mediated by inactivation of SHP-1.

Patients and methods

Patients and cell lines

All patients fulfilled the WHO–EORTC diagnostic criteria for SS,[1] and the presence of an identical T-cell clone was demonstrated in peripheral blood and lesional skin biopsy by *TCR* gene rearrangement studies using BIOMED-2 primer sets.[31] Sézary cell counts were determined at the time of diagnosis and all patients included in the study had a Sézary count >1000 cells/μl^3. Total lymphocyte, CD4 counts and CD4/CD8 ratios were noted at sampling as an indicator of tumour burden. All patient samples were obtained from the nationally approved Cutaneous Lymphoma Research Tissue Bank (07/H10712/106). Healthy control samples were obtained with the approval of the Guy's and St Thomas' Hospital Research Ethics Committee (EC01/301).

A total of 59 patients were involved in this study. For experiments involving freshly isolated enriched tumour cell populations, 18 patients were studied. Multiple samples were available from 10 of the 18 patients, and were used for the functional studies. In addition, genomic DNA from enriched tumour samples from 47 SS patients were analysed for the SHP-1 methylation study.

Primary keratinocytes from healthy skin biopsy samples were available in the department. The CTCL cell lines, HuT78 and SeAx, were gifts from Dr S John (King's College London) and Dr M Vermeer (Leiden University Medical Centre), respectively. MyLa and HEK293 cells were obtained from the ECACC (Salisbury, UK). All cultures were maintained in RPMI containing 10% fetal calf serum and 1% penicillin/streptomycin (Invitrogen, Paisley, UK). SeAx cells were supplemented with interleukin (IL)-2 (25 U/ml).

Enrichment of SS tumour cell populations

At present, there are no tumour-specific cell surface biomarkers available to isolate Sézary cells. We have previously shown that because of the marked heterogeneity of tumour cell populations, isolation of CD4+ T-cells is the most appropriate method to enrich for tumour cells without loss of tumour cell sub-populations.[32,33] Lymphoprep (Axis-shield, Kimbolton, UK) gradient centrifugation was used either directly to isolate peripheral blood lymphocytes or following incubation with RosetteSep CD4+ T-cell enrichment cocktail (Stem Cell Technologies, Grenoble, France) to isolate CD4+ T-cells.

Immunoblotting

Cell lysates were prepared and immunoblotting was performed using standard procedures. Each blot was incubated overnight at 4 °C with anti-STAT3, anti-phospho-STAT3, anti-JAK1, anti-phospho-JAK1, anti-JAK2, anti-phospho-JAK2 (New England Biolabs, Hitchin, UK) or polyclonal anti-SHP-1 (Atlas antibodies AB, Stockholm, Sweden) according to the manufacturer's instructions. Immunoreactivity was detected using peroxide-conjugated anti-mouse or anti-rabbit secondary antibody (Abcam, Cambridge, UK), and was visualised using enhanced chemiluminescence (ECL, GE Healthcare, Chalfont St Giles, UK).

Intracellular flow cytometry

All experiments analysed with multiple antibodies were performed sequentially on the same day. A total volume of 1×10^6 cells/ml were fixed in 1% formaldehyde and then permeabilised in 90% methanol. Following permeabilisation, cells were treated for 1 h with the following primary antibodies; anti-STAT3 (1/100), anti-phospho-STAT3 (1/50), anti-JAK-1 (1/100), anti-phospho-JAK1 (1/50), anti-JAK2 (1/100), anti-phospho-JAK2 (1/50) and anti-SHP-1 (1/150). Cells were then incubated with a fluorescent secondary antibody (Alexa Fluro 488 goat anti-rabbit IgG or Alexa Fluro 588 goat anti-mouse IgG, Invitrogen). To detect background fluorescence, samples were incubated with a rabbit or mouse isotype control (Invitrogen). Flow cytometry analysis was performed on a FACSAriaII (BD Biosciences, Oxford, UK); machine settings were standardized and retained throughout the study; 10 000 events were acquired per sample and delta mean fluorescent intensity was calculated by subtracting the mean fluorescent intensity of the isotype control from the mean fluorescent intensity of the specific antibody using Flowjo software (Tree Star Inc., Ashland, OR, USA).

Methylation-specific PCR

DNA was bisulphite converted using the EZ DNA Methylation-Gold Kit (Zymo Research Corporation, Orange, CA, USA), then amplified using the previously published SHP-1 primers.[34] Methylation and unmethylation-specific PCRs were performed concurrently for each set of samples and each PCR included the following samples: DNA from the Jurkat cell line as a positive control for unmethylated DNA; Jurkat DNA, which had been methylated *in vitro* using the *M.Sss*I CpG methyltransferase enzyme (New England Biolabs) to generate completely methylated DNA.

Pyrosequencing
Bisulphite-converted DNA was subjected to PCR using the primers S1F–biotin-TGTTTTATAGGGTTGTGGTGAGA and S1R–CTCCAAACCCAAATAATACTTCA or S2F–TGTTTTATAGG GTTGTGGTGAGA and S1R–biotin-CTCCAAACCCAAATAATA CTTCA. An aliquot was taken to check for amplification of the correct size product then 20 µl of PCR amplicon was immobilised onto 4 µl of streptavidin sepharose HP beads (GE Healthcare) and a vacuum prep workstation (Biotage AB, Uppsala, Sweden) was used to isolate and wash the beads with bound single-stranded PCR product. These were deposited onto a pyrosequencing plate (Biotage) and sequencing primer S1S–CCTCCACCAACTACTTTT or S2S–GGAGGAGGGAGAGATG annealed. The pyrosequencing reaction was carried out using a PSQ HS 96 machine (Biotage) following the manufacturer's instructions for methylation analysis.

siRNA knockdown
MyLa cells were washed and resuspended to a cell density of 1×10^6 cells/ml. Electroporation was performed using the electroporator Bio-Rad, Gene Pulser II and 4 mm electroporation cuvettes (Flowgen, East Yorkshire, UK). The samples were electroporated at 240 V and 975 µF with 100 nM of either SHP-1-specific or scrambled siRNA (Abgene, Surrey, UK) and cultured for up to 48 h. A total volume of 1×10^6 cells were examined by intracellular flow cytometry (as described above), and the remanants were extracted for total RNA using the RNeasy minikit (Qiagen Ltd, Crawley, UK) and converted into cDNA using the high-capacity cDNA archive kit (Applied Biosystems, Warrington, UK). cDNA was analysed by RT-PCR with SHP1-specific primers[35] and cyclophilin-specific primers (forward: 5′-AAAGCATACGGGTCCTGGCATC-′3; reverse 5′-CGAGTTGT CCACAGTCAGCAATG -3′) to confirm SHP-1 knockdown.

Pan-JAK inhibitor treatment
Cell lines and CD4+ tumour cell populations isolated from SS patients were re-suspended at 1×10^6 cells/ml in complete medium and treated with 0.5 µM of the pan-JAK inhibitor, pyridone 6 (P6) (Merck, Laufelfingen, Switzerland) or a vehicle control (dimethyl sulfoxide) for 120 min.

Detection of apoptosis
Commitment to apoptosis was measured using the Annexin V–PE apoptosis detection kit I (BD Biosciences) and intracellular staining with an antibody against caspase-3 (1/100, Santa Cruz Biotechnology, Heidelberg, Germany). Both assays were quantified using flow cytometry with 10 000 events acquired on a FACSAriaII (BD Biosciences).

Real-time quantitative PCR
cDNA was generated from CD4+ tumour cell populations isolated from SS patients as described above. Real-time PCR was performed on the ABI prism 7000 sequence detection system (Applied Biosystems) using the following optimised TaqMan probe/primer sets: Hs00236329_m1–Bcl-XL, Hs00172036_m1–Mcl-1, Hs00153353_m1–Survivin, Hs00355782_m1–p21, Hs01047580_m1–STAT3, Hs00197982_m1–Bim and Hs99999904_m1–cyclophilin A as an endogenous control. Each sample was analysed in triplicate for both target gene and endogenous control. The $\Delta\Delta C_t$ method was used to determine the fold-change by comparison with the relevant untreated sample.

Mutational studies
DNA from 19 SS patients and 8 healthy controls were amplified. For the regions containing V658 (JAK1) or V617 (JAK2), the following JAK1- and JAK2-specific primer pairs were used (JAK1 forward: 5′-CTGGCCTGAGACATTCCTATG-3′; JAK1 reverse: 5′-CCCCTTTGAAAGAGAACACACT-3′) and (JAK2 forward: 5′-CAAGCATTTGGTTTTAAATTATGGAGTATGT-3′; JAK2 reverse: 5′-TAAATTATAGTTTACACTGACACCTAG-3′). PCR products were labelled using α-^{33}PdCTP as previously described.[36] Denatured PCR products were analysed by single-stranded conformational polymorphism analysis using 6% polyacrylamide gels with and without 5% glycerol. A negative control (deionised water) was performed for each primer pair.

Statistics
Analysis of flow cytometry data comparing JAK–STAT3, SHP-1 expression levels between SS patients and healthy control samples and the apoptosis data was performed using two-tailed *t*-test. Paired *t*-tests with $P<0.05$, indicating statistical significance, were used to analyse SHP-1 siRNA-treated cells and the P6-treated cells.

Results

Constitutive activation of the JAK–STAT3 pathway in primary Sézary cells
The activation status of the JAK–STAT3 pathway was assessed by immunoblotting using whole-cell lysates from enriched tumour cell populations from six SS patients, CD4+ T-cells from two healthy controls and the CTCL cell line MyLa (Figure 1a). All samples expressed STAT3, JAK1 and JAK2, but in contrast to healthy control CD4+ T-cells, all six SS patients and the CTCL cell line showed strong expression of phosphorylated (pSTAT3, pJAK1 and pJAK2) components, consistent with constitutive JAK–STAT3 activation. Furthermore, the observed constitutive STAT3 activation was found to be persistent, as pSTAT3 expression was retained in enriched CD4+ tumour cell populations maintained *in vitro* for a 5-day period in the absence of exogenous cytokine stimulation (Supplementary Figure 1).

Previous studies in CTCL cell lines have suggested that loss or reduced expression of the protein tyrosine phosphatase SHP-1 mediates aberrant activation of the JAK–STAT3 pathway.[28,30] This led us to examine the SHP-1 status in Sézary tumour cell populations. No difference in SHP-1 expression between patients and healthy controls relative to the β-actin loading control (Figure 1a) was apparent.

To validate these data, we extended the study to include 18 SS patients and 6 healthy controls, and quantified expression accurately using intracellular immunofluorescent staining and flow cytometry. JAK–STAT3 activation was confirmed in all 18 patients (Figures 1b–d), which was significantly increased (pSTAT3 $P<0.001$, pJAK1 $P<0.001$ and pJAK2 $P<0.0001$) compared with healthy control samples. In contrast, no significant difference in total unphosphorylated STAT3, JAK1 or JAK2 expression between patients and healthy controls was observed (data not shown). Furthermore, consistent with the immunoblotting data, no loss or significant difference in SHP-1 expression was observed in patients compared with healthy controls (Figure 1e).

STAT3 activation is independent of SHP-1 in primary Sézary cells
Methylation of the SHP-1 promoter has previously been reported in CTCL cell lines,[28,30] therefore, we compared the

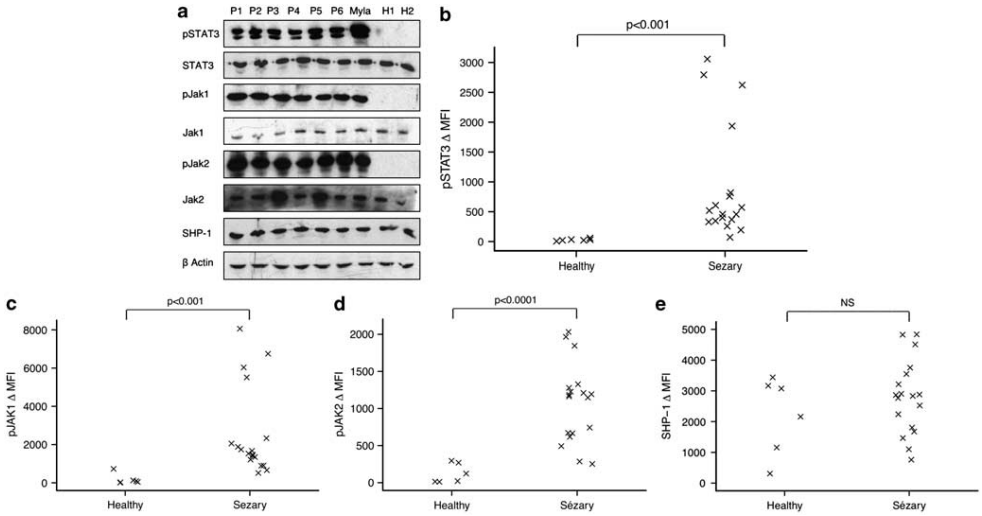

Figure 1 Constitutive activation of the JAK–STAT3 pathway in primary Sézary cells. (**a**) Immunoblot analysis of whole-cell lysates derived from enriched tumour cell populations from six SS patients (P1–P6), CD4+ T-cell from two healthy control samples and the MyLa cell line. Blots are probed with the indicated antibodies against components of the JAK–STAT3 pathway and re-probed with β-actin as loading control. Quantitative flow cytometric analysis of CD4+-enriched tumour samples from 18 SS patients and CD4+ T-cells from 6 healthy control samples of (**b**) pSTAT3 (**c**) pJAK1 (**d**) pJAK2 (**e**) SHP-1. Data are shown as delta mean fluorescent intensity calculated as described in Patients and methods.

methylation status of the SHP-1 promoter in *ex vivo*-enriched Sézary tumour cells, cell lines and CD4+ lymphocytes from 11 healthy donors. Previously published[34] MSP and unmethylation specific (USP) PCR primers were used to amplify bisulphite-converted DNA. Methylation was detected in the CTCL cell lines, Hut78 and SeAx, which correlates with lack of SHP-1 mRNA and protein expression (data not shown) and is consistent with the published findings. In contrast, a weak methylation amplicon was detected in only 1/47 SS patients and 1/11 healthy control samples. Representative MSP/USP data from eight SS patients, eight healthy controls and the CTCL cell lines are shown in Figure 2a.

MSP/USP does not assess the methylation status of all CpG dinucleotides in the CpG island. Therefore, pyrosequencing was used to quantify the methylation status of each CpG dinucleotide in the SHP-1 CpG island in a subset of nine Sézary patient samples, seven healthy control samples and six cell lines. Consistent with SHP-1 expression status (data not shown), MyLa and Jurkat were found to have very low levels of methylation across the SHP-1 CpG island, whereas high levels of methylation were detected in HuT78, SeAx, primary keratinocytes and HEK293 cells. Pyrosequencing analysis also demonstrated very low levels of methylation in both patient tumour cell populations and CD4+ T-cells from healthy controls (Figure 2b), confirming the expression and the MSP data.

These data suggest that activation of JAK–STAT3 pathway in Sézary cells is independent of SHP-1. This was confirmed using siRNA-mediated SHP-1 knockdown in MyLa cells and was validated using SHP-1-specific RT-PCR, intracellular staining and flow cytometry (Figures 2c and d). A significant reduction ($P=0.0001$) in SHP-1 expression was demonstrated in siRNA-transfected cells and importantly no effect on STAT3 phosphorylation was observed (Figure 2e). These data support our *ex vivo* finding that in Sézary cells, activation of STAT3 is not mediated by loss of SHP-1 expression.

JAK inhibition downregulates STAT3 activation and induces apoptosis in primary Sézary cells

Enriched tumour cell populations from 10 of the 18 previously assessed patients were treated with the pan-JAK inhibitor P6 for 120 min. P6 was selected, as previous reports suggest it is a more specific and effective inhibitor of JAK–STAT3 activity compared with AG490 in cell lines.[37,38] Intracellular staining and flow cytometry showed a significant decrease in activation of pJAK1 (Figure 3a, $P=0.005$), pJAK2 (Figure 3b, $P=0.002$) and consequent decrease in activation of pSTAT3 (Figure 3c, $P=0.001$) in all samples treated with the pan-JAK inhibitor. The effect of JAK inhibition on the commitment to apoptosis was assessed in five of these patients and two healthy controls using quantitative flow cytometry to detect cleaved caspase-3 and Annexin V (Figures 4a and b). Apoptosis was strongly induced in tumour cell from all five patients, whereas no induction of apoptosis following P6 treatment was observed in healthy control samples. A concomitant decrease in mRNA expression of the pSTAT3 target and anti-apoptotic genes *Bcl-XL*, *Mcl-1* and *Survivin* was also evident in the tumour cell populations. In contrast, expression of p21 and the proapoptotic gene BIM were both induced in response to P6 treatment as was STAT3 itself (Figure 4c).

JAK1 V658F and JAK2 V617F mutations are not present in primary Sézary cells

To establish whether activating mutations of *JAK1* or *JAK2* are responsible for constitutive activation of the JAK–STAT3

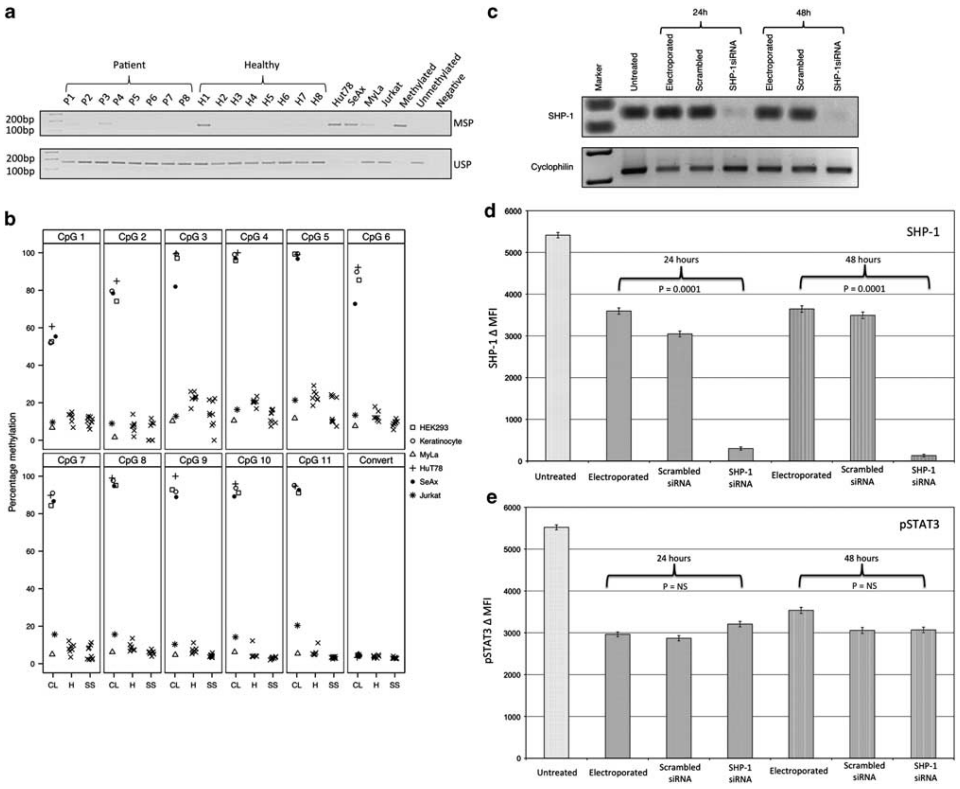

Figure 2 STAT3 activation is independent of SHP-1 in CTCL cells. (**a**) Representative agarose gel of SHP-1 MSP on eight Sézary tumour cell samples, eight healthy controls and four cell lines (**b**) Pyrosequencing across the 11 CpG dinucleotides in the SHP-1 CpG island in nine Sézary samples (SS), seven healthy controls (H) and six cell lines (CL). Convert is the conversion control, which indicates successful bisulphite conversion if <5% (**c**) RT-PCR using specific primer pairs for SHP-1 and cyclophilin using cDNA from MyLa cells, which were untreated, electroporated alone, treated with scrambled or with SHP-1 specific siRNA for 24 or 48 h. (**d, e**) Quantitative flow cytometric analysis of electroporated MyLa cells expressed as delta mean fluorescent intensity, calculated as described in Patients and methods after 24 or 48 h in culture for (**d**) SHP-1 and (**e**) pSTAT3.

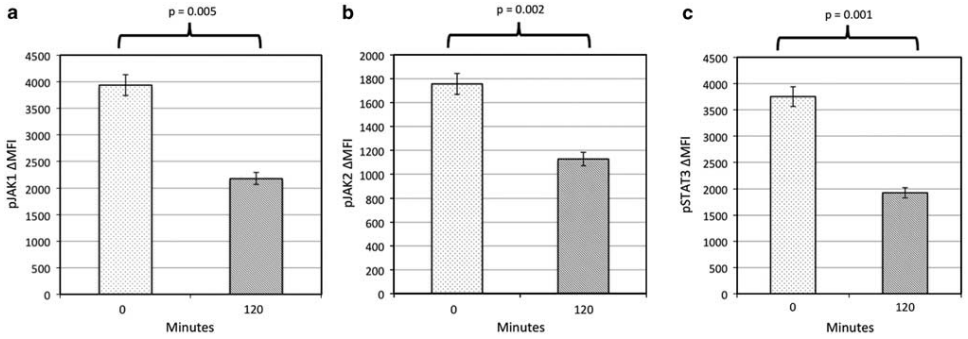

Figure 3 JAK inhibition downregulates STAT3 activation in primary Sézary cells. Quantitative flow cytometric analysis was performed on P6-treated enriched tumour samples from 10 SS patients to determine the effect of P6 on the expression of (**a**) pJAK1 (**b**) pJAK2 (**c**) pSTAT3. Data are expressed as delta mean fluorescent intensity, calculated as described in Patients and methods in untreated (0 min) and P6-treated (120 min) cells.

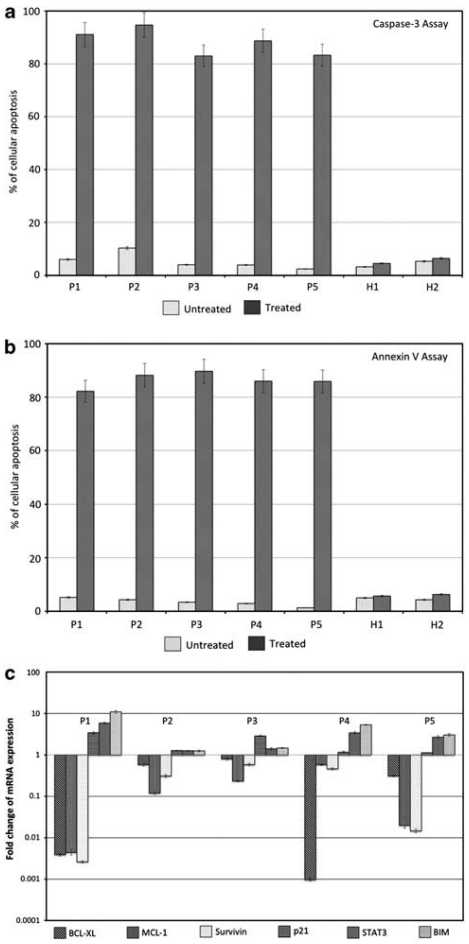

Figure 4 Downregulation of STAT3 activation by pan-JAK inhibition induces apoptosis. Apoptosis analysis was performed on 5 from the 10 P6-treated enriched tumour samples (Figure 3) to determine the downstream effects of P6 on primary (P) tumour and healthy (H) samples (**a**) Caspase-3 apoptosis assay (**b**) Annexin V apoptosis assay (**c**) qPCR of pSTAT3 target genes *Bcl-XL*, *Mcl-1* and *Survivin*, in addition to p21, STAT3 and BIM. The graph denotes the fold change of mRNA expression of P6-treated Sézary samples compared with the untreated Sézary samples.

pathway in Sézary cells, we performed single-stranded conformational polymorphism analysis of the region containing the common V658 (JAK1) and V617 (JAK2) mutations, which are frequently mutated in other malignancies with constitutive activation of the JAK–STAT3 pathway.[39] No band shifts were observed in DNA samples extracted from the enriched tumour cell populations of 19 Sézary patients (data not shown). The CTCL cell lines HuT78, SeAx and MyLa, and the leukaemic cell line Jurkat also did not harbour either mutation.

Discussion

Aberrant activation of STAT3 has been widely reported in a variety of malignancies (reviewed in Al Zaid Siddiquee and Turkson[9] and Yu *et al*.[40]). This study of *ex vivo*-enriched tumour cell populations from a series of SS patients demonstrate that JAK–STAT3 activation is a consistent feature of SS, providing compelling evidence that aberrant STAT3 expression is a significant pathogenetic abnormality in this malignancy. Furthermore, we have shown that in contrast to that reported *in vitro* studies using CTCL-derived cell lines, persistent JAK–STAT3 activation in primary Sézary cell populations is independent of SHP-1. Moreover, treatment of *ex vivo* tumour cells from SS patients with the JAK inhibitor P6 demonstrates that JAK phosphorylation is essential for constitutive activation of STAT3 in SS.

Our data supports previous studies demonstrating constitutive expression of STAT3 in CTCL cell lines,[10–19] and confirm findings in a recent report that showed constitutive and sustained *ex vivo* expression of pSTAT3 over 24 h in PBMCs from a group of four SS/MF patients.[18] In contrast, an earlier study documented strong expression of pSTAT3 in only 2 out of 14 SS patients.[10] However, this study examined total PBMCs rather than enriched tumour cell populations and some patients had low proportions of Sézary cells (1–91%). Therefore, the apparent contrasts to our data may be explained by a low tumour burden in the PBMCs analysed. It has also been suggested that STAT3 activation in SS is not constitutive, but is dependent on exogenous cytokine stimulation, as expression of pSTAT3 was significantly reduced after overnight culture of Sézary cells from three patients.[17] However, another report[18] clearly demonstrated persistent expression of pSTAT3 *in vitro* in the absence of cytokine stimulation, which is consistent with our own observations and supports the conclusion that STAT3 is constitutively activated in SS patients and is independent of exogenous cytokine stimulation.

The underlying mechanism responsible for aberrant STAT3 activation in CTCL has proved elusive, although studies have been mostly restricted to cell lines. The protein tyrosine phosphatase SHP-1 has been proposed as a candidate for aberrant STAT3 activation in CTCL due to its role as a negative regulator of JAK1 and JAK2.[41,42] Previous studies have shown that SHP-1 protein expression is absent in some CTCL cell lines,[28] and immunohistochemical analysis has demonstrated reduced SHP-1 expression in lesional tumour biopsy samples from MF patients with advanced stage disease.[30] Furthermore, studies of anaplastic large cell lymphoma cell lines revealed STAT3 and DNA methyltransferase-mediated epigenetic silencing of SHP-1.[29] However, we found no evidence of SHP-1 downregulation or promoter methylation in primary SS samples when compared with healthy PBMCs, despite using pyrosequencing, which has sufficient sensitivity to detect hypermethylation against a background of normal cells.[33] It has been previously recognised that the immortalisation of cell lines can itself cause aberrant DNA methylation as a result of selective pressures present during the growth of these cells in culture.[43] Given the lack of changes in DNA methylation or protein expression of SHP-1 in primary cells and the absence of an effect of SHP-1 knockdown in MyLa cells, our results suggest that SHP-1 does not contribute to persistent activation of the JAK–STAT3 pathway in SS. Our data, therefore, suggests that in SS and MF, alternative mechanisms may be responsible for aberrant STAT3 activation. This is consistent with studies of other malignancies[40] that have demonstrated multiple mechanisms can lead to aberrant STAT3 activation and also supports recent findings,[2] suggesting that SS and MF may have distinct clinicopathogenetic origins.

The SOCS family of negative STAT regulators is also unlikely to mediate aberrant STAT3 activation in SS, as it has been reported that SOCS3 is expressed at high levels in CTCL cell lines and SS patients.[19] Moreover, the use of a dominant-negative STAT3 in CTCL cell lines was shown to downregulate constitutive expression of SOCS3, demonstrating that SOCS3 expression is a consequence rather than a mediator of aberrant STAT3 activation. Furthermore, no *SOCS3*-associated mutations have been identified in CTCL.[44]

We also detected consistent expression of activated JAK1 and JAK2 in primary SS samples and demonstrate that down-regulation of JAK1 and JAK2 expression using the P6 pan-JAK inhibitor results in significant downregulation of STAT3 expression in primary SS cells. Previous studies of a SS cell line and an MF patient sample *ex vivo* treated with a pan-JAK inhibitor AG490 also showed downregulation of activated STAT3.[13] Although activation of JAK3 in CTCL is well documented, no previous studies of JAK1 and JAK2 have been published.[25,45] Although further experiments are required to elucidate the specific contribution and role of individual JAKs, our findings indicate that aberrant activation of STAT3 is mediated via JAK signalling in SS.

In the last decade, several *JAK* mutations have been identified in acute lymphoblastic leukaemia and myeloproliferative diseases.[46,47] A recent report identified a *JAK3* A572V mutation in 1 of 30 MF patients[48] studied. We have found no evidence for the most common activating mutations, *JAK1* V658F and *JAK2* V617, in primary SS samples. This is perhaps not surprising as the literature suggests that *JAK* mutations, including *JAK2* V617, are uncommon in non-Hodgkin's lymphoma.[49] However, other rare activating *JAK* mutations have been described in various malignancies,[47,50] and therefore, a comprehensive analysis for *JAK* mutations in SS patients is required to fully exclude other activating mutations.

Although an unidentified activating mutation of *JAK1* and/or *JAK2* might explain the aberrant activation of STAT3 in primary SS, aberrant signalling further upstream of *JAK1* and *JAK2* should also be considered. JAKs are activated by a plethora of cytokines and growth factors, as well as by signalling through the T-cell receptor. Studies of CTCL cell lines have shown dysregulation of T-cell activation including constitutive IL-2Rα expression,[13] spontaneous IL-5 production,[14] enhanced secretion of IL-10[ref. 51] and aberrant expression of IL-17.[52] In classical Hodgkin's lymphoma, HSP90 is essential for JAK/STAT signalling, as it activates JAK1 and JAK2.[53] The Ephrin family of tyrosine kinase receptors have also been shown to activate the JAK–STAT3 pathway.[54] Overexpression of one Ephrin family member, EphA4, has been reported in several human cancers, including SS,[55] and therefore it represents a potential mechanism for aberrant JAK–STAT3 activation.

Persistent STAT3 signalling is a major feature of many malignancies and it is well recognised that downstream targets of pSTAT3 include a large number of genes that contribute to apoptotic resistance, differentiation and proliferation.[40] Our *ex vivo* findings of the induction of apoptosis following inhibition of STAT3 activation in Sézary cells, supports the hypothesis that pSTAT3 has a pivotal role in mediating the known resistance to apoptosis. These data confirm several *in vitro* studies using CTCL cell lines, which have induced apoptosis via STAT3 knockdown,[11,12] or STAT3 inhibition with different agents including Curcumin,[18] Cucurbitacin,[17] Panobinostat[15] and Avicin D.[16] Our data suggests that downregulation of the pSTAT3 anti-apoptotic genes *BCL-2*, *Survivin* and *Bcl-XL* contribute to the observed commitment to apoptosis. Furthermore, it is now recognised that unphosphorylated monomeric STATs, including STAT3, regulate gene transcription and have distinct target genes to their phosphorylated isoforms.[6,7] Our findings support these observations as P6 inhibition of JAK–STAT3 phosphorylation induced STAT3 mRNA expression and upregulated expression of BIM, a known target of unphosphorylated monomeric STAT3[refs 6,7] and a pro-apoptotic member of the BCL-2 protein family (reviewed in ref. 56).

In conclusion, by studying *ex vivo*-enriched tumour cell populations from a large cohort of SS patients, we have established that aberrant expression of pSTAT3 is a consistent feature of this malignancy and is likely to be a key pathogenetic abnormality and thus a potential therapeutic target. We have also shown that aberrant STAT3 expression in SS patients is primarily mediated via activation of JAKs. Specifically, we have found no evidence that downregulation of SHP-1, *SHP-1* promoter methylation or common activating mutations of *JAK1/JAK2* is involved in STAT3 activation. Further studies to exclude rare activating mutations of *JAKs* and upstream signalling abnormalities in SS are now required.

Conflict of interest

The authors declare no conflict of interest.

Acknowledgements

We thank Ms Silvia Ferreira for providing expert technical assistance. This work was supported by grants from the British Skin Foundation (RCTM), Guy's and St Thomas' Charitable Foundation and includes support from the 'Skin Matters' fund (CLJ). Support from Guy's & St Thomas' NHS Foundation (TJM) is gratefully acknowledged. We acknowledge the financial support from the Department of Health via the National Institute for Health Research comprehensive Biomedical Research Centre ward to Guy's and St Thomas' NHS Foundation Trust in partnership with King's College London and King's College Hospital NHS Foundation Trust.

References

1 Agar NS, Wedgeworth E, Crichton S, Mitchell TJ, Cox M, Ferreira S *et al*. Survival outcomes and prognostic factors in mycosis fungoides/Sezary syndrome: validation of the revised International Society for Cutaneous Lymphomas/European Organisation for Research and Treatment of Cancer staging proposal. *J Clin Oncol* 2010; **28**: 4730–4739.
2 Campbell JJ, Clark RA, Watanabe R, Kupper TS. Sezary syndrome and mycosis fungoides arise from distinct T-cell subsets: a biologic rationale for their distinct clinical behaviors. *Blood* 2010; **116**: 767–771.
3 Contassot E, Kerl K, Roques S, Shane R, Gaide O, Dupuis M *et al*. Resistance to FasL and tumor necrosis factor-related apoptosis-inducing ligand-mediated apoptosis in Sezary syndrome T-cells associated with impaired death receptor and FLICE-inhibitory protein expression. *Blood* 2008; **111**: 4780–4787.
4 Levy DE, Darnell Jr JE. Stats: transcriptional control and biological impact. *Nat Rev Mol Cell Biol* 2002; **3**: 651–662.
5 Lim CP, Cao X. Structure, function, and regulation of STAT proteins. *Mol Biosyst* 2006; **2**: 536–550.
6 Yang J, Liao X, Agarwal MK, Barnes L, Auron PE, Stark GR. Unphosphorylated STAT3 accumulates in response to IL-6 and activates transcription by binding to NFkappaB. *Genes Dev* 2007; **21**: 1396–1408.
7 Yang J, Stark GR. Roles of unphosphorylated STATs in signaling. *Cell Res* 2008; **18**: 443–451.

8 Bromberg JF, Horvath CM, Besser D, Lathem WW, Darnell Jr JE. Stat3 activation is required for cellular transformation by v-src. *Mol Cell Biol* 1998; **18**: 2553–2558.
9 Al Zaid Siddiquee K, Turkson J. STAT3 as a target for inducing apoptosis in solid and hematological tumors. *Cell Res* 2008; **18**: 254–267.
10 Zhang Q, Nowak I, Vonderheid EC, Rook AH, Kadin ME, Nowell PC *et al.* Activation of Jak/STAT proteins involved in signal transduction pathway mediated by receptor for interleukin 2 in malignant T lymphocytes derived from cutaneous anaplastic large T-cell lymphoma and Sezary syndrome. *Proc Natl Acad Sci USA* 1996; **93**: 9148–9153.
11 Sommer VH, Clemmensen OJ, Nielsen O, Wasik M, Lovato P, Brender C *et al. In vivo* activation of STAT3 in cutaneous T-cell lymphoma. Evidence for an antiapoptotic function of STAT3. *Leukemia* 2004; **18**: 1288–1295.
12 Verma NK, Davies AM, Long A, Kelleher D, Volkov Y. STAT3 knockdown by siRNA induces apoptosis in human cutaneous T-cell lymphoma line Hut78 via downregulation of Bcl-xL. *Cell Mol Biol Lett* 2010; **15**: 342–355.
13 Eriksen KW, Kaltoft K, Mikkelsen G, Nielsen M, Zhang Q, Geisler C *et al.* Constitutive STAT3-activation in Sezary syndrome: tyrphostin AG490 inhibits STAT3-activation, interleukin-2 receptor expression and growth of leukemic Sezary cells. *Leukemia* 2001; **15**: 787–793.
14 Nielsen M, Nissen MH, Gerwien J, Zocca MB, Rasmussen HM, Nakajima K *et al.* Spontaneous interleukin-5 production in cutaneous T-cell lymphoma lines is mediated by constitutively activated Stat3. *Blood* 2002; **99**: 973–977.
15 Shao W, Growney JD, Feng Y, O'Connor G, Pu M, Zhu W *et al.* Activity of deacetylase inhibitor panobinostat (LBH589) in cutaneous T-cell lymphoma models: Defining molecular mechanisms of resistance. *Int J Cancer* 2010; **127**: 2199–2208.
16 Zhang C, Li B, Gaikwad AS, Haridas V, Xu Z, Gutterman JU *et al.* Avicin D selectively induces apoptosis and downregulates p-STAT-3, bcl-2, and survivin in cutaneous T-cell lymphoma cells. *J Invest Dermatol* 2008; **128**: 2728–2735.
17 van Kester MS, Out-Luiting JJ, von dem Borne PA, Willemze R, Tensen CP, Vermeer MH. Cucurbitacin I inhibits Stat3 and induces apoptosis in Sezary cells. *J Invest Dermatol* 2008; **128**: 1691–1695.
18 Zhang C, Li B, Zhang X, Hazarika P, Aggarwal BB, Duvic M. Curcumin selectively induces apoptosis in cutaneous T-cell lymphoma cell lines and patients' PBMCs: potential role for STAT-3 and NF-kappaB signaling. *J Invest Dermatol* 2010; **130**: 2110–2119.
19 Brender C, Nielsen M, Kaltoft K, Mikkelsen G, Zhang Q, Wasik M *et al.* STAT3-mediated constitutive expression of SOCS-3 in cutaneous T-cell lymphoma. *Blood* 2001; **97**: 1056–1062.
20 Yu H, Jove R. The STATs of cancer–new molecular targets come of age. *Nat Rev Cancer* 2004; **4**: 97–105.
21 Levine RL, Gilliland DG. JAK-2 mutations and their relevance to myeloproliferative disease. *Curr Opin Hematol* 2007; **14**: 43–47.
22 Chiarle R, Voena C, Ambrogio C, Piva R, Inghirami G. The anaplastic lymphoma kinase in the pathogenesis of cancer. *Nat Rev Cancer* 2008; **8**: 11–23.
23 Hagemeijer A, Graux C. ABL1 rearrangements in T-cell acute lymphoblastic leukemia. *Genes Chromosomes Cancer* 2010; **49**: 299–308.
24 Kameda T, Shide K, Shimoda HK, Hidaka T, Kubuki Y, Katayose K *et al.* Absence of gain-of-function JAK1 and JAK3 mutations in adult T cell leukemia/lymphoma. *Int J Hematol* 2010; **92**: 320–325.
25 Cornejo MG, Kharas MG, Werneck MB, Le Bras S, Moore SA, Ball B *et al.* Constitutive JAK3 activation induces lymphoproliferative syndromes in murine bone marrow transplantation models. *Blood* 2009; **113**: 2746–2754.
26 Chim CS, Fung TK, Cheung WC, Liang R, Kwong YL. SOCS1 and SHP1 hypermethylation in multiple myeloma: implications for epigenetic activation of the Jak/STAT pathway. *Blood* 2004; **103**: 4630–4635.
27 Sato H, Oka T, Shinnou Y, Kondo T, Washio K, Takano M *et al.* Multi-step aberrant CpG island hyper-methylation is associated with the progression of adult T-cell leukemia/lymphoma. *Am J Pathol* 2010; **176**: 402–415.
28 Zhang Q, Raghunath PN, Vonderheid E, Odum N, Wasik MA. Lack of phosphotyrosine phosphatase SHP-1 expression in malignant T-cell lymphoma cells results from methylation of the SHP-1 promoter. *Am J Pathol* 2000; **157**: 1137–1146.
29 Zhang Q, Wang HY, Marzec M, Raghunath PN, Nagasawa T, Wasik MA. STAT3- and DNA methyltransférase 1-mediated epigenetic silencing of SHP-1 tyrosine phosphatase tumor suppressor gene in malignant T lymphocytes. *Proc Natl Acad Sci USA* 2005; **102**: 6948–6953.
30 Witkiewicz A, Raghunath P, Wasik A, Junkins-Hopkins JM, Jones D, Zhang Q *et al.* Loss of SHP-1 tyrosine phosphatase expression correlates with the advanced stages of cutaneous T-cell lymphoma. *Hum Pathol* 2007; **38**: 462–467.
31 van Dongen JJ, Langerak AW, Bruggemann M, Evans PA, Hummel M, Lavender FL *et al.* Design and standardization of PCR primers and protocols for detection of clonal immunoglobulin and T-cell receptor gene recombinations in suspect lymphoproliferations: report of the BIOMED-2 Concerted Action BMH4-CT98-3936. *Leukemia* 2003; **17**: 2257–2317.
32 Tiemessen MM, Mitchell TJ, Hendry L, Whittaker SJ, Taams LS, John S. Lack of suppressive CD4+CD25+FOXP3+ T cells in advanced stages of primary cutaneous T-cell lymphoma. *J Invest Dermatol* 2006; **126**: 2217–2223.
33 Jones CL, Wain EM, Chu CC, Tosi I, Foster R, McKenzie RC *et al.* Downregulation of Fas gene expression in Sezary syndrome is associated with promoter hypermethylation. *J Invest Dermatol* 2010; **130**: 1116–1125.
34 Oka T, Ouchida M, Koyama M, Ogama Y, Takada S, Nakatani Y *et al.* Gene silencing of the tyrosine phosphatase SHP1 gene by aberrant methylation in leukemias/lymphomas. *Cancer Res* 2002; **62**: 6390–6394.
35 Leon F, Cespon C, Franco A, Lombardia M, Roldan E, Escribano L *et al.* SHP-1 expression in peripheral T cells from patients with Sezary syndrome and in the T cell line HUT-78: implications in JAK3-mediated signaling. *Leukemia* 2002; **16**: 1470–1477.
36 Scarisbrick JJ, Woolford AJ, Russell-Jones R, Whittaker SJ. Loss of heterozygosity on 10q and microsatellite instability in advanced stages of primary cutaneous T-cell lymphoma and possible association with homozygous deletion of PTEN. *Blood* 2000; **95**: 2937–2942.
37 Pedranzini L, Dechow T, Berishaj M, Comenzo R, Zhou P, Azare J *et al.* Pyridone 6, a pan-Janus-activated kinase inhibitor, induces growth inhibition of multiple myeloma cells. *Cancer Res* 2006; **66**: 9714–9721.
38 Berishaj M, Gao SP, Ahmed S, Leslie K, Al-Ahmadie H, Gerald WL *et al.* Stat3 is tyrosine-phosphorylated through the interleukin-6/glycoprotein 130/Janus kinase pathway in breast cancer. *Breast Cancer Res* 2007; **9**: R32.
39 Ghoreschi K, Laurence A, O'Shea JJ. Janus kinases in immune cell signaling. *Immunol Rev* 2009; **228**: 273–287.
40 Yu H, Pardoll D, Jove R. STATs in cancer inflammation and immunity: a leading role for STAT3. *Nat Rev Cancer* 2009; **9**: 798–809.
41 Klingmuller U, Lorenz U, Cantley LC, Neel BG, Lodish HF. Specific recruitment of SH-PTP1 to the erythropoietin receptor causes inactivation of JAK2 and termination of proliferative signals. *Cell* 1995; **80**: 729–738.
42 David M, Chen HE, Goelz S, Larner AC, Neel BG. Differential regulation of the alpha/beta interferon-stimulated Jak/Stat pathway by the SH2 domain-containing tyrosine phosphatase SHPTP1. *Mol Cell Biol* 1995; **15**: 7050–7058.
43 Jones PA, Wolkowicz MJ, Rideout III WM, Gonzales FA, Marziasz CM, Coetzee GA *et al. De novo* methylation of the MyoD1 CpG island during the establishment of immortal cell lines. *Proc Natl Acad Sci USA* 1990; **87**: 6117–6121.
44 Brender C, Lovato P, Sommer VH, Woetmann A, Mathiesen AM, Geisler C *et al.* Constitutive SOCS-3 expression protects T-cell lymphoma against growth inhibition by IFNalpha. *Leukemia* 2005; **19**: 209–213.
45 Krejsgaard T, Vetter-Kauczok CS, Woetmann A, Lovato P, Labuda T, Eriksen KW *et al.* Jak3- and JNK-dependent vascular endothelial growth factor expression in cutaneous T-cell lymphoma. *Leukemia* 2006; **20**: 1759–1766.
46 Flex E, Petrangeli V, Stella L, Chiaretti S, Hornakova T, Knoops L *et al.* Somatically acquired JAK1 mutations in adult acute lymphoblastic leukemia. *J Exp Med* 2008; **205**: 751–758.

47 Mullighan CG, Zhang J, Harvey RC, Collins-Underwood JR, Schulman BA, Phillips LA *et al.* JAK mutations in high-risk childhood acute lymphoblastic leukemia. *Proc Natl Acad Sci USA* 2009; **106**: 9414–9418.
48 Cornejo MG, Boggon TJ, Mercher T. JAK3: a two-faced player in hematological disorders. *Int J Biochem Cell Biol* 2009; **41**: 2376–2379.
49 Lee JW, Soung YH, Kim SY, Nam SW, Park WS, Lee JY *et al.* JAK2 V617F mutation is uncommon in non-Hodgkin lymphomas. *Leuk Lymphoma* 2006; **47**: 313–314.
50 Constantinescu SN, Girardot M, Pecquet C. Mining for JAK-STAT mutations in cancer. *Trends Biochem Sci* 2008; **33**: 122–131.
51 Berger CL, Tigelaar R, Cohen J, Mariwalla K, Trinh J, Wang N *et al.* Cutaneous T-cell lymphoma: malignant proliferation of T-regulatory cells. *Blood* 2005; **105**: 1640–1647.
52 Chong BF, Wilson AJ, Gibson HM, Hafner MS, Luo Y, Hedgcock CJ *et al.* Immune function abnormalities in peripheral blood mononuclear cell cytokine expression differentiates stages of cutaneous T-cell lymphoma/mycosis fungoides. *Clin Cancer Res* 2008; **14**: 646–653.
53 Schoof N, von Bonin F, Trumper L, Kube D. HSP90 is essential for Jak-STAT signaling in classical Hodgkin lymphoma cells. *Cell Commun Signal* 2009; **7**: 17.
54 Lai KO, Chen Y, Po HM, Lok KC, Gong K, Ip NY. Identification of the Jak/Stat proteins as novel downstream targets of EphA4 signaling in muscle: implications in the regulation of acetylcholinesterase expression. *J Biol Chem* 2004; **279**: 13383–13392.
55 van Doorn R, Dijkman R, Vermeer MH, Out-Luiting JJ, van der Raaij-Helmer EM, Willemze R *et al.* Aberrant expression of the tyrosine kinase receptor EphA4 and the transcription factor twist in Sezary syndrome identified by gene expression analysis. *Cancer Res* 2004; **64**: 5578–5586.
56 Youle RJ, Strasser A. The BCL-2 protein family: opposing activities that mediate cell death. *Nat Rev Mol Cell Biol* 2008; **9**: 47–59.

Supplementary Information accompanies the paper on the Leukemia website (http://www.nature.com/leu)

ORIGINAL ARTICLE

Regulation of T-Plastin Expression by Promoter Hypomethylation in Primary Cutaneous T-Cell Lymphoma

Christine L. Jones[1], Silvia Ferreira[1], Robert C.T. McKenzie[1], Isabella Tosi[2], Jacqueline A. Caesar[1], Martine Bagot[3], Sean J. Whittaker[1] and Tracey J. Mitchell[1]

T-plastin (PLS3) is an actin-bundling protein normally expressed in epithelial cells but absent in cells of hematopoietic origin. Aberrant PLS3 expression has been demonstrated in lymphocytes from Sézary syndrome (SS) patients and has been proposed as a biomarker for SS; however, the mechanism underlying dysregulation of PLS3 has not been determined. In this study, PLS3 mRNA expression was demonstrated in 21/35 (60%) SS patients and in 3/8 (38%) mycosis fungoides patients, all of whom had clonal blood involvement. No evidence for PLS3 mutations within coding or promoter regions was found, but significant hypomethylation of CpG dinucleotides 95–99 within the PLS3 CpG island was observed and this was restricted to the PLS3+ population. A polyclonal antibody specific to PLS3 was raised to examine coexpression of PLS3 with a panel of T-cell differentiation markers. All PLS3+ cells were CD3+CD4+ and CD26−, suggesting that loss of CD26 is consistently associated with gain of PLS3, whereas all other markers were distributed heterogeneously. However, a patient-specific TCR copy number assay also demonstrated heterogeneity in PLS3 expression in tumor cell populations. Importantly, our findings demonstrate PLS3 expression in the majority of SS patients and provide insight into the molecular regulation of PLS3 expression in CTCL.

Journal of Investigative Dermatology (2012) **132,** 2042–2049; doi:10.1038/jid.2012.106; published online 12 April 2012

INTRODUCTION

Primary cutaneous T-cell lymphoma (CTCL) is the second most common form of extranodal non-Hodgkin's lymphoma with an incidence of 7.7 in 1,000,000 person-years (Bradford *et al.*, 2009). Mycosis fungoides (MF) is the most prevalent form of CTCL, accounting for 54% of cases (Bradford *et al.*, 2009). In MF, the tumor cells are usually restricted to the skin compartment, and prognosis is generally favorable with a 5-year overall survival of 78% (Agar *et al.*, 2010). Sézary syndrome (SS) is a closely related but more aggressive subtype in which a leukemic clone of T cells is present in the peripheral blood. SS is associated with a poor prognosis and a 5-year overall survival of only 26% (Agar *et al.*, 2010).

[1]*Skin Tumour Unit, St John's Institute of Dermatology, Division of Genetics and Molecular Medicine, King's College London, London, UK;* [2]*Cutaneous Medicine Theme, NIHR Biomedical Research Centre, Guy's and St Thomas' NHS Foundation Trust and King's College London, London, UK and* [3]*Department of Dermatology, Hôpital Saint Louis, Paris, France*

Correspondence: Tracey J. Mitchell, St John's Institute of Dermatology, 9th Floor, Tower Wing, Guy's Hospital, London SE1 9RT, UK. E-mail: tracey.mitchell@kcl.ac.uk

Abbreviations: cDNA, complementary DNA; CGI, CpG island; CTCL, cutaneous T-cell lymphoma; MF, mycosis fungoides; PBL, peripheral blood lymphocyte; qPCR, quantitative reverse transcriptase–PCR; SS, Sézary syndrome

Received 9 November 2011; revised 2 February 2012; accepted 15 February 2012; published online 12 April 2012

Diagnosis of the various subtypes of CTCL is made using a combination of clinical, histological, and immunophenotypic features, because there is a lack of biomarkers unique to the disease or its subtypes. In SS, a measure of circulating tumor burden can be obtained by visual inspection of a blood smear to quantify those cells with abnormal cerebriform nuclei. However, Sézary cells are morphologically heterogeneous and can be difficult to distinguish from normal activated T cells based on morphology alone.

Previous studies have suggested a characteristic immunophenotype typical of SS, including loss of CD7 (Haynes *et al.*, 1981), loss of CD26 (Jones *et al.*, 2001), and the presence of CD158k (Bagot *et al.*, 2001). Increasingly, these differentiation markers are being used in research studies to enrich for the tumor cells (Contassot *et al.*, 2008; Yoon *et al.*, 2008). However, a study comparing the use of the different phenotypic markers as diagnostic tools concluded that no individual marker is present in all cases, and that a combination of markers is required for flow cytometric diagnosis (Klemke *et al.*, 2008). In addition, tumor cells have been identified in FACS-sorted CD7- and CD26-positive subsets from SS patient samples using a clone-specific TCR PCR (Steinhoff *et al.*, 2009), suggesting that these markers may not be appropriate for enrichment of the tumor cell population.

T-plastin (PLS3) is an actin-bundling protein, the expression of which is restricted to epithelial cells with replicative

potential (Lin *et al.*, 1993). A closely related isoform, L-plastin, is normally expressed only in hematopoietic cells, but ectopic expression of L-plastin has been reported in epithelial malignancies including colon and breast cancers (Lin *et al.*, 1993). This appears to be critical in some tumors for enhancing migration and invasion (Foran *et al.*, 2006). Aberrant expression of PLS3 mRNA was first identified in a complementary DNA (cDNA) array–based study of peripheral blood mononuclear cells from 48 SS patients (Kari *et al.*, 2003) and was proposed as a potential diagnostic biomarker. Similar findings were reported by a representational difference analysis study of mRNA derived from CD4+/CD7-enriched tumor cells from nine SS patients, which demonstrated high levels of PLS3 mRNA expression in Sézary cells and confirmed PLS3 protein expression by western blot analysis in one patient (Su *et al.*, 2003). Subsequent studies including our own have identified that high levels of PLS3 mRNA expression is a common feature of Sézary cells (van Doorn *et al.*, 2004; Nebozhyn *et al.*, 2006; Tiemessen *et al.*, 2006; Booken *et al.*, 2008; Capriotti *et al.*, 2008; Tang *et al.*, 2010). However, the mechanism by which aberrant expression of PLS3 occurs in SS has not yet been determined. A key potential mechanism that may contribute to the dysregulation of PLS3 expression in SS is promoter methylation, as the *PLS3* gene harbors a 1,585 bp CpG island (CGI), which may be differentially methylated in Sézary cells compared with healthy T cells.

As PLS3 is not normally expressed by any cell of hematopoietic origin, it has potential as a Sézary cell biomarker and as a tool to evaluate the utility of other proposed markers for the identification of SS tumor cells. Here we assess the extent of PLS3 expression in CTCL and undertake a detailed investigation of potential regulatory mechanisms. We further show that an antibody against PLS3 can be used to identify a subset of malignant circulating cells in SS and characterize in detail the immunophenotype of this subset of malignant cells.

RESULTS

PLS3 is expressed in the majority of SS patients

To establish the prevalence of PLS3 in our patient cohort, the expression of PLS3 mRNA was determined in CD4+ peripheral blood lymphocytes (PBLs) by quantitative reverse transcriptase–PCR (qPCR). qPCR detected a minimal amount of PLS3 mRNA in 11 healthy controls representing one thousandth of the amount of cyclophilin mRNA present. A threshold for positive detection of PLS3 mRNA was set at one hundredth of the amount of cyclophilin mRNA, using this definition 60% (21/35) of SS patients expressed PLS3. A group of 18 MF patients, 8 of whom had advanced-stage disease (Stage IV) with no morphological evidence of Sézary cells but with a T-cell clone identical to that observed in the skin (Stage B0b) and 10 of whom had skin-restricted disease (Stage IB–III B0a) were also examined. Of the eight MF patients with peripheral blood involvement, three expressed PLS3 (38%), whereas all those with skin-restricted disease were PLS3 negative. Comparison of average PLS3 mRNA expression among the three groups demonstrated a significant increase in PLS3 expression in SS patients compared with healthy controls ($P<0.05$; Figure 1). The expression of PLS3 was also compared with measures of tumor burden such as total lymphocyte count, CD4+ count, and CD4/CD8 ratio, and demonstrated only a weak correlation ($\rho=0.33$, $P=0.008$) with the percentage of CD4+ T cells.

The absence of coding or promoter mutations in the *PLS3* gene

To address whether mutational events may be responsible for aberrant PLS3 expression, PBL mRNA from six SS patients was sequenced using primer sets that covered the entire coding sequence and 953 bp of the 1,111 bp 3′-untranslated region. No mutations were detected within the PLS3 coding sequence and 3′-untranslated region of the six patients examined. A C/G polymorphism was observed in exon 1,390 bp upstream of the translational start site in two patients. Further investigation revealed this site to be a known single-nucleotide polymorphism, rs757124. As PLS3 mRNA was found with the C variant in four patients and the G variant in two patients, we conclude that this single-nucleotide polymorphism is not influencing the expression of PLS3.

The promoter region of 12 SS patients was also sequenced to establish whether other polymorphisms might be associated with aberrant PLS3 expression. This cohort included three SS patients not expressing PLS3 mRNA, eight SS patients expressing PLS3, and one MF patient expressing PLS3. The only polymorphisms detected within the region 1,845 bp upstream of the transcriptional start site corresponded to known single-nucleotide polymorphisms in this region (Table 1). Although a much larger cohort is required to conclusively test for an association between genotype and PLS3 expression, no clear pattern emerged from the 12 patients studied.

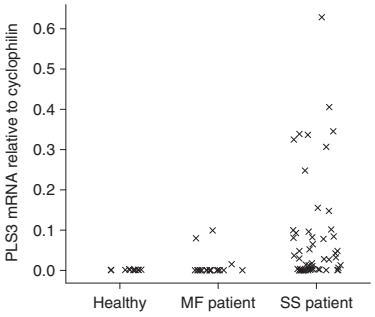

Figure 1. T-plastin (PLS3) mRNA is aberrantly expressed in CD4+ lymphocytes from Sézary syndrome (SS) patients. Quantitative reverse transcriptase–PCR (qPCR) was used to assess the expression of PLS3 mRNA in CD4+ lymphocytes from 11 healthy controls, 18 mycosis fungoides (MF) patients, and 35 SS patients. The housekeeping gene *Cyclophilin* was used as a normalization control. A significant difference between healthy and SS patient expression was demonstrated by one-way analysis of variance (ANOVA).

Table 1. Genotypes of the three SNPs within the T-plastin (PLS3) upstream region

Sample	PLS3 expression	rs3813931	rs1557770	rs757124
R67	+	C/C	T/T	G/G
R73	–	C/C	T/G	G/C
R82	+	ND	G/G	C/C
R83	+	C/C	T/T	G/G
R84	+	C/C	T/T	G/G
R85	+	C/C	T/T	G/G
R89	+	C/C	T/T	G/G
R118 (MF)	+	C/C	T/T	G/G
R122	–	T/T	T /T	C/C
R125	+	C/C	T/G	G/C
R126	–	C/C	T/T	C/C
R133	+	C/C	T/T	G/G

Abbreviations: MF, mycosis fungoides; ND, not determined; SNP, single-nucleotide polymorphism.

Site-specific hypomethylation may contribute to aberrant PLS3 expression

Although Lin *et al.* (1999) found that the PLS3 CGI was unmethylated in primary lymphocytes, the assay used only investigated those CpG sites that were within the restriction site of *Eag*I, *Nru*I, and *Pvu*I. Therefore, we used direct sequencing of bisulfite-converted DNA to examine the methylation of the entire PLS3 CGI. The majority of the CGI was observed to be unmethylated in healthy controls; however, one small region containing CpG dinucleotides 95–99 was found to contain methylation in four healthy lymphocyte samples but not in keratinocytes, which express PLS3 (Figure 2a).

To investigate this region further, a pyrosequencing assay was designed and used to quantify methylation in PBL samples taken from 24 healthy controls and 36 SS patients. Healthy PBLs were found to contain an average of 32% methylation of CpG dinucleotides 95–99, which was significantly greater than the 21% methylation observed in PLS3+ patient samples ($P<0.05$). An average methylation level of 46% was detected in PLS3− samples, which was not significantly different from the healthy PBL samples (Figure 2b).

Development of an antibody against PLS3

We tested the two commercially available PLS3 antibodies by western blotting and observed a lack of specificity and sensitivity. Therefore, a polyclonal antibody was raised against a PLS3 antigen and specificity was demonstrated by western blotting (Figure 3a). Expression status of PLS3 protein in SS PBLs was broadly consistent with the expression status of PLS3 mRNA. Expression of PLS3 protein was demonstrated in 8/11 SS samples shown to express PLS3 mRNA by qPCR, whereas 2/3 SS samples with PLS3 mRNA levels below the threshold showed no PLS3 protein expression. In the one SS sample where PLS3 was detected at the protein level but not the mRNA level, the quantity of PLS3 mRNA was just below the threshold for PLS3 expression. Immunostaining of PBLs from one PLS3-positive SS patient demonstrated PLS3 protein expression in a proportion of lymphocytes and suggested that the PLS3 protein is localized in the cytoplasm (Figure 1b).

PLS3+ cells are CD3+CD4+ and CD26− and heterogeneous for other markers

Multiparameter flow cytometry was used to examine the correlation of PLS3 expression with other immunophenotypic markers including CD3, CD4, CD45RO, CD7, CD26, CD25, and CD158k. PLS3+ cells were demonstrated in 11 of 16 SS samples by flow cytometry, and in all cases the PLS3+ population also expressed CD3 and CD4 (Figure 4). In those samples expressing PLS3, the PLS3+ cells comprised between 3 and 76% of the CD4+ PBLs (data not shown).

Next, we examined the distribution of various phenotypic markers within the PLS3+ and PLS3− populations (Figure 5). Notably, in all 11 samples the CD4+PLS3+ population showed almost complete loss of CD26, whereas the corresponding CD4+PLS3− subsets expressed a significantly greater proportion of CD26 ($P=0.0006$), suggesting that loss of CD26 is associated with gain of PLS3. However, no other significant association was found between any of the other differentiation markers and PLS3 status. Notably, a wide range of CD45RO expression was observed, with four patients demonstrating a significantly lower proportion ($P<0.05$) and three patients showing a significantly greater proportion ($P<0.05$) of CD45RO+ in the CD4+ subset than the healthy control average of 47% (Figure 5). Although the distribution of expression between PLS3− and PLS3+ subsets is variable, in three patients showing significant reduction of CD45RO expression, the PLS3 expression was confined to the CD45RO− population.

PLS3 expression is enriched in cells with the tumor-specific TCR gene rearrangement

To assess whether PLS3 expression is heterogeneous in tumor cells from individual patients, we used FACS to isolate PLS3+ and PLS3− cell populations from one well-characterized SS patient (R164). These cell populations were analyzed for the presence of the patient-specific clonal TCR-β gene rearrangement using a qPCR assay. The PLS3+ population contained 84% (confidence interval 69–99% $P<0.05$) cells with the tumor-specific clonal TCR-β gene rearrangement, whereas the PLS3− population contained 28% (confidence interval 14–43% $P<0.05$) cells with the tumor-specific clonal TCR-β gene rearrangement.

PLS3-positive cells show hypomethylation of CpG sites 95–99

DNA from the PLS3− and PLS3+ populations was also analyzed for the methylation status of the PLS3 CGI at sites 95–99. In the pre-sort sample, DNA methylation across these sites was 16%, whereas after sorting DNA from the PLS3+ subset, which represented 79% of the pre-sort sample, was found to be 10% methylated and DNA from the PLS3− subset was 43% methylated.

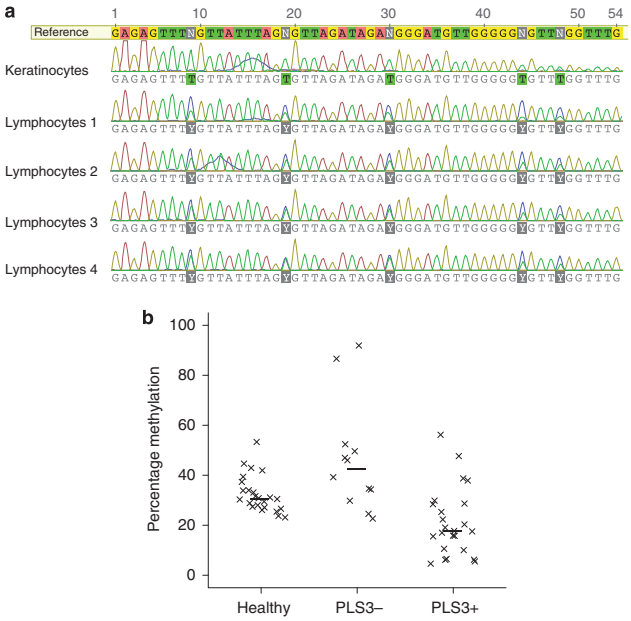

Figure 2. CpG dinucleotides 95–99 are partially methylated in healthy lymphocytes, unmethylated in healthy keratinocytes, and show reduced methylation in lymphocytes from Sézary syndrome (SS) patients expressing T-plastin (PLS3). (**a**) Bisulfite-converted DNA from four healthy lymphocyte samples and one healthy keratinocyte sample were sequenced to assess DNA methylation across the PLS3 CpG island (CGI). The section shown covers CpG dinucleotides 95–99. The bisulfite-converted reference sequence shows potentially methylated cytosine residues (N) and the resultant C + T mixed base (Y) highlighted in gray. (**b**) Pyrosequencing of bisulfite-converted DNA was used to measure methylation of CpG dinucleotides 95–99 in lymphocytes from 24 healthy controls, and in tumor cells from 12 PLS3-negative (PLS3−) and 24 PLS3-positive (PLS3 +) SS patients. The median of each group is represented by a horizontal line. A significant difference in methylation was demonstrated between healthy and PLS3 + groups by one-way analysis of variance (ANOVA).

DISCUSSION

We have shown that aberrant expression of PLS3 is observed in 60% of SS patients and 38% of MF patients with peripheral blood involvement (stage B0b). No mutations were found in the coding or regulatory regions of the *PLS3* gene to account for aberrant PLS3 expression in CTCL. Consistent with other studies, no evidence of DNA methylation was found across the bulk of the CGI (Lin *et al.*, 1999; Oprea *et al.*, 2008); however, in a region that has not previously been investigated, methylation was found in healthy lymphocytes but not in keratinocytes, which correlates with PLS3 expression. In contrast, this region was hypomethylated in lymphocytes from PLS3 + SS patients. Furthermore, sorting of the PLS3 + and PLS3− populations demonstrated that hypomethylation was restricted to the PLS3 + population. These observations strongly suggest that methylation of this region may contribute to the silencing of PLS3 expression in healthy lymphocytes and that loss of methylation may lead to aberrant PLS3 expression in Sèzary cells. Further longitudinal studies are now required to address whether therapies that reduce tumor burden are associated with the reversal of the observed hypomethylation.

We have previously demonstrated that Sézary cells are present within CD4 + CD26 + , CD4 + CD26−, CD4 + CD25−, and CD4 + CD25 + populations by quantifying PLS3 mRNA within sorted cell subsets (Jones *et al.*, 2010; Tiemessen *et al.*, 2006). In this study, we further explored the correlation between T-cell differentiation marker expression and PLS3 expression using an antibody specific for PLS3. In all samples, PLS3 expression was observed to be restricted to CD3 + CD4 + T cells. We found that loss of CD26 was significantly associated with the PLS3 + subpopulation, whereas loss of CD7 and gain of CD158k were not. We also observed that tumor cells were not exclusively confined to the CD45RO + population as widely reported (Willemze *et al.*, 1997). Indeed, in three samples with significant loss of CD45RO, we were able to confirm that PLS3 expression was confined to the CD45RO− population. Similar results have been reported recently, showing heterogeneity in CTCL tumor cells in both CD45RO and CD45RA expression (Campbell *et al.*, 2010). The study by Campbell *et al.* also identified significant differences in the expression of cell differentiation markers and addressins in SS and MF patients with significant blood involvement (leukemic CTCL)

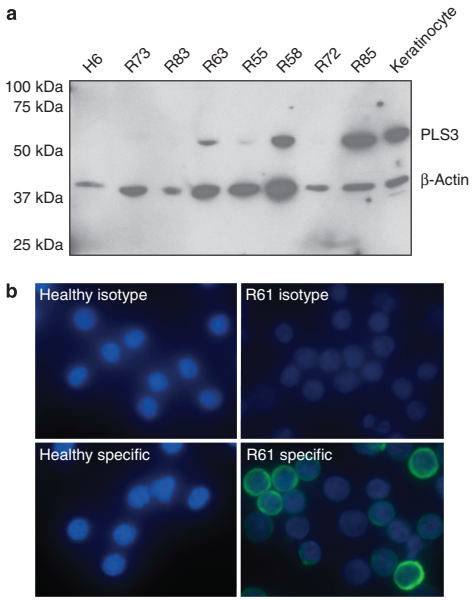

Figure 3. A newly generated antibody is specific for the detection of T-plastin (PLS3) protein. (**a**) Western blot analysis to determine PLS3 expression in primary keratinocytes, and lymphocyte samples from one healthy control, 6 Sézary syndrome (SS) patients shown to express PLS3 mRNA (R83, R63, R55, R58, R72, R85), and one SS patient who did not express PLS3 mRNA (R73). PLS3-specific bands are at the expected size of 70 kDa. β-Actin (40 kDa) is included as a loading control. (**b**) Immunostaining to detect PLS3 expression. Healthy CD4+ lymphocytes and SS patient lymphocytes (R61) were cytospun onto slides, fixed in 1% paraformaldehyde, permeabilized with ice-cold methanol, and then immunostained using the PLS3-specific antibody or a rabbit polyclonal isotype control. Goat anti-rabbit Alexa Fluor 488 (green) was used to visualize the staining, and nuclei were counterstained with 4,6-diamidino-2-phenylindole (DAPI; blue).

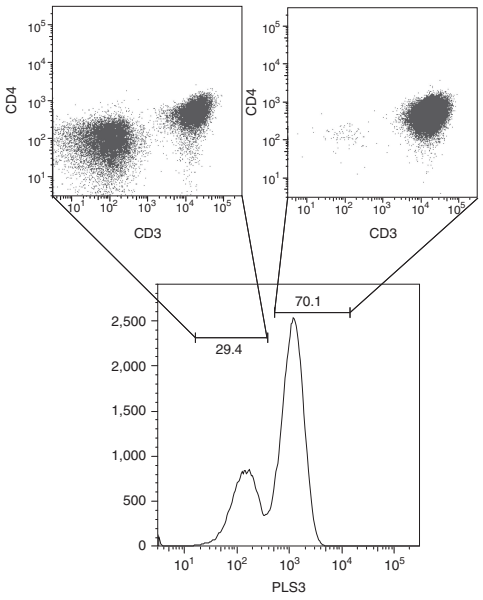

Figure 4. T-plastin (PLS3)-positive cells are CD3+CD4+. Lymphocytes were stained with fluorescent antibodies against CD3, CD4, CD45RO, CD25, CD26, CD7, CD158k, and PLS3, and then examined by flow cytometry. Viable lymphocytes were gated into PLS3− and PLS3+ populations to allow examination of CD3 and CD4 scatterplots. The example shown is taken from Sézary syndrome (SS) patient sample R164.

compared with MF patients with skin-restricted disease. Circulating tumor cells from leukemic patients were found to express high levels of the lymph node–homing receptors CCR7/L-selection and CD27, a phenotype consistent with central memory T cells. MF tumor cells derived from lesional skin lacked expression of the lymph node–homing markers but expressed high levels of the skin-homing receptors CCR4 and CLA, a phenotype in keeping with skin-resident effector memory T cells. Thus, it was proposed that SS and MF arise from distinct functional T-cell subsets. As we did not include such markers, our data do not address the functional T-cell subset origin of CTCL tumor cells. However, the PLS3 antibody described may facilitate future validation of the model proposed by Campbell *et al.* by using PLS3 expression to identify CTCL tumor cells in effector versus central memory T-cell populations, although heterogeneity in PLS3 expression within tumor cell populations may confound data interpretation.

The wide range of proportions of PLS3+ cells observed suggests that PLS3 expression is confined to a substantial subset of tumor cells rather than the whole population. This hypothesis is further supported by the detection of tumor cells within the PLS3-negative population in one patient. This effectively precludes the use of PLS3 sorting to isolate tumor cells in SS patients expressing PLS3.

Although loss of CD7 and CD26 and gain of CD158k have been proposed as diagnostic tools, it is not established whether any of these markers can be used to quantify tumor burden accurately. Our observations of phenotypic heterogeneity within the tumor population are supported by a previous study, which determined that tumor cells are not restricted to CD7− or CD26− subpopulations (Steinhoff *et al.*, 2009). This supports our conclusion that cell sorting based upon these phenotypic markers is likely to identify only a subset of tumor cells, although still potentially including reactive cells. Therefore, isolation of the CD4+ subset still provides the most reliable approach for the enrichment of the tumor population in SS.

To quantify tumor cells within sorted cell subsets, we have developed a patient-specific real-time TCR assay based upon those used in acute lymphoblastic leukemia (Bruggemann *et al.*, 2004; van der Velden and van Dongen, 2009). We

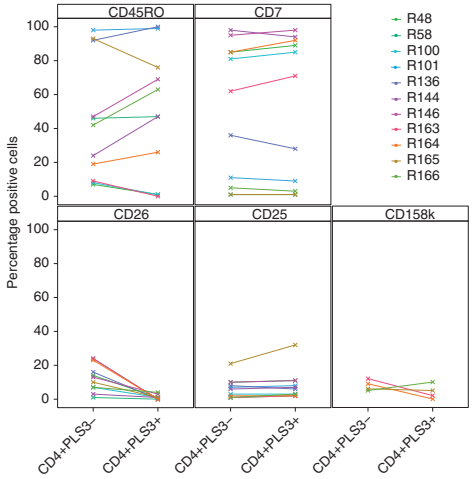

Figure 5. T-cell differentiation marker expression is heterogeneous between PLS3+ and PLS3− subsets. Lymphocytes were stained with fluorescent antibodies against CD3, CD4, CD45RO, CD25, CD26, CD7, CD158k, and PLS3, and then examined by flow cytometry. Viable cells were gated into CD4+PLS3S3− and CD4+PLS3+ populations, and then the percentage of positive cells was quantified for every other differentiation marker (CD45RO, CD7, CD26, CD25, and CD158k) in each subset.

chose to utilize a genetic assay rather than Vβ antibodies to enhance the specificity of detection and to avoid excluding cells where cell surface TCR was not expressed. Patient-specific real-time TCR copy number assays have the potential for future use in quantifying tumor burden, allowing detailed monitoring of response to therapies.

PLS3 and L-plastin are closely related actin-bundling proteins, which normally demonstrate tissue-specific expression (Lin *et al.*, 1993). However, aberrant L-plastin expression has been demonstrated in a wide range of epithelial malignancies (Lin *et al.*, 1993) and shown to induce proliferation and invasion in colon cancer cells (Foran *et al.*, 2006). In healthy tissue, L-plastin becomes phosphorylated upon leukocyte activation (Wabnitz *et al.*, 2007) and leukocytes deficient for L-plastin are incapable of killing pathogens despite showing normal migration, adhesion, spreading, and phagocytosis (Chen *et al.*, 2003). PLS3 has been proposed to have a role in DNA damage repair (Sasaki *et al.*, 2002; Ikeda *et al.*, 2005) in healthy tissue and is overexpressed in cisplatin-resistant (Hisano *et al.*, 1996) and UV-resistant (Higuchi *et al.*, 1998) cells. Given the importance of actin cytoskeletal dynamics in the formation of the immunological synapse and the dysregulation of T-cell signaling observed in CTCL, aberrantly expressed PLS3 may interfere with the assembly of the immunological synapse. Further investigation is necessary to determine the functional role of aberrant PLS3 expression in CTCL.

In conclusion, we have determined the prevalence of PLS3 expression in a large cohort of SS patients and developed an antibody specific for PLS3, which should provide a valuable tool for further studies into the functional role of PLS3. We have demonstrated that hypomethylation of CpG dinucleotides 95–99 in the PLS3 CGI is a likely mechanism responsible for aberrant expression of PLS3 in Sézary cells. Longitudinal studies are now required to assess the prognostic relevance of aberrant PLS3 expression in CTCL. We further conclude that the expression of T-cell differentiation markers in SS patients is heterogeneous and that CD4 expression remains the most reliable approach for enrichment of tumor cells.

MATERIALS AND METHODS

Patient material

Patient lymphocytes were obtained from a nationally approved research tissue bank (07/H10712/106) in accordance with the Declaration of Helsinki Principles of 1975, as revised in 1983. Lymphocytes were isolated using Lymphoprep (Axis-Shield, Kimbolton, UK) gradient centrifugation, whereas CD4+ lymphocytes were obtained by incubating blood with RosetteSep CD4+ T-cell enrichment cocktail (Stem Cell Technologies, London, UK) before Lymhoprep gradient centrifugation. Diagnosis was made using the WHO-EORTC diagnostic criteria for CTCL (Willemze *et al.*, 2005). All SS patients had an identical T-cell clone detected in lesional skin and peripheral blood as demonstrated by TCR gene rearrangement studies using BIOMED-2 primer sets (van Krieken *et al.*, 2007).

Quantitative RT-PCR

RNA was isolated from CD4+ lymphocytes using the RNeasy mini kit (Qiagen, Crawley, UK), followed by conversion into randomly primed cDNA using the high-capacity cDNA archive kit (Applied Biosystems, Warrington, UK). Quantitative RT-PCR was performed on an ABI Prism 7000 (Applied Biosystems) using optimized TaqMan probe/primer sets for PLS3 (Hs00192406_m1) and the endogenous control Cyclophilin A (Hs99999904_m1).

Sequencing

DNA was isolated using standard procedures; cDNA was generated as described above; bisulfite conversion was performed using the Epitect bisulfite kit (Qiagen). Primer sequences and cycling conditions are available on request. PCR products were sequenced by Geneservice (London, UK) using the original PCR primers and additional sequencing primers. Data were examined using Geneous (Drummond *et al.*, 2011) with a 25% peak height similarity cutoff to detect potential mutations.

Pyrosequencing

Pyrosequencing was performed as described in Jones *et al.* (2010) using the following primers: PLS39599_F-5′-TGGAGTGGGGGT TAATGGTAT-3′, PLS39599_R-5′-CCTCCCAATCCCTCTTAACAAA-3′ and sequencing primers PLS39599_SF-5′-TTAAGTGGGTTGGA GAGT-3′, PLS39599_SR-5′-AATCCCTCTTAACAAACC-3′.

Antibody generation

Antibody production was performed by Cambridge Research Biochemicals (Billingham, UK) using the antigenic peptide

Ac-MATTQISKDELDELKC-amide. Antisera were subjected to affinity purification on thiopropyl sepharose 6B derivatized with the antigen followed by elution using Glycine.

Western blotting

Western blotting was carried out using standard procedures. Commercial antibodies against PLS3 used were ab45769 (AbCam, Cambridge, UK) and sc-16655-R (Santa Cruz Biotechnology, Santa Cruz, CA). Anti-β-actin (AbCam) was used as a loading control.

Flow cytometry

Lymphocytes were stained with LIVE DEAD Fixable Aqua dye (Life Technologies, Paisley, UK) before incubation with APC-αCD26 (Miltenyi Biotech, Bisley, UK) and APC-Cy7-αCD158k (gift from Dr Bagot conjugated using Innova Lightening-Link kit, Innova Bioscience, Cambridge, UK) or appropriate isotype controls. Following fixation and permeabilization, cells were incubated with PE-Cy7-αCD3 (eBioscience, Hatfield, UK), PE-TxR-αCD4 (Caltag-Medsystems, Little Balmer, UK), PacificBlue-αCD45RO (Biolegend, Cambridge, UK), PE-Cy5-αCD7 (eBioscience), PE-αCD25 (eBioscience), and DyLight488-αPLS3 (in-house antibody conjugated using Pierce amine-reactive DyLight dye kit, Thermo Fisher Scientific, Rockford, IL), or appropriate isotype controls. Flow cytometry acquisition and sorting was performed on a FACSAria II (BD Biosciences, Oxford, UK), and data were analyzed using the FlowJo software (Tree Star, Ashland, OR).

Patient clone–specific qPCR assay

PCR/SSCP with the BIOMED-2 TCR-β primers was performed as described in Fraser-Andrews *et al.* (2001) using the diagnostic sample from SS patient R164. Clonal bands were sequenced (Geneservice) using multiplexed forward or reverse BIOMED-2 primers. A rearrangement-specific forward primer was designed to overlap V, D, and N regions. J region–specific reverse primer and probe were synthesized according to published sequences. Quantitative PCR was performed on an ABI 7000, and the assay was validated using the diagnostic sample as a positive control and pooled healthy lymphocyte DNA as a negative control. Sensitivity was tested and a standard curve generated by spiking a synthetic positive control into pooled healthy lymphocyte DNA. Patient-specific Ct values were normalized against the Ct values from two diploid genomic control regions (SDC4 and BCMA) to calculate the proportion of tumor cells present in each cell subset.

Statistics

Comparison between two groups was made using Student's *t*-test, whereas comparisons among three groups were made by analysis of variance. All statistical tests were performed using the R statistical software package (http://www.r-project.org/).

CONFLICT OF INTEREST

The authors state no conflict of interest.

ACKNOWLEDGMENTS

This work was supported by grants from the Guy's and St Thomas' Charitable Foundation ''Skin Matters'' fund (C.L.J.). Support from Guy's and St Thomas' NHS Foundation Trust (to T.J.M) is gratefully acknowledged. We acknowledge financial support from the Department of Health via the National Institute for Health Research (NIHR) comprehensive Biomedical Research Centre award to Guy's and St Thomas' NHS Foundation Trust in partnership with King's College London and King's College Hospital NHS Foundation Trust.

REFERENCES

Agar NS, Wedgeworth E, Crichton S *et al.* (2010) Survival outcomes and prognostic factors in mycosis fungoides/Sézary syndrome: validation of the revised International Society for Cutaneous Lymphomas/European Organisation for Research and Treatment of Cancer staging proposal. *J Clin Oncol* 28:4730–9

Bagot M, Moretta A, Sivori S *et al.* (2001) CD4 (+) cutaneous T-cell lymphoma cells express the p140-killer cell immunoglobulin-like receptor. *Blood* 97:1388–91

Booken N, Gratchev A, Utikal J *et al.* (2008) Sézary syndrome is a unique cutaneous T-cell lymphoma as identified by an expanded gene signature including diagnostic marker molecules CDO1 and DNM3. *Leukemia* 22:393–9

Bradford PT, Devesa SS, Anderson WF *et al.* (2009) Cutaneous lymphoma incidence patterns in the United States: a population-based study of 3884 cases. *Blood* 113:5064–73

Bruggemann M, van der Velden VH, Raff T *et al.* (2004) Rearranged T-cell receptor beta genes represent powerful targets for quantification of minimal residual disease in childhood and adult T-cell acute lymphoblastic leukemia. *Leukemia* 18:709–19

Campbell JJ, Clark RA, Watanabe R *et al.* (2010) Sezary syndrome and mycosis fungoides arise from distinct T-cell subsets: a biologic rationale for their distinct clinical behaviors. *Blood* 116:767–71

Capriotti E, Vonderheid EC, Thoburn CJ *et al.* (2008) Expression of T-plastin, FoxP3 and other tumor-associated markers by leukemic T-cells of cutaneous T-cell lymphoma. *Leuk Lymphoma* 49:1190–201

Chen H, Mocsai A, Zhang H *et al.* (2003) Role for plastin in host defense distinguishes integrin signaling from cell adhesion and spreading. *Immunity* 19:95–104

Contassot E, Kerl K, Roques S *et al.* (2008) Resistance to FasL and tumor necrosis factor-related apoptosis-inducing ligand-mediated apoptosis in Sezary syndrome T-cells associated with impaired death receptor and FLICE-inhibitory protein expression. *Blood* 111:4780–7

Drummond AJ, Ashton B, Buxton S *et al.* (2011) Geneious v5.4, Available from http://www.geneious.com/

Foran E, McWilliam P, Kelleher D *et al.* (2006) The leukocyte protein L-plastin induces proliferation, invasion and loss of E-cadherin expression in colon cancer cells. *Int J Cancer* 118:2098–104

Fraser-Andrews EA, Russell-Jones R, Woolford AJ *et al.* (2001) Diagnostic and prognostic importance of T-cell receptor gene analysis in patients with Sezary syndrome. *Cancer* 92:1745–52

Haynes BF, Metzgar RS, Minna JD *et al.* (1981) Phenotypic characterization of cutaneous T-cell lymphoma. Use of monoclonal antibodies to compare with other malignant T cells. *N Engl J Med* 304:1319–23

Higuchi Y, Kita K, Nakanishi H *et al.* (1998) Search for genes involved in UV-resistance in human cells by mRNA differential display: increased transcriptional expression of nucleophosmin and T-plastin genes in association with the resistance. *Biochem Biophys Res Commun* 248:597–602

Hisano T, Ono M, Nakayama M *et al.* (1996) Increased expression of T-plastin gene in cisplatin-resistant human cancer cells: identification by mRNA differential display. *FEBS Lett* 397:101–7

Ikeda H, Sasaki Y, Kobayashi T, *et al.*, (2005) The role of T-fimbrin in the response to DNA damage: silencing of T-fimbrin by small interfering RNA sensitizes human liver cancer cells to DNA-damaging agents. *Int J Oncol* 27:933–40

Jones CL, Wain EM, Chu CC, *et al.*, (2010) Downregulation of Fas gene expression in Sezary syndrome is associated with promoter hypermethylation. *J Invest Dermatol* 130:1116–25

Jones D, Dang NH, Duvic M, *et al.*, (2001) Absence of CD26 expression is a useful marker for diagnosis of T-cell lymphoma in peripheral blood. *Am J Clin Pathol* 115:885–92

Kari L, Loboda A, Nebozhyn M *et al.* (2003) Classification and prediction of survival in patients with the leukemic phase of cutaneous T cell lymphoma. *J Exp Med* 197:1477–88

Klemke C-D, Brade J, Weckesser S *et al.* (2008) The diagnosis of Sézary syndrome on peripheral blood by flow cytometry requires the use of multiple markers. *Br J Dermatol* 159:871–80

Lin C, Lau A, Huynh T *et al.* (1999) Differential regulation of human T-plastin gene in leukocytes and non-leukocytes: identification of the promoter, enhancer, and CpG island. *DNA Cell Biol* 18:27–37

Lin CS, Park T, Chen ZP *et al.* (1993) Human plastin genes. Comparative gene structure, chromosome location, and differential expression in normal and neoplastic cells. *J Biol Chem* 268:2781–92

Nebozhyn M, Loboda A, Kari L *et al.* (2006) Quantitative PCR on 5 genes reliably identifies CTCL patients with 5% to 99% circulating tumor cells with 90% accuracy. *Blood* 107:3189–96

Oprea GE, Kröber S, McWhorter ML *et al.* (2008) Plastin 3 is a protective modifier of autosomal recessive spinal muscular atrophy. *Science* 320:524–7

Sasaki Y, Itoh F, Kobayashi T *et al.* (2002) Increased expression of T-fimbrin gene after DNA damage in CHO cells and inactivation of T-fimbrin by CpG methylation in human colorectal cancer cells. *Int J Cancer* 97:211–6

Steinhoff M, Schöpp S, Assaf C *et al.* (2009) Prevalence of genetically defined tumor cells in CD7 as well as CD26 positive and negative circulating T-cell subsets in Sézary syndrome. *Leuk Res* 33:88–99

Su MW, Dorocicz I, Dragowska WH *et al.* (2003) Aberrant expression of T-plastin in Sezary cells. *Cancer Res* 63:7122–7

Tang N, Gibson H, Germeroth T *et al.* (2010) T-plastin (PLS3) gene expression differentiates Sezary syndrome from mycosis fungoides and inflammatory skin diseases and can serve as a biomarker to monitor disease progression. *The British journal of dermatology* 162:463–6

Tiemessen MM, Mitchell TJ, Hendry L *et al.* (2006) Lack of suppressive CD4+CD25+FOXP3+ T cells in advanced stages of primary cutaneous T-cell lymphoma. *J Invest Dermatol* 126:2217–23

van der Velden VHJ, van Dongen JJM (2009) MRD detection in acute lymphoblastic leukemia patients using Ig/TCR gene rearrangements as targets for real-time quantitative PCR. *Methods Mol Biol* 538:115–50

van Doorn R, Dijkman R, Vermeer MH *et al.* (2004) Aberrant expression of the tyrosine kinase receptor EphA4 and the transcription factor twist in Sézary syndrome identified by gene expression analysis. *Cancer Res* 64:5578–86

van Krieken JHJM, Langerak AW, Macintyre EA *et al.* (2007) Improved reliability of lymphoma diagnostics via PCR-based clonality testing: report of the BIOMED-2 Concerted Action BHM4-CT98-3936. *Leukemia* 21:201-6

Wabnitz GH, Köcher T, Lohneis P *et al.* (2007) Costimulation induced phosphorylation of L-plastin facilitates surface transport of the T cell activation molecules CD69 and CD25. *Eur J Immunol* 37:649–62

Willemze R, Jaffe ES, Burg G *et al.* (2005) WHO-EORTC classification for cutaneous lymphomas. *Blood* 105:3768–85

Willemze R, Kerl H, Sterry W *et al.* (1997) EORTC classification for primary cutaneous lymphomas: a proposal from the Cutaneous Lymphoma Study Group of the European Organization for Research and Treatment of Cancer. *Blood* 90:354–71

Yoon JS, Newton SM, Wysocka M *et al.* (2008) IL-21 enhances antitumor responses without stimulating proliferation of malignant T cells of patients with Sézary syndrome. *J Invest Dermatol* 128:473–80